Performance Analysis of Energy Efficient Spectrum Sensing Techniques in Cognitive Radio Networks

THESIS

Submitted in partial fulfillment

of the requirements for the degree of

DOCTOR OF PHILOSOPHY

by

RAJALEKSHMI KISHORE

Under the Supervision of

PROF. RAMESHA C. K.

and

Co-Supervision of

PROF. K. R. ANUPAMA

BITS Pilani

Pilani|Dubai|Goa|Hyderabad

BIRLA INSTITUTE OF TECHNOLOGY & SCIENCE, PILANI

2018

BIRLA INSTITUTE OF TECHNOLOGY & SCIENCE, PILANI

CERTIFICATE

This is to certify that the thesis entitled **"Performance Analysis of Energy Efficient Spectrum Sensing Techniques in Cognitive Radio Networks"**, submitted by **Rajalekshmi Kishore** ID. No. **2012PHXF0401G** for award of Ph.D. of the Institute embodies original work done by her under our supervision.

Signature of the Supervisor:

Name in capital letters : **PROF. RAMESHA C. K.**

Designation : **ASSOCIATE PROFESSOR**

Department of Electrical & Electronics Engineering

Date : 1/9/2018

Signature of the Co-Supervisor

Name in capital letters : **PROF. K. R. ANUPAMA**

Designation : **PROFESSOR**

Department of Electrical & Electronics Engineering

Date : 1/9/2018

DECLARATION

I, Rajalekshmi Kishore, hereby declare that this thesis entitled "Performance Analysis of Energy Efficient Spectrum Sensing Techniques in Cognitive Radio Networks" submitted by me under the guidance and supervision of Prof. Ramesha C. K. and Prof. K. R. Anupama, is a bonafide research work. I also declare that it has not been submitted previously in part or in full to this University or any other University or Institution for award of any degree.

Signature of the Student : Rajalekshmi 01/09/2018

Name in capital letters : **RAJALEKSHMI KISHORE**

ID. N0. of the student : **2012PHXF0401G**

Date : 01-09-2018

Abstract

Cognitive radio network (CRN), that employs dynamic spectrum access (DSA) to opportunistically coexist with a primary user network, is expected to support a large number of connected devices for a variety of wireless related applications. In this regard, DSA, where the unlicensed users, or secondary users (SUs), can opportunistically access an underutilized spectrum of the licensed users, or primary users (PUs), is the de facto solution for the realization of dynamic spectrum sharing, which is envisioned to be an integral part of the future 5G communication systems. A fundamental feature of CRN is spectrum sensing by which one can obtain the spectrum usage status of the PU. Conventional cooperative sensing (CCS) is preferred due to its resilience to multipath fading and hidden node problem. CCS is carried out in two consecutive phases, namely, the sensing phase, where each CR carries out sensing, and a reporting phase, where each CR shares its decision with a fusion center (FC) which makes a global decision. Thus, CCS consumes a significant amount of energy, which is a challenge for successful deployment of SU network. Moreover, the necessity to periodically sense and an increase in the number of channels to be sensed, further increases the energy demand. Hence, one of the main factor that limits the implementation of cognitive radio network especially in battery powered terminal is due to its high energy consumption. Towards this end, energy efficient cooperative spectrum sensing in a CR network is the focus of this research. Energy efficiency in a CR network can be increased by either increasing the network throughput, or decreasing the total energy consumption. A significant improvement in energy efficiency can be achieved by (a) ensuring proper cooperation among the nodes, (b) optimally assigning a subset of nodes for spectrum sensing for a given PU channel, and (c) by employing techniques like compressed sensing to reduce the communication overhead between the sensors and FC.

In this thesis, energy-efficient schemes for CCS are proposed under the above mentioned scenarios. The proposed work includes energy efficiency analysis due to a reduction in sensor reporting overhead, sensor-to-channel assignment in energy harvesting-based heterogeneous cognitive radio network (HCRN), and the energy efficiency analysis of the compressed sensing-based collaborative sensing scheme. To begin with, the energy efficiency of superior selective reporting (SSR)-based schemes for CCS in cognitive radio networks is studied. The maximization of energy efficiency (EE) for the SSR scheme is proposed as a multiple variable-based, non-convex optimization problem and approximations to reduce it to a quasi-convex optimization problem is provided. The errors due to these approximations are shown to be negligible. The SSR scheme is designed to optimize the energy consumption, which enhances the EE. Alternatively, EE can also be improved by increasing the achievable throughput. Towards this end, a novel variation on the SSR scheme called the opportunistic SSR (OSSR) scheme, was proposed and its EE analysis

is carried out. The tradeoff between the performances of the SSR and OSSR schemes is shown to be the implicit tradeoff between achievable throughput and energy consumption. The regimes where OSSR is preferred over SSR and vice-versa, in terms of EE are discussed. Also, through an extensive numerical study, it was shown that both SSR and OSSR schemes outperform the CCS schemes that employ the OR and AND fusion rules, in terms of EE.

The performance of SSR scheme is also analyzed in a multi-channel heterogeneous cognitive radio wireless sensor network (HCRWSN) which employs energy harvesting nodes for spectrum sensing. Initially, the average achievable network throughput of the optimal CCS scheme which employs the L-out-of-M fusion rule and the SSR scheme is analyzed. Next, for both CCS and SSR schemes, a nonlinear integer programming problem is formulated to find throughput-optimal set of spectrum sensors scheduled to sense a particular channel, with a given PU interference and energy harvesting constraints. The problem is solved by using the cross entropy (CE) method, and the advantages of the CE algorithm in comparison to the exhaustive search, and the greedy algorithm is discussed. Finally, the tradeoff between the average achievable throughput of SSR and CCS schemes is analyzed to highlight the regime where the SSR scheme is better than the optimal CCS scheme. It is shown that this inherent tradeoff is between the channel available time and the detection accuracy. Numerical results show that as the number of spectrum sensors increases, the channel available time gets a larger priority in an HCRWSN, as opposed to detection accuracy.

Finally, a study on the compression limit, and trade-off between the achievable throughput and energy consumption of CR network employing compressed conventional collaborative sensing (CCCS) scheme is carried out. The expressions for the achievable throughput, energy consumption and EE of CCCS scheme is derived and a multiple variable, non-convex optimization problem is formulated to find out the optimum compression level that maximizes energy efficiency, subject to interference constraints on the primary network. Approximations to reduce it to a convex optimization problem are provided and it is shown that the errors due to these approximations are negligible. It is shown that the EE achieved due to the CCCS scheme is higher than that of the CCS scheme under the same predefined conditions, and the increase in the EE is due to the considerable decrease in the energy consumption, which is especially significant with higher number of sensors.

In all the above mentioned scenarios, a detailed performance study, comparing the energy efficiency of the proposed techniques, is presented, and their relative advantages are discussed. Most importantly, it is interesting to note that each study resulted in a performance trade-off, which are also discussed in detail.

Acknowledgements

I would like to express my sincere gratitude to my supervisor, Prof. Ramesha C. K. for his patient guidance, warm encouragement and invaluable advice throughout the course of my Ph.D. study. He was always understanding of the difficulties and the challenges one inevitably faces during the seemingly never ending Ph.D. study. His positive outlook and endless support inspired me and gave me the confidence and motivation needed to finish this work. His careful and insightful reviews contributed enormously to the production of this thesis. It was truly a great privilege working with him.

I would like to thank my Co-Supervisor, Prof. K. R. Anupama, for giving me the opportunity to pursue my Ph.D. in this Institution and all the support and encouragement throughout my Ph.D. study period.

My sincere gratitude also goes to Late Prof. Sanjeev Aggarwal, fromer Director, BITS Pilani, K. K. Birla Goa Campus, for all his help and support. It was due to his push that I was able to find an in-house campus, which greatly reduced my research-related workload and increased my research productivity. I would also like to thank the Doctoral Advisory Committee members for my thesis, Dr. Narayan Suresh Manjarekar and Dr. Lucy J. Gudino for taking the time and effort to review the progress of my research work and providing me with their insightful comments.

I would extend my sincere thanks to Prof. A. Amalin Prince, HOD of EEE Department, for his constant support and encouragement at various levels.

I thank Prof. G. Raghurama, Director, BITS Pilani, K. K. Birla Goa Campus, Prof. Bharat M. Deshpande, Associate Dean, ARD, Prof. Prasanta Kumar Das, Prof. Sunil Bhand, Dean, SRCD and Prof. D. M. Kulkarni, Dean, Administration, BITS, Pilani, K.K. Birla Goa Campus, for giving me an opportunity to carry out research studies at the institute and also by providing necessary infrastructure and facilities to carry out my work.

I express my sincere gratitude to Prof. Sanjeev Gurugopinath, Professor, PES University, Bangalore, for his invaluable insights and suggestions. This work would not have been possible without his guidence, support, and encouragement on a daily basis. His own zeal for perfection, passion towards research has always inspired me to do more. I have learned various aspects of academic research, right from problem formulation to the analysis and presentation of results, from him. Thank you, Prof. Sanjeev, for all the support.

I also extend my sincere thanks to Dr. Gautam G. Bacher, DRC Convener, for his support and motivation.

I acknowlege with due gratitude to the faculty members of EEE department Prof. Anita Agrawal, Prof. M. K. Deshmukh, Dr. Nitin Sharma, Dr. Pravin Mane, Dr. Sarang Dhongdi and Dr. C. B. K. Murthy for their constant motivation and support. I also extend my sincere thanks to Ms. Parul Sahu, for her continous support and help during my intial days in the campus.

My heartfelt thanks to my fellow Ph.D scholors from Maths department, Santosh Kumar Bhal, Shah Parth Mukeshbhai, Aloysius Godinho for all their professional help that they have extended to me throughout. My special gratitude to Praveen G.B. and Hima Bindu and all other friends Selva Ganapathy, Khairnar Vikas Vishnu, Saif Dilavar, Athokpam Bharatbushan, Kadam Bhushan Vinayak, Joshi Abhishek Dilip, Gibin Chacko George, Chithira and Mouna for their moral support and motivation, which drives me to give my best.

I would extend my sincere thanks to Mr. Sameer Chodankar, Mr. Anil Lamani, Mr. Pushparaj Paradkar, and Mr. Shivaraj Rathod, lab technicians for their constant help during my research work.

Words cannot express the feelings I have for my parents for their constant support, love and encouragement to carry out my research work. I appreciate and treasure everything they have taught me. My mother has been my constant source of inspiration and I have learned from my father the value of hard work and dedication leads to success.

It is my fortune to gratefully acknowledge the unfailing emotional support of my parents-in-law and their faith in me. They were always beside me during the happy hard moments to motivate me. I deeply thank for their unconditional trust, timely encouragement and endless support.

Finally, I would like to acknowledge my husband Kishore. He has been a constant source of strength and inspiration. I would not be where I am today without his support and constant encouragement. I can honestly say that it was only his determination and constant encouragement that ultimately made it possible for me to see this thesis through to the end.

I would like to thank my beloved son, Govinda, who is my constant source of joy and happiness and whose presence ease all life difficulties and make it worthwhile.

Above all, I thank God Almighty for all the blessings bestowed upon me and for granting me the strength and patience to complete this work.

Rajalekshmi Kishore

This thesis is dedicated to my son Govinda

Contents

List of Figures

List of Tables

Abbreviations

CR	**C**ognitive **R**adio
CCS	**C**onventional **C**operative **S**ensing
CE	**C**ross **E**ntropy
CCCS	**C**onventional **C**ollaborative **C**ompressed **S**ensing
CS	**C**ompressed **S**ensing
CLRS	**C**ross **L**ayer **R**econfiguration **S**cheme
DSA	**D**ynamic **S**pectrum **A**ccess
ED	**E**nergy **D**etector
EE	**E**nergy **E**fficiency
EH	**E**nergy **H**arvesting
EGC	**E**qual **G**ain **C**ombining
FC	**F**usion **C**enter
HCRWSN	**H**etrogeneous **C**ognitive **R**adio **W**ireless **S**ensor **N**etwork
HD	**H**ard **D**ecision
HWSN	**H**etrogeneous **W**ireless **S**ensor **N**etwork
LR	**L**ikelihood **R**atio
LLR	**L**og **L**ikelihood **R**atio
MRC	**M**aximum **R**atio **C**ombining
NP	**N**yman **P**earson
OFDM	**O**rthogonal **F**requency **D**ivision **M**ultiple **A**cess
OCR	**O**verlay **C**ognitive **R**adio
OSA	**O**ppertunistic **S**pectrum **A**ccess
OSSR	**O**ppertunistic **S**uperior **S**elective **R**eproting

SE	**S**pectral **E**fficiency
SS	**S**pectral **S**ensing
SSR	**S**uperior **S**elective **R**eproting
SWIPT	**S**imultaneous **W**ireless **I**nformation **P**ower **T**ransfer
SSDFA	**S**pectrum **S**ensing **D**ata **F**alsification **A**ttack
UCR	**U**nderlay **C**ognitive **R**adio

Chapter 1

Introduction

1.1 Introduction

The ever-increasing data traffic in radio communication systems, calls for new methods of handling and managing the existing radio spectrum resources. This demand, along with a shortage of existing spectrum resource, has inspired researchers to come up with the idea of cognitive radio (CR), introduced in fundamental works by J. Mitola III [2]–[3]. The works of J. Mitola III, have also stimulated investigation in the field of efficient spectrum sharing and dynamic spectrum access, which are considered an integral part of future 5G communication systems [4]. The CR technology employs dynamic spectrum access (DSA) to opportunistically coexist with licensed users, also referred to as primary users (PU). CR aims to determine the availability of considered frequency band with atmost probability. This may essentially be achieved based on the knowledge about scheduled primary activities, known as database, or based on the real-time measurement of the PU's activity, known as spectrum sensing. The latter solution was initially considered as the main aspects for future CR systems, but due to long-standing open research issues in the implementation of reliable sensing methods, the interest in databases grew significantly [5], [6]. However, investigation on spectrum sensing is still highly encouraged, as sensing can complement and extend the information provided by databases.

1.2 Spectrum Sensing

The objective of spectrum sensing (SS) is to detect the existence of a PU by a cognitive entity or secondary user (SU) in any particular band of frequency. Energy detector, matched filter detector, feature detection technique and wavelet technique are various spectrum sensing techniques which have been proposed in this context, as described in [7], [8],[9].

The spectrum sensing decision D_i made by the secondary user to detect the primary user signal s_i can be represented as:

$$D_i = \begin{cases} \mathcal{H}_0 & \text{if } Y_i = n_i \\ \mathcal{H}_1 & \text{if } Y_i = h_i s_i + n_i, \end{cases} \qquad i = 1, 2, ...Z \tag{1.1}$$

where Z is the number of observations used for detection, $\mathcal{H}_0$ is the hypothesis that the spectrum is vacant, and $\mathcal{H}_1$ is the hypothesis that the spectrum is occupied. A test-statistic represented by T$(\cdot)$ is calculated based on the recorded observations. If the test statistic is greater than a chosen threshold, denoted by δ, then hypothesis $\mathcal{H}_1$ is declared true. Otherwise, $\mathcal{H}_0$ is declared true. Mathematically, the detector is represented as

$$T(Y_1, ...Y_Z) \underset{\mathcal{H}_0}{\overset{\mathcal{H}_1}{\gtrless}} \delta \tag{1.2}$$

Most popular local sensing techniques such as, energy detector [10], cyclostationarity- based detector [11], matched filter- based detector [12] and Bayesian detector [13],[14] have been proposed and studied extensively. The energy detector senses the state of the PU by calibrating the power of obtained signal [15]. Cyclostationarity-based detection exploits the cyclostationarity features of the primary signals; however, it does not make full use of the characteristics of the modulated signals [11]. The matched filter-based detector correlates the received signal with a copy of the transmitted signal. Although it is computationally simple, it assumes knowledge of the primary user signal, which may not be feasible in general [12]. In Bayesian detector (BD), the effect of the prior probabilities are taken into account and the detection threshold is chosen to minimize a convex combination of the false-alarm and signal detection probabilities [14]. However, prior investigations have proved that the sensing is not accurate enough when carried

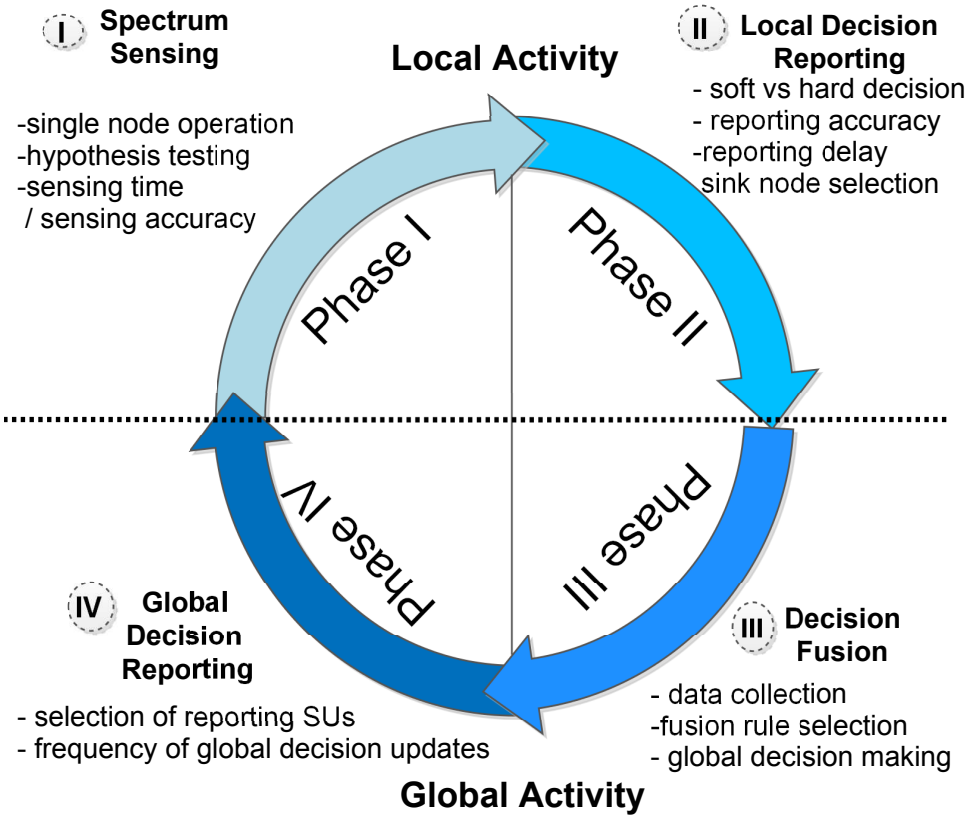

Figure 1.1. Steps involved in Cooperative Spectrum Sensing

out locally by a single device [16, 17], and hence, cooperative sensing is preferred for spectrum sensing for its resilience to multipath fading [18, 19]. Hence, it is agreed that applying cooperation between the nodes is one of the ways to improve the consistency of spectrum sensing.

1.3 Cooperative Spectrum Sensing

In cooperative spectrum sensing (CSS), each node in the network reports its local sensing result to a fusion center, which makes an overall decision about the availability of the primary spectrum. Thus, cooperative SS is carried out in four consecutive phases, as illustrated in Figure 1.1.

i. Local spectrum sensing by single node

ii. Local spectrum sensing decision reporting

iii. Decision fusion

iv. Global decision reporting

Each of these phases will be discussed in detail in the subsequent sections.

1.3.1 Local Spectrum Sensing by Single Node

The main objective of local SS is to sense the presence or absence of a PU signal by SU. The quality of sensing is characterized by

i. Probability of detection P_d - The probability that SU correctly declares the presence of PU, given the true hypothesis to be $\mathcal{H}_1$

ii. Probability of missed-detection P_{md} - The probability that SU incorrectly declares the absence of PU, given the true hypothesis to be $\mathcal{H}_1$.

iii. Probability of false alarm P_f - The probability that SU incorrectly declares the presence of PU when the PU is inactive.

Maximizing the detection probability and minimizing the false alarm probability will improve the detection reliability. However, optimization of these two metrics are contradictory goals [20], i.e., lowering the requirement for detection threshold leads to increase in detection probability and consequently to an increase in false alarm probability. Similarly, increasing the detection threshold reduces both detection and false alarm probability. Thus, it is important to sustain a tradeoff that maintains low false alarm rate and high detection rate for every sensing scheme. To attain this tradeoff, Bayesian test and Neyman-Pearson test are the most popular approaches used. In Neyman-Pearson (NP) formulation, the goal is to maximize the probability detection, subjected to a constraint on the probability of false alarm. Alternatively, in Bayesian approach, the effect of the prior probabilities are taken into account and the detection threshold is chosen to minimize a convex combination of the false-alarm and signal detection probabilities.

Once all the sensors/nodes procures individual sensing decisions with a given detection accuracy measured by P_d and P_f, the next stage is to share this sensing result with other nodes or fusion center to generate global, improved-quality decision.

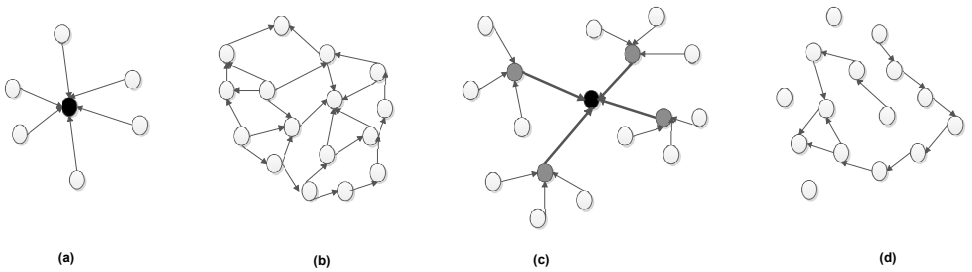

Figure 1.2. Classification of cooperative spectrum sensing (a) centralized, (b) distributed, (c) cluster-based, (d) relay-based

1.3.2 Sensing Decision Reporting

Local decision on the availability of vacant spectrum in a given band, made by the individual node, can be shared to the fusion center or neighboring nodes through a lossless channel. This method of decision reporting, known as hard-decision combining, is very brief and easy-to-decode and hence decision fusion and global decision can be easily achieved, whereas in soft-decision reporting scheme, sensing information with an assumed level of accuracy is encoded and reported. Thus, soft decision reporting increases global detection quality. However, due to the large data overhead, computational complexity increases in soft-metric reporting. In an energy-efficient perspective, the size of the sensing report should be limited, and practically, it can be achieved by adopting compressed sensing (CS) - reducing the sampling rate at the sub-Nyquist rate [21], which further reduces the sensing time duration and greatly favors energy saving. For this reason, the CS is proposed as an efficient approach for improving the energy efficiency in cognitive radio network.

The preparation of local sensing decision in the form of decision reports is followed by the process of sharing the local observation with the selected nodes or the fusion center. There are several methods by which these local observations can be conveyed to other nodes which rely on: a) the location of fusion center (FC), b) the sensing channel quality and c) the reporting channel availability [22]. The classification of cooperative spectrum sensing is presented in the following subsection.

1.3.2.1 Classification of cooperative sensing

Cooperative spectrum sensing can be classified based on how local sensing nodes share the sensing reports within the network as follows:

- Centralized Cooperative Sensing
- Distributed Cooperative Sensing
- Cluster-based Cooperative Sensing
- Relay-based Cooperative Sensing

In centralized cooperative sensing, the fusion center (FC) generates a global decision based on sensing decisions collected from the nodes and broadcasts the global decision back to nodes. In Figure.1.2, a such a centralized topology is presented. Unlike centralized cooperative sensing, distributed cooperative sensing does not rely on an FC for making the cooperative decision [20]. In this case, sensing nodes communicate among themselves and converge to a unified decision on the presence or absence of PUs. Figure.1.2b illustrates the cooperation in the distributed manner. When the distance between the nodes are larger, the reporting channel distance will also be larger and in such a scenario, a cluster-based scheme is adopted. In the cluster-based approach, a closed group, which is known as a cluster, is formed by geographically neighboring nodes. Each cluster selects a cluster head, [20]. All nodes in a cluster report their local decisions to the cluster head, which forwards, the decisions collected to the FC. This is illustrated in Figure.1.2c. The cluster-based scheme introduces additional overhead in sharing the sensing information for organizing cluster nodes and for cluster heads selection. If a node has poor reporting channel quality, relaying is employed in which sensing information by the individual nodes is transmitted based on the channel condition of individual nodes. In such cooperation, the sensing messages are relayed by another node to the FC or a selected node. This is illustrated in Figure.1.2d. The method of relaying introduces additional delay in the network where the information is relayed by a number of secondary nodes [20].

1.3.3 Decision Fusion

After the local sensing results are collected, the fusion center or selected sink node should perform decision fusion using various fusion rules [23],[24–26] to get the global decision [27]. Various fusion rules such as L-out-of-M-rule, AND rule, OR rule, Majority rule are possible, and their global decisions are based on local sensing information from secondary nodes [20].

1.3.4 Global Decision Reporting

The final phase of cooperative sensing is to share the global decision on the spectrum vacancy. In the centralized topology, the FC shares the global decision by broadcasting its decision to all other cooperative nodes. However, in a distributed topology, nodes acquire their neighbors' sensing result during the local decision reporting stage. In the cluster-based approach, the cluster heads are responsible to report the global decisions back to the nodes within a cluster.

1.4 Performance Evaluation Metrics of CSS Scheme

The overall performance of CSS is based on the detection accuracy, which is a combination of the detection and false-alarm probabilities [28]. A comprehensive metric which includes both detection and false alarm probability is the error probability P_e and is expressed as follows:

$$P_e = P(\mathcal{H}_0)P_f + P(\mathcal{H}_1)(1 - P_d) = P(\mathcal{H}_0)P_f + P(\mathcal{H}_1)P_{md} \tag{1.3}$$

Low values of P_e indicate high detection accuracy which favors other aspects of the network performance. Yet another important evaluation metrics for the CRN performance are the achievable throughput and total energy consumption. The average achievable throughput (R) is defined as the average achievable data rate by the scheduled secondary nodes, while the energy consumption (E) is defined as the average energy consumed during local sensing, results reporting and data transmission by the secondary nodes [28]. Notice that detection accuracy affects both the throughput and energy consumption. However, there exists a trade-off between the achievable throughput and energy consumption, since increase in average achievable throughput may increase energy consumption and vice versa. Thus, energy efficiency is a general metric that combines both of them. Energy efficiency (EE) is defined as the ratio between the achievable throughput to the total energy consumption, and measured in $Bits/Hz/Joule$ [28]. Mathematically, EE is expressed as follows:

$$Energy\ Efficiency\ (EE) = \frac{Throughput\ (R)}{Energy\ consumed\ (E)} Bits/Hz/J \tag{1.4}$$

Note that the EE metric represents the overall performance of a CR system, by jointly taking into account the achievable network throughput in terms of the detection accuracy, and the overall energy consumption. Apparently, EE represents a fair indicator of the whole performance of cognitive radio network.

In a network where cognition capabilities are involved to access the licensed spectrum, an essential criterion is to guarantee PU protection against interference generated by the CR system. As primary users can use its spectrum at any moment, sensing should be a continuous process which results in an increased energy consumption and a larger delay in making a decision on the availability of the spectrum due to the sensing overhead. This makes energy efficiency an important issue to be addressed in practical implementation of cooperative spectrum sensing [29–31] in CR networks.

1.5 Energy Efficient Cooperative Spectrum Sensing

This section provides an outline of the energy efficiency aspects of cooperative sensing in terms of tradeoff impact and the classification of energy saving techniques in cooperative sensing in CRN. In an energy saving context, the following tradeoffs are identified in each phase of CSS.

1.5.1 Tradeoff in Single-Node Sensing

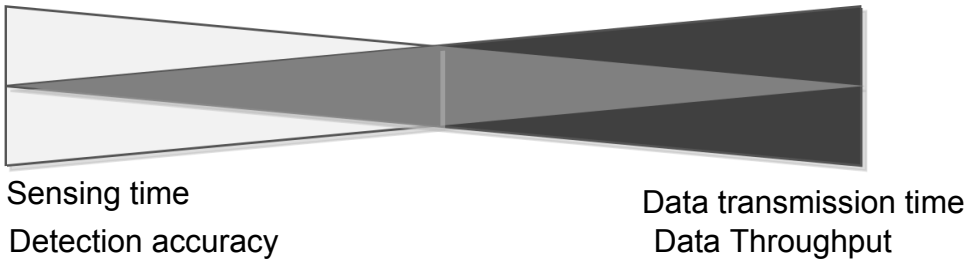

Figure 1.3. Sensing time- data transmission time tradeoff

One of the key tradeoffs in spectrum sensing is to regulate the sensing duration and the data transmission duration [20]. The first one influences sensing reliability, thereby increasing the PU protection, and the second increases the SU spectral efficiency, which is illustrated in Figure 1.3.

Thus, both influence the energy efficiency of a CR system [20]. Therefore, the sensing duration has to be carefully maintained in order to achieve a given level of sensing reliability [20].

1.5.2 Tradeoff in Sensing Decision Reporting

In the context of energy saving, it is easy to indicate the trade-off between the accuracy and granularity of sensing decision transmitted and the energy and time needed for this action. The higher the granularity of the transferred sensing decision, the higher the generated traffic in the network and energy consumption in that particular phase, but at the same time, the more detailed and accurate the message delivered to the fusion centre.

1.5.3 Tradeoff in Sink Node Selection

Energy consumed during sink node selection mainly depends on the number of links between the nodes involved in exchanging of information [20]. However, this tradeoff is highly influenced by the topology selection which was mentioned in the previous section.

1.5.4 Tradeoff in the Decision Fusion

A tradeoff exists between the detection accuracy in decision made by a fusion center and the EE. If the detection probability is low, the number of collisions with a PU increases, which increases the re-transmissions for both the PU and the SU. This leads to a lower energy efficiency. However, this tradeoff can be handled to an extent by assuming the level of uncertainty to a constant. Even in this scenario, the tradeoff will depend highly on the topology [20].

1.5.5 Tradeoff in the Global Decision Reporting

This phase of cooperative sensing requires the delivery of the global decision to all nodes. However, the tradeoffs between detection accuracy and energy efficiency still occur when the

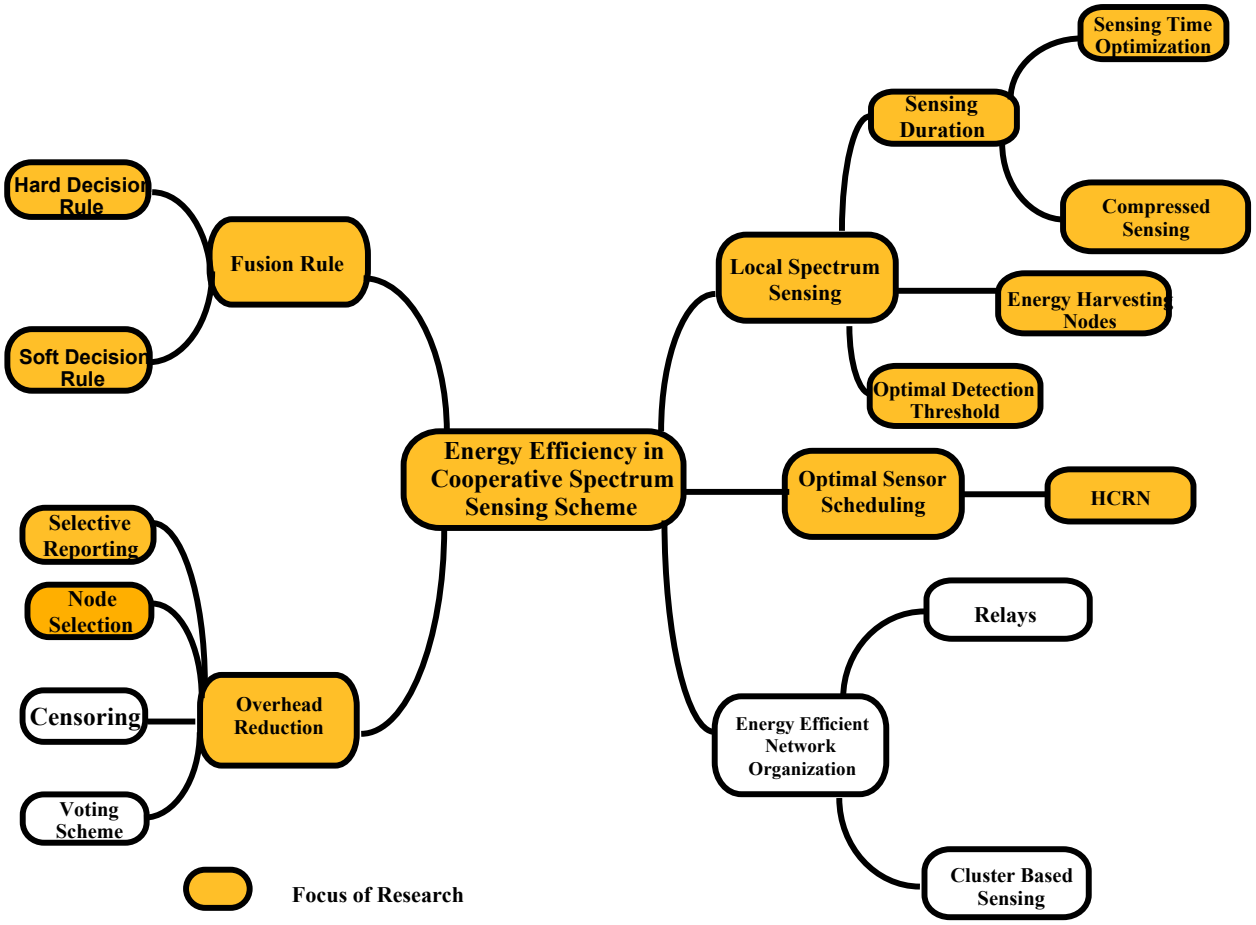

Figure 1.4. Classification of energy efficient cooperative spectrum sensing

global decisions are transmitted to all nodes or the cluster heads receive the decision and further transmit the decision report to individual nodes within the cluster.

The identification of the prevailing tradeoffs in each phase of cooperative sensing shows that there exist a variety of methods by which optimization of the energy efficiency in CSS networks is possible. Based on the aforementioned EE analysis of CSS, the classification of energy efficiency of CSS techniques are discussed in detail in the following section.

1.6 Classification of Energy Efficient CSS

Based on the possible energy savings, following are the classification of energy efficient cooperative spectrum sensing technique, as shown in Figure 1.4:

- **Energy Efficient Local Sensing Phase** :

  Reduction in sensing time or number of collected samples are the ways to attain energy efficiency in local spectrum sensing. As the number of acquired samples is reduced,

the energy consumption reduces. However, this reduction in energy consumption is only possible with reduction in performance. Energy efficiency can be further improved by optimization of the detection threshold which is used for the differentiation of decision variable to decide on the binary hypothesis of presence and absence of the primary user in a given spectrum.

Another promising technology for improving energy efficiency in local spectrum sensing phase is energy harvesting (EH). It allows wireless devices to capture and store ambient energy such as solar, wind and ambient radio power to generate power [32]. Thus, deployment of energy harvesting aided spectrum sensors takes care of the energy efficiency in an energy- constrained CR network.

- **Fusion and Decision Rules Selection** : Energy savings in decision fusion phase is possible if an efficient fusion of local sensing decisions is considered at the fusion center. Further improvement in EE can be attained by adapting the decision fusion threshold on the basis of wireless channel condition [20].

- **Optimization of Number of Cooperative Nodes** : Energy efficiency in CSS can be improved by reducing the sensing overhead which can be achieved either by selective sensing [33] or selective decision reporting [34]. Thus, it is advantageous to avoid the nodes that offer only a relatively small value addition to the network energy efficiency metrics at a higher energy cost.

- **Optimal Sensor Scheduling** : In a multi-channel system, the benefits of assigning users to sense channels in parallel must also be considered to improve the energy efficiency of the network. A sensing schedule, for each user to sense the assigned channel at different sensing moments, must be thus created to optimize system performance.

- **Energy Efficient Network Organization** : The EE can also be improved by efficient network organization. The energy devoted to interchange decision information in CSS should be considered more carefully. Thus, by choosing network topology based on the scenario, energy efficiency can be improved to a greater extent.

1.7 Challenges in Energy Efficient Cooperative Spectrum Sensing

The open challenges regarding energy efficient cooperative sensing scheme is to maintain detection accuracy and efficient resource utilization to satisfy the requirements of the sustainable green cognitive radio network. Towards this end, a few of the open challenges includes the following:

1.7.1 Effect of Cooperation Overhead

Most of the existing cooperative sensing schemes focus on attaining detection performance accuracy, where all the SUs reports their sensing results to FC or to the respective nodes which results in considerable amount of energy consumption. Hence, reduction of overhead in cooperation detection has received considerable research attention. Only a few cooperation overhead issues have been discussed in the existing literature. For example, in [35], only the number of cooperative CR users and the sensing time-throughput tradeoff are considered in forming utility functions. While cooperative gain is important in the sensing scheme, proper modeling of cooperation overhead can reveal achievable cooperative gain and energy saving. In [34], only the sensor with the highest received SINR reports its decision to the center SU. This scheme is called as superior selective reporting (SSR) scheme. However, the study in [34] was restricted to the detection performance of SSR scheme, under the NP framework. The detection performance of SSR scheme under Bayesian framework is given in Appendix D [36].

Another interesting aspect related to energy efficient CSS is achieved by optimization of sensing time and/or number of sensing nodes that maximizes the energy efficiency. But energy efficiency analysis in SSR scheme is more challenging as both overhead reduction and optimization of parameters such as sensing time and number of nodes are to be considered while analyzing the energy efficiency of cooperative sensing scheme.

1.7.2 Effect of Multichannel Sensing

Apart from conventional CRN, another network where spectrum sensing is challenging is heterogeneous cognitive radio wireless sensor network (HCRWSNs) where multiple sensors are assigned to sense more than one channel. Hence, frequent scanning is required to obtain higher detection accuracy to protect the PU from the interference caused by SU [37]. However, in energy-constrained networks which are traditionally powered by batteries, frequent spectrum sensing will increase the energy consumption. Consequently, energy conservation becomes a critical design issue for HCRWSNs. Several attempts are made to reduce energy consumption by incorporating energy-harvesting based spectrum sensors. But the disadvantage is that a reduction in channel available time occurs due to the need to report all the associated local decisions to the fusion center (FC), which decreases the channel available time as the number of SUs increases. This leads to another open challenge on how to further reduce the sensing overhead and to improve the channel available time for data transmission.

1.7.3 Effect of compressed sensing in a cooperative scenario

Compressed sensing is a promising wideband, energy efficient sensing technique and is an efficient approach for energy saving in CRN scenario. However, due to the sub-Nyquist-rate sampling and insufficient number of samples, a weak PU signal with a nearby strong signal may not be properly reconstructed for detection by the SU in a wideband spectrum. Thus, it is a challenge to achieve the detection sensitivity by compressed sensing in a wide-band spectrum. Most of the existing literature aims at the signal reconstruction performance [38], or sensing performance [21, 39], but has not considered energy efficiency.

The main goal of this thesis is to analyze energy efficiency of various cooperative spectrum sensing methods based on overhead reduction, multichannel and multiuser sensing and reduction in number of sensing samples. The main contribution of this thesis is discussed in the next section.

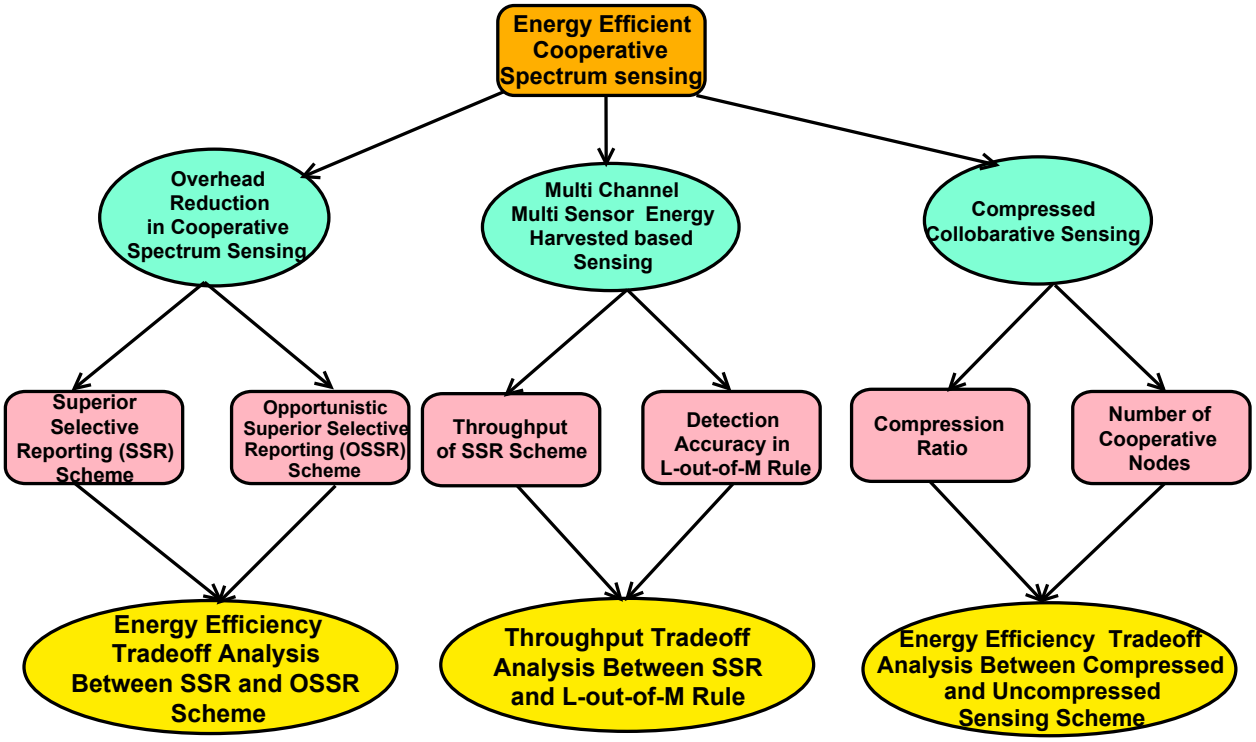

Figure 1.5. Contribution of Thesis

1.8 Contribution of the Thesis

As highlighted in Figure.1.5, based on achievable throughput, energy consumed and energy efficiency, the performances of superior selective reporting scheme (SSR), opportunistic SSR scheme, heterogeneous CR network (HCRN) and collaborative compressed sensing scheme (CCCS) for cooperative spectrum sensing in CR network are analytically evaluated and specific contributions in each of these analysis are listed below.

1. The energy efficiency of the SSR scheme is studied in terms of the detection threshold, the sensing time allocation factors denoted by β and η, and the required number of SUs for cooperation. The maximization of EE of SSR is posed as a multiple variable, non-convex optimization problem, and approximations to reduce this to a quasi-convex optimization are discussed. The accuracy of the approximation is studied. The optimal detection threshold, time allocation factors and the number of cooperative SUs are derived. Through numerical results, it is shown that the SSR scheme outperforms the conventional cooperative sensing (CCS) schemes employing the OR and AND-fusion rules.

2. Extending the analysis of selective reporting-based sensing scheme, a novel variation on the SSR scheme, namely the OSSR scheme, is proposed and analyzed following a method similar to that of SSR scheme. The tradeoff in energy efficiency performances of SSR and OSSR schemes are referred to the tradeoff between energy consumption and the achievable throughput of both the schemes. Through numerical results, it is shown that the SSR and OSSR schemes outperform the conventional cooperative sensing (CCS) schemes employing the popular OR and AND-fusion rules. In particular, it is highlighted that SSR outperforms all the other schemes in several scenarios. In other words, it is shown that minimizing the energy consumption takes a priority over maximizing the achievable throughput in a CRN, in several scenarios.

3. The average achievable throughput of an SSR-based, multi-channel HCRWSN is analyzed in terms of channel available time and detection accuracy. The problem of finding an optimal set of spectrum sensors scheduled for spectrum sensing for each channel such that the average network throughput is maximized is formulated and solved by employing the cross entropy (CE) algorithm. The advantages of the CE algorithm in contrast to the exhaustive search algorithm and a greedy algorithm are established. Through numerical results, it is shown that as the number of sensors increases, the SSR-based scheme outperforms the optimal CCS scheme in terms of average achievable throughput. A tradeoff between the average achievable throughput of SSR and CCS schemes is studied, which is the inherent tradeoff between the channel available time and detection accuracy. It was shown that as the number of spectrum sensors increases, the channel available time gets a larger priority in a HCRWSN than the detection accuracy.

4. The energy efficiency analysis of the compressed conventional collaborative sensing (CCCS) scheme for cognitive radio networks is considered, and a study on the compression limit and trade-off between the achievable throughput and energy consumption of the network is carried out. First, the expressions for the achievable throughput, energy consumption and energy efficiency of CCCS scheme are derived. Later, a multi-variable, non-convex optimization problem is formulated to find out the optimum compression level that maximizes energy efficiency, subject to interference constraints on the primary network. Approximation to reduce it to convex optimization problem is provided, and it is highlighted that the error due to these approximations are negligible. It is shown that the

energy efficiency achieved due to the CCCS scheme is higher than that of the conventional collaborative sensing scheme under the same predefined conditions. It was shown that the increase in the energy efficiency is due to the considerable decrease in energy consumption, which is especially significant with higher number of sensors.

1.9 Organization of the Thesis

The thesis is organized as follows:

- **Chapter 1:** This chapter explains the basics of cooperative spectrum sensing in cognitive radio network, steps involved in CSS and their classification. In addition, the energy efficient aspects of CSS in terms of tradeoff impact and the classification of energy-saving techniques in CSS are discussed in detail. Contribution of the thesis are highlighted in the end.

- **Chapter 2:** As an overview of methods adopted in the past to improve the energy efficiency of various CSS scheme, detailed literature review is presented in this chapter.

- **Chapter 3:** In this chapter, the EE of the SSR spectrum sensing scheme is studied, in terms of the detection threshold, the sensing time allocation factors and the required number of SUs for cooperation. The optimal detection threshold, time allocation factors and the number of cooperative SUs are derived. With a detailed numerical analysis, the performance of the SSR scheme and the conventional cooperative sensing (CCS) schemes employing the OR and AND-fusion rules are investigated.

- **Chapter 4:** Extending the analysis of selective reporting-based sensing scheme, in this chapter, a novel variation on the SSR scheme, namely the OSSR scheme, is proposed and analyzed following a method similar to that of SSR scheme. The tradeoff in energy efficiency performances of SSR and OSSR schemes are referred to the tradeoff between energy consumption and the achievable throughput of both the schemes. The performance of the SSR and OSSR schemes are compared with the conventional cooperative sensing (CCS) schemes employing the popular OR and AND-fusion rules. The advantages of the SSR and OSSR schemes are highlighted, and the performance benefits relative to conventional CSS scheme are illustrated through numerical analysis.

- **Chapter 5:** In this chapter, the average achievable throughput of an SSR-based, multi-channel HCRWSN is analyzed in terms of channel available time and detection accuracy. The problem of finding an optimal set of spectrum sensors scheduled for spectrum sensing for each channel such that the average network throughput is maximized, formulated and solved by employing the cross entropy (CE) algorithm. The advantages of the CE algorithm in contrast to the exhaustive search algorithm and greedy algorithm are established. The advantages of the SSR scheme in comparison with the optimal CCS scheme are highlighted, and the performance benefits relative to CCS scheme are illustrated through numerical analysis. A tradeoff between the average achievable throughput of SSR and CCS schemes is studied, which is the inherent tradeoff between the channel available time and detection accuracy.

- **Chapter 6:** In this chapter, the energy efficiency of the compressed conventional collaborative (CCCS) spectrum sensing scheme is studied in terms of the required number of sensors involved in collaboration and the compression ratio that satisfies a given primary user detection constraints. The tradeoff between reducing the number of samples in a compressive sensing-based measurement scheme and achievable energy efficiency of CCCS considering different signal models such as deterministic and random signal are studied. Energy efficiency improvement in CCCS scheme, when compared to uncompressed collaborative sensing scheme, are illustrated and the advantages of CCCS scheme, are highlighted through numerical analysis.

- **Chapter 7:** The outcomes of research work carried out are summarized in this chapter. Also, further improvements that can be done in this research area are listed.

Chapter 2

Literature Survey

2.1 Introduction

Spectrum efficiency and energy efficiency are two critical issues in wireless communication networks. Cognitive radio has received much research attention recently, as a promising paradigm to improve the spectrum usage efficiency [40]. Energy efficiency design is particularly important for a CR scenario, because it not only involves the greenhouse problem and operational expenditure, but it is also prerequisite to achieve high utilization of the limited transmission power consumed to support additional signal processing requirements for the CR system, such as spectrum sensing and decision reporting overhead [40]. Thus, EE has received a lot of research interest. Another important reason for considering EE as a performance metric is due to the fact that it represents the overall performance of a CR network, as it is capable of jointly taking into account the detection accuracy, the average throughput and the overall energy consumption. The combination of these factors in a single metric has made the EE as a significant metric for analyzing the quality of CR network. Moreover, optimizing the EE in CR networks not only reduces the environmental impact, but also cuts deployment costs to enable economical green wireless networks [40]. This chapter provides an overview of available research activities that are aimed at improving the detection accuracy, spectral efficiency or throughput, reducing energy consumption and improving the EE of cooperative spectrum sensing applied to CR networks.

2.2 Literature Review

The efforts made in the past to improve the performance of spectrum sensing techniques in cognitive radio in terms of detection accuracy, spectral efficiency and energy efficiency using different techniques can be grouped according to several scenarios. The classifications based on four main directions on attaining energy efficiency are listed in Table 2.1. General observations for each classification are discussed in detail in the following subsections.

2.2.1 Energy Efficient Local Spectrum Sensing Phase

Focusing on achieving EE in local spectrum sensing, an immediate and natural way of achieving energy saving is by reducing the sensing duration or employing compressed sensing irrespective of the adopted sensing method. Thus, sensing time is a critical parameter for sustaining the spectrum sensing performance. Varying the sensing time gives rise to a tradeoff between the detection accuracy and spectral efficiency. To balance the energy inefficiency of continuous spectrum sensing and the unreliability issue of periodic spectrum sensing, Gan et al. [41] optimized the sampling rate and sensing time to minimize the total sensing power across multiple channels, while maintaining the sensing reliability constraints. In [42], the authors considered spectrum sensing scheme where the SU adaptively performs spectrum sensing for either one or two periods based on the first sensing result. Specifically, this allows the SU to perform the spectrum sensing again to confirm that the PU is indeed idle when the first sensing result indicates the PU is idle, which leads to a better protection for the PU. In addition, based on the different activity level of the PU, the sensing interval can be adjusted to further improve the energy efficiency. A similar scenario was also examined in [43] where the optimization problem was formulated to optimize the sensing period using recently introduced optimization technique, namely Jaya algorithm, to maximize the discovery of spectrum opportunities while maintaining the sensing overhead and interference time within user defined value. Different from [43], the authors in [44] have investigated a cluster-based collaborative spectrum sensing scheme to maximize energy efficiency by considering optimized parameters such as the number of clusters, local detection threshold and time fraction under collision constraint and false alarm probability constraint. It was shown that there exists a unique time fraction to maximize the energy efficiency when meeting performance constraints.

Table 2.1. Energy efficient approaches in cooperative spectrum sensing

A. Energy efficient local spectrum sensing phase			
Features	**Advantages**	**Disadvantages**	**References**
Sensing time optimization	• Reduction in energy consumption	• Decreased detection performance	[41]-[44]
Detection threshold optimization	• Processing load reduction in each sensing node • Optimization of sensing time	• Incorrect threshold selection may affect sensing reliability	[45]- [49]
Reduced number of samples	• Processing load reduction • Reduced data to send and process • Shorter sensing time	• Less reliable sensing • Good for non-sparse signal	[50]-[55]
Energy harvesting nodes	• Do not require battery backup. • Better energy utilization	• If energy harvesting is based on solar power, it is unpredictable source of energy.	[56]-[57]
B. Energy efficiency by overhead reduction			
Features	**Advantages**	**Disadvantages**	**References**
Sensing node selection	• Reduction in the number of sensing nodes • No energy consumption by inactive nodes • Quality of the reported message can be improved by proper selection of the reporting node	• Detection accuracy degradation • Additional data acquisition is required for proper selection of reporting nodes	[58] -[63]
Reporting node selection	• Quality of the reported message can be improved by proper selection of the reporting node	• Additional data acquisition is required for proper selection of reporting nodes	[30][64]
Censoring of reports nodes	• Censoring of faulty or malicious nodes • No energy consumption for reporting by censored nodes • Reduction in number of reporting nodes	• Faulty censoring process may lead to wrong decision • Finding the analytical thresholds for censoring is hard	[65],[66], [67]
Voting scheme	• Reduced number of control messages • Low demand for additional data (nodes, SNR, location)	• Malicious nodes may affect performance	[68]-[71]

Table 2.1 (*Continued*)

C. Energy efficient fusion and decision rule			
Features	**Advantages**	**Disadvantages**	**References**
Selection of fusion rule	• Fusion rule decides the type and nature of reporting information send to the fusion center • Fusion rule can be selected depending on the required QoS	• Cooperative nodes has to be updated for every change of the fusion rule	[72], [73]
Soft/Hard reporting	• Depending on the transmission rate soft or hard decision reporting can be chosen • Adaptation of the traffic related to data reporting	• Tradeoff between the accuracy of each report and amount of data volume needed to deliver	[74],[75], [76]
Selective decision reporting	• Reduction of traffic overhead	• Negative effect on accuracy of detection report delivered to the fusion center	[74]
D. Energy efficient network organization			
Features	**Advantages**	**Disadvantages**	**References**
Multichannel heterogeneous network	• Multiple channels will be available which enhances the throughput when compared to conventional network	• CSS should be implemented over several channels to increase the number of available channels which increases the complexity • Detection within a minimal time bound over multiple channels is a challenging problem	[77]- [80]
Relay-based network	• Reduction of the transmit power of the reporting node due to shorter distance	• Due to processing of information from other nodes, energy consumption in relaying node is increased • Data delivery to the fusion center causes additional delay	[81]-[82]
Cluster-based network	• Shorter transmission link enhances energy saving	• Delay in sharing sensing report • Additional overhead in cluster heads selection and organizing nodes into clusters	[83]- [88]

Energy efficiency may be further enhanced by compressed sensing (CS) which was recently proposed to reduce the sampling rate below the Nyquist rate, without a significant loss in

the performance [50]. The energy consumption in spectrum sensing, mainly caused by the analog-to-digital converter (ADC), is proportional to the sensing time duration and the sampling rate [51, 52]. However, at any instance of time, only a small subset of channels are occupied by PUs, making the wideband spectrum sparser in the frequency range. Such sparsity of wideband spectrum is taken as an advantage in compressed sensing (CS). Thus, when compared to the conventional wideband spectrum sensing, compressed sensing reduces the sampling rate at the sub-Nyquist rate [54, 89] which further reduces the sensing time duration and greatly favors energy saving. For this reason, the CS-based spectrum sensing methods have been proposed as an efficient approach for improving the energy efficiency [55] in cognitive radio network. Despite its attractiveness as an energy efficient technique, compressed sensing suffers from a few major drawbacks which limit its applicability in practice. A CS based sensing scheme incurs a certain performance loss due to compression, when compared to the conventional sensing scheme while detecting non-sparse signals. This performance degradation can be seen as a loss in the detection performance to improve the energy efficiency. Thus, to compensate the performance loss due to compression, the authors in [53] proposed a collaborative compressive detection (CCD) framework in which a group of spatially distributed nodes sense the presence of PU independently and send a compressed summary of observations to the fusion center (FC) where a global decision is made. It was shown that through collaboration the performance loss due to compression can be recovered. However, the study [53], did not consider energy efficiency and was restricted to the detection performance of CCD, where it is evident that an increase in either the compression ratio (c) (keeping number of collaborative nodes N fixed) or the N (keeping c fixed)decreases the probability of error exponentially.

Another possibility of improving the EE is to optimize the sensing threshold. In [45–47] the authors investigate the effects of detection threshold optimization for a fixed sensing time which may result in contradictory goals. However, joint optimization of sensing durations and detection thresholds of SUs is necessary for finding a spectrum hole effectively. It was shown in [48] that the joint optimization of sensing parameters such as detection threshold and sensing time can considerably improve system performance to detect a spectrum hole. This work was then extended to the case for minimization of the average detection time as well as joint maximization of the aggregate opportunistic throughput in [49]. Specifically, the joint optimization approach can considerably improve system performance in terms of the mean time to detect a spectrum hole

and also the aggregate opportunistic throughput of both primary and secondary users, relative to the scenarios where only a single sensing variable is considered.

Yet another way of achieving energy efficiency in local spectrum sensing is energy harvesting by local sensing nodes, which manages to improve both channel utilization and meet the requirement of green communications [56],[90]- [93]. It has been shown that combining energy harvesting (EH) techniques with CR can simultaneously improve the spectrum efficiency and energy efficiency [94, 95]. Moreover, powering the mobile devices by harvested energy [96] from ambient sources and/or external transmission activities makes the wireless networks to be self-sustaining for a longer duration. More recently, the radio frequency (RF) powered CR networks [97, 98] have been proposed and studied for CR, where a CR transmitter harvests energy when the primary user is present, and utilizes it for the data transmission when the spectrum is vacant. This protocol is known as the harvest-then-transmit (HTT) mode [99, 100]. A major disadvantage with this functionality is the drastic reduction in secondary throughput when the harvested energy is low and/or when the data transmission time is less. To overcome this drawback, the concept of simultaneous wireless information and power transfer (SWIPT) was introduced [101], which has attracted significant research attention ever since [57],[102]. In 5G communication systems, the SWIPT technology can be of fundamental importance for energy and information transmission across CR networks.

2.2.2 Energy Efficiency by Overhead Reduction

The strength of the cooperative solutions, which reflects in the recorded observations, lies in the diversity offered by multiple nodes operating at different locations and in a variety of channel conditions [20]. However, incorporating a large number of sensing devices consumes more power, and results in only a small fraction of detection improvement. Naturally, reducing the number of active nodes may result in a small overall probability of detection. Therefore, choosing the right number of nodes is a way to the improve energy efficiency. This choice depends on the node selection criterion to reduce the energy consumption with an acceptable constraint on performance degradation. To address this issue of reducing the cooperative overhead, while simultaneously taking advantage of cooperative sensing, the authors in [58], proposed a two-step spectrum sensing scheme, where only one or a few selected sensors are involved in the first step,

but the second step occurs for cooperative sensing when the outcome of the first step is uncertain to make a decision in the presence of PUs. This enhances the probability of detection and reduces consumed energy as well as communication overhead, within a reasonable sensing time. Sensing overhead generally degrades the throughput performance. The prior work, to resolve this problem, proposed algorithms either to decrease the time spent in sensing or to decrease the number of SUs participating in sensing. In [59], the authors proposed a joint resource allocation (RA) strategy considering the time and energy consumed for spectrum sensing to maximize the throughput while satisfying the target detection performance. Furthermore, to reduce the additional resources used in spectrum sensing, the right censored order statistics-based cooperative spectrum sensing scheme is adopted, which produces the criterion for deciding the set of reporting SUs. By jointly designing the time and energy for sensing, the proposed joint resource allocation scheme in [59] provides the improvement of spectral efficiency. In the context of extending the life time of a network, ON/OFF mode of each sensors can be scheduled in a cooperative manner. However, frequent ON/OFF switching of sensor nodes will generate an adverse impact and makes the network vulnerable and unreliable. Thus, optimizing the scheduling order to reduce the switch frequency using greedy heuristic algorithm is proposed in [60] to obtain the minimum node switch with low computational complexity.

However, [58–60] foresee that all SUs report their sensing results to an FC, as similar to the CCS scheme, leading to considerable energy consumption. Hence, reduction of overhead in cooperative detection by selective reporting has also received considerable research attention [69, 103, 104]. In [69], reporting SUs were chosen based on the best individual detection performance. The best sensor set selection scheme was proposed as a non-cooperative game in [104]. A key feature that these works highlight is that the energy inefficiency occurs due to the need to report all the local decisions to the FC, which increases linearly with the number of SUs [105, 106]. Reduction in the sensing overhead was successfully mitigated in a spectrum sensing (SS) strategy discussed in [34], where a network of N sensors carry out SS along with a center SU, but cooperation is employed only when the center SU decides that the spectrum is vacant. That is, only the sensor with the highest received SNR reports its decision to the center SU. This scheme is termed as superior selective reporting (SSR) scheme. However, the study in [34] was restricted to the detection performance of SSR, where it was shown that the SSR achieves a larger probability of detection compared to the case where FC employs OR fusion rule.

A slight variation on the above mentioned work is the censoring algorithm, in which only selected nodes are permitted to transmit their sensing report, which saves energy during the reporting stage. Furthermore, the censoring scheme is more consistent when compared to the node selection-based sensing scheme, because the censoring of nodes are done after performing spectrum sensing by individual nodes.

Censoring scheme based on the double-detection threshold was proposed in [107] to reduces the transmission overhead between CR and FC without significantly affecting the receiver operating characteristics. The performance of the above mentioned CR network has been assessed in terms of the average number of normalized transmitted sensing bits, the total error probability and the optimal number of CR users that ensures minimum error probability, where it was shown that the censoring probability saturates rapidly for an average number of nodes and is independent of the number of CR nodes leading to low energy consumption [20]. Further investigation on censoring was proposed in [67], under the constraints on minimum false alarm probability and maximum detection probability, where censoring and sleeping are adopted. Moreover, a detailed analysis in [67] on energy consumption in the network based on sleeping rates and optimum censoring demonstrates that these values complement significant increase in energy savings.

In previous works, efficient node selection criterion is based on the estimated SNR, probability of detection and correlation to name a few. In [62] and [63], the criterion of efficient node selection is based on the observed SNR. User selection based on uncorrelated decisions across SUs was employed in [103], where a dedicated error-free channel was assumed for reporting individual sensing results. In practical scenario, it is to be noted that, proper estimation of SNR is not always possible. Moreover, interchanging messages to find the specific SNR value may not be energy efficient. Hence, in [68, 71] the voting scheme is proposed based on the sensing result of own decision of the FC, and the global decisions. The voting schemes introduced in [68], called the confidence voting, work on limiting the unreliable decision transmissions by demanding each node to compute a confidence metric. The local and global decisions are collated in a hard decision scenario whereas in the case of co-incidence scenario, the confidence metric is incremented or decremented [20]. The confidence metrics are computed during the training period and only the nodes with the highest confidence metrics are allowed to report their decisions to the fusion center. The authors in [68] claim 40% energy saving for confidence voting algorithm. Yet another voting scheme presented in [69] is called the collision detection scheme which is

based on node selection with the highest correctness measure. The correctness measure signifies the number of times a node gives correct decisions when the global false decision is that the PU is not absent. Cooperative sensing involves the nodes with the highest correctness. The main advantage of the voting-based scheme is that it requires limited number of control messages which reduces the sensing overhead. Since these voting-based scheme relay on the opinion of the majority, they have a major drawback especially in a scenario where the most of SUs face a bad channel condition between the PU and themselves. In such scenarios, the FC votes for the decision of unreliable nodes with a larger confidence resulting in a decision worse than the conventional scheme. Moreover, the presence of malicious SUs can degrade the performance of voting based schemes.

Most of the above mentioned work on overhead reduction in CSS have considered throughput enhancement or energy consumption reduction separately. On the otherhand, it is essential to consider EE as a comprehensive metric which is capable of jointly taking into account the achievable throughput, the overall energy consumption and the detection accuracy. Hence, studying the performance of a CR network based on EE is essential.

2.2.3 Energy Efficient Fusion and Decision Rule

Another approach to reduce energy consumption is to optimize the fusion rule which may decrease the energy consumption to a greater extent. Hard and soft decision are the two types of decisions, transfered from nodes to FC. The performance analysis and comparison of hard and soft decision based approaches for the cooperative spectrum sensing in the presence of reporting channel errors was carried out in [72], where the soft decision combination is proved to be more robust to channel impairments. However, in [72], the associated complexity and transmission overhead are not considered. The energy consumption and detection probability of fusion rules such as likelihood ratio rule (LR), maximum ratio combining rule (MRC) and equal gain combining rule (EGC) under parameters such as frame length for each rule, number of nodes and SNR are analyzed in [108]. The results exhibits a better performance for EGC in both energy saving and detection probability for a short frame length, less number of nodes and low SNR. Energy efficiency maximization by optimizing number k in the k-out-of-N fusion rule together with detection threshold is proposed in

[73]. The obtained results presents that the joint optimization of number of users and the decision threshold, can achieve an energy efficiency of 2 bits/Hz/Joule for various SNRs.

Soft decision combining schemes provide optimal detection performance by combining the actual sensed information from the SUs, resulting in a high cooperation overhead in terms of time, computational complexity, and bandwidth. Alternatively, hard decision combining schemes offer lower cooperation overhead, but achieves sub-optimal detection performance. In order to utilize the advantage of both soft and hard decision-based cooperative sensing, combined hard/soft decision-based CCS scheme is presented in [74–76]. The authors in [74] proposed a method based on the log-likelihood ratio (LLR) based cooperative spectrum sensing scheme with hard-soft combining at the fusion centre (FC), where the SUs perform a local LLR-based detection employing two thresholds. If the locally sensed information falls in between the two threshold values, then the actual sensed information is reported to the FC and weighted soft combining is performed at FC, else the local binary decisions are reported to FC and hard combining is performed. Further, a second stage hard combining employing AND/OR rule is performed at FC considering the previous decisions. The authors concluded that the proposed scheme gives a near optimal performance with a slight increase in the cooperation overhead.

2.2.4 Sustainable Cognitive Wireless Sensor Networks

The limited power available with each sensor in a WSN usually results in a short life time of WSNs, which directly affects the sustainability of network. Some solutions are proposed in the literature to enhance the sustainability, by employing efficient data transmission in a WSN. Wang et al. [109] proposed a time adaptive schedule algorithm (TASA) for data collection from WSN to cloud along with a minimum cost spanning tree (MST)-based routing method to save on the transmission cost. They showed that their proposed method considerably reduces latency and optimizes energy consumption, which makes the sensor-cloud pair sustainable. To prolong the network life time, a sustainable WSN has been considered in [110] from the perspective of energy-aware communication coverage, where the two types of sensor nodes, namely, energy-rich nodes (ERN) and energy-limited nodes (ELN) are deployed. Throughput-optimal resource allocation policy design for sustainable energy harvesting-based WSN (EHWSN) has been widely addressed in [111] and [90]. Xu et al. [111] investigate the utility-optimal data sensing and transmission in

an EHWSN, with heterogeneous energy sources such as power grids and utilizing the harvested energy. They also analyzed the tradeoff between the achieved network utility and cost due to the energy utilized from the power grid. Zhang et al. in [90] developed an optimization framework to guarantee sensor-sustainability in the EH-based CRN (EHCRSN), where the parameters such as stochastic energy harvesting, energy consumption, spectrum utilization and spectrum access processes are designed in an optimal way. An aggregate network utility optimization framework based on a Lyapunov cost-based optimization was developed for the design of online energy management, spectrum management and resource allocation. They also demonstrated that the outcome of the work can be used as a guide for designing a practical EHCRN, which guarantees PU protection and sensors sustainability at the same time. However, note that these existing methods only offer sustainability of network and are unable to effectively ensure the balance between overall performance, reduction in overhead and network resource utilization.

2.2.5 Sensor Scheduling

Energy-aware sensor scheduling in WSN has also attracted significant research attention. In [112], the authors proposed a new priority-based traffic scheduling for CR communication on smart grids, considering channel-switch and spectrum sensing errors, and a system utility optimization problem for the considered communication system was formulated. Such a scheduling scheme was shown to serve as a new paradigm of the future CR-based smart grid communication network. More recently, in order to avoid large overhead and delay, smart scheduling of a collaborative sequential sensing-based wide band detection scheme was proposed in [113] to effectively detect PU activity in a wide band of interest. A sensor selection scheme was proposed in [69] to find a set of sensors with the best detection performance for cooperative spectrum sensing, which does not require a priori knowledge of the PU SNR. The throughput of the CR network is optimized in [114], by scheduling the spectrum sensing activities based on the residual energy of each sensor. Liu et al. in [114] proposed an ant colony-based energy-efficient sensor scheduling algorithm to optimally schedule a set of sensors to provide the required sensing performance and to increase the overall CR system throughput. It was demonstrated that the proposed algorithm outperforms a greedy algorithm, and the genetic algorithm, with a lower computational complexity. However, the sensors employed in the above system model are energy-constrained

battery powered sensors and not sensors equipped with energy harvesting. These scheduling strategies do not specifically consider the tradeoff between network performance and resource spectrum utilization in a CR-based WSN. Moreover, the overhead of network resources caused by the cooperative sensing strategies is not accounted for in the existing methods, which is a key factor. Thus, the problem of sensor scheduling in a CR-based WSN needs to be considered in terms of a collective network utility and efficiency performance.

2.2.6 Energy Efficient Network Organization

With vastly increasing wireless traffic demands, realization of a HWSN suffers from disadvantages such as severe interference [115], which affects its spectral efficiency. A heuristic solution to mitigate this problem is to integrate the cognitive radio (CR) technology [2] with HWSN [116], collectively termed as heterogeneous cognitive radio wireless sensor networks (HCRWSN) [117]. In an HCRWSN, the deployed sensors periodically scan a primary user spectrum to detect the availability of vacant channels and the network assigns data transmission over them, while guaranteeing a given PU interference level [118]. However, the periodic sensing increases the energy consumption, which is a critical issue in battery operated sensor networks. Therefore, an HCRWSN with energy harvesting spectrum sensors [119] has been proposed to enhance both spectrum and energy efficiencies [77–79].

A new spectrum sensing scheme based on spatial-temporal opportunistic detection is proposed in [120], in which a 2D cognitive wireless sensor network (CWSN) topology model is employed. It was shown that the proposed scheme not only has a desirable property to process the spectrum-heterogeneous problem in spatial-temporal 2D sensing environment but satisfactory detection performance can be achieved with less energy consumption as well. By jointly considering the constraints on sensing accuracy, efficiency and overhead, which are quantitatively characterized by the energy consumption, multi-channel CSS strategies, are modeled in [37] to maximize the aggregate opportunistic throughput of SUs. It was demonstrated that optimal CSS scheme is effective in improving channel utilization for SUs with low interference to PUs.

A multiband cooperative spectrum sensing and resource allocation framework for the internet-of-things (IoT) in cognitive 5G networks can significantly reduce energy consumption

for spectrum sensing compared to the conventional single-band scheme. Towards this end, an optimization problem was formulated in [121] to determine a minimum number of channels to be sensed by each IoT node in the multiband approach to minimize the energy consumption for spectrum sensing while satisfying probabilities of detection and false alarm requirements. Moreover, a cross-layer reconfiguration scheme (CLRS) for dynamic resource allocation was proposed in IoT applications with different quality-of-service (QoS) requirements including data rate, latency, reliability, economic price, and environment cost. The proposed scheme, i.e., CLRS, efficiently allocates resources to satisfy QoS requirements through opportunistic spectrum access. In order to increase the detection probability in weak channel conditions, the neighboring nodes cooperate with each other which includes relaying the sensing messages by another node to the FC or to a selected node [81],[122, 123]. In [124], an optimization framework for a wireless sensor network is given whereby, the optimal relay selection and power allocation are performed subject to signal-to-noise ratio constraints. The proposed approach determines whether a direct transmission is preferred for a given configuration of nodes, or a relay-based cooperative transmission should be used. An energy-efficient power allocation for orthogonal frequency division multiplexing (OFDM) based relay-aided cognitive radio networks with imperfect spectrum sensing is considered in [82], where the authors show that the proposed algorithms can obtain a good tradeoff between energy and capacity of the network. In [123], energy-efficient cooperative spectrum sensing with relay switching over Rayleigh fading channels is proposed and analyzed. By not activating all the available relays at all time, power and transmission resources of the relays are saved. In the first scheme, when relaying is activated, a switch-and-test (SWT) policy based on the energy received from the relaying path is used. To enhance the detection performance of SWT, in the second scheme, a switch-and-selection-test (SST) policy is considered. Both SWT and SST schemes integrate the relay switching and spectrum sensing into one step, which further saves the power and time of relay processing.

Solution proposed in [83, 84], for energy consumption minimization is cluster and forward scheme, where the nodes are dynamically placed in cluster groups. The node with the best channel gain, in each group, is opted as the cluster head. In [87], a cluster-based MAC protocol is designed in which channel sensing scheme is analyzed to reduce the total consumed energy. It is shown that there is a correlation between the number of sensed channels and EE, and the best overall performance is guaranteed by cluster-based sensing for three channels. A cluster-based

collaborative spectrum sensing scheme from the energy efficiency perspective is analyzed in [88], by considering optimization parameters like the number of clustered CSs, local detection threshold and time fraction to maximize the energy efficiency under collision constraint and false-alarm probability constraint.

In this section, the key CSS aspects to maximize energy efficiency were identified. However, optimization of one parameter increases the detection performance but generally at the expense of computational complexity. Therefore, the effect of enabling energy efficiency in CR network can be analyzed from a fundamental tradeoff perspective which is elaborated in the next section.

2.2.7 Fundamental Tradeoffs in CR Networks

This section discusses the ways of achieving higher energy efficiency in CR networks from a fundamental tradeoffs perspective to achieve a large energy efficiency (EE). In view of EE, the tradeoffs identified are listed in Table 2.2 as QoS, PU interference, overhead, throughput, energy consumption, cooperative gain and security, which are the critical network design dimensions. These tradeoffs are analyzed focusing on the energy efficiency.

2.2.8 Energy Efficiency vs. Quality of Service Trade-off

Mechanisms to improve the QoS may contradict the requirements of the EE. Moreover, there are other complicating factors such as interference limitations, power budget of the CR system, and imperfect channel sensing which are inherent in nature, are to be considered in a CR network [1]. Hence, this tradeoff issue is prominent while allocating resources for CRNs [125]. QoS for CRNs have been examined from an opportunistic spectrum access (OSA) perspective and it is observed that disruptions from SUs or PUs involved in OSA protocols cause challenges in QoS deployment. In this regards, the QoS can be realized in three directions, namely,

- PU centric approach
- SU centric approach
- Hybrid approach

Table 2.2. Fundamental tradeoffs for energy efficiency in cognitive radio networks [1]

Tradeoff	Description	Reference
Energy efficiency vs. QoS tradeoff	• EE requirement may be contradictory to the QoS improvement mechanisms	[125]
Energy efficiency vs. PU interference tradeoff	• Frequent sensing increases the energy consumption and causes higher overhead but improves the sensing performance, which is of major concern for tuning the EE vs. PU interference tradeoff	[126]
Sensing vs. Throughput tradeoff	• Maximizing sensing accuracy may be contradictory to enhancing the network throughput	[127]-[129]
Overhead vs. Throughput tradeoff	• More sensing overhead for SUs, the less throughput the CR network can achieve.	[130]
Spectral efficiency vs. energy efficiency tradeoff	• SE improvement due to the involvement of multiple SU nodes, leads to reduction in EE.	[93], [131]- [134]
Energy efficiency vs. security tradeoff	• Integration of security protocols in CRs results in additional overhead at both the transmitter and the receiver which affects the EE of the network due to increase in energy consumption.	[135],[136]

PU centric approach focuses to protect the QoS of PUs while employing OSA. In this scenario, reduction of miss detection probability is very important and EE dimension is not critical [1]. Hence, the main constraint is not to disturb the incumbent users while retaining QoS. The second approach, SU centric QoS, is where the environment is divided by prioritizing the SUs while safe guarding the PUs. In this scenario, the solution space of the problem becomes larger as the interference limitations are relaxed. In this approach, the objective is to reduce the false alarm probability as much as possible. For both of the above approaches, the specific detection accuracy can be attained by improving either sensing time and sampling frequency or SNR. Increasing the sensing time is the only viable solution as the PU's SNR is beyond the control of the CRN, and the sampling frequency is device-dependent. However, the periodic nature of sensing results in more energy consumption of the network. The third approach, hybrid approach, a natural extension of PU centric approach and SU centric approach, is to have a hybrid situation where the QoS of the PUs and SUs are evaluated in a more flexible manner and not differentiated categorically.

2.2.9 Energy Efficiency vs. PU Interference Tradeoff

The CR operation's fundamental constraint is that the secondary users must not cause harmful interference to the primary user communication. In other words, the resulting interference due to SU transmission at nearby PUs must be well below the tolerable interference limits for underlay CRNs, and the simultaneous transmission time with the PUs must be considerably short for overlay CRNs [1]. Two scenarios which causes interference to PU are: misdetection of PU and reappearance of PU. To deal with the first scenario, the CRs must have high detection accuracy (P_d) which reduces the probability of collision with the PU. This demands for a high P_d, which can be attained using various techniques such as longer sensing duration, cooperative sensing and higher sampling frequency. But these high detection accuracy solutions may lead to higher energy consumption. In the reappearing PU scenario, due to the nature of periodic sensing, the CR network may interfere with the PU network irrespective of the achieved high detection accuracy. In the periodic sensing, a reappearing PU does not get detected until the next sensing period. But frequent sensing increases the energy consumption and sensing overhead which directly affects the throughput. Hence, EE vs. PU interference tradeoff puts forward a challenge to decide on the sensing and transmission durations [126]. To cope up with these two scenarios, a CR may choose to be conservative at the sensing phase and/or at the transmission phase of the cognitive cycle. The solution to address this challenge is to adjust the sensing accuracy and the sensing duration by considering the PU traffic pattern [126] and at the transmission phase the solution is to control the interference by regulating the transmission power.

2.2.10 Sensing vs. Throughput Trade-off

The sensing slot duration is a critical parameter for maximizing the achievable throughput for the secondary users under the constraint that the primary users is protected to a sufficient level. The average sensing time should be designed such that the secondary user by maintaining certain level of detection accuracy can find at least one available out-band channel which improves its throughput [137]. Based on this fact, a collision-throughput tradeoff problem was formulated in [127] based on the sensing time requirement and the traffic pattern of primary users to find optimal value for the frame duration of CR operation so that the throughput of the CR network

is maximized. It was shown that there exists an optimal frame duration for a given sensing slot duration to obtain the best tradeoff. Similar sensing throughput tradeoff analysis was carried out in [128] to maximize both detection accuracy and EE of a CR network. Another adaptive spectrum sensing scheme is formulated based on the first sensing result to provide better protection for PU. In other words, when the first sensing result indicates the idle status of PU, the SU performs spectrum sensing once again to reconfirm the availability of spectrum band. This adaptive sensing scheme maximizes the energy efficiency in an energy-constrained CR sensor networks, by adjusting the sensing duration according to the PU activity. The study in [128], confirms that the proposed scheme improves both the spectrum sensing performance and the EE compared with other existing methods. Imperfect spectrum sensing and multi-channel access contention impacts the tradeoff between the interference to PUs and throughput achieved by the SUs. Imperfect spectrum sensing and multi-channel access contention are jointly considered in [129] in which the sensing-throughput tradeoff problem is formulated by taking the interference probability as the optimization constraint. It was concluded that the throughput performance of SUs can be improved significantly by relaxing the requirement of sensing reliability. Moreover, it was demonstrated that the throughput performance of SUs when the realistic multi-channel scenario is taken into account is worse than the single-channel scenario.

2.2.11 Overhead vs. Throughput Tradeoff

Cooperative spectrum sensing is a viable sensing technique to enhance the spectral utilization efficiency of SUs while ensuring the quality of service of PU. Intuitively, the more SUs are involved in sensing, the more sensing accuracy the CR can be achieved, whereas the more sensing overhead the SUs consume, the less throughput the CR network can achieve. Towards this end, the authors in [130] investigated overhead-throughput tradeoff over Rayleigh-fading channels in a cooperative CR network that consists of a number of the SUs employing energy detectors and a single decision fusion center. Considering the tradeoff, the authors proved that there is an optimal set of the sensing length and the number of SUs that maximize the throughput of an SU network.

2.2.12 Spectral Efficiency vs. Energy Efficiency Trade-off

Increasing spectrum-efficiency (SE) as well as energy efficiency (EE) has attracted much attention recently due to the fact that the future wireless networks needs to address the issues of high throughput and low power consumption. However, the objective for optimizing SE sometimes conflicts with the one for optimizing EE, and the methods for improving EE may result in a decrease in SE [131, 132]. The authors in [93], analyzed the problem of joint optimization of sensing duration and decision threshold by maximizing EE while satisfying SE requirement. The tradeoff between SE and EE was also illustrated. But the conventional CSS model was considered for the analysis which increases the sensing overhead as the number of SUs increases. A general framework to evaluate the tradeoff between energy efficiency and spectral efficiency in three cognitive radio networks paradigms, namely underlay CRNs (UCRNs), overlay CRNs (OCRNs), and interweave CRNs (ICRNs), was proposed in [134]. It was shown that the ICRN can achieve the best SE and the UCRN can achieve the best EE, under the same transmission requirements. Different from [134], a CR framework is developed in [133] to study the secure SE and EE in underlay random CR networks. A joint secure SE-EE optimization problem was formulated with a tradeoff factor which provides the optimal transmission power and intensity of the SU transmitters. It is proved that with an increase of the preference for secure SE, a relatively large transmission power and/or intensity are preferred to jointly maximize the secure SE and EE, and with the increase of the intensity of eavesdroppers, a relatively small transmission power and/or a relatively large intensity are preferred to jointly maximize the secure SE and EE.

2.2.13 Energy Efficiency vs. Security Trade-off

The effect of multiple malicious users on the energy efficiency of a cognitive radio network was studied in [135], in which low-overhead security protocol is proposed to address spectrum sensing data falsification (SSDF) attacks under a tradeoff between energy efficiency and security. Based on the analytic study in [135], the optimal number of security bits required to maximize energy efficiency is provided. From the perspective of EE, considerable improvement was shown. Furthermore, it was shown that optimal number of bits depends explicitly on the selected fusion rule, the number of malicious users and the number of legitimate users.

A similar study was conducted in [136] to find an optimal length of message authentication code (MAC) and an optimal number of cooperative SUs to maximum EE, which is a promising solution to avoid SSDF attack. It was shown that the cooperative spectrum sensing scheme based on MAC can resist SSDF attacks as well as improve energy efficiency.

2.3 Chapter Summary

In this chapter, the various methods to increase the EE of cooperative spectrum sensing have been analyzed. The main points from the literature survey are summarized as follows.

1. Even though several aspects of CSS which can be subject to optimization are identified in the literature previously, the key challenges in accurate EE modeling and optimization for CSS network arises from the fact that there exist a plethora of elements that have to be considered in the optimization process.

2. Optimization of any one parameter increases the reliability of detection at the expense of computational complexity which further increases the energy consumption.

3. To develop an energy efficient cooperative sensing technique, the overhead in cooperative sensing has to be reduced without compromising the detection accuracy, so that such cooperative sensing scheme can be utilized in energy constrained environment.

4. Efforts have been made to improve the performance of CSS with respect to throughput, energy consumption and energy efficiency. Conventional cooperative sensing scheme is replaced by the node selective-based sensing scheme which has shown an improvement in the detection accuracy. Although these techniques have shown improvement in the detection performance, the analysis of energy efficiency in node selective-based CSS with optimization of parameters such as detection threshold, sensing time and number of nodes involved in cooperation has not been explored in the literature.

5. Most of the existing literature focus on methods to improve the detection accuracy or perfect reconstruction of the received signal after compressed spectrum sensing. Although the compressed sensing-based cooperative sensing scheme has been analyzed in terms of

detection errors, energy efficiency analysis of compressed collaborative sensing scheme by optimizing compression ratio and number of nodes has not been explored in the cooperative sensing framework. In other words an important question that remained unanswered is as follows: For a given compression ratio, $\mathtt{c}$, what should be the number of nodes N, to maximize the energy efficiency?

In this thesis, many of the above questions are successfully answered and a study to improve the performance of cooperative spectrum sensing in CRN in terms of average achievable throughput, energy consumption and energy efficiency is presented. To start with, the idea is to improve energy efficiency by reducing the cooperative overhead and maintaining the detection accuracy simultaneously. Towards this end, in the next chapter, an analysis of energy efficiency using superior selective reporting-based cooperative sensing scheme by optimizing detection threshold, sensing time and number of nodes involved in sensing such that the energy efficiency is maximized.

Chapter 3

Energy Efficiency Optimization for Superior Selective Reporting-Based Spectrum Sensing

3.1 Introduction

In this work, the EE analysis of the SSR scheme proposed in [34] are presented by deriving the expressions for energy consumption and achievable throughput of the SSR scheme. EE optimization problem is formulated subjected to several constraints. As this problem is highly non-convex, some approximations to reduce it to a quasi-convex optimization problem are presented. Later, it is highlighted that these approximations are sufficiently accurate. The motivation to consider the SSR scheme is threefold. Firstly, it saves the sensing overhead to a considerable extent, particularly when the probability of detection of the center SU is high. Secondly, this scheme does not require a dedicated control channel to forward the decision. Finally, since all the SUs do not report their decisions, interference to PU system is reduced, when compared to the conventional cooperative sensing (CCS) scheme. EE of the SSR scheme has not been considered earlier in the literature. In this work, note that the reporting channels is assumed to be error-free for analytical simplicity and does not consider the impairments such as

dispersiveness in the reporting channels [138].
The main contributions of this work are as follows:

- The EE of the SSR spectrum sensing scheme is studied, in terms of the detection threshold, the sensing time allocation factors and the required number of SUs for cooperation.
- The maximization of EE of SSR is posed as a multiple variable, non-convex optimization problem, and approximations to reduce this to a quasi-convex optimization are discussed. The tightness of the approximation is studied.
- The optimal detection threshold, time allocation factors and the number of cooperative SUs are derived.
- Through numerical results, it is shown that the SSR scheme outperforms the conventional cooperative sensing (CCS) schemes employing the OR and AND-fusion rules.

The remainder of this chapter is organized as follows. The system model and review the CCS and SSR schemes is presented in Sections 3.2, 3.2.1and 3.2.2 respectively. Performance analysis of CCS and SSR scheme are provided in 3.2.3. The energy efficiency optimization problem for the SSR scheme is proposed in Section 3.3, and approximations, reformulation and analysis are provided in Section 3.4. Results and conclusions are provided in Sections 3.5 and 3.6 respectively.

3.2 System Model

Consider a cognitive radio (CR) network depicted in Figure 3.1, with N co-located nodes (denoted by $C_1, \ldots, C_N$), that carry out spectrum sensing to exploit the under-utilization of the licensed band of a primary transceiver pair, denoted by (PU_{tx}, PU_{rx}), opportunistically. A separate CR fusion-node also called as a secondary user (SU) – which aims for an opportunistic communication at a given time is labeled as the center SU, and is denoted by F. The individual CR nodes $C_1, \ldots, C_N$ carry out energy-based spectrum sensing, and their decisions are used in a co-operative manner by the center SU, which will be explained in detail later. The PU signal is assumed to be a complex-valued PSK signal and the noise to be circularly symmetric Gaussian random variable with variance σ^2 [137]. Let h_{C_iF} and h_{PF} denote the fading coefficient of the channel from C_i,

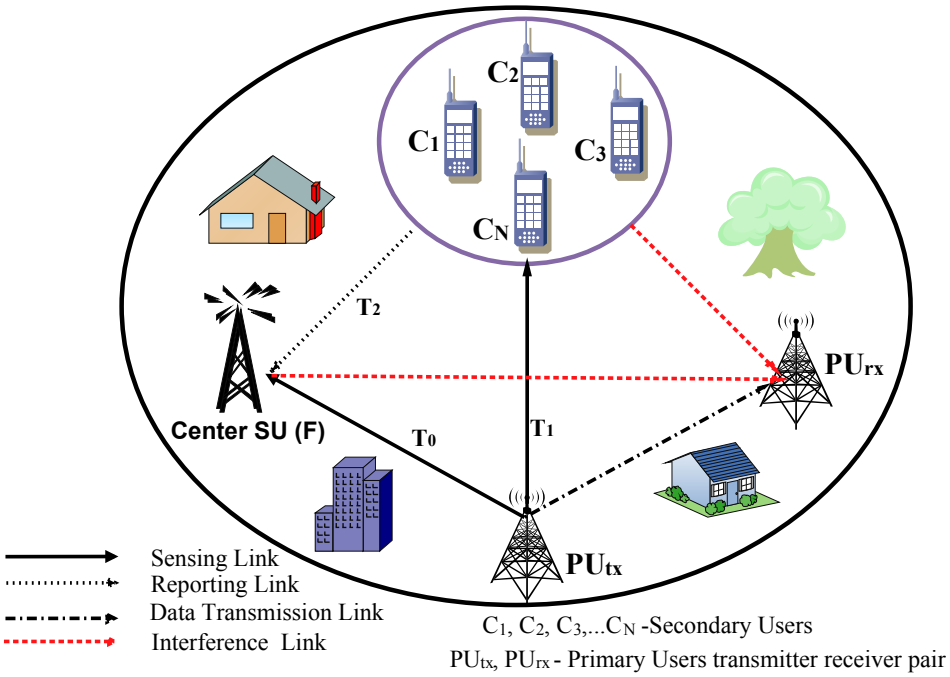

Figure 3.1. System model for Superior Selective Reporting (SSR) Scheme

$i = 1, \ldots, N$ to the center SU(F), and PU_{tx} and center SU, respectively. Let γ_{C_i} and γ_P denote the signal-to-noise ratio (SNR) over the link from the CR node C_i, $i = 1, \ldots, N$ to the center SU and the link from PU transmitter PU_{tx}, to the center SU respectively. Without loss of generality, it is assumed that, at a given time, the center SU has a perfect knowledge of noise variance σ^2, h_{C_iF}, h_{PF}, γ_{C_i} and γ_P [34]. Next, the superior sensing based reporting schemes and the conventional cooperative sensing schemes are revisited.

3.2.1 Conventional Cooperative Sensing (CCS) Scheme

Conventional cooperative sensing (CCS) scheme is a common technique, where each time frame of duration T_{Total} seconds consists of two phases, namely, the sensing phase (T) and the transmission phase ($T_{Total} - T$). Energy-based sensing is employed during the sensing phase for a duration of τ seconds, where the center SU and all the CR nodes employ sensing. Subsequently, the remaining duration of the sensing time, that is $T - \tau$, is further divided into N sub-slots for the transmission of the individual decisions by the nodes $\{C_i, i = 1, \ldots, N\}$ to the center SU [139–141].

To save the sensing overhead, it is assumed that each sensor transmits a one-bit decision over a dedicated, error free channel. Therefore, as shown in Figure 3.2, the sensing duration adds to

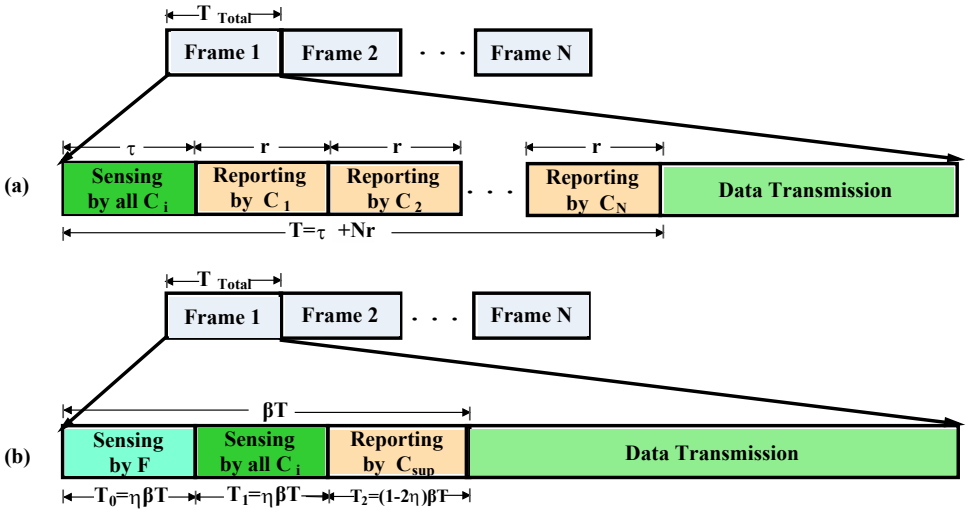

Figure 3.2. Time slot format for (a) CCS scheme and (b) SSR scheme.

a total of $T = \tau + Nr$ units, where r denotes the time-duration of each sub-slots. Hence, the sensing time T increases linearly with N, which increases the energy consumption and decreases the throughput. At the end of time slot T, the center SU combines these decisions by using a suitable fusion rule – such as AND [142], OR [143] or MAJORITY rules [144], and broadcasts its global decision to all the nodes. The sensing duration of CCS scheme, and the energy consumption increase with an increase in N. To reduce the sensing time and energy consumption, a selective reporting based cooperative spectrum sensing scheme, namely superior selective reporting (SSR) scheme was proposed, which is explained next.

3.2.2 Superior Selective Reporting (SSR) Scheme

The SSR scheme, originally proposed in [34], has multiple advantages over the CCS scheme, as the center SU receives the decision only from a superior SU, which is selected as described in next section. It should be noted that in [34], the study of SSR scheme was limited to its detection performance in comparison to the CCS scheme, whereas in this work its energy efficiency performance is studied by calculating the achievable throughput and energy consumption. As shown in Figure 3.2, the SSR scheme has two sensing time allocation factors, namely η and β [34]. In a given time frame of T_{Total} seconds, the center SU carries out spectrum sensing for a duration of T_0 seconds. If the decision of the center SU favors hypothesis $\mathcal{H}_1$, then the center SU broadcasts a message saying that the primary user is present, indicating the duration $T_{Total} - T_0$

not to be engaged in communication. In this case, no cooperation from other CR nodes is utilized. In the case when the center SU decides in favor of hypothesis $\mathcal{H}_0$, it requests for a cooperation from the other nodes, and nodes $C_1, \ldots, C_N$ carry out sensing for a duration of T_1. Later, among the nodes that favor $\mathcal{H}_1$, the node with the highest SNR reports back its decision to the center SU, on the same channel, for a time duration of T_2 seconds, which is inversely proportional to its SNR. This node is termed as the superior SU, which is selected as decribed in section 3.2.3.2. For analytical simplicity, it is assumed that this report is error-free. However, it should be noted that the performance of SSR would degrade further in the case of dispersive reporting channel errors [138], and hence the presented performance can be considered as an upper bound for practical purposes. Also, the mobility aspects of the PU [145] is ignored, since each SU would then require an exact knowledge of the change in network topology due to the movement of PU, which makes the analysis more complex. Moreover, as considered in [69],[106], the interference to PUs induced by final decision reporting can be ignored, since the transmission duration of such reporting is relatively short in comparison to the duration of the sensing phase. In fact, the final decision can be declared by using a power control method discussed in [34] to sufficiently protect primary transmissions.

Algorithm 1 : Selective reporting algorithm

Consider the N SU nodes $C_i, i = 1, \ldots, N$.
procedure LOCAL SENSING BY CENTER SU, F
    for time duration T_0 **do**
        Calculate energy-based test statistic, i.e., $T_E(y) = \frac{1}{M} \sum_{n=1}^{M} |y(n)|^2$
        Calculate threshold, ε, by fixing the probability of false-alarm
        if $(T(r) \geq \varepsilon)$ **then**
            Center SU(F) claims the presence of PU
            Broadcast local decision and stop spectrum sensing
        else
            Local sensing by other SUs (C_i) at time slot T_1
            Form detection set, Φ, as the set of sensors claiming presence of PU
            if (Φ = empty) **then**
                Center SU(F) claims the absence of PU
            else
                Select *Superior* SU as discussed in Sec. 3.2.3.2
            end if
        end if
        Selected Superior SU reports its local decision to center SU, F
        Broadcast final detection result by center SU, F, to other SUs
    end for
end procedure

As opposed to the CCS scheme, only a portion $0 \leq \beta \leq 1$ of the detection time T is required in the SSR scheme. The duration βT includes sensing and reporting times, and is divided into the previously defined T_0, T_1 and T_2, where $T_0 = T_1 = \eta\beta T$, for some $0 \leq \eta \leq 1$, which indicates the sensing duration of center SU and the nodes C_i, $i = 1, \ldots, N$ and $T_2 = \beta T - T_0 - T_1$ indicates the reporting time of the superior SU. Cooperative sensing procedure in SSR scheme is described in Algorithm 1.

3.2.3 Performance Analysis with Energy Detection

As mentioned earlier, energy detection (ED) is employed to detect the presence of the PU. In this section, the performance analysis of energy detection in CCS, SSR and OSSR schemes are discussed.

3.2.3.1 CCS Scheme

For the CCS scheme, probabilities of signal detection and false-alarm at each SU are given by [137]

$$P_{f,i} = Q\left(\left(\frac{\varepsilon_i}{\sigma^2} - 1\right)\sqrt{u_0}\right) \triangleq \varphi(u_0, \varepsilon_i), \tag{3.1}$$

$$P_{d,i} = Q\left(\left(\frac{\varepsilon_i}{\sigma^2} - \gamma_i - 1\right)\sqrt{\frac{u_0}{2\gamma_i + 1}}\right) \triangleq \varphi(u_0, \varepsilon_i, \gamma_i), \quad i = 1, 2, ...N \tag{3.2}$$

where $u_0 = \tau f_s$, is the time-bandwidth product, i.e., τ is the signal duration, f_s is the sampling frequency, ε_i denotes the detection threshold at node C_i, and γ_i denotes the received SNR at node C_i. Also, $Q(\cdot)$ indicates the complementary cumulative distribution function of a standard Gaussian random variable. The threshold ε_i can be computed from (3.1) as

$$\varepsilon_i = \sigma^2 Q^{-1}\left(\frac{P_{f,i}}{\sqrt{u_0}}\right) + 1 \tag{3.3}$$

In the CCS scheme, the center SU combines the decisions from all nodes C_i, $i = 1, \ldots, N$ using the AND, OR or MAJORITY rules [142]. Following this, the global probabilities of false-alarm

and signal detection, for the OR rule, respectively, are given by [143]

$$P_f^{CCS,OR} = \left[1 - \prod_{i=1}^{N} \left(1 - P_{f,i}\right)\right] = 1 - (1 - P_{f,i})^N \tag{3.4}$$

$$P_d^{CCS,OR} = \left[1 - \prod_{i=1}^{N} \left(1 - P_{d,i}\right)\right] = 1 - (1 - P_{d,i})^N \tag{3.5}$$

For the AND fusion rule, the probabilities are given by [26]

$$P_f^{CCS,AND} = \prod_{i=1}^{N} P_{f,i} = \left(P_{f,i}\right)^N \tag{3.6}$$

$$P_d^{CCS,AND} = \prod_{i=1}^{N} P_{d,i} = \left(P_{d,i}\right)^N \tag{3.7}$$

The overall detection probability of the CCS scheme is obtained by fixing $P_{f,i}$ to a predefined level. For a comparative study, the CCS scheme with AND and OR fusion rules is discussed in this chapter, which have associated advantages and disadvantages [26, 143].

3.2.3.2 SSR Scheme

Recall that for the SSR scheme, the sensing duration for the individual SUs are given by $T_0 = T_1 = \eta\beta T$, where T is the sensing duration of the CCS scheme, and is given by $T = \tau + Nr$. The superior SU is selected from the detection set to report to the center SU, in time T_2, when the decision of the center SU is in favor of $\mathcal{H}_1$. Following this, the superior reporting SU node, C_{sup}, can be described as:

$$C_{sup} = \underset{C_i \epsilon \Phi}{\arg\max} \left(\frac{\gamma_{C_i}|h_{C_iF}|^2}{1 + \theta\gamma_P|h_{PF}|^2}\right) = \underset{C_i \epsilon \Phi}{\arg\max} \left(\gamma_{C_i}|h_{C_iF}|^2\right), \tag{3.8}$$

where $\Phi \triangleq \{C_i : C_i \text{ decides } \mathcal{H}_1\}$ is the detection set obtained in time slot T_2. The scenario considered for spectrum sensing problem is as follows. The cognitive radio network is assumed to be far from the primary network, such that the primary SNR at each node is nearly equal. Hence, γ_P is same across all nodes. Additionally, CR network is assumed to be clustered in a relative small area, which makes the quantity $|h_{PF}|$ for each node to be approximately the same. Hence,

maximization given in the first equality is the same as that given in the second equality, since the denominator is approximately equal across all nodes.

The procedure to choose the superior SU is as follows. The SUs that detect the presence of PU constitute a detection set Φ. Each SU $\{C_i \in \Phi\}$ sets off a timer at the end of sensing phase, with each initial values $\{T_i, C_i \in \Phi\}$ set inversely proportional to its received SNR $\gamma_{C_i}|h_{C_iF}|^2$ as in [34]. i.e., $\mathtt{T}_i = \frac{\omega}{(\gamma_{C_i}|h_{C_iF}|^2)}$, for some $\omega \in \mathbb{R}^+$. The SU with highest SNR exhausts its timer first and reports to the center SU. This SU is the superior SU among the cooperative SUs in Φ. Only the superior SU sends its local decision to center SU in time slot T_2. Channel reciprocity [1] is assumed between center SU and the other SUs [34]. In addition, the selected superior SU transmits a short duration flag packet, signaling its presence. All other SUs, waiting for their timer to expire, back off immediately as soon as they receives this flag [146].

The method of calculating the received SNR is as described in [146]. Each SU node carries out the following procedure to assist the center SU to select the superior SU, in SSR schemes. When requested for cooperation, each SU at the end of its sensing duration sets a timer which is inversely proportional to the SNR of the channel between the center SU(F) and other SUs, obtained from a CTS packet broadcast by center SU. Each SUs in the detection set overhears the CTS packet and estimates the instantaneous wireless channel SNR between the center SU(F) and other SUs (C_i). This instantaneous SNR is used to calculate the particular channel gain (h_{C_iF}), which is used to initialize the timer. Channel reciprocity is assumed between the center SU and other SUs, and a perfect clock synchronization is assumed across the SUs [34]. In [146], the authors show that the overhead of such user selection is a small fraction of the coherence interval with collision probability less than 0.6%. Therefore, the energy consumed during the process of selection of superior SU is neglected in this analysis.

The probabilities of false-alarm and signal detection at the center SU and other SUs (C_i) using energy detector are given, respectively, as [147]

$$P_{f,F}^{SSR} = P_{f,C_i}^{SSR} = Q\left(\left(\frac{\varepsilon_i}{\sigma^2} - 1\right)\sqrt{u_1}\right) = \varphi(u_1, \varepsilon_i, 0), \quad i = 1, \ldots, N \tag{3.9}$$

$$P_{d,F}^{SSR} = Q\left(\left(\frac{\varepsilon_i}{\sigma^2} - \gamma_F - 1\right)\sqrt{\frac{u_1}{2\gamma_F + 1}}\right) \triangleq \varphi(u_1, \varepsilon_i, \gamma_F), \quad P_{d,C_i}^{SSR} = \varphi(u_1, \varepsilon_i, \gamma_{C_i}) \tag{3.10}$$

[1] The center SU and other SUs operate in a fixed time-division multiple-access (TDMA) manner, which is commonly considered in existing studies [34],[69, 103–106] where a common channel is shared between SUs.

where $u_1 = \eta\beta T f_s$, γ_F is the SNR of center SU and γ_{C_i} is the SNR of other SUs. As indicated earlier, only the decision of C_{sup} is reported in the slot T_2. From Figure 3.2, $T_2 = (1-2\eta)\beta T$. Note that energy detector is used to evaluate the performance of conventional and proposed sensing scheme. The results obtained in this work is extended to Bayesian detector case which is shown in Appendix D. Then, the probability that F receives an incorrect decision in favor of $\mathcal{H}_1$ from C_{sup} in T_2 slot for SSR is obtained as [34]

$$P_{f,C,1}^{SSR} = \sum_{i=1}^{2^N-1} \left[\prod_{C_l \in \Phi_i} P_{f,C_l}^{SSR} \prod_{C_m \in \overline{\Phi}} (1 - P_{f,C_m}^{SSR}) \right] = 1 - (1 - P_{f,C_i}^{SSR})^N. \tag{3.11}$$

Here Φ_i is the i^{th} possible combination of elements among the total 2^N elements in detection set Φ, and $\overline{\Phi}$ is the complement of the detection set Φ. Hence, the overall probability of false-alarm at the center SU in the SSR scheme is given by [34]

$$P_f^{SSR} = P_{f,F}^{SSR} + (1 - P_{f,F}^{SSR}) P_{f,C,1}^{SSR} \tag{3.12}$$

Similarly, the probability that the center SU, correctly receives the decisions from other SUs $C_i, i = 1, \ldots, N$ in favor of $\mathcal{H}_1$ in T_2 slot is shown to be

$$P_{d,C,1}^{SSR} = \sum_{i=1}^{2^N-1} \left[\prod_{C_l \in \Phi_i} P_{d,C_l}^{SSR} \prod_{C_m \in \overline{\Phi}} (1 - P_{d,C_m}^{SSR}) \right] = 1 - (1 - P_{d,C_i})^N, \tag{3.13}$$

following which, the final detection probability of SSR can be calculated as [34]

$$P_d^{SSR} = P_{d,F}^{SSR} + (1 - P_{d,F}^{SSR}) P_{d,C,1}^{SSR} \tag{3.14}$$

The main aspect of the SSR scheme is to design the optimal values of η and β. In the earlier work [34], the optimal values for η and β were designed based on an upper bound and lower bound constraints on probabilities of false-alarm and signal detection, respectively. In this work, the optimal values of η, β and N, is designed such that the energy efficiency is maximized.

3.3 Formulation of Energy Efficiency Optimization for the SSR Scheme

The ratio of average throughput to the average energy consumption is defined as the energy efficiency of a CR system [140, 148]. In the following, the average throughput, average energy consumption for SSR scheme in CR network is discussed and later the governing optimization problem of designing η, β and N is provided such that the energy efficiency is maximized.

In a CR network with SSR scheme, the average throughput achievable depends on the communication between PU and SUs, categorized into four scenarios elaborated below.

S1. The first scenario corresponds to the case when PU is present, and the network correctly identifies its presence. This case can be further divided into two cases which correspond to the situation where the decision in favor of $\mathcal{H}_1$ is made at the end of slot T_0 (i.e., by the center SU), which occurs with probability $P(\mathcal{H}_1)P_{d,F}^{SSR}$ and in the case when center SU incorrectly declares $\mathcal{H}_0$, but is corrected by the node C_{sup} at the end of slot T_2, which occurs with probability $P(\mathcal{H}_1)(1-P_{d,F}^{SSR})P_{f,C,1}^{SSR}$. Observe that in both these cases, the SUs do not transmit data and the throughput achieved is zero.

S2. The second scenario covers the case when PU is absent but incorrectly declared as present by the network. Again, this case has two sub-cases. The first case corresponds to the situation where the center SU makes a false-alarm, which occurs with probability $P(\mathcal{H}_0)P_{f,F}^{SSR}$. The second case corresponds to the situation where although the center SU correctly observes the spectrum to be empty, the node C_{sup} incorrectly declares the presence of the PU, which occurs with probability $P(\mathcal{H}_0)(1-P_{f,F}^{SSR})P_{f,C,1}^{SSR}$. Since the CR network misses a transmission opportunity in this case, the throughput achieved is given by $-\phi\mathtt{C}(T_{Total}-\beta T)$, where ϕ is a suitably chosen penalty factor [149].

S3. The third scenario corresponds to the scenario when both center SU and the node C_{sup} make incorrect decision that the PU is absent, when it is actually present. In this situation, which occurs with probability $P(\mathcal{H}_0)(1-P_{d,F}^{SSR})(1-P_{d,C,1}^{SSR})$, the network transmits and causes interference to the PU. However, even this being the case, a partial throughput of $\kappa_c\mathtt{C}(T_{Total}-\beta T)$ units can still be achieved for some $0 \leq \kappa_c < 1$.

S4. The last scenario corresponds to where the achievable throughput is maximum. This covers the situation when the PU is absent and both center SU and C_{sup} makes correct decisions, which occurs with probability $P(\mathcal{H}_0)(1 - P_{f,F}^{SSR})(1 - P_{f,C,1}^{SSR})$. In this case, the average throughput for the duration of $T_{Total} - \beta T$ is denoted as $\mathtt{C}(T_{Total} - \beta T)$ units, where $\mathtt{C}$ denotes the average data rate of SU transmission.

Table 3.1. Energy consumption and throughput achieved by the CRN for different scenarios

CCS Scheme			SSR Scheme		
Scenario	Energy(J)	Throughput (bitz/Hz)	Scenario	Energy(J)	Throughput (bitz/Hz)
$P(\mathcal{H}_1)P_d^{CCS}$	N$P_s\,\tau$ + N P_t r	0	$P(\mathcal{H}_1)P_{d,F}^{SSR}$	P_sT_0	0
			$P(\mathcal{H}_1)(1-P_{d,F}^{SSR})\,P_{d,C,1}^{SSR}$	$P_s\,T_0$+N $P_s\,T_1$ +P_tT_2	
P(H_0)P_f^{CCS}	N$P_s\,\tau$ + NP_tr	-ϕC(T_{Total} - T)	P(H_0)$P_{f,F}^{SSR}$	P_sT_0	-ϕC(T_{Total} - βT)
			P(H_0)(1-$P_{f,F}^{SSR}$)$P_{f,C,1}^{SSR}$	$P_s\,T_0$+N $P_s\,T_1$ +P_tT_2	
P(H_1)(1-P_d^{CCS})	N$P_s\,\tau$ + NP_tr +P_t(T_{Total} - τ-Nr)	κ_cC(T_{Total} - T)	P(H_1)(1-$P_{d,F}^{SSR}$)*(1-$P_{d,C,1}^{SSR}$)	$P_s\,T_0$+N $P_s\,T_1$ +P_tT_2+P_t(T_{Total} - βT)	κ_cC(T_{Total}-β T)
P(H_0)(1-P_f^{CCS})	N$P_s\,\tau$ + NP_tr +P_t(T_{Total} - τ-Nr)	C(T_{Total} - T)	P(H_0)(1-$P_{f,F}^{SSR}$)*(1-$P_{f,C,1}^{SSR}$)	$P_s\,T_0$+N $P_s\,T_1$ +P_tT_2 +P_t(T_{Total} - βT)	C(T_{Total}-β T)

3.3.1 Average Throughput

Considering all the above cases, the average throughput of the SSR scheme is given by

$$\begin{aligned} R_{SSR}(\varepsilon,\eta,\beta,N) = {} & P(\mathcal{H}_0)\left[(1-P_{f,F}^{SSR})(1-P_{f,C,1}^{SSR})\right](T_{Total}-\beta T)\mathtt{C} \\ & + \kappa_c P(\mathcal{H}_1)\left[(1-P_{d,F}^{SSR})(1-P_{d,C,1}^{SSR})\right]\mathtt{C}(T_{Total}-\beta T) \\ & - \phi P(\mathcal{H}_0)\left[P_{f,F}^{SSR}+(1-P_{f,F}^{SSR})(P_{f,C,1}^{SSR})\right](T_{Total}-\beta T)\mathtt{C} \end{aligned} \tag{3.15}$$

for some $0 \leq \kappa_c < 1$, and $\phi \geq 0$.

Note that for the CCS scheme, the average throughput is given by

$$\begin{aligned} R_{CCS}(N,\tau) = {} & P(\mathcal{H}_0)(1-P_f^{CCS})(T-\tau-Nr)\mathtt{C} + \kappa_c\mathtt{C}(T_{Total}-T)P(\mathcal{H}_1)(1-P_d^{CCS}) \\ & -\phi\mathtt{C}(T_{Total}-T)P(\mathcal{H}_0)P_f^{CCS}. \end{aligned} \tag{3.16}$$

3.3.2 Energy Consumption

In this section, the energy consumed by the SU network for the above mentioned four scenarios are discussed. Recall that P_s and P_t denote the power required for each SU node for sensing and transmission, respectively. The energy consumption for the SSR scheme across all the scenarios mentioned above along with the achievable throughput and energy consumption for the CCS scheme are listed in Table. 3.1. Following these cases,

$$E_{SSR}(\varepsilon,\eta,\beta,N) = X_s(P_sT_0) + Y_s(P_sT_0 + NP_sT_1 + P_tT_2) + Z_s(P_sT_0 + NP_sT_1 + P_tT_2 + P_t(T_{Total} - \beta T), \quad \text{with} \tag{3.17}$$

$$X_s = P(\mathcal{H}_1)P_{d,F}^{SSR} + P(\mathcal{H}_0)P_{f,F}^{SSR}, \tag{3.18}$$

$$Y_s = P(\mathcal{H}_1)(1 - P_{d,F}^{SSR})P_{d,C,1}^{SSR} + P(\mathcal{H}_0)(1 - P_{f,F}^{SSR})P_{f,C,1}^{SSR}, \quad \text{and} \tag{3.19}$$

$$Z_s = P(\mathcal{H}_1)(1 - P_{d,F}^{SSR})(1 - P_{d,C,1}^{SSR}) + P(\mathcal{H}_0)(1 - P_{f,F}^{SSR})((1 - P_{f,C,1}^{SSR}). \tag{3.20}$$

On the other hand, the energy consumption for the CCS scheme vide Table 6.1 is given by

$$E_{CCS}(N,\tau) = X_c(NP_s\tau + NP_tr) + Y_c(NP_s\tau + P_t(T_{Total} - \tau)), \quad \text{where} \tag{3.21}$$

$$X_c = P(\mathcal{H}_1)P_d^{CCS} + P(\mathcal{H}_0)P_f^{CCS}, \quad \text{and} \tag{3.22}$$

$$Y_c = P(\mathcal{H}_1)(1 - P_d^{CCS}) + P(\mathcal{H}_0)(1 - P_f^{CCS}). \tag{3.23}$$

3.3.3 Energy Efficiency

First consider the CCS scheme, the energy efficiency, measured in (bits/Hz/J), of the CR network is expressed as

$$EE_{CCS}(N,\tau) = \frac{R_{CCS}(N,\tau)}{E_{CCS}(N,\tau)}. \tag{3.24}$$

When both P_d^{CCS} and P_f^{CCS} tends to zero, the network decides that PU is absent and starts data transmission, which improves the average throughput, but with lesser detection accuracy. On the other hand when both P_d^{CCS} and P_f^{CCS} tends to one, PU is declared to be present and the bandwidth is not utilized effectively. The energy efficiency maximization for the CCS scheme is given by

$$\mathcal{OP}_{CCS}: \max_{\varepsilon,\tau,N} \quad EE_{CCS}(\varepsilon,\tau,N) \tag{3.25}$$

$$\text{s.t.} \begin{cases} P_f^{CCS} \leq \overline{P_f}, \\ P_d^{CCS} \geq \overline{P_d}, \\ 0 \leq \tau \leq T, \\ 1 \leq N \leq N_{max}, \end{cases} \tag{3.26}$$

for some $0 < \overline{P_f} < \overline{P_d} < 1$. This problem has been earlier considered with AND [26] and OR fusion rules [150].

On the other hand, in the SSR scheme, since a single SU is required to report its local decision to the center SU, sensing overhead can be significantly reduced which in turn reduces the energy consumption. Also, the saved sensing time and energy can be utilized for data transmission by SU, which potentially enhances the secondary throughput. This leads to the eventual improvement in energy efficiency in contrast to the CCS scheme. The energy efficiency of the SSR scheme is:

$$EE_{SSR}(\varepsilon,\eta,\beta,N) = \frac{R_{SSR}(\varepsilon,\eta,\beta,N)}{E_{SSR}(\varepsilon,\eta,\beta,N)}. \tag{3.27}$$

The energy efficiency optimization problem governing the SSR scheme is given by,

$$\mathcal{OP}_{SSR}: \max_{\varepsilon,\eta,\beta,N} \quad EE_{SSR}(\varepsilon,\eta,\beta,N) \tag{3.28}$$

$$\text{s.t.} \begin{cases} P_f^{SSR} \leq \overline{P_f} \\ P_d^{SSR} \geq \overline{P_d}, \\ 0 \leq \beta \leq 1, \\ 0 \leq \eta \leq 1/3, \\ 1 \leq N \leq N_{max}, \end{cases} \tag{3.29}$$

for some $0 < \overline{P_f} < \overline{P_d} < 1$. Notice that the constraint $0 \leq \eta \leq 1/3$ ensures that $T_0, T_1, T_2 \geq 0$. The IEEE 802.22 standard [151], enforce requirements for the upper bound on the probability of

signal detection and lower bound on the probability of false-alarm to be 0.9 and 0.1, respectively.

The above mentioned optimization problem is non-convex. For the ease of analysis, the cost function for the above problem is approximated and the conditions under which the problem can be reduced to a convex optimization problem is mentioned. The details are provided in the next section.

3.4 Approximation, Problem Reformulation and Analysis

In this section, an approximation of EE_{SSR} is provided and the optimization problem $\mathcal{OP}_{SSR}$ is reformulated. On a general note, the channel detection probability should be large enough to limit the collision between the primary and cognitive transmission. Therefore, $P(\mathcal{H}_0) > P(\mathcal{H}_1)$, $P_{d,F}^{SSR} > P_{f,F}^{SSR}$, $P_{d,C,1}^{SSR} > P_{f,C,1}^{SSR}$, $P_d^{SSR} > P_f^{SSR}$. For the ease of analysis, the average throughput in (3.15) can be approximated by the above inequalities, and setting $\kappa_c = 0$ as

$$\tilde{R}_{SSR} \approx (T - \beta T)P(\mathcal{H}_0)\mathtt{C}\left\{(P_{f,F}^{SSR} + (1 - P_{f,F}^{SSR})P_{f,C,1}^{SSR})(-\Phi) + (1 - P_{f,F}^{SSR})(1 - P_{f,C,1}^{SSR})\right\} \quad (3.30)$$

Assuming that $P_{f,F}^{SSR} = P_{f,C_i}^{SSR} = P_f$,

$$\tilde{R}_{SSR} \approx P(\mathcal{H}_0)\mathtt{C}(T_{Total} - \beta T)\left\{-\Phi + (\Phi + 1)(1 - P_f)^{N+1}\right\}. \quad (3.31)$$

Similarly an approximate expression for E_{SSR} can be written as

$$\begin{aligned}\tilde{E}_{SSR} \approx P_s T_0 - [NP_s T_1 + P_t T_2]\left\{P(\mathcal{H}_1)P_{d,F}^{SSR} + P(\mathcal{H}_0)P_{f,F}^{SSR}\right\} + \\ P_t(T_{Total} - \beta T)\left\{P(\mathcal{H}_0)(1 - P_{f,F}^{SSR})(1 - P_{f,C_i}^{SSR})\right\}. \quad (3.32)\end{aligned}$$

Assuming that $P_{f,F}^{SSR} = P_{f,C_i}^{SSR} = P_f$, and $P_{d,F}^{SSR} = P_{d,C_i}^{SSR} = P_d$, further simplification of (3.17) gives

$$\begin{aligned}\tilde{E}_{SSR} \approx PsT_0 - [NP_s T_1 + P_t T_2]\{P(\mathcal{H}_1)P_d \\ + P(\mathcal{H}_0)P_f - 1\} + P(\mathcal{H}_0)P_t(T_{Total} - \beta T)(1 - P_f)^{N+1}. \quad (3.33)\end{aligned}$$

Now, the approximated energy efficiency can be written as

$$\tilde{EE}_{SSR}(\varepsilon, \beta, \eta, N) \approx \frac{\tilde{R}_{SSR}(\varepsilon, \eta, \beta, N)}{\tilde{E}_{SSR}(\varepsilon, \beta, \eta, N)}. \tag{3.34}$$

The accuracy of the approximate throughput and energy consumption equations given in (3.31) and (3.33), respectively, in relation to the actual expressions given in (3.15) and (3.17), and the consequence of the approximate energy efficiency in (3.34) will be discussed in the Sec. 3.5. Hereafter, $\frac{\tilde{R}_{SSR}(\varepsilon,\eta,\beta,N)}{\tilde{E}_{SSR}(\varepsilon,\beta,\eta,N)}$ will be used instead of $\frac{R_{SSR}(\varepsilon,\eta,\beta,N)}{E_{SSR}(\varepsilon,\beta,\eta,N)}$ as an objective function in this analysis. Consequently, the optimization problem $\mathcal{OP}_{SSR}$ can be reformulated as

$$\mathcal{OP}1_{SSR}: \max_{\varepsilon,\eta,\beta,N} \quad \tilde{EE}_{SSR}(\varepsilon, \eta, \beta, N) = \frac{\tilde{R}_{SSR}(\varepsilon, \eta, \beta, N)}{\tilde{E}_{SSR}(\varepsilon, \beta, \eta, N)} \tag{3.35}$$

$$\text{s.t.} \begin{cases} P_f^{SSR} \leq \overline{P_f} \\ P_d^{SSR} \geq \overline{P_d}, \\ 0 \leq \beta \leq 1, \\ 0 \leq \eta \leq 1/3, \\ 1 \leq N \leq N_{max}, \end{cases} \tag{3.36}$$

Next, a detailed analysis on obtaining the optimal detection threshold, the number of cooperative users and sensing time to maximize the energy efficiency given in $\mathcal{OP}1_{SSR}$ is provided.

3.4.1 Optimal Detection Threshold

Here, the optimal value of the detection threshold ε that satisfies the detection performance constraint is given in problem $\mathcal{OP}1_{SSR}$. Theorem 3.2 gives the expression for the optimal threshold ε^* and the required condition corresponding to the optimization problem in $\mathcal{OP}1_{SSR}$. Lemma 3.1 is stated and proved the following lemma before theorem 3.2.

Lemma 3.1. *The throughput of the SSR scheme is non-negative, i.e.,* $\tilde{R}_{SSR} \geq 0$*, if the penalty factor* (ϕ) *is chosen to meet the condition (D1)* $\frac{\Phi+1}{\Phi} \geq \frac{1}{[1-P_f(\varepsilon)]^{N+1}}$

Proof. The proof is straightforward and can be obtained by directly setting $\tilde{R}_{SSR} \geq 0$ in (3.31) and rearranging the equation.

Theorem 3.2. *The constraint $P_d^{SSR} \geq \overline{P_d}$ in the optimization problem $\mathcal{OP}1_{SSR}$ is satisfied with equality. Consequently, the optimal detection threshold is given by*

$$\varepsilon^* = \sigma^2 \left[(\gamma + 1) + \sqrt{\frac{2\gamma + 1}{\eta \beta T f_s}} Q^{-1} \left[1 - (1 - \bar{P}_d)^{\frac{1}{N+1}} \right] \right]. \tag{3.37}$$

Proof. The partial derivative of $\tilde{EE}_{SSR}$ with respect to ε, after some algebraic simplification, can be shown to be

$$\frac{\partial \tilde{EE}_{SSR}}{\partial \varepsilon} = -G(\varepsilon) \frac{\partial P_f}{\partial \varepsilon}, \tag{3.38}$$

where $G(\varepsilon) = \frac{[V_0(\varepsilon) - V_1(\varepsilon)]}{E_{SSR}^2(\varepsilon)^2}$, and the functions $V_0(\varepsilon)$ and $V_1(\varepsilon)$ are given as

$$V_0(\varepsilon) = P(\mathcal{H}_0) \mathtt{C} (T_{Total} - \beta T) \left[(\phi + 1)(N + 1)(1 - P_f(\varepsilon))^N \right] E_{SSR}(\varepsilon) \geq 0, \text{ and} \tag{3.39}$$

$$V_1(\varepsilon) = R_{SSR}(\varepsilon) P(\mathcal{H}_0) \left([N P_s \eta \beta T + P_t \eta \beta T] + P_t (T_{Total} - \beta T)(N + 1)(1 - P_f)^N \right). \tag{3.40}$$

Now, note that the first derivative of $P_f(\varepsilon)$ with respect to ε is given by

$$\frac{\partial P_f}{\partial \varepsilon} = -\frac{1}{\sigma^2} \sqrt{\frac{\eta \beta T f_s}{2\pi}} \exp \left(\frac{-(\frac{\varepsilon}{\sigma^2} - 1)^2 \eta \beta T f_s}{2} \right) \leq 0. \tag{3.41}$$

Since $\frac{\partial P_f}{\partial \varepsilon} \leq 0$, it is sufficient to prove that $G(\varepsilon) = [V_0(\varepsilon) - V_1(\varepsilon)] \geq 0$, to establish that $\frac{\partial \tilde{EE}_{SSR}}{\partial \varepsilon} \geq 0$. It is already seen that $V_0(\varepsilon) \geq 0$. Since $V_1(\varepsilon)$ depends on $\tilde{R}_{SSR}(\beta)$, $V_1(\varepsilon)$ will be non-negative if the condition (D1) holds, vide lemma 3.1. Therefore, under the conditions stated in lemma 3.1, $[V_0(\varepsilon) - V_1(\varepsilon)] \geq 0$.

Therefore, $(\frac{\partial \tilde{EE}_{SSR}}{\partial \varepsilon}) \geq 0$. This implies that the optimal threshold to maximize the objective function $\mathcal{OP}1_{SSR}$ should be large, which happens if the constraint $P_d^{SSR} = \bar{P}_d$ is satisfied. Any other smaller ε, must satisfy the constraint $P_d^{SSR} > \bar{P}_d$ for a given value of N, β and η. Note that the constraint $P_d^{SSR} = \bar{P}_d$ can still be satisfied when $P_{d,F}^{SSR}$ and P_{f,C_i}^{SSR} are equal. Setting $P_{d,F}^{SSR} = P_{d,C_i}^{SSR} = P_{d,i}$ gives $P_d^{SSR} = 1 - [1 - P_{d,i}]^{N+1}$. Following this, the equation for the optimal detection threshold ε^* is obtained. This completes the proof.

3.4.2 Optimal Values of β and η

In this section, an analysis to find the optimal values of η and β is provided. First, the optimal value of η is described in the following lemma.

Lemma 3.3. *The optimal value of η that maximizes the cost function in the optimization problem $\mathcal{OP}1_{SSR}$ is given by $\eta^* = \frac{1}{3}$.*

Proof. It is shown in AppendixA that $\frac{\partial \tilde{EE}_{SSR}(\eta)}{\partial \eta} \geq 0$ for every $0 \leq \eta \leq 1/3$. Thus $\eta^* = \frac{1}{3}$.

Following the results from Theorem 3.2 and Lemma 3.3, for a given N and β, optimization problem $\mathcal{OP}1_{SSR}$ can be simplified to $\mathcal{OP}2_{SSR}$ as:

$$\mathcal{OP}2_{SSR}: \max_{\beta,N} \quad EE_{SSR}(\epsilon^*, \eta^*, \beta, N) \tag{3.42}$$

$$\text{s.t.} \begin{cases} P_f^{SSR} \leq \overline{P_f}, \\ 0 \leq \beta \leq 1, \\ 1 \leq N \leq N_{max}. \end{cases} \tag{3.43}$$

The following theorem gives the conditions under which optimal β can be obtained.

Theorem 3.4. *Let β_{min} be defined as below. Then, the objective function in $\mathcal{OP}3_{SSR}$ is quasi-concave for all $\beta \in (\beta_{min}, 1)$, with*

$$\beta_{min} = \left[\frac{Q^{-1}\left(1 - (1-\overline{P}_f)^{\frac{1}{N+1}}\right)}{\left(\frac{\varepsilon^*}{\sigma^2} - 1\right)\left(\sqrt{\eta T f_s}\right)} \right]^2. \tag{3.44}$$

Proof. The first-order derivative of $\tilde{EE}_{SSR}$ with respect to β can be written as

$$\frac{\partial \tilde{EE}_{SSR}}{\partial \beta} = -\left[V_0(\beta) - V_1(\beta)\right] \frac{\partial P_f}{\partial \beta} + V_2(\beta), \tag{3.45}$$

where $V_0(\beta)$, $V_1(\beta)$ and $V_2(\beta)$ are given by

$$V_0(\beta) = P(\mathcal{H}_0)\mathtt{C}(T_{Total} - \beta T)\left[(\Phi+1)(N+1)(1-P_f)^N\right]\tilde{E}_{SSR}(\beta), \tag{3.46}$$

$$V_1(\beta) = P(\mathcal{H}_0)\left\{(NP_s\eta\beta T + (1-2\eta)\beta T) + P_t(T_{Total} - \beta T)(1-P_f)^N(N+1)\right\}\tilde{R}_{SSR}(\beta). \tag{3.47}$$

$$V_2(\beta) = -\tilde{R}_{SSR}(\beta)\left[\frac{T\tilde{E}_{SSR}(\beta)}{T_{Total}-\beta T} + P_s\eta T - [NP_s\eta T + P_t(1-2\eta)T](P(\mathcal{H}_0)(\overline{P_d}+P_f)+1)\right.$$
$$\left. -P(\mathcal{H}_0)P_tT(1-P_f)^{N+1}\right] \tag{3.48}$$

From (3.45), the first-order derivative of P_f with β, i.e., $\frac{\partial P_f}{\partial \beta}$ is given by

$$\frac{\partial P_f(\beta,\varepsilon^*)}{\partial\beta} = -\sqrt{\frac{\eta T f_s}{8\pi\beta}}\left(\frac{\varepsilon^*}{\sigma^2}-1\right)\exp\left(\frac{-(\frac{\varepsilon^*}{\sigma^2}-1)^2\eta\beta T f_s}{2}\right) \leq 0. \tag{3.49}$$

Therefore, P_f is a monotonically decreasing function of β.

Based on the above analysis, it is shown in Appendix A that, when $\beta \to 0$, $\frac{\partial P_f}{\partial\beta} \to -\infty$ and hence $[V_0(\beta) - V_1(\beta)] \geq 0$. Thus, when $V_2(\beta)$ is close to 0, $\lim_{\beta\to 0}\frac{\partial E E_{SSR}(\beta)}{\partial\beta} \geq 0$. On the other hand, when $\beta \to 1$, and ϕ meets the requirement (D1) stated in lemma 3.1, it is shown in Appendix A that $V_0(\beta)$ is a decreasing function of β and $V_1(\beta)$ is an increasing function of β, in the range $\beta_{min} \leq \beta \leq T$. Therefore, $\frac{\partial \tilde{E E}_{SSR}}{\partial\beta}$ is a decreasing function in β for $\beta_{min} \leq \beta \leq 1$, given that $V_2(\beta) \leq 0$. Hence, $\frac{\partial \tilde{E}_{SSR}}{\partial\beta}$ first increases and then decreases with respect to $\beta \in (\beta_{min}, 1)$. In other words, the cost function in $\mathcal{OP}2_{SSR}$ is quasi-concave in β.

Theorem 3.4 establishes that the objective function is quasi-concave in a given range of β, and hence techniques such as direct search method, golden search method, bi-section, Newton–Raphson method, etc. [152–154] can be used to calculate the root of the objective in $\mathcal{OP}2_{SSR}$. Based on the analytic development, a simple search algorithm is proposed to obtain the optimal values of ε, η, β and N for the optimization problem in $\mathcal{OP}1_{SSR}$, which is summarized in Algorithm 2. This completes the analysis of energy efficiency of the SSR scheme.

Algorithm 2 : Optimizing variables ε, β, and N

Set $P_s, P_t, T_{Total}, \tau, N, \beta_0, P(\mathcal{H}_0), P(\mathcal{H}_1), \overline{P_f}, \overline{P_d}$
procedure INITIALIZE $\beta = \beta_0, \eta = 1/3, P_d^{SSR} = \overline{P_d}, EE_{SSR}(0) = 0$ (,)
Initialize $\zeta \in \mathbb{R}$ such that $EE_{SSR}(N+1) - EE_{SSR}(N) < \zeta$
    To select optimal ε, β, N
    for do $N = 1 : N_{max}$
        Calculate ε using (3.37)
        Calculate β_{min} using (3.44)
        Compute EE_{SSR} using (3.28) with $\varepsilon(N)$ and $\beta_{min}(N)$
        Go to Step 5 if $EE_{SSR}(N+1) - EE_{SSR}(N) > \zeta$
        Stop iteration and return the optimal
        Calculate $EE_{SSR}(N, \varepsilon^*, \beta^*)$
    end for
end procedure
Return $\max(EE_{SSR})$ and the corresponding $N, \varepsilon^*, \beta^*$,

3.5 Numerical Results and Discussion

In this section, the performances of SSR, CCS-AND, and CCS-OR schemes are discussed, in terms of energy efficiency. MATLAB is used as a simulation tool. The parameter values are fixed as follows. The target probabilities $\overline{P_d}$ and $\overline{P_f}$, are fixed to be 0.9 and 0.1, respectively. The prior probability $P(\mathcal{H}_0) = 0.75$. The total frame duration is assumed to be $T_{Total} = 200$ ms. The sampling frequency at the local SUs is assumed to be $f_s = 1$ MHz, and the sensing power $P_s = 0.1$ W. The sensing time, τ, and reporting time, r, of CCS scheme is set to 100 μs. The achievable rate of secondary transmission is chosen to be $\mathtt{C} = \log_2(1 + \text{SNR}_s) = 6.6582$ bits/sec/Hz, where the SNR_s for the secondary transmission is assumed to be $\text{SNR}_s = 20$ dB. The transmission power of individual sensors, P_t, is assumed to be 3 W. The number of users, N, is set to minimum of 10 following the condition (D1) in lemma 3.1, unless otherwise stated. Also, $\kappa_c = \phi = 0.5$.

Figure 3.3 shows the variation of $EE_{SSR}(\varepsilon^*, \eta^*, \beta, N)$ and $\tilde{EE}_{SSR}(\varepsilon^*, \eta^*, \beta, N)$ vs. β for different values of SNR. It can be observed that all the cost functions are quasi-concave with respect to β, and that there exists a good match between the actual and approximate cost functions for SSR in (3.27) and (3.34), respectively. Also, as expected, EE increases as SNR increases. For the rest of the analysis, we chose number of available SUs, N to be a fixed number for the ease of analysis. Moreover, we are interested in characterizing the energy efficiency performance for a fixed value of N. This characterization serves as a corner-case design, for a given value of the design parameter N.

Figure 3.4 shows the variation of optimal β, (β^*) as a function of SNR for different values of N. This curve highlights the fact that the optimal values of β are nearly equal for the actual and approximate energy efficiency for SSR. The decrease in β^* with an increase in SNR is intuitive, since it results in a better detection performance, which in turn results in better throughput and hence better efficiency. Therefore, in subsequent discussion, performance analysis is considered only based on the approximated optimization problem for SSR.

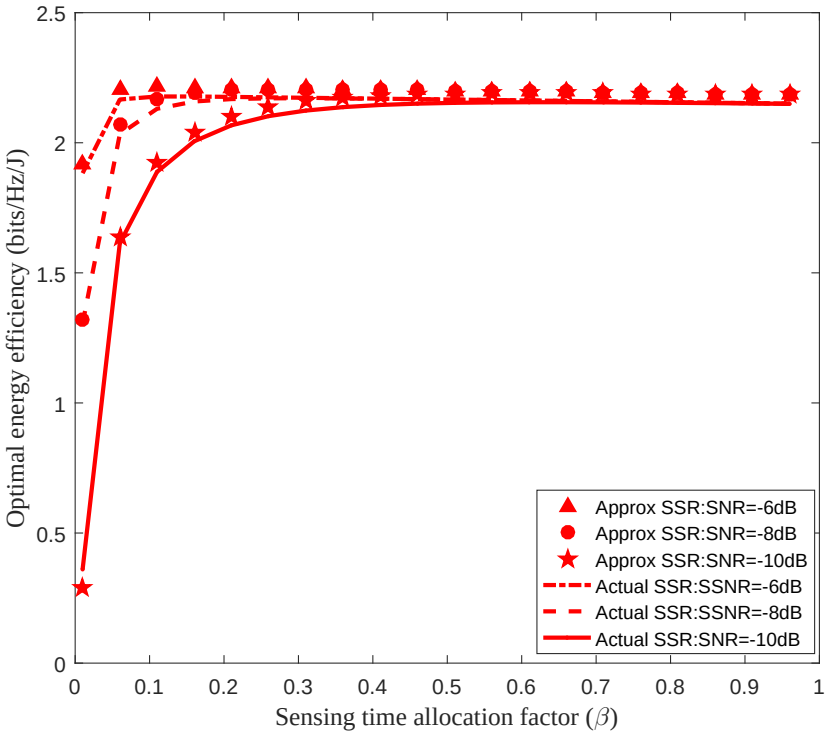

Figure 3.3. Variation of EE with β for SSR scheme.

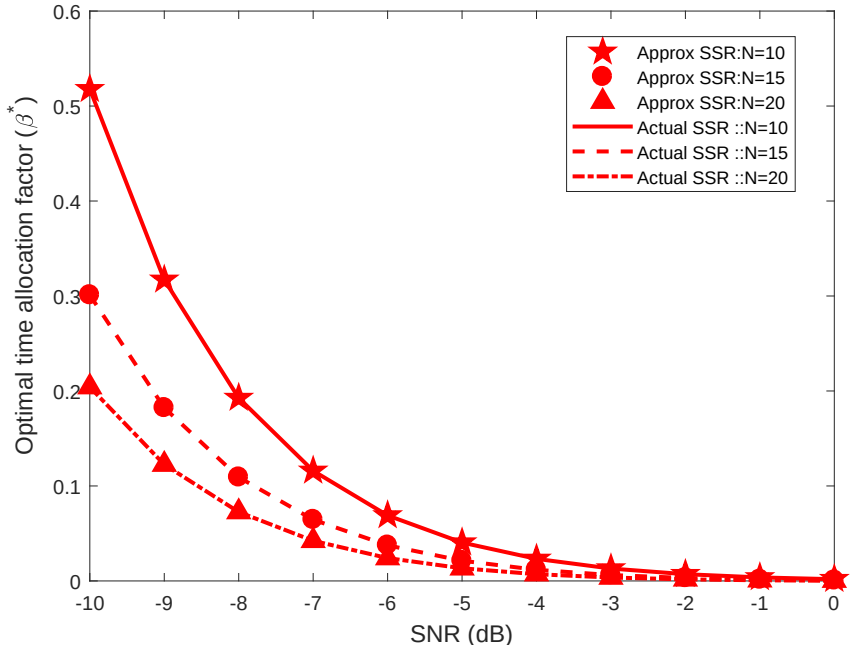

Figure 3.4. Variation of the optimal β with SNR (dB).

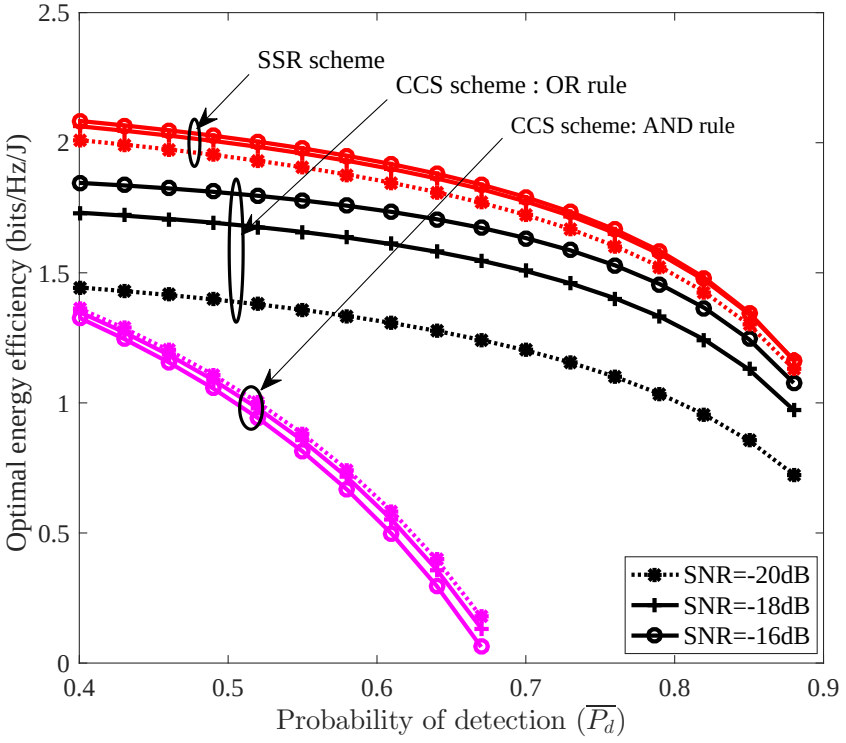

Figure 3.5. Variation of EE with $\overline{P_d}$ for SSR, CCS-AND, and CCS-OR schemes, $N = 10$.

In Figure 3.5, the variation of optimal energy efficiency for SSR, CCS-AND and CCS-OR schemes, with respect to a desired level probability of detection, $\overline{P}_d$ is plotted. The condition (D1) described in lemma 3.1 dictates that $N \geq 10$, and hence N is chosen to be 10. Note that this small value of N is fair to the CCS-AND rule, which is known to perform well only for low N. The performance of all the techniques increase with a decrease in $\overline{P}_d$, since a lower tolerance on the probability of miss detection improves the average throughput and energy consumption. However, the rate of improvement in energy efficiency is rather low for around $\overline{P}_d \leq 0.75$. Most importantly, the SSR scheme outperforms both CCS-OR and CCS-AND schemes.

Next, EE of SSR schemes with respect to the penalty factor ϕ is considered in Figure 3.6. N and κ_c are chosen to be $N = 13$, and $\kappa_c = 0.5$. It is straightforward to see that the energy efficiency decreases with an increase in ϕ. Again, the SSR scheme consistently offers the best performance in comparison with other schemes. In Figure 3.7 the performance of SSR schemes is plotted for different values of the partial throughput factor κ_c, for $N = 13$ and $\phi = 0.5$. An increase in partial throughput factor indicates that the SSR scheme exploits the maximum channel availability time to enhance the achievable throughput, for a given SNR.

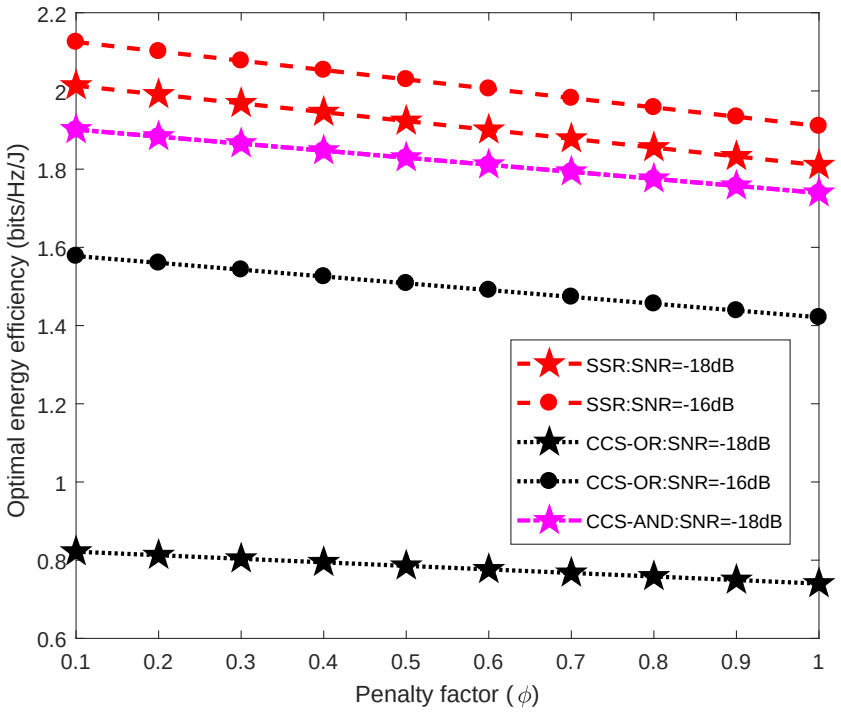

Figure 3.6. Variation of optimal energy efficiency with the penalty factor (ϕ) and $N = 13$.

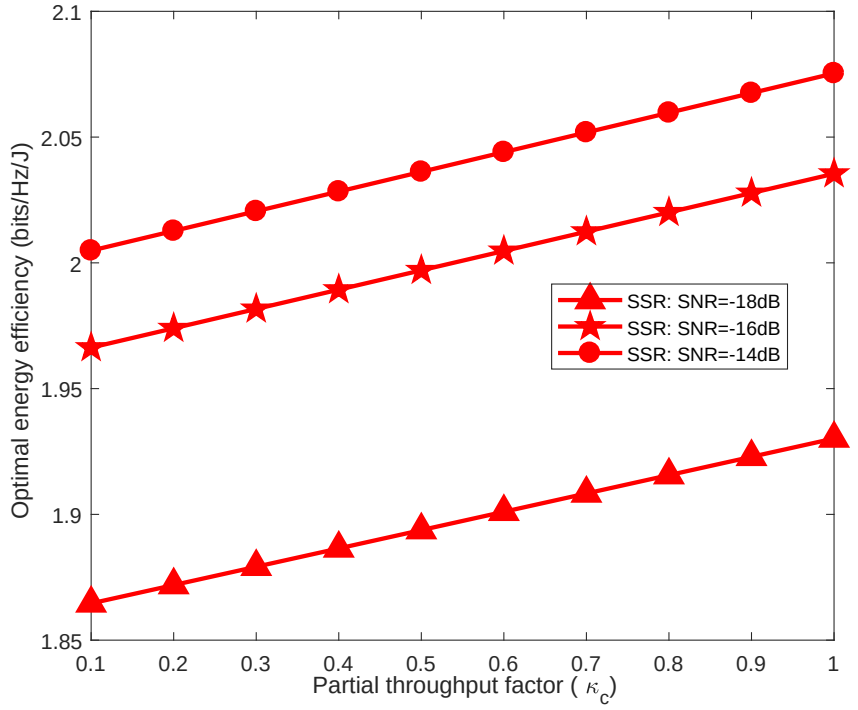

Figure 3.7. Variation of optimal energy efficiency with partial throughput factor (κ_c) and $N = 13$.

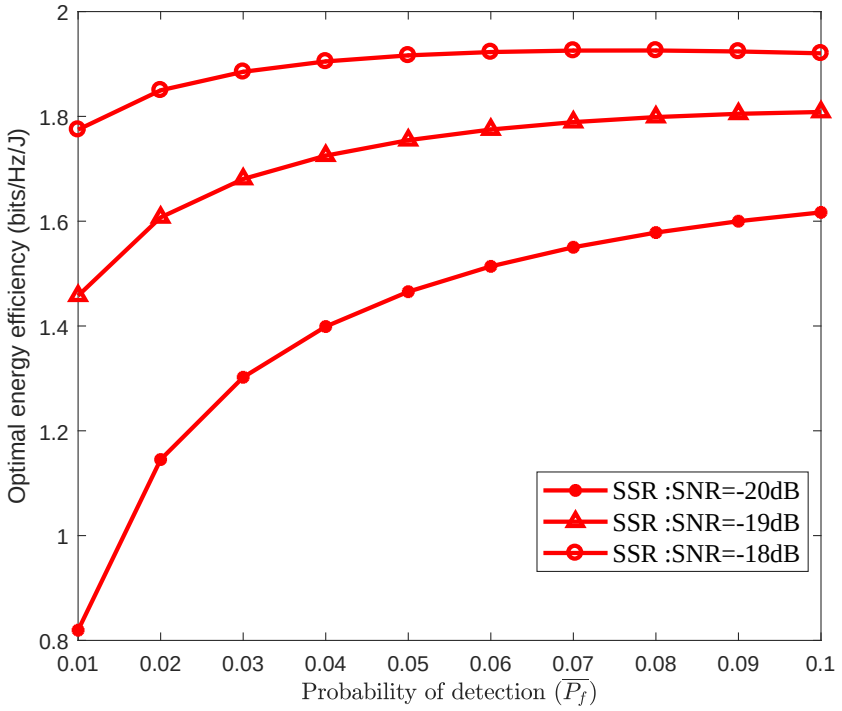

Figure 3.8. Variation of optimal energy efficiency with false alarm probability ($\overline{P}_f$) and $N = 10$.

Figure 3.8 shows the variation of energy efficiency with the tolerance limit on the false-alarm probability, $\overline{P}_f$, with $N = 10$. As expected, the performance of SSR scheme increase with an increase in the tolerance limit. As expected, the performance of SSR scheme improves as the SNR increases.

Figure 3.9 shows the variation of actual and approximate energy efficiency values for SSR scheme with η, for $N = 30$. Apart from reiterating on an earlier note that the approximate efficiency is close to the actual value, this plot also signifies the variation of the performance of SSR with η is monotone, and hence the choice of $\eta^* = \frac{1}{3}$ is justified.

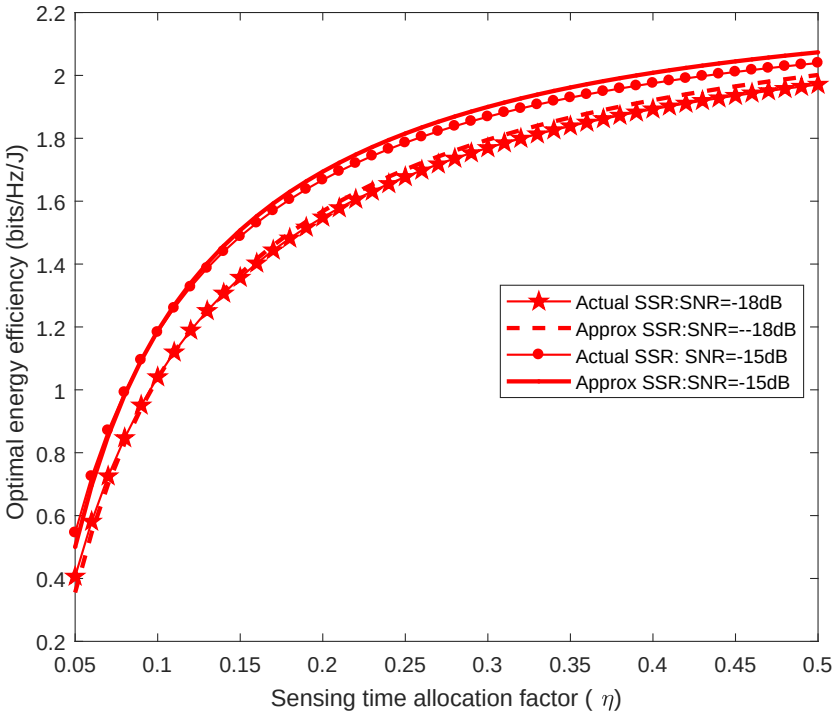

Figure 3.9. Variation of energy efficiency with sensing time allocation factor (η) and $N = 30$.

3.6 Summary

The energy efficiency of superior selective reporting (SSR)-based scheme for spectrum sensing is considered, and its achievable throughput, energy consumption and energy efficiency is derived. The energy efficiency maximization for the SSR scheme is formulated as a non-convex, multiple variable optimization problem, and approximating it to a quasi-concave optimization problem is

discussed, and showed that this approximation holds with sufficient accuracy. Through numerical results, it was shown that the energy efficiency achieved by the SSR scheme is larger as compared to the conventional cooperative sensing schemes based on OR and AND rules.

However, there is an associated disadvantage with the SSR scheme. The scheme demands cooperation from the other sensors only when the center user declares the licensed band to be vacant. Otherwise, the center user does not communicate in the data transmission slot of a given time frame. The gain in energy efficiency in SSR scheme is related to the reduction in energy consumption; this comes at the expense of achievable throughput. However, in a typical CRN, achievable throughput may be of higher priority in comparison to the energy consumption. Therefore, in the next chapter, novel modification on the SSR scheme, termed as the opportunistic SSR (OSSR) scheme, is proposed which gives priority to spectrum vacant times – and hence, the achievable throughput – as opposed to the energy consumption. The energy efficiency of the OSSR scheme is analyzed and the tradeoff between SSR and OSSR is explored, which is the implicit tradeoff between the throughput and energy consumption, respectively.

Chapter 4

Opportunistic Superior Selective Reporting Technique for Energy Efficient Cooperative Spectrum Sensing

4.1 Introduction

The gain in energy efficiency in SSR scheme discussed in previous chapter is related to reduction in energy consumption, which comes at the expense of achievable throughput. However, in a typical CRN, increasing bit rate or achievable throughput may be of higher priority in comparison to the energy consumption. Therefore, this chapter tackles the balance between the achievable throughput and energy consumption of selective reporting based cooperative sensing scheme in CRN by introducing a novel modification on the SSR scheme termed as the opportunistic SSR (OSSR) scheme which gives priority to spectrum vacant times and hence, the achievable throughput – as opposed to the energy consumption.

When the center SU decides that the spectrum is vacant, the network uses the licensed bandwidth for communication. Cooperative sensing is employed when the spectrum is declared to be occupied, in the hope that the superior sensor declares the spectrum to be available. Therefore, this greedy technique gives priority to spectrum vacant times – and hence, the achievable throughput – as opposed to the energy consumption. Note that since the energy efficiency is defined as the ratio between achievable throughput and energy consumption, both OSSR and SSR schemes are expected to follow a trend, where the implicit tradeoff is between the throughput and energy consumption, respectively. This tradeoff is explored and the scenarios where SSR outperforms OSSR and vice-versa is described. The main contributions of this chapter are summarized as below.

- A novel variation on the SSR scheme, namely the OSSR scheme, is proposed in this chapter and its energy efficiency is studied, in terms of the detection threshold, the sensing time allocation factors and the required number of SUs for cooperation, that satisfies a given primary user interference constraint.
- The maximization of energy efficiency of OSSR is posed as a multiple variable, non-convex optimization problem, and the approximations that reduce this problem to a quasi-concave optimization are discussed. The tightness of the approximation is studied.
- The optimal detection threshold, time allocation factors and the number of SUs required for cooperation are derived.
- The tradeoff in energy efficiency of SSR and OSSR schemes are referred to the tradeoff between energy consumption and the achievable throughput of both the schemes.
- Through numerical results, it is shown that the SSR and OSSR schemes outperform the conventional cooperative sensing (CCS) schemes employing the popular OR and AND-fusion rules. In particular, it is highlighted that SSR outperforms all the other schemes in several scenarios and it is shown that minimizing the energy consumption takes a priority over maximizing the achievable throughput in a CRN, in several scenarios.

The remainder of this chapter is organized as follows. The OSSR scheme is proposed and its performance is studied in Section 4.2. The energy efficiency formulation, approximations, and

analysis of the OSSR scheme are presented in Sections 4.3, 4.4 and 4.5. The results and discussion are presented in Section 4.6 and concluding remarks are provided in Section 4.7.

4.2 Opportunistic Superior Selective Reporting (OSSR) Scheme

As discussed earlier in the SSR scheme, the cooperation among the SUs is employed (in terms of the superior SU) when the decision of the center SU favors hypothesis $\mathcal{H}_0$; otherwise, it is not utilized. Note that the SSR approach, reduces the energy consumption, and is pessimistic. To elaborate, if the center SU incorrectly declares in favor of $\mathcal{H}_1$ given the true hypothesis to be $\mathcal{H}_0$, an opportunity to transmit for a duration of $T_{Total} - T_0$ is not exploited, even though it results in lesser energy consumption. To overcome this disadvantage, a slightly modified version of the SSR scheme, called the opportunistic SSR (OSSR) scheme is proposed in this chapter. The system model and the time-slot structure for OSSR remains the same as that of the SSR scheme (Figure 3.1), with the following change in the strategy. In time slot T_0, the center SU utilizes the cooperation from the other nodes when it favors $\mathcal{H}_1$ in contrast to $\mathcal{H}_0$ in case of SSR, and does not employ cooperation when it decides in favor of $\mathcal{H}_0$. Therefore, in OSSR scheme, emphasis is on the achievable throughput in contrast to the emphasis on the energy consumption as in SSR scheme. In other words, the energy efficiency performance of SSR scheme vis-á-vis OSSR scheme is the tradeoff between achievable throughput and energy consumption.

4.2.1 Performance Analysis of OSSR with Energy Detection

Energy detection (ED) is employed to detect the presence of the PU. In this section, the performance analysis of energy detection in OSSR schemes is discussed.

The probabilities of detection and false-alarm for CCS scheme employing OR and AND fusion rules are respectively given by

$$P_f^{CCS,OR} = \left[1 - \prod_{i=1}^{N} \left(1 - P_{f,i}\right)\right] = 1 - (1 - P_{f,i})^N, \tag{4.1}$$

$$P_d^{CCS,OR} = \left[1 - \prod_{i=1}^{N} \left(1 - P_{d,i}\right)\right] = 1 - (1 - P_{d,i})^N, \tag{4.2}$$

and

$$P_f^{CCS,AND} = \prod_{i=1}^{N} P_{f,i} = \left(P_{f,i}\right)^N \tag{4.3}$$

$$P_d^{CCS,AND} = \prod_{i=1}^{N} P_{d,i} = \left(P_{d,i}\right)^N. \tag{4.4}$$

The overall detection probability of the CCS scheme is obtained by fixing $P_{f,i}$ to a predefined level. Similarly, for the SSR scheme, the probabilities of detection and false-alarm are respectively given by

$$P_{f,C,1}^{SSR} = \sum_{i=1}^{2^N-1} \left[\prod_{C_l \in \Phi_i} P_{f,C_l}^{SSR} \prod_{C_m \in \overline{\Phi}} (1 - P_{f,C_m}^{SSR}) \right] = 1 - (1 - P_{f,C_i}^{SSR})^N. \tag{4.5}$$

Here Φ_i is the i^{th} possible combination of elements among the total 2^N elements in detection set Φ, and $\overline{\Phi}$ is the complement of the detection set Φ. Now, the overall probability of false-alarm at the center SU in the SSR scheme is given by [34]

$$P_f^{SSR} = P_{f,F}^{SSR} + (1 - P_{f,F}^{SSR}) P_{f,C,1}^{SSR} \tag{4.6}$$

Similarly, the probability that the center SU, F, correctly receives the decisions from other SUs $C_i, i = 1, \ldots, N$ in favor of $\mathcal{H}_1$ in T_2 slot is shown to be

$$P_{d,C,1}^{SSR} = \sum_{i=1}^{2^N-1} \left[\prod_{C_l \in \Phi_i} P_{d,C_l}^{SSR} \prod_{C_m \in \overline{\Phi}} (1 - P_{d,C_m}^{SSR}) \right] = 1 - (1 - P_{d,C_i})^N, \tag{4.7}$$

following which, the final detection probability of SSR can be calculated as [34]

$$P_d^{SSR} = P_{d,F}^{SSR} + (1 - P_{d,F}^{SSR}) P_{d,C,1}^{SSR} \tag{4.8}$$

Following the analysis similar to the SSR scheme, the probability that F receives an incorrect decision in favor of $\mathcal{H}_0$ from C_{sup} in T_2 slot for OSSR is obtained as

$$P_{f,C,1}^{OSSR} = \sum_{i=1}^{2^N-1} \left[\prod_{C_l \in \Phi_i} P_{f,C_l}^{SSR} \prod_{C_m \in \overline{\Phi}} (1 - P_{f,C_m}^{SSR}) \right] = 1 - (1 - P_{f,i})^N. \tag{4.9}$$

Now, the overall probability of false-alarm at the center SU in the OSSR scheme is given by

$$P_f^{OSSR} = 1 - \left\{ (1 - P_{f,F}^{OSSR}) + P_{f,F}^{OSSR} (1 - P_{f,C,1}^{OSSR}) \right\} \tag{4.10}$$

Similarly, the probability that F correctly receives the decisions from other SUs $\{C_i, i = 1, \ldots, N\}$ in favor of $\mathcal{H}_0$ in T_2 slot is shown to be

$$P_{d,C,1}^{OSSR} = \sum_{i=1}^{2^N-1} \left[\prod_{C_l \in \Phi_i} (1 - P_{d,C_l}^{OSSR}) \prod_{C_m \in \overline{\Phi}} P_{d,C_m}^{OSSR} \right] = 1 - (1 - P_{d,C_i})^N, \tag{4.11}$$

following which, the final detection probability of OSSR can be calculated as

$$P_d^{OSSR} = 1 - \left\{ (1 - P_{d,F}^{OSSR}) + P_{d,F}^{OSSR} (1 - P_{d,C,1}^{OSSR}) \right\} \tag{4.12}$$

In the next section, the main contributions of this chapter is discussed, i.e., analysis on the achievable throughput, energy consumption and energy efficiency of the OSSR scheme which follows the same trend corresponding to the SSR scheme considered in the previous chapter.

4.3 Formulation of Energy Efficiency Optimization for the OSSR Scheme

As mentioned earlier, energy efficiency is defined as the ratio of average throughput to the average energy consumption of a CR system [140, 148]. In the following, the details on the average throughput, average energy consumption for the CR network with OSSR scheme is described and later the governing optimization problem of designing η, β and N is provided such that the energy efficiency is maximized.

Table 4.1. Energy consumption and throughput achieved by the OSSR for different scenarios

Scenario	**Energy(joules)**	**Throughput(bits/Hz)**
$P(\mathcal{H}_1)\ P_{d,F}^{OSSR}\ P_{d,C,1}^{OSSR}$	$P_s\ T_0$+N $P_s\ T_1$	0
$P(\mathcal{H}_0)\ P_{f,F}^{OSSR} P_{f,C,1}^{OSSR}$	$P_s\ T_0$+N $P_s\ T_1$	$-\phi\mathtt{C}(T_{Total} - \beta T)$
$P(\mathcal{H}_1)\ (1 - P_{d,F}^{OSSR})$	$P_s\ T_0 + P_t(T_{Total} - T_0)$	$\kappa_c\mathtt{C}(T_{Total} - T_0)$
$P(\mathcal{H}_1)\ P_{d,F}^{OSSR}$ (1-$P_{d,C,1}^{OSSR}$)	$P_s\ T_0$+N $P_s\ T_1$+$P_tT_2 + P_t(T_{Total} - \beta T)$	$\kappa_c\mathtt{C}(T_{Total} - \beta T)$
$P(\mathcal{H}_0)\ (1 - P_{f,F}^{OSSR})$	$P_s\ T_0 + P_t(T_{Total} - T_0)$	$\mathtt{C}(T_{Total} - T_0)$
$P(\mathcal{H}_0)(P_{f,F}^{OSSR})\ (1 - P_{f,C,1}^{OSSR})$	$P_s\ T_0$+N $P_s\ T_1$+$P_tT_2 + P_t(T_{Total} - \beta T)$	$\mathtt{C}(T_{Total} - \beta T)$

In a CR network with OSSR scheme, the average throughput achievable depends on the communication between PU and SUs, and is categorized into four scenarios elaborated below.

S1. The first scenario corresponds to the case when PU is present, and the network correctly identifies its presence. This case corresponds to the situation where the decision is in favour of $\mathcal{H}_1$ is made at the end of time slot T_0 (i.e., by the center SU), and as a result it seeks cooperation from the other nodes, where node C_{sup} will also make a correct decision that the PU is present at the end of slot T_2, which occurs with probability $P(\mathcal{H}_1)\ P_{d,F}^{OSSR}\ P_{d,C,1}^{OSSR}$. Observe that in this scenario, the SU do not transmit data and the throughput achieved is zero.

S2. The second scenario covers the case when PU is absent but incorrectly declared as present by the network. This case corresponds to the situation where the the center SU make a false alarm, which favours $\mathcal{H}_1$ at the end of time slot T_0 by the center SU, and again it seeks cooperation from the other nodes, where node C_{sup} will also make an incorrect decision that the PU is present at the end of slot T_2, which occurs with probability $P(\mathcal{H}_0)\ P_{f,F}^{OSSR} P_{f,C,1}^{OSSR}$. Since the CR network misses a transmission opportunity, the throughput achieved in this case is given by $-\phi\mathtt{C}(T_{Total} - \beta T)$, where ϕ is a suitably chosen penalty factor [149].

S3. The third case corresponds to the scenario when both center SU and the node C_{sup} make incorrect decision that the PU is absent, when it is actually present. This case can be further divided in to two cases which corresponds to the situation where the decision in favour of $\mathcal{H}_0$ is made at the end of slot T_{Total} by the center SU, which occurs with the probability $P(\mathcal{H}_1)\ (1 - P_{d,F}^{OSSR})$ and in the case when center SU correctly declares $\mathcal{H}_1$, but the node C_{sup} incorrectly declares $\mathcal{H}_0$ with the probability $P(\mathcal{H}_1)\ P_{d,F}^{OSSR}$ (1-$P_{d,C,1}^{OSSR}$). However, even when this is the case, a partial throughput of $\kappa_c\mathtt{C}(T_{Total} - \beta T)$ units can still be achieved for some $0 \leq \kappa_c < 1$.

S4. The last case corresponds to where the achievable throughput is maximum. Again this case has two sub-cases. The first case corresponds to the situation where the center SU make a correct decision of absence of PU which occurs with probaility $P(\mathcal{H}_0)\ (1 - P_{f,F}^{OSSR})$. The second case corresponds to the situation where although center SU incorrectly declares the presence of PU, the node C_{sup} correctly declares the spectrum to be empty. This covers the situation when the PU is absent and both center SU and C_{sup} makes correct decisions, which occurs with probability $P(\mathcal{H}_0)(P_{f,F}^{OSSR})\ (1-P_{f,C,1}^{OSSR})$. In this case, the average throughput for the duration of $T_{Total} - \beta T$ is denoted as $\mathtt{C}(T_{Total} - \beta T)$ units, where $\mathtt{C}$ denotes the average data rate of SU transmission.

4.4 Energy Efficiency Analysis for the OSSR Scheme

Similar to the analysis in SSR, the achievable throughput and the energy consumption of the OSSR scheme can be divided into various scenarios, as detailed in Table. 4.1. It can be shown that the equations for the average throughput and energy consumption for OSSR are given by

$$\begin{aligned} R_{OSSR}(\varepsilon,\eta,\beta,N) &= \mathtt{C}(T_{Total}-T_0)\left\{P(\mathcal{H}_1)(1-P_{d,F}^{OSSR})\kappa_c + P(\mathcal{H}_0)(1-P_{f,F}^{OSSR}))\right\} \\ &+ \mathtt{C}(T_{Total}-\beta T)\left\{P(\mathcal{H}_1)P_{d,F}^{OSSR}(1-P_{d,C,1}^{OSSR})\kappa_c + P(\mathcal{H}_0)P_{f,F}^{OSSR}(1-P_{f,C,1}^{OSSR})\right. \\ &\left. -\phi P(\mathcal{H}_0)P_{f,F}^{OSSR}P_{f,C,1}^{OSSR}\right\}, \end{aligned} \tag{4.13}$$

$$\begin{aligned} E_{OSSR}(\varepsilon,\eta,\beta,N) &= P_sT_0 + NP_sT_1\left\{P(\mathcal{H}_1)P_{d,F}^{OSSR} + P(\mathcal{H}_0)P_{f,F}^{OSSR}\right\} \\ &+ [P_tT_2 + P_t(T_{total}-\beta T)]\left\{P(\mathcal{H}_1)P_{d,F}^{OSSR}(1-P_{d,C,1}^{OSSR}) + P(\mathcal{H}_0)(P_{f,F}^{OSSR})\right\} \\ &(1-P_{d,C,1}^{OSSR}) + P_t(T_{total}-T_0)\left\{1 + P(\mathcal{H}_1)P_{d,F}^{OSSR} - P(\mathcal{H}_0)P_{f,F}^{OSSR}\right\}. \end{aligned} \tag{4.14}$$

Recall that P_s and P_t denote the power required for each SU node for sensing and transmission, respectively. The energy consumption and average throughput for the OSSR scheme across all the scenarios mentioned are listed in Table 4.1.

The energy efficiency for the OSSR scheme is given by

$$EE_{OSSR}(\varepsilon,\eta,\beta,N) = \frac{R_{OSSR}(\varepsilon,\eta,\beta,N)}{E_{OSSR}(\varepsilon,\eta,\beta,N)} \tag{4.15}$$

Now, the energy efficiency optimization problem governing the OSSR scheme is given by

$$\mathcal{OP}_{OSSR} : \max_{\varepsilon,\eta,\beta,N} \quad EE_{OSSR}(\varepsilon,\eta,\beta,N) \tag{4.16}$$

$$\text{s.t.} \begin{cases} P_f^{OSSR} \leq \overline{P_f}, \\ P_d^{OSSR} \geq \overline{P_d}, \\ 0 \leq \beta \leq 1, \\ 0 \leq \eta \leq 1/3, \\ 1 \leq N \leq N_{max}, \end{cases} \tag{4.17}$$

for some $0 < \overline{P_f} < \overline{P_d} < 1$. Yet again, the above mentioned optimization problem is non-convex, and for the ease of analysis, the cost function of the above problem as in the SSR case is approximated. The details are provided in the next section.

4.5 Approximation and Problem Reformulation

Using the same set of assumptions as in the SSR case, the approximate throughput for OSSR scheme can be written as

$$\tilde{R}_{OSSR}(\varepsilon,\eta,\beta,N) \approx \mathtt{C}(T_{Total} - T_0)\left\{P(\mathcal{H}_0)(1 - P_{f,F}^{OSSR})\right\} + \mathtt{C}(T_{Total} - \beta T) \left\{P(\mathcal{H}_0)P_{f,F}^{OSSR}(1 - P_{f,C,1}^{OSSR}) - \phi P(\mathcal{H}_0)P_{f,F}^{OSSR}P_{f,C,1}^{OSSR}\right\}. \tag{4.18}$$

Assuming that $P_{f,F}^{OSSR} = P_{f,C_i}^{OSSR} = P_f$,
Further simplification gives

$$\tilde{R}_{OSSR}(\varepsilon,\eta,\beta,N) \approx \mathtt{C}(T_{Total} - T_0)\left\{P(\mathcal{H}_0)(1 - P_f)\right\} + \mathtt{C}(T_{Total} - \beta T) \left\{P(\mathcal{H}_0)P_f(-\phi + (\phi+1)(1 - P_f)^N\right\}. \tag{4.19}$$

Similarly approximate $\tilde{E}_{OSSR}$ can be written as

$$\begin{aligned}\tilde{E}_{OSSR}(\varepsilon,\eta,\beta,N) \approx\ & P_sT_0 + NP_sT_1[P(\mathcal{H}_1)P_{d,F}^{OSSR} + P(\mathcal{H}_0)P_{f,F}^{OSSR}] \\ & + [P_tT_2 + P_t(T_{Total} - \beta T)][P(\mathcal{H}_0)P_{f,F}^{SSR}(1 - P_{f,C,1}^{OSSR})] \\ & + P_t(T_{Total} - T_0)[1 - P(\mathcal{H}_1)P_{d,F}^{OSSR} - P(\mathcal{H}_0)P_{f,F}^{OSSR}]. \end{aligned} \tag{4.20}$$

Assuming that $P_{f,F}^{OSSR} = P_{f,C_i}^{OSSR} = P_f$, and $P_{d,F}^{OSSR} = P_{d,C_i}^{OSSR} = P_d$,
Further approximation gives

$$\begin{aligned}\tilde{E}_{OSSR}(\varepsilon,\eta,\beta,N) \approx\ & P_sT_0 + NP_sT_1[P(\mathcal{H}_1)P_d + P(\mathcal{H}_0)P_f] \\ & + [P_tT_2 + P_t(T_{Total} - \beta T)][P(\mathcal{H}_0)P_f(1 - P_f)^N] \\ & + P_t(T_{Total} - T_0)[1 - P(\mathcal{H}_1)P_d - P(\mathcal{H}_0)P_f]. \end{aligned} \tag{4.21}$$

Finally, the approximate energy efficiency can be written as

$$\tilde{EE}_{OSSR}(\varepsilon,\eta,\beta,N) \approx \frac{\tilde{R}_{OSSR}(\varepsilon,\eta,\beta,N)}{\tilde{E}_{OSSR}(\varepsilon,\eta,\beta,N)}, \tag{4.22}$$

and the optimization problem $\mathcal{OP}_{OSSR}$ can be reformulated as

$$\mathcal{OP}1_{OSSR}: \max_{\varepsilon,\eta,\beta,N} \quad \tilde{EE}_{OSSR}(\varepsilon,\eta,\beta,N) = \frac{\tilde{R}_{OSSR}(\varepsilon,\eta,\beta,N)}{\tilde{E}_{OSSR}(\varepsilon,\beta,\eta,N)} \tag{4.23}$$

$$\text{s.t.} \begin{cases} P_f^{OSSR} \leq \overline{P_f}, \\ P_d^{OSSR} \geq \overline{P_d}, \\ 0 \leq \beta \leq 1, \\ 0 \leq \eta \leq 1/3, \\ 1 \leq N \leq N_{max}, \end{cases} \tag{4.24}$$

The following theorem gives the optimal detection threshold that maximizes the objective function in $\mathcal{OP}1_{OSSR}$.

Theorem 4.1. *The constraint $P_d^{OSSR} \geq \overline{P_d}$ in the optimization problem $\mathcal{OP}1_{OSSR}$ is satisfied with equality. Consequently, the optimal detection threshold is given by*

$$\varepsilon^* = \sigma^2 \left[(\gamma + 1) + \sqrt{\frac{2\gamma + 1}{\eta \beta T f_s}} Q^{-1} \left(\sqrt{\frac{\overline{P_d}}{N}} \right) \right] \tag{4.25}$$

Proof. See Appendix B.

Now, by similar arguments used in the SSR case in the previous chapter, it can be shown that it is sufficient to choose the detection threshold such that the constraint $P_d^{OSSR} \geq \overline{P_d}$ is satisfied with equality. Since

$$P_d^{OSSR} = \overline{P_d} = P_d\{1 - [1 - P_d]^N\}, \tag{4.26}$$

the expression for the optimal detection threshold ε^* can be obtained directly.

Following the above result, the problem $\mathcal{OP}1_{OSSR}$ can be simplified in to $\mathcal{OP}2_{OSSR}$ as given by

$$\mathcal{OP}2_{OSSR} : \max_{\varepsilon^*, \eta, \beta, N} \quad \tilde{EE}_{OSSR}(\varepsilon^*, \beta, \eta, N) \tag{4.27}$$

$$\text{s.t.} \begin{cases} P_f^{OSSR} \leq \overline{P_f}, \\ 0 \leq \beta \leq 1, \\ 0 \leq \eta \leq 1/3, \\ 1 \leq N \leq N_{max}. \end{cases} \tag{4.28}$$

For the OSSR case, it is not straightforward to obtain closed form expression for $\frac{\partial EE_{OSSR}}{\partial \beta}$, and therefore, the optimal values β^* and η^* have to be numerically calculated. However, similar to the case of SSR scheme, β_{min} has a closed form expression and is given by

$$\beta_{min} = \left[\frac{1}{\left(\frac{\varepsilon^*}{\sigma^2} - 1\right)\left(\sqrt{\eta T f_s}\right)} Q^{-1} \left(\sqrt{\frac{\overline{P_d}}{N}} \right) \right]^2 \tag{4.29}$$

Based on the analytic development, search algorithm use in SSR scheme is used here to obtain the optimal values of ε, η, β and N for the optimization problem in $\mathcal{OP}1_{OSSR}$, which is summarized in Algorithm 3.

Algorithm 3 : Optimizing variables ε, β, and N

Set $P_s, P_t, T_{Total}, \tau, N, \beta_0, P(\mathcal{H}_0), P(\mathcal{H}_1), \overline{P_f}, \overline{P_d}$
procedure INITIALIZE $\beta = \beta_0, \eta = 1/3, P_d^{OSSR} = \overline{P_d}, EE_{OSSR}(0) = 0$ (,)
Initialize $\zeta \in \mathbb{R}$ such that $EE_{OSSR}(N+1) - EE_{OSSR}(N) < \zeta$
    $\boldsymbol{To\ select\ optimal}\ \varepsilon, \beta, N$
    for do $N = 1 : N_{max}$
        Calculate ε using (4.25)
        Calculate β_{min} using (4.29)
        Compute EE_{OSSR} using (4.16) with $\varepsilon(N)$ and $\beta_{min}(N)$
        Go to Step 5 if $EE_{OSSR}(N+1) - EE_{OSSR}(N) > \zeta$
        Stop iteration and return the optimal
        Calculate $EE_{OSSR}(N, \varepsilon^*, \beta^*)$
    end for
end procedure
Return $\max(EE_{OSSR})$ and the corresponding $N, \varepsilon^*, \beta^*$,

4.6 Numerical Results and Discussion: SSR vs. OSSR

In this section, the performances of OSSR in terms of energy efficiency is discussed and compared with that of SSR scheme analyzed in the previous chapter and the CCS schemes such as AND-based CCS, and OR-based CCS schemes, in terms of energy efficiency. MATLAB is used as a simulation tool. The parameter values are fixed as follows. The target probability of detection, $\overline{P_d}$, and false-alarm probability, $\overline{P_f}$, was chosen to be 0.9 and 0.1, respectively. The prior probabilities $P(\mathcal{H}_0)$ and $P(\mathcal{H}_1)$ was set to 0.75 and 0.25, respectively. The total frame duration was assumed to be $T_{Total} = 200$ ms. The sampling frequency at the local SUs was assumed to be $f_s = 1$ MHz, and the sensing power $P_s = 0.1$ W. The sensing time, τ, and reporting time, r, of CSS scheme was set to 100 μs. The achievable rate of secondary transmission was chosen to be $\mathtt{C} = \log_2(1 + \text{SNR}_s) = 6.6582$ bits/sec/Hz, where the SNR_s for the secondary transmission was assumed to be $\text{SNR}_s = 20$ dB. The transmission power of individual sensors, P_t, was assumed to be 3 W. The number of available users, N, was set to minimum of 10 following the condition (D1) in lemma 3.1, unless otherwise stated. Also, the partial throughput factor, κ_c, and the penalty factor, ϕ, was set to be 0.5 each.

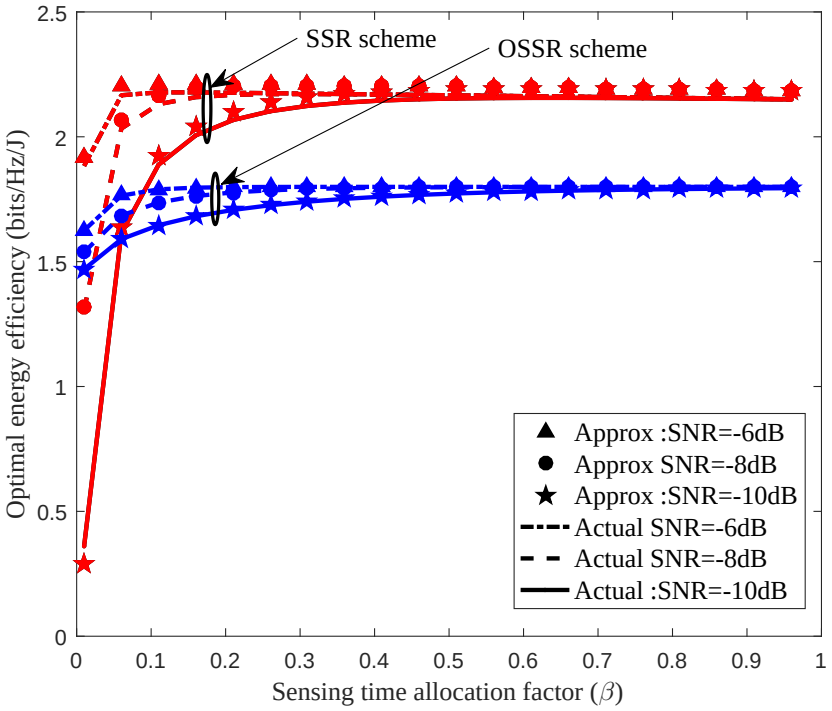

Figure 4.1. Variation of energy efficiency with β for SSR and OSSR schemes.

Figure 4.1 shows the variation of $EE_{SSR}(\varepsilon^*, \eta^*, \beta, N)$, $\tilde{EE}_{SSR}(\varepsilon^*, \eta^*, \beta, N)$, $EE_{OSSR}(\varepsilon^*, \eta^*, \beta, N)$ and $\tilde{EE}_{OSSR}(\varepsilon^*, \eta^*, \beta, N)$ versus β for different values of SNR. N is set as 10. It can be observed that all the cost functions are quasi-concave with respect to β, and the good match between the actual and approximation cost functions for SSR in (3.27) and (3.34), respectively, and those corresponding to OSSR validate the argument of considering the optimization of functions $\tilde{EE}_{SSR}(\varepsilon^*, \eta^*, \beta, N)$ and $\tilde{EE}_{OSSR}(\varepsilon^*, \eta^*, \beta, N)$. Also, as expected, the energy efficiency in all cases increases with an increase in SNR. For the rest of the analysis, we chose number of available SUs, N to be a fixed number for the ease of analysis. Moreover, we are interested in characterizing the energy efficiency performance for a fixed value of N. This characterization serves as a corner-case design, for a given value of the design parameter N.

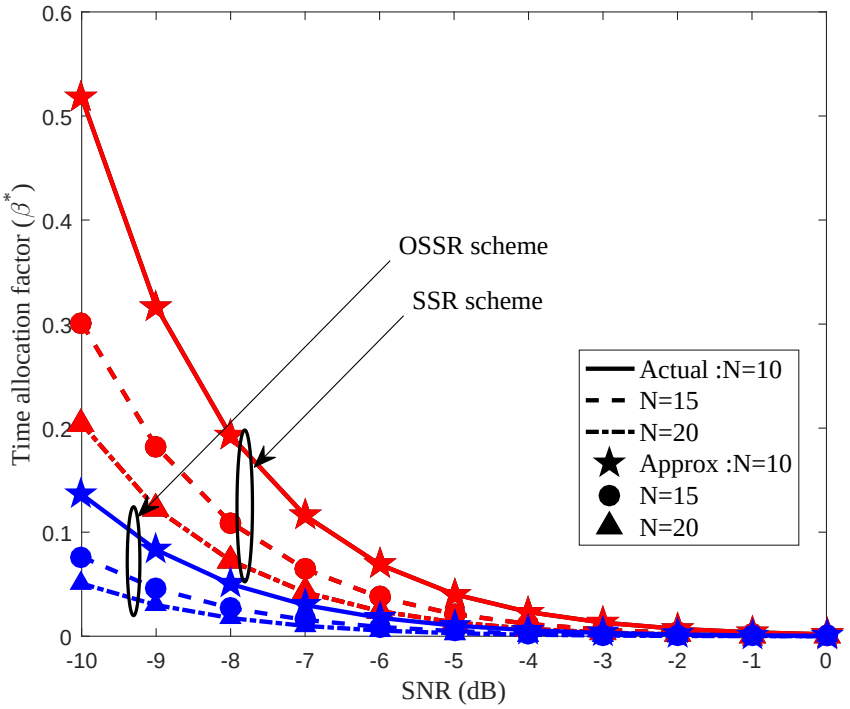

Figure 4.2. Variation of the optimal sensing time allocation factor (β) with SNR (dB).

Figure 4.2 shows the variation of β^*, the optimal β, as a function of SNR for different values of N. This curve highlights the fact that the optimal values of β are nearly equal for the actual and approximate energy efficiency for both SSR and OSSR. The decrease in β^* with an increase in SNR is intuitive, since it results in a better detection performance, which in turn results in better throughput and better efficiency. From Figures. 4.1 and 4.2, the performance analysis was considered only based on the approximated optimization problems for SSR and OSSR for subsequent discussions.

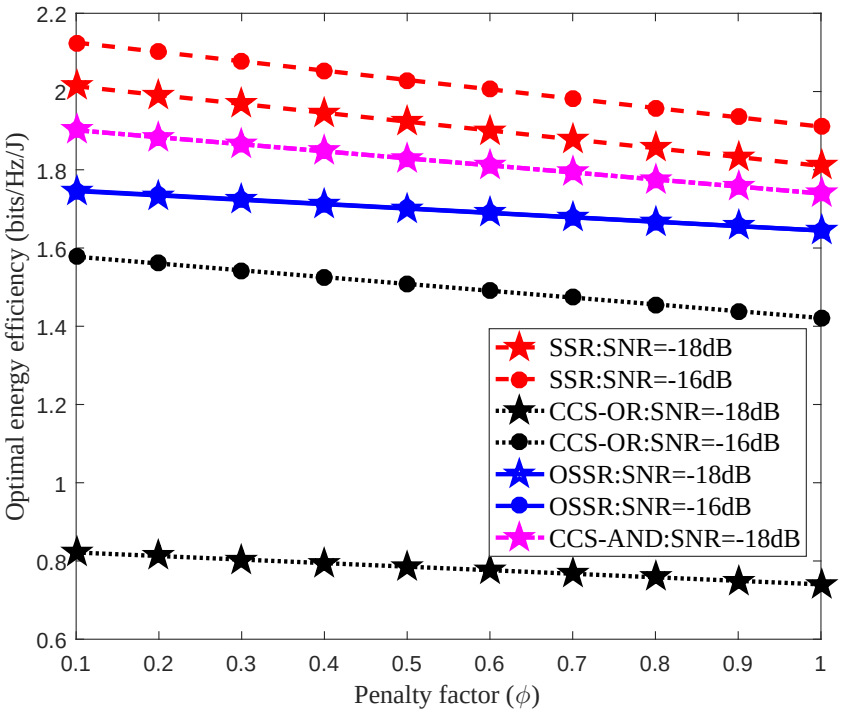

Figure 4.3. Variation of optimal energy efficiency with the penalty factor (ϕ) and $N = 13$.

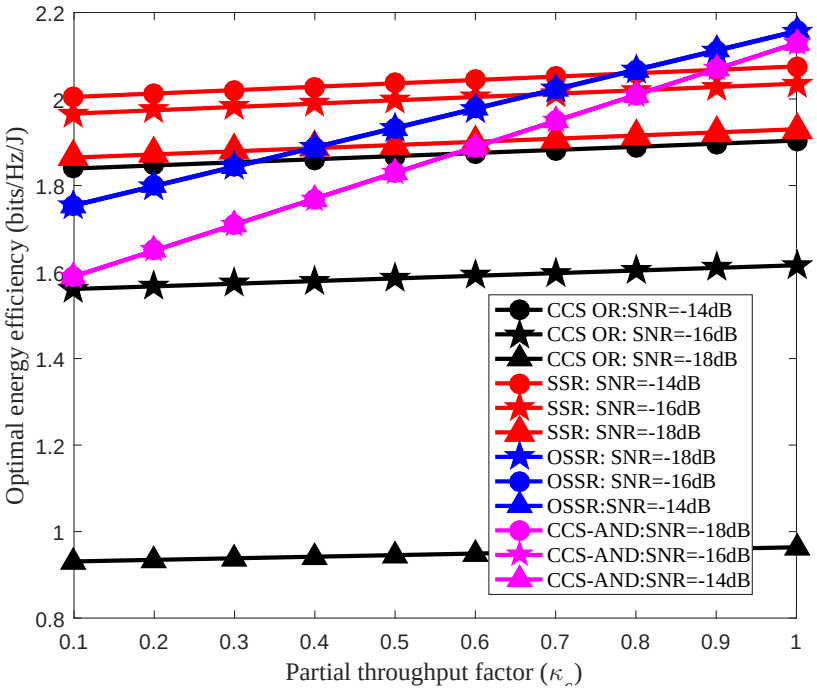

Figure 4.4. Variation of optimal energy efficiency with partial throughput factor (κ_c) and $N = 13$.

Next, the performance of all the schemes with respect to the penalty factor ϕ is considered in Figure 4.3. N is chosen to be 13, and $\kappa_c = 0.5$. It is evident that the energy efficiency decreases with an increase in ϕ, across all schemes. Again, the SSR scheme consistently offers the best performance in comparison with other schemes. However, the situation depicted in Figure 4.4 favors OSSR, where the performance of all the schemes are plotted for different values of the partial throughput factor κ_c, for $N = 13$ and $\phi = 0.5$. Since the OSSR scheme exploits the channel availability time to enhance the achievable throughput, for a given SNR, there exists a nontrivial κ_c above which OSSR outperforms SSR as well as the other schemes. Note that the improvement in the efficiency of the CCS-AND rule is due to the fact that it saves largely on energy consumption with a reduced throughput.

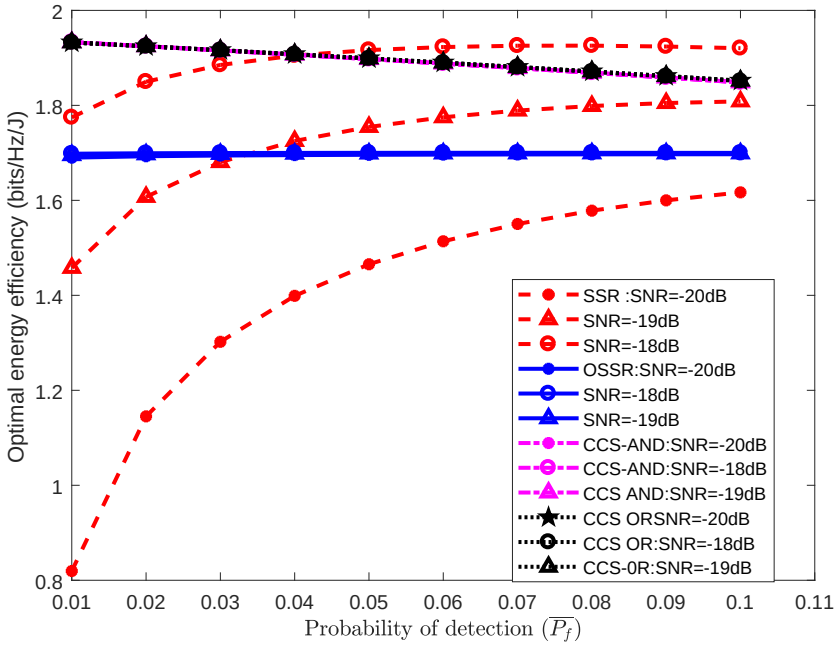

Figure 4.5. Variation of optimal energy efficiency with false alarm probability $(\overline{P}_f)$ and $N = 10$.

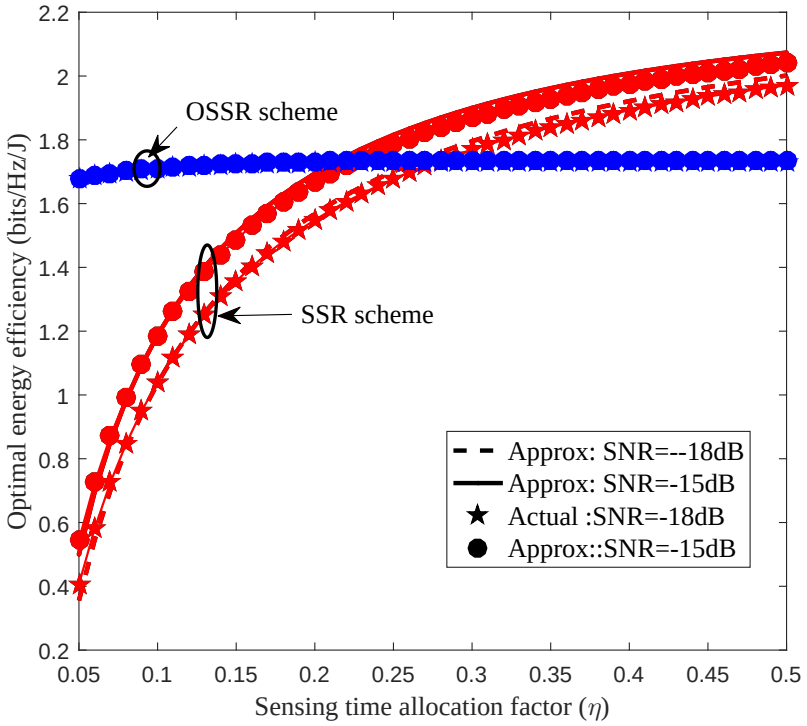

Figure 4.6. Variation of energy efficiency with sensing time allocation factor (η) and $N = 30$.

Figure 4.5 shows the variation of energy efficiency with the tolerance limit on the false-alarm probability, $\overline{P}_f$, with $N = 10$. As expected, the performance of all schemes increase with an increase in the tolerance limit. The SSR scheme performs the best as the SNR increases. At low SNRs, OSSR outperforms SSR, but offers no significant gain as SNR increases. The CCS methods also do not offer significant performance gain with SNRs, but outperform both SSR and OSSR schemes for low values of $\overline{P}_f$. This increase in energy efficiency is due to the saving in energy consumption.

Figure 4.6 shows the variation of actual and approximate energy efficiency values for SSR and OSSR schemes with η, for $N = 30$. Apart from reiterating on an earlier note that the approximate efficiency is close to the actual value, this plot also signifies the following. The variation of the performance of SSR with η is monotone, and hence the choice of $\eta^* = \frac{1}{3}$ is justified. However, it can be observed that η^* for OSSR can be arbitrary, and has to be chosen as $\eta^* = \max\{\eta^*, 1/3\}$ to ensure the non-negativity of time slots T_0, T_1 and T_2.

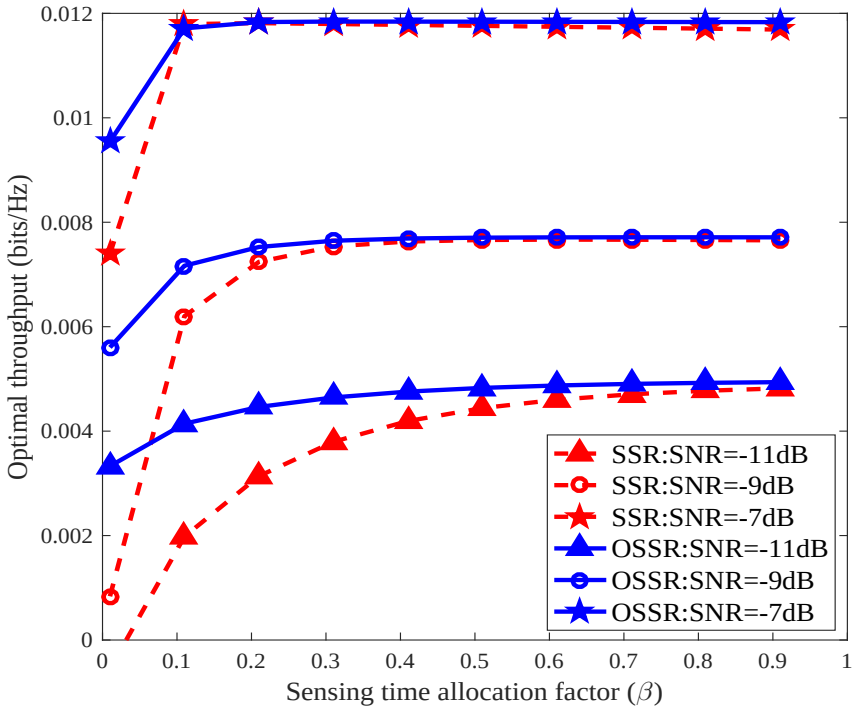

Figure 4.7. Variation of achievable throughput with sensing time allocation factor (β) and $N = 30$.

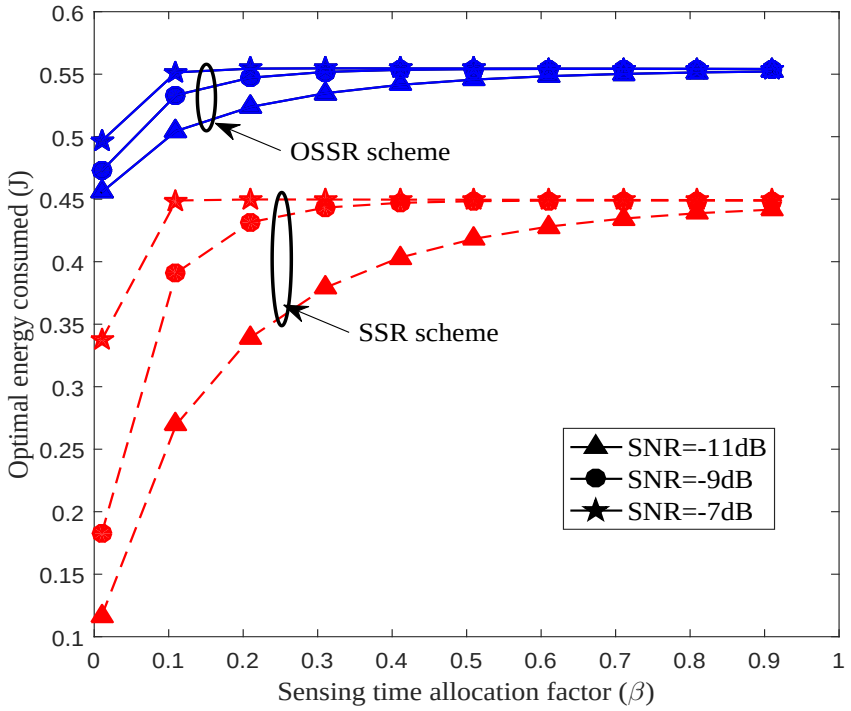

Figure 4.8. Variation of optimal energy consumption with sensing time allocation factor (β) and $N = 30$.

Finally, the tradeoff between the optimal performances of SSR and OSSR schemes are discussed. The achievable throughput and energy consumption for the optimal ε^*, η^*, and N on both SSR and OSSR schemes with respect to parameter β are shown in Figures. 4.7 and 4.8, respectively. For each value of SNR, as expected, the OSSR scheme yields a larger throughput, at the expense of larger energy consumption, as opposed to the SSR scheme which saves the consumed energy at the loss of throughput.

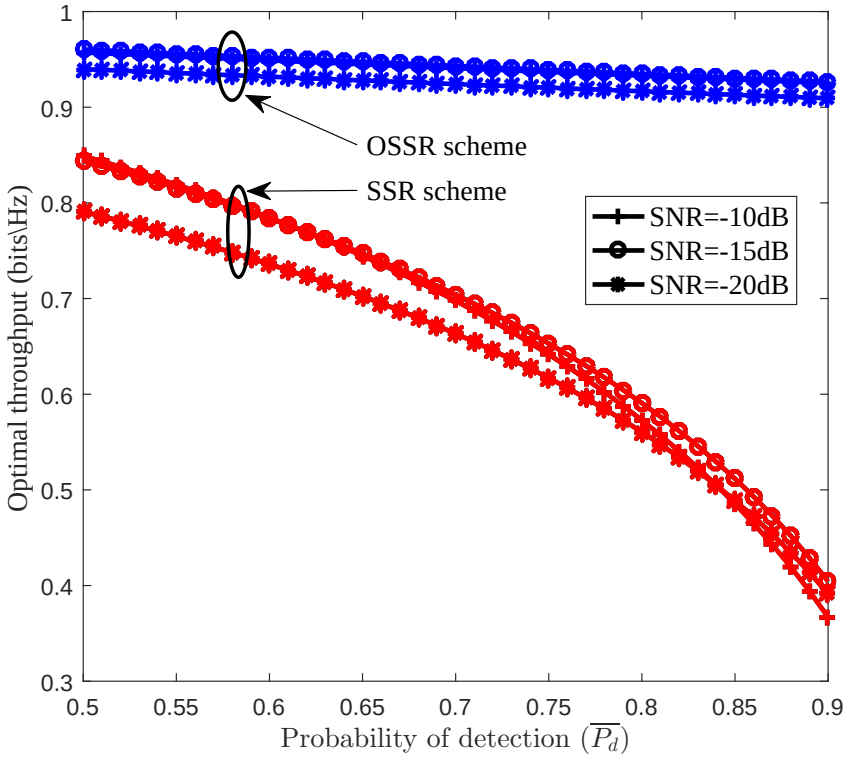

Figure 4.9. Variation of achievable throughput with detection probability ($\overline{P}_f$) and $N = 30$.

A similar trend can be seen in Figures. 4.9 and 4.10, where the throughput and energy consumption performance comparison is carried out for different values of $\overline{P}_d$. Interestingly, the throughput reduction and an increase in energy saving occurs at a faster rate in SSR as opposed to OSSR. Based on these trends, one would expect that the energy efficiency performance of both the schemes to be comparable in many cases. However, as seen in the previous plots (Figures. 4.3–4.6), the SSR scheme outperforms OSSR in many scenarios. This indicates that the energy consumption gets a larger priority in a CRN, as opposed to the achievable throughput. In other words, in the scenarios such as green cognitive radio communication systems, SSR scheme

is a better choice. However, in the scenarios where the saving of sensing and transmission energy is not a main concern, OSSR scheme could be employed.

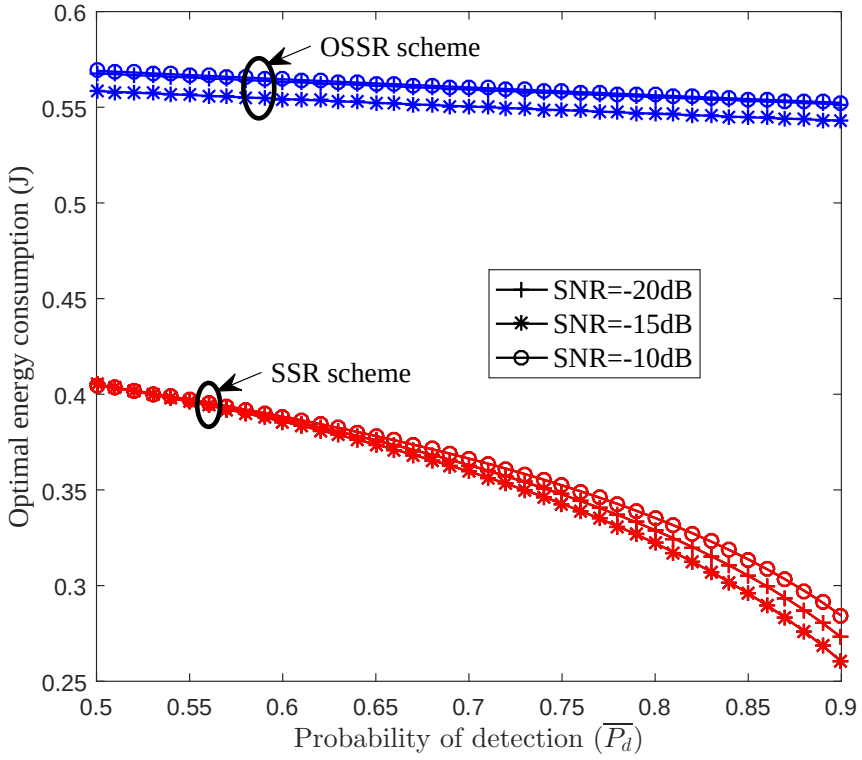

Figure 4.10. Variation of optimal energy consumption with detection probability ($\overline{P}_f$)and $N = 30$.

4.7 Summary

A variant of the SSR scheme called the opportunistic superior selective reporting (OSSR) scheme was proposed, and its energy efficiency analysis was carried out. Through numerical results, it was shown that the SSR and OSSR techniques outperform the conventional AND and OR fusion rule-based energy efficient schemes, and discussed the regimes where OSSR is preferred over SSR and vice-versa, in terms of the energy efficiency. It is shown that the trade off between the performances of SSR and OSSR schemes is the implicit trade off between the energy consumption and average throughput. Moreover, it is shown that the SSR scheme outperforms OSSR scheme in many scenarios. This indicates that the energy consumption gets a larger priority in a CRN, as opposed to the achievable throughput and therefore, in the scenarios such as green cognitive radio

systems, SSR scheme is a better choice. However, in the scenarios where the saving of sensing and transmission energy is not a main concern, OSSR scheme could be employed.

Another possibility of introducing energy efficiency in CCS is by optimally assigning a subset of nodes for spectrum sensing for a given PU channel. Therefore, it is beneficial to find optimal subset of nodes for spectrum sensing especially in energy constrained multichannel heterogeneous cognitive radio sensor network (HCRWSN). Towards this end in the next chapter, the performance of a multichannel heterogeneous cognitive radio network which employs energy harvesting nodes is analyzed and their relative advantages and tradeoffs are discussed.

Chapter 5

Throughput Efficient Selective Reporting based Spectrum Sensing in Heterogeneous Cognitive Radio Networks with Energy Harvesting Nodes

5.1 Introduction

Heterogeneous wireless sensor networks (HWSN) are envisioned to tailor the recent growth of wireless data services [155],[156]. With vastly increasing wireless traffic demands, realization of HWSN suffers from disadvantages such as drastic interference [115], which affects its spectral efficiency. A heuristic solution to mitigate this problem is to integrate the cognitive radio (CR) technology [2] with HWSN [116], collectively termed as *heterogeneous cognitive radio wireless sensor networks* (HCRWSN) [117]. In an HCRWSN, the deployed sensors periodically scan a primary user (PU) spectrum to detect the availability of vacant channels and the network assigns

data transmission over them, while guaranteeing a given PU interference level [118]. However, the periodic sensing increases the energy consumption, which is a critical issue in battery operated sensor networks. Thus energy harvesting (EH) is considered as one of the effective approaches for improving the energy efficiency of WSNs. EH-enabled sensors can harvest energy from either radio signals or ambient energy sources which enable them to operate continuously without battery replacement. Since spectrum sensors perform spectrum scanning at a much higher rate than data sensing which depletes the battery energy much faster than the data sensors, the average energy efficiency can be improved by using energy harvested spectrum sensors. Therefore, an HCRWSN with energy harvesting (EH) spectrum sensors [119] has been proposed to enhance both spectrum and energy efficiencies [77],[78],[79],[80].

In this chapter, an analysis on the throughput performance of an SSR-based, multi-channel HCRWSN is presented, and an optimization problem that maximizes the average achievable throughput is formulated to find the best sensor-to-channel assignment vector, subject to energy harvesting and interference constraints. Throughput analysis of a multi-channel HCRWSN, utilizing the SSR-based scheme has not been considered earlier in the literature.

The main contributions of this chapter are summarized as below.

- The average achievable throughput of an SSR-based, multi-channel HCRWSN is analyzed in terms of channel available time and detection accuracy.
- The problem of finding an optimal set of spectrum sensors scheduled for spectrum sensing for each channel such that the average network throughput is maximized, is formulated and solved by employing the cross entropy (CE) algorithm. The advantages of the CE algorithm in contrast to the exhaustive search algorithm, and a greedy algorithm are established.
- Through numerical results, it is shown that as the number of sensors increases, the SSR-based scheme outperforms the optimal CCS scheme in terms of average achievable throughput.
- A tradeoff between the average achievable throughput of SSR and CCS schemes is studied, which is the inherent tradeoff between the channel available time and detection accuracy. In other words, it is shown that as the number of spectrum sensors increases, the channel available time gets a larger priority in a HCRWSN than the detection accuracy.

The remainder of this chapter is organized as follows. The system model for multi-channel HCRWSN employing the SSR scheme is presented in Section 5.2. The spectrum sensor scheduling problem that maximizes the average achievable throughput for the SSR scheme is formulated and analyzed in Section 5.3. The results and discussions are presented in Section 5.4, and conclusions are provided in Section 5.5.

5.2 System Model

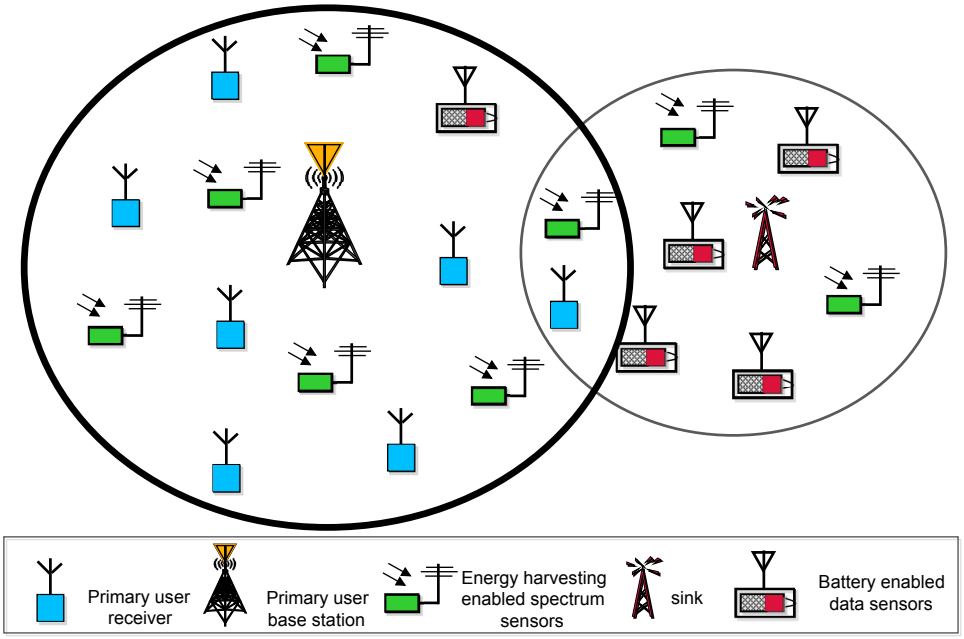

Figure 5.1. System model of the HCRWSN.

Consider a heterogeneous cognitive radio wireless sensor network (HCRWSN) with the following three types of nodes: M EH-enabled spectrum sensors, N battery powered data sensors and a sink or a fusion center, FC [117] as shown in Figure 5.1. It is assumed that the PUs are distributed within the coverage area of the HCRWSN. The licensed spectrum is divided into K non-overlapping channels of equal bandwidth W. The data sensors utilize the vacant channels declared by the spectrum sensors, on a priority basis. The FC controls the scheduling of both the spectrum sensors and data sensors. The scheduling of spectrum sensors is considered in this work. The set of spectrum sensors for each channel is assigned using the cross entropy (CE) algorithm, as discussed in [117]. It is assumed that each spectrum sensor can sense multiple orthogonal channels simultaneously [157, 158]. For cooperation in sensing, the superior selective reporting

(SSR) scheme [34] is used, which is explained in the next section. Later, the sink assigns the available channels to the data sensors for data transmission.

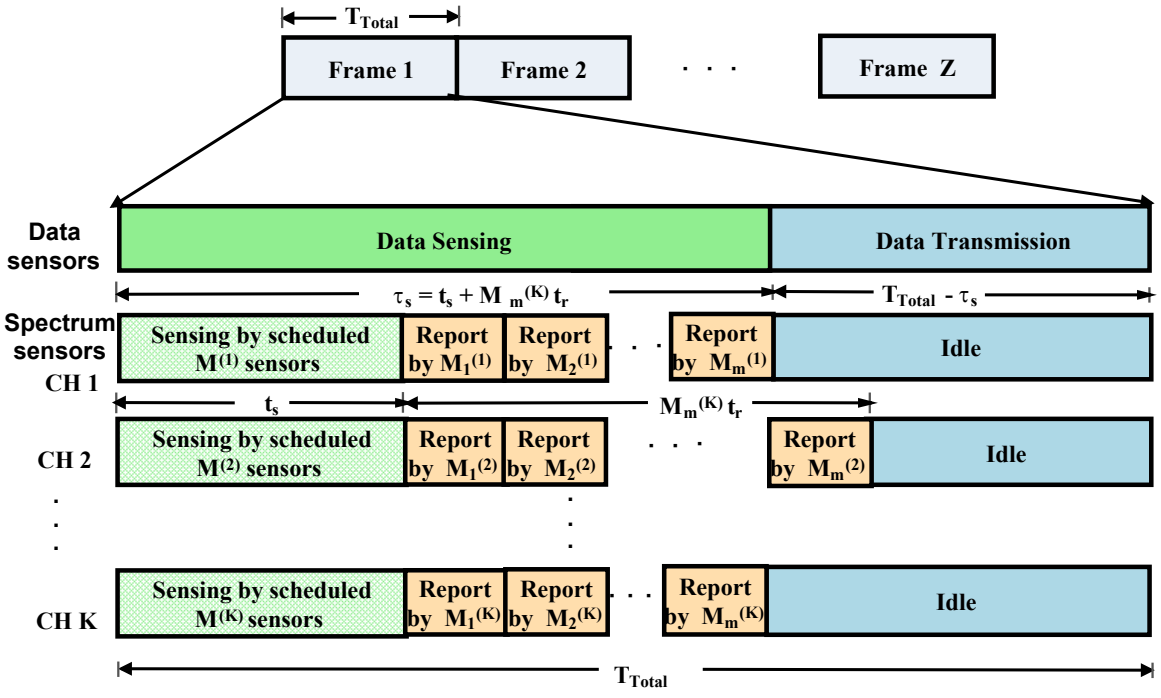

(a)

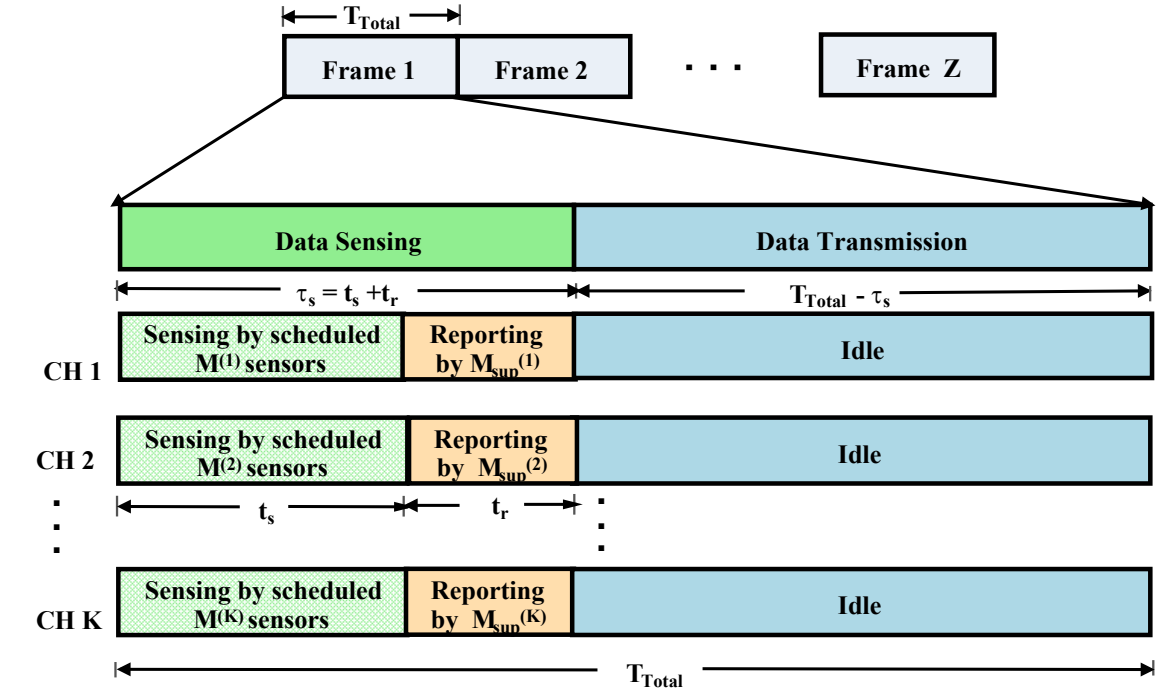

(b)

Figure 5.2. Frame structure of the HCRWSN for (a) CCS scheme and (b) SSR scheme.

The frame structure of HCRWSN is as shown in Figure 5.2. Periodic sensing is carried out with a frame period of T_{Total} seconds. Each frame duration is divided into two phases, namely, sensing phase and data transmission phase, given by τ_s and $T_{Total} - \tau_s$ units, respectively. In the sensing duration τ_s, a preassigned optimal subset of the M spectrum sensors, denoted by $M^{(k)}$, $k = 1, 2, \ldots, K$, simultaneously sense the presence of PU for a time t_s, and one among these $M^{(k)}$ sensors is selected based on their SNR to report its decision to the sink during reporting time slot t_r, corresponding to each channel. The advantage of employing the SSR scheme is that it increases the throughput and reduces the sensing overhead, when compared to conventional cooperative sensing (CCS) scheme using the OR rule [92]. Meanwhile, the data sensors collect information, and when the sink identifies all the available channels, the data sensors transmit data by utilizing all the available channels in the data transmission phase for a duration $T_{Total} - \tau_s$.

5.2.1 Conventional Cooperative Sensing (CCS) Scheme

Conventional cooperative sensing (CCS) scheme is a common technique employed during the sensing phase for a duration of t_s seconds, where a set of spectrum sensors are assigned to sense k^{th} channel for sensing. Subsequently, the remaining duration of the sensing time, that is $\tau_s - t_s$, is further divided into $M^{(k)}$ sub-slots for the transmission of the individual decisions by the nodes $\{M_m^{(k)}, m = 1, \ldots, M,\ k = 1, \ldots, K\}$ to the sink (fusion center) [139–141]. To save on the sensing overhead, it is assumed that each sensor transmits a one-bit decision over a dedicated, error free channel. Therefore, as shown in Figure 5.2(a), the sensing duration adds to a total of $\tau_s = t_s + M^{(k)} t_r$ units, where t_r denotes the reporting time-duration of each sub-slots. Hence, the sensing time τ_s increases linearly with $M^{(k)}$, which decreases the channel available time and hence the average achievable throughput. At the end of time slot τ_s, the sink collects the sensing results from all the scheduled spectrum sensors and combines these decisions by using a suitable fusion rule such as the AND rule [142], OR rule [143] or the L-out-of-M rule [144], and estimates the availability of the channels. In this work, the L-out-of-M rule is considered, since it is known to be Bayesian optimal [159]. The sensing duration of CCS scheme increases with $M^{(k)}$. To reduce the sensing overhead, a selective reporting based cooperative spectrum sensing scheme, namely superior selective reporting (SSR) scheme has been proposed [34], which is briefly explained next.

5.2.2 Superior Selective Reporting (SSR)-Based Sensing Scheme

The SSR scheme, originally proposed in [34], has multiple advantages over the CCS scheme that employs the OR rule, as the sink receives the decision only from the superior sensor, denoted by $M_{sup}^{(k)} = \underset{M_m \in \Phi_k}{\arg\max} \left(\gamma_{M_m} |h_{M_m,FC}|^2 \right)$, $m = 1, \ldots, M$, which is selected based on the received SNR between the FC and sensors across all sensors. The set of spectrum sensors $M^{(k)}$ that detect the presence of PU constitute a detection set Φ_k, $k = 1, \ldots, K$. Each sensor $\{M_m \in \Phi_k\}$ sets off a timer at the end of sensing phase, with each initial values $\{\mathtt{T}_m, M_m \in \Phi_k\}$ set inversely proportional to its received SNR $\gamma_{M_m} |h_{M_m,FC}|^2$ [34], where γ_{M_m} and $h_{M_m,FC}$ denote the SNR and the fading coefficient of the channel from the FC to M_m, $m = 1, \ldots, M$, respectively, i.e., $\mathtt{T}_m = \mu / (\gamma_{M_m} |h_{M_m,FC}|^2)$, for some $\mu \in \mathbb{R}^+$. The sensor with highest SNR, termed as the superior sensor, exhausts its timer first and reports to the FC. Hence, only the superior sensor sends its local decision to sink in time slot t_r by transmitting a short duration flag packet, signaling its presence. All other sensors, waiting for their timer to expire, back off immediately as soon as they hear this flag packet[146].

5.2.3 Performance Analysis with Energy Detection

As mentioned earlier, energy detector (ED) is employed in this work to detect the presence of the PU. In this section, the performance analysis of energy detection strategies that employ CCS and SSR schemes are discussed.

5.2.3.1 CCS Scheme

For the CCS scheme, probabilities of signal detection and false-alarm at m^{th} sensor sensing k^{th} channel are given by [117]

$$P_f(m,k) = Q\left(\left(\frac{\varepsilon}{\sigma^2} - 1 \right) \sqrt{U} \right) \triangleq \overline{P_f}, \tag{5.1}$$

$$P_d(m,k) = Q\left(\frac{Q^{-1}(\overline{P_f}) - \sqrt{U}\gamma_{mk}}{\sqrt{2\gamma_{mk} + 1}} \right), \tag{5.2}$$

where $Q(\cdot)$ is the complementary CDF of the standard Gaussian distribution, and γ_{mk} denotes the received SNR from the PU at the k^{th} channel by the m^{th} sensor. U is the average number of samples of the received signal at the m^{th} spectrum sensors on the k^{th} channel. The PU signal is assumed to be a complex-valued PSK signal and the noise is circularly symmetric complex Gaussian with zero mean and variance σ^2 [160]. Without loss of generality, the detection threshold ε is set to be the same for all the sensors. The overall probabilities of false-alarm and detection at the k^{th} channel for the CCS scheme [140] is obtained by fixing $P_f(m,k)$ to a predefined level $\overline{P_f} \in (0,1)$, as

$$\begin{aligned} G_f^{ccs}(k) &= \sum_{n=L^{(k)}}^{M^{(k)}} \binom{M^{(k)}}{n} P_f(m,k)(1-P_f(m,k))^{M^{(k)}-n} \\ &= \sum_{n=L^{(k)}}^{M^{(k)}} \binom{M^{(k)}}{n} \overline{P_f}(1-\overline{P_f})^{M^{(k)}-n} \qquad (5.3) \\ G_d^{ccs}(k) &= \sum_{n=L^{(k)}}^{M^{(k)}} \binom{M^{(k)}}{n} P_d(m,k)(1-P_d(m,k))^{M^{(k)}-n}, \qquad (5.4) \end{aligned}$$

where the total number of cooperating sensors for sensing k^{th} channel is $M^{(k)}$, and the value of L determines the fusion rule used. The optimum value of L is given by [159]

$$L_{opt}^{(k)} = \min\left(M^{(k)}, \left\lceil \frac{\log\left(\frac{P(\mathcal{H}_0)}{1-P(\mathcal{H}_0)}\right) + M^{(k)} \log\left(\frac{1-P_f(m,k)}{P_m(m,k)}\right)}{\log\left\{\left(\frac{1-P_m(m,k)}{P_f(m,k)}\right)\left(\frac{1-P_f(m,k)}{P_m(m,k)}\right)\right\}} \right\rceil \right), \qquad (5.5)$$

where only those $P_f(m,k)$ and $P_m(m,k)$ values for $m \in M^{(k)}$ are used to evaluate (5.5) for each $k = 1, \ldots, K$. If $L^{(k)}$ is chosen as either $M^{(k)}$, 1 or $\lceil M^{(k)}/2 \rceil$, the L-out-of-M rule reduces to the AND, OR or Majority fusion rules, respectively. As mentioned previously, the optimum fusion rule with L as given in (5.5) is considered. However, for a comparative study, the CCS scheme with AND and OR rules are considered later, which have their associated advantages and disadvantages [26, 143].

5.2.3.2 SSR Scheme

The method of choosing the superior SU and calculating the received SNR is followed as described in [34, 92]. The probabilities of false-alarm, $G_f(k)$, and signal detection, $G_d(k)$, at the FC are given, respectively, as [147]

$$G_f(k) = \sum_{j=1}^{2^{M^{(k)}}-1} \left[\prod_{m \in \Phi_{j,k}} P_{f,C_l}^{SSR} \prod_{m \in \overline{\Phi}_{j,k}} (1 - P_{f,C_m}^{SSR}) \right] \tag{5.6}$$

$$= 1 - (1 - \overline{P_f})^{M^{(k)}}, \tag{5.7}$$

$$G_d(k) = 1 - \prod_{m=1}^{M^{(k)}} (1 - P_d(m,k))^{M^{(k)}}. \tag{5.8}$$

Here, $\Phi_{j,k}$ is the j^{th} nonempty sub-collection of detection set Φ_k, and $\overline{\Phi}_{j,k}$ is the complement of $\Phi_{j,k}$. In contrast to the optimal CCS scheme with L-out-of-M fusion rule, the advantage of the SSR scheme is in saving the reporting time t_r, which increases the channel available time for data transmission vide Figure 5.2, and thereby improving the average achievable throughput for secondary transmission over the k^{th} channel. Next, the main contribution of this chapter is considered, i.e., an optimization problem is formulated for finding the best subset of spectrum sensors per channel, $M^{(k)}$, to maximize the network throughput for a given PU interference constraint.

5.3 Problem Formulation: Optimal Scheduling

The average number of bits transmitted by the data sensors across all K channels in one time duration is defined as the average achievable throughput of a HCRWSN [117]. Consider a sensor-to-channel assignment matrix $\mathbf{J} \in \{0,1\}^{M \times K}$. Let the $(m,k)^{\text{th}}$ element $[\mathbf{J}]_{m,k}$, $m = 1, \ldots, M$, $k = 1, \ldots, K$ of 1 indicate that the sensor m is scheduled for spectrum sensing for channel k, and 0 otherwise. This work aims to find the optimal $\mathbf{J}$ that maximizes the average throughput in the considered HCRWSN. The average achievable throughput depends on the available time for data transmission, probability that favors the inactive state of PU, $P(\mathcal{H}_0)^{(k)}$, of the k^{th} channel, $P_f(m,k)$, $P_d(m,k)$, and the channel capacity, $\mathtt{C}$. The PU dynamics over each

channel is modeled as a stationary exponential ON-OFF random process [117], with the average available time of the k^{th} channel being the product of stay-over time and the stationary probability. Let $T_{ON}^{(k)} = 1/\lambda_0^{(k)}$ and $T_{OFF}^{(k)} = 1/\lambda_1^{(k)}$ be the average values of the stay-over time of the ON state and OFF state of k^{th} channel respectively, where $\lambda_0^{(k)}$ denotes the transition rate from the ON state to OFF state on the k^{th} channel and $\lambda_1^{(k)}$ denotes the transition rate in the opposite direction. The stationary probabilities of the ON and OFF states of PU on each channel are given by [117]

$$P(\mathcal{H}_1)^{(k)} = \frac{\lambda_1^{(k)}}{\lambda_1^{(k)} + \lambda_0^{(k)}}, \quad P(\mathcal{H}_0)^{(k)} = \frac{\lambda_0^{(k)}}{\lambda_1^{(k)} + \lambda_0^{(k)}}. \tag{5.9}$$

The average achievable network throughput under four possible scenarios are as listed as below.

S1. In this scenario, the spectrum sensors successfully detect the absence of PUs with probability $P(\mathcal{H}_0)^{(k)}\ (1 - G_f(k))$. The throughput for this scenario is expressed as $P(\mathcal{H}_0)^{(k)}\left[1-\bar{P}_f\right]^{\sum_{m=1}^{M}[J]_{m,k}}$ $I_{d,SSR}^{(k)}\,\mathtt{C}^{(k)}(T_{Total}-\tau_s)$, where $I_{d,SSR}^{(k)}$ is a binary variable introduced as a constraint to satisfy the PU protection requirement are respectively, defined as

$$I_{d,SSR}^{(k)} = \begin{cases} 1 & \text{if } 1 - G_d(k) < \overline{PM}_{thr}, \\ 0 & \text{otherwise.} \end{cases} \tag{5.10}$$

Similarly, the throughput for the CCS case can be obtained for this scenario (Table 5.1) via the corresponding indicator function defined as:

$$I_{d,CCS}^{(k)} = \begin{cases} 1 & \text{if } 1 - G_d^{ccs}(k) < \overline{PM}_{thr}, \\ 0 & \text{otherwise.} \end{cases} \tag{5.11}$$

That is, in both cases, if the probability of miss of the k^{th} channel exceeds a predefined threshold $\overline{PM_{thr}} \in (0, 1)$, the decision is said to be unreliable for communication over the k^{th} channel.

S2. Here, the sensors correctly detect the PU as active, with probability $P(\mathcal{H}_1)^{(k)}G_d(k)$, which results in no throughput. Similarly, no throughput can be achieved in the CCS case.

S3. In this scenario, the sensors falsely detect the PU to be present, with probability $P(\mathcal{H}_0)^{(k)}G_f(k)$. Here, since the CR network misses a transmission opportunity, the throughput achieved is given by $P(\mathcal{H}_0)^{(k)}\left[1-(1-\overline{P}_f)^{\sum_{m=1}^{M}[\mathbf{J}]_{m,k}}\right]\ I_{d,SSR}^{(k)}\ \mathtt{C}^{(k)}\ (T_{Total}-\tau_s)(-\phi)$, where $\phi \in (0,1)$ is a suitably chosen penalty factor.

S4. In this scenario, the sensors make an incorrect decision that the PU is absent, with probability $P(\mathcal{H}_1)^{(k)}(1-G_d(k))$. The network causes interference to the PU, with a partial throughput of $\kappa\ P(\mathcal{H}_1)^{(k)}\left[1-P_d(m,k)\right]^{\sum_{m=1}^{M}[\mathbf{J}]_{m,k}}\ I_{d,SSR}^{(k)}\ \mathtt{C}^{(k)}\ (T_{Total}-\tau_s)$, with some $\kappa \in (0,1)$.

The throughput achieved due to the CCS and SSR schemes across all the scenarios are listed in Table . 5.1. Following these cases, average achievable throughput of the SSR scheme is given by:

$$R_{SSR}=\sum_{k=1}^{K}\Bigg\{P(\mathcal{H}_0)^{(k)}\big[1-\overline{P}_f\big]^{\sum\limits_{m=1}^{M}[\mathbf{J}]_{m,k}}-\phi P(\mathcal{H}_0)^{(k)}\left[1-(1-\overline{P}_f)^{\sum\limits_{m=1}^{M}[\mathbf{J}]_{m,k}}\right]+P(\mathcal{H}_1)^{(k)}[1-P_d(m,k)]^{\sum\limits_{m=1}^{M}[\mathbf{J}]_{m,k}}\kappa\Bigg\}I_{d,SSR}^{(k)}\ \mathtt{C}^{(k)}(T_{Total}-\tau_s), \tag{5.12}$$

for some $0 \leq \kappa < 1$, and $\phi \geq 0$. On the other hand, the average achievable throughput for the CCS scheme vide Table. 5.1 is given by

Table 5.1. Throughput achieved for different scenarios using CCS and SSR schemes.

CCS Scheme		SSR Scheme	
Scenario	Throughput (bitz/Hz)	Scenario	Throughput (bitz/Hz)
S1: $P(\mathcal{H}_0)^{(k)}(1-G_f^{ccs}(k))$	$I_{d,CCS}^{(k)}\,\mathtt{C}^{(k)}(T_{Total}-(t_s+M^{(k)}t_r))$	$P(\mathcal{H}_0)^{(k)}(1-G_f(k))$	$I_{d,SSR}^{(k)}\,\mathtt{C}^{(k)}(T_{Total}-(t_s+t_r)$
S2: $P(\mathcal{H}_1)^{(k)}G_d^{ccs}(k)$	0	$P(\mathcal{H}_1)^{(k)}G_d(k)$	0
S3: $P(\mathcal{H}_0)^{(k)}G_f^{ccs}(k)$	$I_{d,CCS}^{(k)}\,\mathtt{C}^{(k)}\,(T_{Total}-(t_s+M^{(k)}t_r))(-\phi)$	$P(\mathcal{H}_0)^{(k)}G_f(k)$	$I_{d,SSR}^{(k)}\,\mathtt{C}^{(k)}\,(T_{Total}-(t_s+t_r))(-\phi)$
S4: $P(\mathcal{H}_1)^{(k)}(1-G_d^{ccs}(k))$	$I_{d,CCS}^{(k)}\,\mathtt{C}^{(k)}\,(T_{Total}-(t_s+M^{(k)}t_r))(\kappa)$	$P(\mathcal{H}_1)^{(k)}(1-G_d(k))$	$I_{d,SSR}^{(k)}\,\mathtt{C}^{(k)}\,(T_{Total}-(t_s+t_r))(\kappa)$

For the spectrum sensor scheduling problem, the constraints are set related to the energy harvesting (EH) dynamics to facilitate the sustainability of the sensors. In a given frame T_{Total}, the energy consumption of each sensor should not exceed the EH rate, i.e., $\big(\sum_{k=1}^{K}[\mathbf{J}]_{m,k}\big)e_s \leq \delta_m\, T_{Total}\ \forall m$, where δ_m is the EH rate. Now, the problem to find the optimum $\mathbf{J}$ that maximizes R_{SSR} can be formulated as follows:

$$\mathcal{OP}_{SSR}: \max_{\mathbf{J}} \quad R_{SSR} \tag{5.13}$$

$$\text{s.t.} \quad \begin{cases} \big(\sum_{k=1}^{K}[\mathbf{J}]_{m,k}\big)e_s \leq \delta_m\, T_{Total}, \quad \forall\, m \\ [\mathbf{J}]_{m,k} = \{0,1\}, \quad \forall m,k \end{cases} \tag{5.14}$$

Similarly, the throughput optimization problem governing the CCS scheme is given by

$$\mathcal{OP}_{CCS}: \max_{\mathbf{J}} \quad R_{CCS} \tag{5.15}$$

$$\text{s.t.} \quad \begin{cases} \big(\sum_{k=1}^{K}[\mathbf{J}]_{m,k}\big)e_s \leq \delta_m\, T_{Total}, \quad \forall\, m \\ [\mathbf{J}]_{m,k} = \{0,1\}, \quad \forall m,k \end{cases} \tag{5.16}$$

From (5.12), it is clear that as more channels are assigned to a given set of sensors, i.e., as $\sum_{k=1}^{K}[\mathbf{J}]_{m,k}$ increases, the value of $(1-\overline{P}_f)^{\sum_{m=1}^{M}[\mathbf{J}]_{m,k}}$ decreases, and $I_{d,SSR}$ tends to unity. Therefore, there is a tradeoff between the values of $(1-\bar{P}_f)^{\sum_{m=1}^{M}[\mathbf{J}]_{m,k}}$ and $I_{d,SSR}$. As a consequence, as M increases, there exist a tradeoff between the detection accuracy and the channel available time, which affects the average achievable throughput of the network. The optimization problem $\mathcal{OP}_{CCS}$ and $\mathcal{OP}_{SSR}$, are integer programming problem, that can be solved by using exhaustive search method. However, this leads to a search space of 2^{MK} elements which are computationally expensive. Hence, the cross entropy (CE) algorithm is applied as discussed in [117]. Therefore, the problem $\mathcal{OP}_{SSR}$ is transformed into the following unconstrained optimization problem, by applying a penalty of $\omega \in \mathbb{R}^{+}$ for violating any of the constraints [117]:

$$\max_{\mathbf{J}} \quad R_{SSR} - \omega I_{\left(\sum\limits_{k=1}^{K}[\mathbf{J}]_{m,k}e_s > \delta_m T_{Total}\right)}, \tag{5.17}$$

The unconstrained optimization problem for CCS case can be written as

$$\max_{\mathbf{J}} \quad R_{CCS} - \omega I_{\left(\sum_{k=1}^{K} [\mathbf{J}]_{m,k} e_s > \delta_m T_{Total}\right)}, \tag{5.18}$$

where $I(\cdot)$ is the indicator function. When the solution violates the constraints, the objective function evaluates to a negative value, which is discarded. The CE algorithm is implemented as discussed below [117]. Initially, the iteration counter is set as $i = 1$ to $i_{\max} \in \mathbb{Z}^+$. Let $\mathbf{C}$ be the set of all possible K-dimensional binary vectors, with $|\mathbf{C}| = 2^K$. To begin with, the row vectors of $\mathbf{J}$ are drawn from the matrix $\mathbf{C}$. Now, Z samples of channel matrix, defined as $\mathbf{V}^{(z)} = \mathbf{v}_{m,\mathbf{c}}^{(z)}, 1 \leq m \leq M, \mathbf{c} \in \mathbf{C}$, $z = 1, \ldots, Z$ of size $M \times 2^K$. Here, $\mathbf{v}_{m,\mathbf{c}}^{(z)}$ denotes the $\mathbf{c}^{\text{th}}$ column vector or $\mathbf{V}^{(z)}$. These column vectors are generated based on a probability mass function (PMF) matrix $\mathbf{Q}^{(i)} = \mathbf{q}_{m,\mathbf{c}}^{(i)}, 1 \leq m \leq M, \mathbf{c} \in \mathbf{C}$, where $\mathbf{q}_{m,\mathbf{c}}^{(i)}$ denotes the probability vector that the sensor m is scheduled to sense the channel k in vector $\mathbf{C}$. Now, the cost function in (5.17) is calculated for each sample z, and arrange them in descending order.ρ ($0 \leq \rho \leq 1$) fraction of sorted objective function values $\mathcal{OP}_{SSR}^{(z)}$ are retained and all other values are discarded. Let the smallest chosen value of the objective function be η, corresponding to the index $\lceil \rho Z \rceil$. In each step, the PMF matrix is updated as $\mathbf{q}_{m,\mathbf{c}}^{(i+1)} = \frac{\sum_{z=1}^{Z} \mathbf{v}_{m,\mathbf{c}}^{(z)} I_{(O^z \geq \eta)}}{\lceil \rho Z \rceil}$. The algorithm is stopped after $i_{\max}$ iterations, and the resultant $\mathbf{V}^{(z)}$ is selected to map the solution, i.e., the optimal $\mathbf{J}$. To summarize, each iteration of the CE algorithm consists of the steps described in Algorithm 4. Similar procedure is carried out to evaluate the optimal $\mathbf{J}$ for the CCS scheme.

5.4 Results and Discussion

In this section, the performance of SSR-based sensing scheme in HCRWSN is discussed in terms of average achievable throughput, and compare its performance with the CCS scheme following the L-out-of-M rule, with an optimum L chosen as in [159]. We evaluate the performance of the CE algorithm in the spectrum-sensing phase through performing simulations using MATLAB. The parameter values are set as mentioned in Table. 5.2. The sensors are randomly placed in a circular area where the primary user coexists. The channel gain from PU transmitter to the sensor is calculated as $1/D^{\alpha}$, where D is the distance between PU and the spectrum sensors and α is the

Algorithm 4 : Cross Entropy (CE) algorithm

procedure INITIALIZATION
Step 1:
    for i $\leftarrow$ 1 to $i_{\max}$ **do**
        $\mathbf{q}_{m,\mathbf{c}}^{(1)} = 1/|\mathbf{C}| = 1/2^K$
        for z $\leftarrow$ 1 to Z **do**
Step 2: Generate Z samples of matix $\mathbf{V}^{(z)}$ based on PMF matix $\mathbf{Q}^{(i)} = \mathbf{q}_{m,\mathbf{c}}^{(i)}$
        end for
Step 3:
        for z $\leftarrow$ 1 to Z **do**
      Calculate the Objective function in (5.17) $\mathcal{OP}_{SSR}^{(z)}$
        end for
Step 4: Arrange $\{\mathcal{OP}_{SSR}^{(z)}, z = 1, \ldots, Z\}$ in the decreasing order
Step 5:
        Retain $0 \leq \rho \leq 1$ fraction of sorted values $\{\mathcal{OP}_{SSR}^{(z)}\}$ and discard others.
        Let the smallest chosen value of $\mathcal{OP}_{SSR}^{(z)}$ be η, corresponding to the index $\lceil \rho Z \rceil$.
Step 6:
        for j $\leftarrow$ 1 to M **do**
            for $\mathbf{c} = 1 : \mathbf{C}$ **do** Update $\mathbf{q}_{m,c}^{i+1}$ using
                $\mathbf{q}_{m,\mathbf{c}}^{(i+1)} = \frac{\sum_{z=1}^{Z} \mathbf{v}_{m,\mathbf{c}}^{(z)} I_{(O^z \geq \eta)}}{\lceil \rho Z \rceil}$.
            end for
        end for
    end for
Step 7:
    Return $\mathbf{V}^{(z)}$
Step 8:
        The channels-to-sensors assignment in $\mathbf{V}^{(z)}$ is mapped to the channels-to-sensors assignment in $\mathbf{J}$ which is a solution to the original optimization problem $\mathcal{OP}_{SSR}^{(z)}$.
end procedure

path-loss exponent. The achievable rates by data sensors are chosen to be $C = \log_2(1 + SNR) = 6.658$ bits/sec/Hz [117].

Table 5.2. Parameter Settings

Parameters	**Settings**
Number of spectrum sensors M	10
Number of data sensors N	30
Target false alarm probability $\bar{P_f}$	0.1
Target miss- detection probability $\bar{P_m}$	0.1
Number of Licensed channel	7
Bandwidth of the licensed channel W	6MHz
Path-loss exponent α	3.5
Transition rate of PU from ON state to OFF state λ_0^k	0.6,0.8,1,1.2,1.4,1.6,1.8
Transition rate of PU from OFF state to ON state,λ_1^k	0.4,0.8,0.6,1.6,1.2,1.4,1.8
Total frame length T_{Total}	100msec
Sampling rates of spectrum sensors U	6000
Duration of spectrum sensing phase τ_s	7msec
Duration of spectrum sensing by	
assigned sensors on each channel t_s	6msec
Duration of reporting sensing results to sink t_r	1msec
Sensing power of spectrum sensors P_s	0.1W
Transmission power of data sensors P_t	0.22W
Energy consumption per spectrum sensing	0.11mJ
Fraction of samples retained in CE algorithm ρ	0.6
Stopping threshold ϵ	10^{-3}
partial throughput factor κ	0.5
Penalty factor for miss detection ϕ	0.5
SNR of secondary transmission	20dB

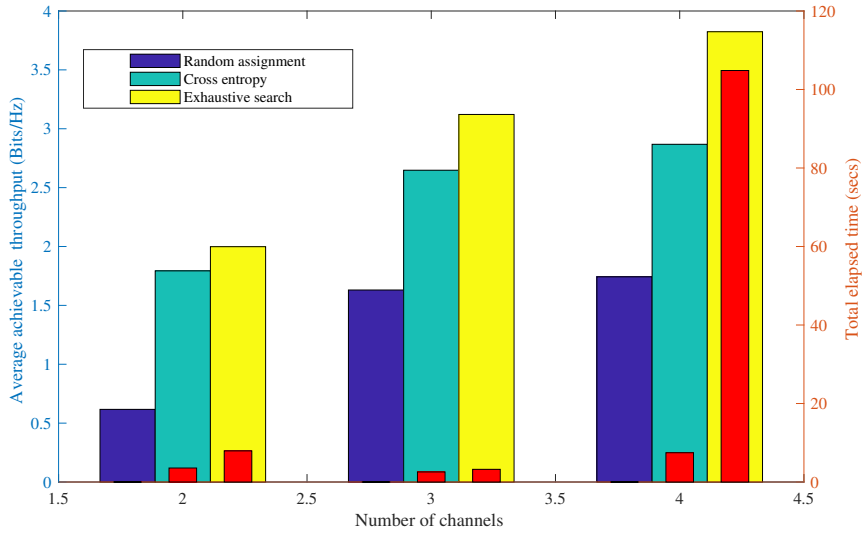

Figure 5.3. Average achievable throughput vs Number of channels for SSR based CE-algorithm,random assignment and exhaustive search method.

The variation of throughput with different number of licensed channels, K, is shown in Figure. 5.3. For illustration purposes, $M = 3$ is chosen, so that a solution using the exhaustive search can be quickly evaluated. The average achievable throughput of SSR-based approach using the CE

algorithm is compared with the random assignment and exhaustive search. Set of all possible assignments are considered in exhaustive search to find the optimal set, whereas a licensed channel is randomly assigned to spectrum sensors in random assignment. As shown in Figure. 5.3, the average achievable throughput obtained by the SSR-based CE algorithm is about 75%–90% of that obtained by the exhaustive search. In contrast, the total elapsed time for the evaluation using the exhaustive search method is about 14 times larger than that using the CE algorithm, when K is increased to 4. As K further increases, the elapsed time increases exponentially for the exhaustive search. Thus, the SSR-based CE algorithm attains the maximum throughput with much lesser computation time when compared to exhaustive search. Figure 5.4 shows the comparison between the performance of the CE algorithm and that of a greedy algorithm [161], for different values of EH rates. The greedy algorithm assigns channel to each sensor sequentially that gives the maximum achievable throughput. It is shown that the CE algorithm outperforms greedy algorithm in terms of achievable throughput, over a range of EH rates.

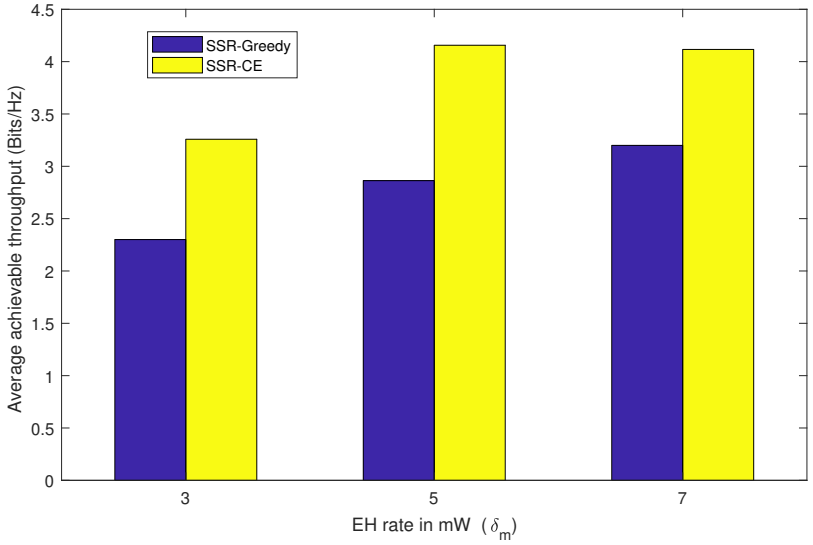

Figure 5.4. Comparison of CE algorithm and greedy algorithm performance for a range of EH rates.

The stability of CE-algorithm with respect to the average throughput is shown in Figure. 5.5. Here, the convergence of CE algorithm with the number of iterations can be seen, for different EH rate values. As expected, the average throughput increases with EH rate. Figure 5.6 shows the convergence result of CE algorithm with respect to the sensing phase duration τ_s ranging from as low as 2 ms to a relatively high value such as 15 ms, for a fixed EH rate of 7 mW. Note that the achievable throughput first increases with an increase in τ_s and later decreases as τ_s is increased

further. This concave behavior is due to the sensing-throughput tradeoff [160]. Figure 5.7 shows the impact of the fine-tuning CE algorithm parameter, i.e., fraction of samples retained, ρ, on the number of iterations and average throughput. It is evident from both the plots that CE on SSR performs better than CE on L-out-of-M rule. Moreover, the CE algorithm converges quickly with small ρ.

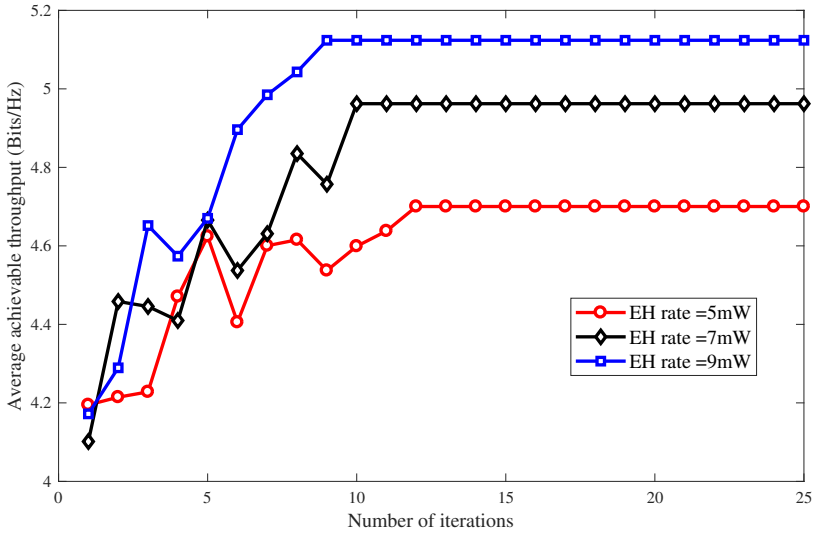

Figure 5.5. Average achievable throughput vs Number of Iteration for different EH rate.

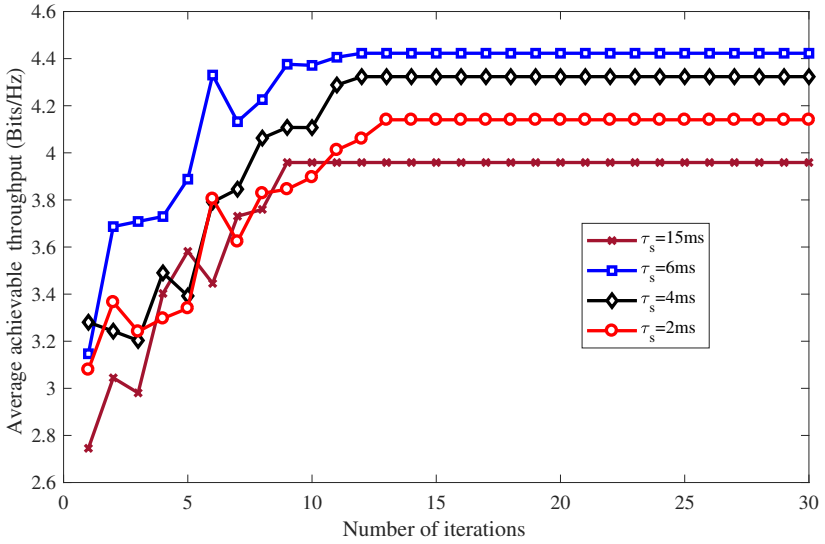

Figure 5.6. Average achievable throughput vs Number of iteration for different sensing phase duration τ_s.

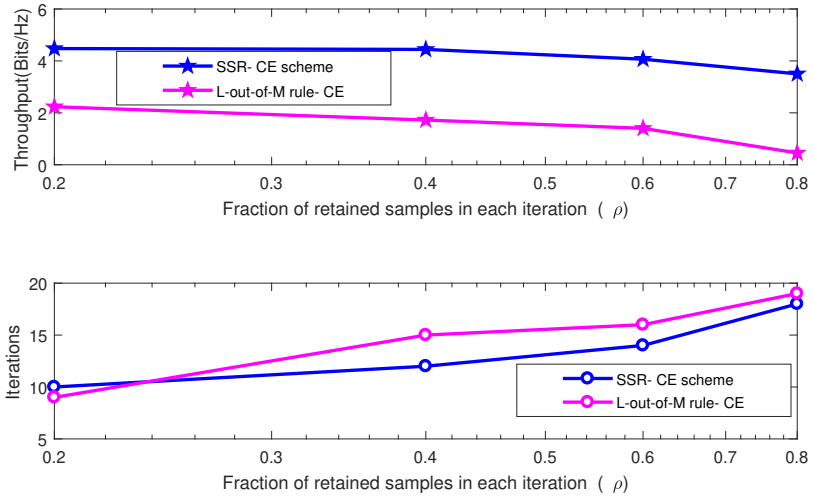

-

Figure 5.7. Impact of the fraction of retained samples ρ on the performance of the CE algorithm

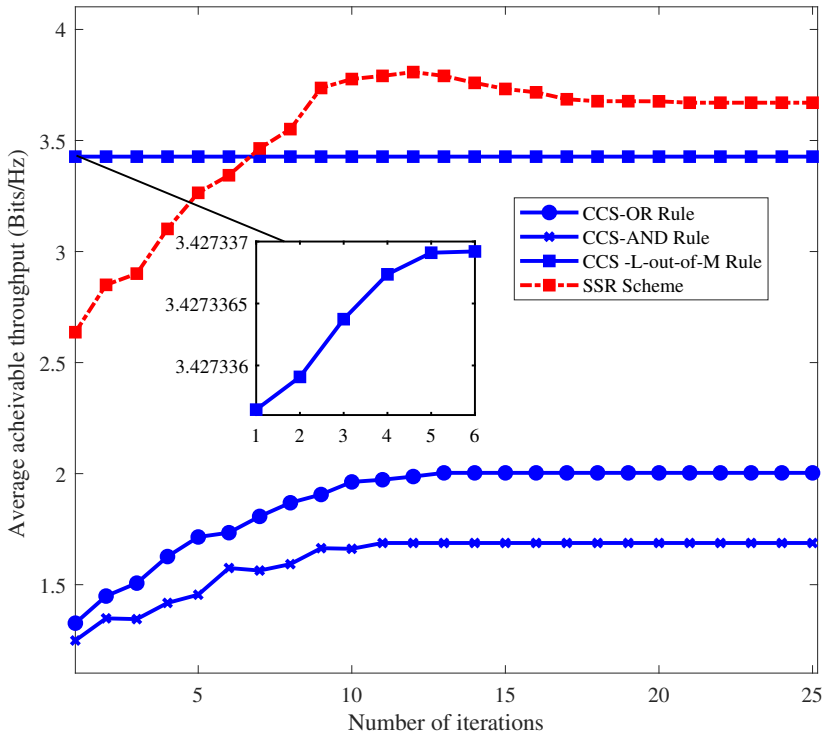

Figure 5.8. Average throughput vs Number of iteration.

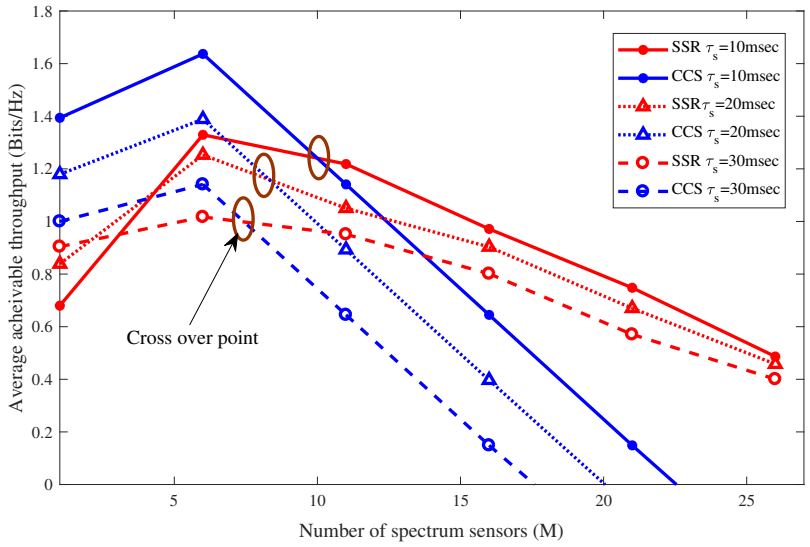

Figure 5.9. Average achievable throughput vs Number of spectrum sensors, M.

Now, for a network with $M = 15$ and $K = 7$, the average achievable throughput of SSR-based CE algorithm is compared with conventional fusion rules such as OR, AND, and L-out-of-M rule, as shown in Figure. 5.8. In the SSR scheme, since only one sensor reports its decision to the sink, it performs better than the CCS scheme employing L-out-of-M, OR and AND rules. As expected, the L-out-of-M rule performs the best among the CCS schemes, when optimum value of L is chosen [159]. Finally, the tradeoff between the optimal performances of SSR-based multichannel scheme with that of the L-out-of-M rule based CCS scheme is discussed. The variation of average achievable throughput with M, for different sensing times τ_s is shown in Figure. 5.9. When M is less, the L-out-of-M rule yields a larger throughput due to the better detection accuracy at the expense of relatively less channel available time, as opposed to the SSR scheme which saves the channel available time, but loses out on detection accuracy. Interestingly, as M increases, the SSR scheme outperforms the CCS scheme, since even though the detection accuracy of the CCS scheme increases, it loses out on the channel available time. Hence, this tradeoff yields a regime where SSR is preferred over L-out-of-M rule-based CCS scheme. Inherently, this tradeoff is between the detection accuracy and channel available time for secondary data transmission. Therefore, as M increases, the channel available time gets a larger priority as opposed to the detection accuracy in the HCRWSN, resulting in SSR scheme as a better choice. However, in the scenario where the detection accuracy is a main concern, L-out-of-M rule can still be employed.

5.5 Summary

The maximum achievable throughput of SSR-based spectrum sensing in a multichannel HCRN is considered. The impact of EH rate on maximum achievable throughput of SSR scheme is investigated. It is shown that the achievable throughput increases with EH rate by optimally scheduling the spectrum sensors to sense a particular channel. Through numerical results, it is shown that SSR-based multichannel scheduled sensing scheme outperforms the CCS scheme employing the optimal L-out-of-M rule, and the tradeoff between the average achievable throughput of both schemes are analyzed. It is shown that this tradeoff is the inherent tradeoff between the channel available time and the detection accuracy, and the regime where SSR is preferred over CCS scheme is also discussed. The results show that the SSR scheme outperforms CCS scheme when the number of spectrum sensors is large, and therefore, the channel available time gets a larger priority in a HCRWSN than the detection accuracy. Hence, in a scenario where spectral efficiency needs to be improved, SSR is a better choice; CCS should be employed in the scenario where the PU protection and detection accuracy are important.

Further increase of energy efficiency can be achieved by employing compressive sensing where sampling rate is reduced at the sub-Nyquist-rate and takes a shorter sensing duration which promotes energy saving but at the cost of performance degradation which directly affects the achievable throughput. One way to overcome this degradation is by employing collaborative sensing. Thus next chapter gives a complete analysis of energy efficiency of compressed conventional collaborative sensing (CCCS) scheme focusing on balancing the tradeoff between energy efficiency and detection accuracy in cognitive radio environment.

Chapter 6

Energy Efficiency Analysis of Compressive Collaborative Sensing Scheme in Cognitive Radio Networks

6.1 Introduction

The energy consumption in spectrum sensing, mainly caused by the analog-to-digital converter (ADC), is proportional to the sensing time duration and the sampling rate [51],[52]. However, at any instance of time, only a minority of channels are occupied by PUs in WSS, making the wideband spectrum sparser in the frequency range. Such sparsity of wideband spectrum is taken as an advantage in compressed sensing (CS) and recently been proposed to reduce the sampling rate below the Nyquist rate [50]. Thus compressed sensing, when compared to the conventional WSS, reduces the sampling rate at the sub-Nyquist rate [54] which further reduces the sensing time duration and greatly favors energy saving. For this reason, the CS-based spectrum sensing methods have been proposed as an efficient approach for improving the energy efficiency [55] in cognitive radio network.

Despite its attractiveness as an energy efficient sensing technique, CS suffers from a few major drawbacks which limit its applicability in practice. A CS based sensing scheme incurs a certain performance loss due to compression, when compared to the conventional sensing scheme, while detecting non sparse signals. This performance loss can be seen as sacrifice to improve energy efficiency in terms of detection performance. Thus to compensate the performance loss due to compression, the authors in [53] proposed collaborative compressive detection (CCD) framework in which group of spatially distributed nodes sense the presence of PU independently and send a compressed summary of observations to the fusion center (FC) where a global decision is made. It was shown that through collaboration the performance loss due to compression can be recovered. However, the study [53], never addressed energy efficiency and was restricted to the detection performance of CCD, where it is evident that an increase in either the compression ratio c (keeping number of collaborative nodes N fixed) or the N (keeping c fixed), the probability of error decreases exponentially.

In this work, it is shown that a similar trend can be seen with energy efficiency as a metric. In particular, expressions for energy consumption and achievable throughput of the Collaborative Compressive Conventional Detection (CCCS) scheme is derived. Next, an expression for energy efficiency of CCCS is derived, and an optimization problem that maximizes the energy efficiency subjected to constrain on detection and false alarm probability is formulated. As this problem is highly non-convex, some approximations to reduce it to a convex optimization problem is provided. Later, it is shown that these approximations are sufficiently accurate.

The motivation to consider the CCCS is threefold. First, it reduces the sampling rate at the sub Nyquist rate and takes a shorter sensing duration which promotes energy saving. Second, since it utilizes collaborative sensing scheme the achievable detection performance can be maintained to a target limit. Finally, since it promotes energy saving and ensures detection performance, the energy efficiency is guaranteed. In the process of determining optimal system parameters such as optimal compression ratio and number of active nodes, an attempt is made to answer the question : For a given compression ratio, c, what should be the number of nodes N, to maximize the energy efficiency ?

Energy efficiency of compressed sensing in wideband cognitive radio networks was studied in [162], where the authors showed that by optimizing the sampling rate, energy efficiency can be maximized. It is proved that sparser the wideband spectrum, higher the energy efficiency and

lower the energy consumption. But their analysis was restricted to compressed sensing in sparse signal condition. However in this work both compressed and collaborative sensing was considered to guarantee both dimensionality reduction and detection performance that favors improvement in energy efficiency to a greater extend. An analysis on EE for the CCCS scheme has not been considered earlier in the literature. The main contributions of this chapter are summarized as below.

- The energy efficiency of the CCCS spectrum sensing scheme is studied in terms of the required number of sensors involved in collaboration and the compression ratio that satisfies a given primary user detection constraints.
- The maximization of energy efficiency of CCCS is posed as a non-convex optimization problem, that optimizes the compression rate c, and number of sensors involved for cooperation.
- The Number of sensors required (N) and the compression ratio (c) are derived in terms of SNR and the required detection accuracy.
- The tradeoff between reducing the number of samples in a compressive sensing based measurement scheme and achievable energy efficiency of CCCS considering different signal models such as deterministic and random signal are studied. In both cases, it is shown that the energy efficiency is improved by either increasing the compression ratio c or by increasing the number of collaborative nodes N.
- Through numerical result, it is shown that in comparison with the uncompressed sensing scheme, the compressed sensing scheme reduces the sampling rate and take a shorter sensing and reporting time duration both of which are greatly favorable to energy saving which improves the energy efficiency of the system to a greater extent. In other words, it also tells us how many nodes are needed to collaborate to compensate for the loss due to compression. Moreover it was inferred that the improvement in energy efficiency can be obtained by optimizing either the compression ratio c (keeping N fixed) or the number of collaborating nodes N (keeping c fixed).

The remainder of this chapter is organized as follows. The system model for CCCS scheme is proposed and review of CCCS and CCS schemes for random signal case is provided in Secs. 6.2.

The energy efficiency optimization problem for the CCCS scheme is proposed in Section 6.3, and approximations, reformulation and detailed analysis are provided in Section 6.4. The energy efficiency formulation, approximations, and analysis for deterministic signal case is presented in Section 6.5. The results are presented in Section 6.6 and concluding remarks are provided in Section 6.7.

6.2 System Model

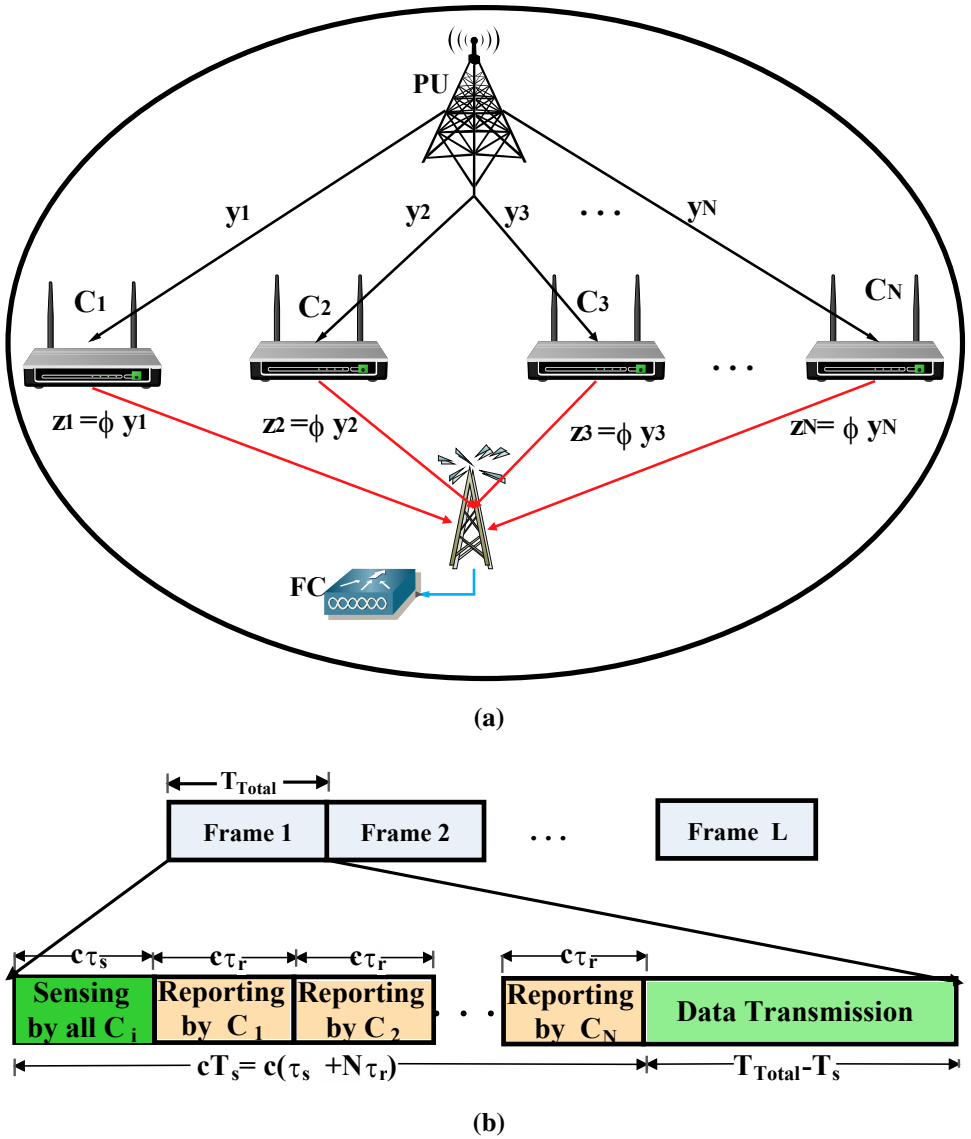

Figure 6.1. (a) System model for Collaborative Compressive Conventional Detection (CCCS) Scheme ; (b) Time slot structure for CCCS Scheme

Consider a cognitive radio (CR) network (CRN) – as depicted in Figure 6.1(a) – with N CR nodes denoted by $C_1, \ldots, C_N$ that record P observations each from a licensed band owned by a primary user (PU). First the conventional cooperative sensing (CCS) framework is described. The CR nodes forward their observation vectors over a lossless link to a fusion center (FC), where these observations are fused to make an overall decision on the availability of the primary spectrum. The hypothesis testing problem governing this scenario is:

$$\begin{aligned} \mathcal{H}_0 &: \mathbf{y}(n) = \mathbf{w}(n) \\ \mathcal{H}_1 &: \mathbf{y}(n) = \mathbf{x}(n) + \mathbf{w}(n), \quad n = 1, \ldots, N, \end{aligned} \tag{6.1}$$

where $\mathbf{w}(n)$ represents the $P \times 1$ noise vector, whose entries are assumed to be independent and identically distributed (i.i.d.), Gaussian random variables with zero mean and variance σ_w^2, and $\mathbf{x}(n)$ represents the $P \times 1$ primary signal vector, whose statistics is also assumed to be i.i.d. Gaussian with zero mean and variance σ_x^2. In other words, if $\mathcal{N}(\boldsymbol{\mu}, \boldsymbol{\Sigma})$ denotes a Gaussian random vector with mean vector $\boldsymbol{\mu}$ and covariance matrix $\boldsymbol{\Sigma}$, then $\mathbf{w}(n) \sim \mathcal{N}(\mathbf{0}, \sigma_w^2 \mathrm{I}_P)$, and $\mathbf{x}(n) \sim \mathcal{N}(\mathbf{0}, \sigma_x^2 \mathrm{I}_P)$, where I_P is a $P \times P$ identity matrix.

Now, the conventional compressive collaborative sensing (CCCS) framework is considered. Here, instead of $P \times 1$ vector $\mathbf{y}(n)$, each node sends an $M \times 1$ compressed vector $\mathbf{z}(n)$ to the FC, with $M < P$. The collection of these M-length universally sampled observations is given by $\{\mathbf{z}(n) = \boldsymbol{\phi}\mathbf{y}(n), n = 1, \ldots, N\}$, where $\boldsymbol{\phi}$ is an $M \times P$ compression matrix, which is assumed to be same across all nodes. With this setup, the hypothesis testing problem in (6.1) reduces to:

$$\begin{aligned} \mathcal{H}_0 &: \mathbf{z}(n) = \boldsymbol{\phi}\mathbf{w}(n) \\ \mathcal{H}_1 &: \mathbf{z}(n) = \boldsymbol{\phi}\mathbf{x}(n) + \boldsymbol{\phi}\mathbf{w}(n), \quad n = 1, \ldots, N, \end{aligned} \tag{6.2}$$

The FC receives the observation matrix $\mathbf{Z} = [\mathbf{z}(1) \cdots \mathbf{z}(N)]$, and makes a decision on the availability of the primary spectrum.

6.2.1 Performance Analysis of CCCS Scheme

Let π_0 be the prior probability that the channel is vacant. Upon collecting the observation matrix $\mathbf{Z}$, the FC employs likelihood ratio test (LRT), which is optimal. The LRT is devised as follows.

$$\prod_{n=1}^{N} \frac{f(\mathbf{z}(n);\mathcal{H}_1)}{f(\mathbf{z}(n);\mathcal{H}_0)} \underset{\mathcal{H}_0}{\overset{\mathcal{H}_1}{\gtrless}} \lambda_L, \tag{6.3}$$

where $f(\mathbf{z}(n);\mathcal{H}_0)$ and $f(\mathbf{z}(n);\mathcal{H}_1)$ represent the PDF of $\mathbf{z}(n)$ under $\mathcal{H}_0$ and $\mathcal{H}_1$, respectively, given by

$$f(\mathbf{z}(n);\mathcal{H}_0) = \frac{\exp\left(-\frac{\mathbf{z}^T(n)(\sigma_w^2\boldsymbol{\phi}\boldsymbol{\phi}^T)^{-1}\mathbf{z}(n)}{2}\right)}{(2\pi)^{M/2}|\sigma_w^2\boldsymbol{\phi}\boldsymbol{\phi}^T|^{1/2}}, \text{ and} \tag{6.4}$$

$$f(\mathbf{z}(n);\mathcal{H}_1) = \frac{\exp\left(-\frac{\mathbf{z}^T(n)((\sigma_x^2+\sigma_w^2)\boldsymbol{\phi}\boldsymbol{\phi}^T)^{-1}\mathbf{z}(n)}{2}\right)}{(2\pi)^{M/2}|(\sigma_x^2+\sigma_w^2)\boldsymbol{\phi}\boldsymbol{\phi}^T|^{1/2}}. \tag{6.5}$$

Substituting in (6.3) and simplifying gives

$$\left[\frac{|\sigma_w^2\boldsymbol{\phi}\boldsymbol{\phi}^T|^{1/2}}{|(\sigma_x^2+\sigma_w^2)\boldsymbol{\phi}\boldsymbol{\phi}^T|^{1/2}}\right]^N \exp\left[-\sum_{n=1}^{N}\left(\frac{\mathbf{z}^T(n)(\boldsymbol{\phi}\boldsymbol{\phi}^T)^{-1}\mathbf{z}(n)}{2(\sigma_x^2+\sigma_w^2)} - \frac{\mathbf{z}^T(n)(\boldsymbol{\phi}\boldsymbol{\phi}^T)^{-1}\mathbf{z}(n)}{2\sigma_w^2}\right)\right] \underset{\mathcal{H}_0}{\overset{\mathcal{H}_1}{\gtrless}} \lambda_L. \tag{6.6}$$

Recalling that $\mathbf{z}(n) = \boldsymbol{\phi}\mathbf{y}(n)$, it is easy to see that the above test reduces to the form

$$T(\mathbf{Y}) \triangleq \sum_{n=1}^{N} \mathbf{y}^T(n)\boldsymbol{\phi}^T(\boldsymbol{\phi}\boldsymbol{\phi}^T)^{-1}\boldsymbol{\phi}\mathbf{y}(n) \underset{\mathcal{H}_0}{\overset{\mathcal{H}_1}{\gtrless}} \lambda, \tag{6.7}$$

where λ the detection threshold, which is chosen based on either the Neyman-Pearson criterion [163], or the Bayesian criterion [164, 165]. In this work, the Neyman-Pearson framework is considered, where the errors are controlled independently. For the ease of characterizing the performance of the above test in (6.6), it is assumed that the linear mapping $\boldsymbol{\phi}$ satisfies the ϵ-embedding property, as considered in [53]. Designing a $\boldsymbol{\phi}$ that satisfies the ϵ-embedding property is beyond the scope of current study. Let $\gamma \triangleq \frac{\sigma_x^2}{\sigma_w^2}$ denote the average received SNR at a CR node, and $\widehat{\mathbf{P}} \triangleq \boldsymbol{\phi}^T(\boldsymbol{\phi}\boldsymbol{\phi}^T)^{-1}\boldsymbol{\phi}$ denote the orthogonal projection matrix. For large value of the product

NM, it can be shown that the test statistic under both $\mathcal{H}_0$ and $\mathcal{H}_1$ is distributed as [53]

$$\frac{T(\mathbf{Y})}{\sigma_k^2} \overset{NM\to\infty}{\sim} \begin{cases} \mathcal{N}(NM, 2NM), & \text{under } \mathcal{H}_0 \\ \mathcal{N}(NM, 2NM), & \text{under } \mathcal{H}_1 \end{cases} \tag{6.8}$$

where $k = 0, 1$, that is, $\sigma_0^2 = \sigma_w^2$, and $\sigma_1^2 = \sigma_x^2 + \sigma_w^2$.

Following (6.8), the probability of false-alarm at the FC can be written as [53]

$$\begin{aligned} P_f^{CCCS} &\triangleq P(T(\mathbf{Y}) > \lambda | \mathcal{H}_0) \\ &= Q\left(\frac{\frac{\lambda}{\sigma_w^2} - NM}{\sqrt{2NM}}\right) = Q\left(\frac{\frac{\lambda}{P\sigma_w^2} - \mathsf{c}N}{\sqrt{2\mathsf{c}NP}}\right). \end{aligned} \tag{6.9}$$

Similarly, the probability of detection at the FC can be written as [53]

$$\begin{aligned} P_d^{CCCS} &= P(T(\mathbf{Y}) > \lambda | \mathcal{H}_1) \\ &= Q\left(\frac{\frac{\lambda}{\sigma_x^2+\sigma_w^2} - NM}{\sqrt{2NM}}\right) = Q\left(\frac{\frac{\lambda}{P(\sigma_x^2+\sigma_w^2)} - \mathsf{c}N}{\sqrt{2\mathsf{c}NP}}\right). \end{aligned} \tag{6.10}$$

Note that the expressions for P_f^{CCCS} and P_d^{CCCS} depend on the value of c, which dictates the loss in the detection accuracy due to the compressed measurements $\{\mathbf{z}(n), n = 1, \ldots, N\}$. Since the detection accuracy is also a function of N, it can be improved by increasing N. In other words, the loss in detection due to compression can be recovered by increasing the number of collaborative nodes. This observation is shown in Figure 6.2, where the variation of P_d^{CCCS} across γ is plotted, with $P_f^{CCCS} = 0.1$, for different values of c and N. The case of $\mathsf{c} = 1$ corresponds to Nyquist sampling, i.e., the CCS approach. As c decreases, P_d^{CCCS} decreases, which can be increased to a desired level by increasing N. Interestingly, as N increases, even though the probability of detection – and consequently, the achievable throughput of the secondary network – increases, the total energy consumption in the secondary network also increases, thereby decreasing the energy efficiency. Hence, a study of design of the optimal system parameters c and N, that maximize the energy efficiency is of interest. In other words, an attempt has been made to seek answers to the following questions. Given that the secondary network uses a compression ratio c, how large should N be such that the energy efficiency is maximized? Also, given a secondary setup with N nodes, how small can be the compression ratio c, such that the energy efficiency is maximized?

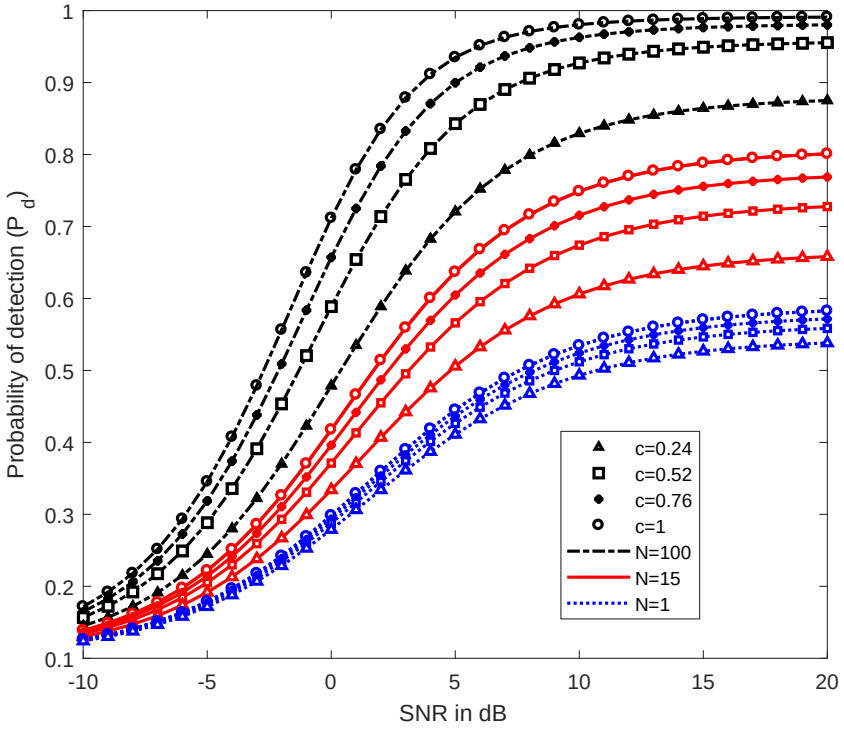

Figure 6.2. Variation of probability of detection, P_d^{CCCS}, for different values of average SNR, γ. Probability of false-alarm, $P_f^{CCCS} = 0.1$. Note that as c decreases, P_d^{CCCS} decreases. However, P_d^{CCCS} can be increased to a desired level by increasing N.

To answer these questions – the main contribution of this chapter, the expressions for the average achievable throughput, average energy consumption and energy efficiency of the CR network was derived, and formulated the governing optimization problem in the next section.

6.3 Energy Efficiency and Problem Formulation

As mentioned in the previous section, the objective is to find the optimal number of the compression ratio c for a given N (and the optimal N for a given c), such that the energy efficiency in the CR network is maximized, subject to constraints on sensing errors. In this section, the governing optimization problem is formulated. Before that, the average achievable throughput and the average energy consumption in the CR network in each time slot is derived, and later the energy efficiency of the network is derived.

Table 6.1. Achievable throughput and energy consumption by the CR network employing CCCS, for scenarios S1-S4.

Scenario	**Probability**	**Energy Consumed (J)**	**Achievable Throughput (bits/Hz)**
S1	$\pi_1 \, P_d^{CCCS}$	$NP_s\mathtt{c}\tau_s$+$NP_t\mathtt{c}\tau_r$	0
S2	$\pi_0 \, P_f^{CCCS}$	$NP_s\mathtt{c}\tau_s$+$NP_t\mathtt{c}\tau_r$	$-\phi\mathcal{C}(T_{Total}-\mathtt{c}T_s)$
S3	$\pi_1 \, (1 - P_d^{CCCS})$	$NP_s\mathtt{c}\tau_s$+$NP_t\mathtt{c}\tau_r + P_t(T_{Total} - \mathtt{c}T_s)$	$\kappa_c\mathcal{C}(T_{Total} - \mathtt{c}T_s)$
S4	$\pi_0 \, (1 - P_f^{CCCS})$	$NP_s\mathtt{c}\tau_s$+$NP_t\mathtt{c}\tau_r + P_t(T_{Total} - \mathtt{c}T_s)$	$\mathcal{C}(T_{Total} - \mathtt{c}T_s)$

In a CR network with CCCS, the average achievable throughput and the average energy consumption depend on the communication link between the PU node and the sensing nodes, which can be calculated based on four scenarios denoted by **S1**-**S4**, detailed below.

S1. The first scenario corresponds to the case when PU is present, and the FC correctly declares its presence, which occurs with probability $\pi_1 P_d^{CCCS}$. Hence, the CR nodes do not transmit data and the throughput achieved is zero.

S2. The second scenario covers the case when PU is absent but incorrectly declared as present by the FC, which occurs with probability $\pi_0 P_f^{CCCS}$. Since the CR network misses a transmission opportunity in this case, the achievable throughput in this case is calculated as $-\phi\mathcal{C}(T_{Total} - \mathtt{c}T_s)$, where $T_s = (\tau_s + N\tau_r)$, $\mathcal{C}$ is the capacity of the secondary link, and $\phi \in (0, 1)$ is a suitably chosen penalty factor [149].

S3. In the third scenario, FC makes an incorrect decision that the PU is absent, when it is actually present, which occurs with probability $\pi_0(1 - P_d^{CCCS})$. In this case, the CR network transmits and causes interference to the PU. Even with the interference to the PU, the CR communication achieves a partial throughput of $\kappa_c\mathcal{C}(T_{Total} - \mathtt{c}T_s)$ units, for some $\kappa_c \in [0, 1)$.

S4. The last scenario corresponds to the case when the PU is absent and the FC declares it correctly, which occurs with probability $\pi_1(1 - P_f^{CCCS})$. In this case, the achievable throughput is maximum, and is given by $\mathcal{C}(T_{Total} - \mathsf{c}T_s)$ units.

The achievable throughput, along with the energy consumed in each of the above scenarios are listed in Table 6.1, where P_s and P_t denote the power required for each SU node for sensing and data transmission, respectively.

Considering all the above cases, the average throughput of the CCCS scheme is given by

$$\begin{aligned} R_{CCCS}(\lambda, \mathsf{c}, N) = & \pi_0(1 - P_f^{CCCS})(T_{Total} - \mathsf{c}T_s)\mathcal{C} \\ & + \kappa_c \mathcal{C}(T_{Total} - \mathsf{c}T_s)\pi_1(1 - P_d^{CCCS}) \\ & - \phi\mathcal{C}(T_{Total} - \mathsf{c}T_s)\pi_1 P_f^{CCCS}. \end{aligned} \tag{6.11}$$

Similarly, the average energy consumption for the CCCS scheme vide Table. 6.1 is given by

$$\begin{aligned} E_{CCCS}(\lambda, \mathsf{c}, N) = & (NP_s\mathsf{c}\tau_s + NP_s\mathsf{c}\tau_r) \\ & + P_t(T_{Total} - T_s)\left(1 - \pi_1 P_d^{CCCS} - \pi_0 P_f^{CCCS}\right). \end{aligned} \tag{6.12}$$

The energy efficiency, measured in (bits/Hz/J), of the CR network is given by

$$EE_{CCCS}(\lambda, \mathsf{c}, N) \triangleq \frac{R_{CCCS}(\lambda, \mathsf{c}, N)}{E_{CCCS}(\lambda, \mathsf{c}, N)}. \tag{6.13}$$

The goal here is to design the system parameters – λ and c, for a given N, or λ and N, for a given c, such that the energy efficiency $EE_{CCCS}(\lambda, \mathsf{c}, N)$ is maximized, subject to constraints on the sensing errors.

For a given c, the governing optimization problem is:

$$\mathcal{OP}_{CCCS}^{(N)} : \max_{\lambda, N} \quad EE_{CCCS}(\lambda, \mathsf{c}, N) \tag{6.14}$$

$$\text{s.t.} \quad \begin{cases} P_f^{CCCS} \leq \overline{P}_f, \\ P_d^{CCCS} \geq \overline{P}_d, \end{cases} \tag{6.15}$$

and for a given N, the governing optimization problem is:

$$\mathcal{OP}^{(\mathsf{c})}_{CCCS} : \max_{\lambda,\mathsf{c}} \quad EE_{CCCS}(\lambda, \mathsf{c}, N) \tag{6.16}$$

$$\text{s.t.} \quad \begin{cases} P_f^{CCCS} \leq \overline{P}_f, \\ P_d^{CCCS} \geq \overline{P}_d, \end{cases} \tag{6.17}$$

for some $0 \leq \overline{P}_f < \overline{P}_d \leq 1$. The IEEE 802.22 standard [151], for e.g., enforces requirements for the upper bound on the probability of signal detection and lower bound on the probability of false-alarm to be 0.9 and 0.1, respectively.

The problems given in (6.14) and (6.16) are hard to solve, because the expression for $EE_{CCCS}(\lambda, \mathsf{c}, N)$ calculated from (6.13) is lengthy. Hence, for the ease of analysis, the cost function in the above problems are approximated, and mention the conditions under which the problem can be reduced to a convex optimization problem. Later, in Sec. 6.6, it is highlighted that the errors due to these approximations are negligible.

6.4 Approximation, Reformulation and Analysis

In this section, an approximation of EE_{CCCS} is provided and optimization problems (6.14) and (6.16) are reformulated. On a general note, the apriori probability of channel availability should be large enough to maintain the detection accuracy. That is, it is assumed that $\pi_0 > \pi_1$, and $P_d^{CCCS} > P_f^{CCCS}$, which is justified in a typical CR scenario [31],[166]. Following this, the average throughput in (6.11) can be approximated by the above inequalities and setting $\kappa_c = 0$ as

$$\tilde{R}_{cccs}(\lambda, \mathsf{c}, N) \approx \pi_0 \mathcal{C}(T_{Total} - \mathsf{c}T_s) \left(1 - (1+\phi) P_f^{CCCS}\right). \tag{6.18}$$

Similarly $E_{CCCS}(\lambda, \mathsf{c}, N)$ can be approximated as

$$\begin{aligned} \tilde{E}_{cccs}(\lambda, \mathsf{c}, N) \approx & (NP_s \mathsf{c}\tau_s + NP_s \mathsf{c}\tau_r) \\ & + P_t(T_{Total} - \mathsf{c}T_s)\pi_0(1 - P_f^{CCCS}). \end{aligned} \tag{6.19}$$

Consequently, $EE_{CCCS}(\lambda, \mathsf{c}, N)$ can be approximated as

$$\tilde{EE}_{cccs}(\lambda, \mathsf{c}, N) = \frac{\tilde{R}_{cccs}(\lambda, \mathsf{c}, N)}{\tilde{E}_{cccs}(\lambda, \mathsf{c}, N)}, \tag{6.20}$$

and the optimization problems $\mathcal{OP}^{(N)}_{CCCS}$ and $\mathcal{OP}^{(\mathsf{c})}_{CCCS}$ can be respectively reformulated as

$$\mathcal{OP}1^{(N)}_{CCCS} : \max_{\lambda, N} \qquad \tilde{EE}_{cccs}(\lambda, \mathsf{c}, N) = \frac{\tilde{R}_{cccs}(\lambda, \mathsf{c}, N)}{\tilde{E}_{cccs}(\lambda, \mathsf{c}, N)} \tag{6.21}$$

$$\text{s.t.} \quad \begin{cases} P_f^{CCCS} \leq \overline{P}_f, \\ P_d^{CCCS} \geq \overline{P}_d, \end{cases} \tag{6.22}$$

and

$$\mathcal{OP}1^{(\mathsf{c})}_{CCCS} : \max_{\lambda, \mathsf{c}} \qquad \tilde{EE}_{cccs}(\lambda, \mathsf{c}, N) = \frac{\tilde{R}_{cccs}(\lambda, \mathsf{c}, N)}{\tilde{E}_{cccs}(\lambda, \mathsf{c}, N)} \tag{6.23}$$

$$\text{s.t.} \quad \begin{cases} P_f^{CCCS} \leq \overline{P}_f, \\ P_d^{CCCS} \geq \overline{P}_d. \end{cases} \tag{6.24}$$

Later, in Sec. 6.6, it is shown that the errors due to these approximations are negligible.

Note that P_d^{CCCS} and P_f^{CCCS} are dependent on c and N, only through their product $\mathsf{c}N$. The following theorem provides the solution to the optimal threshold, λ^*, for the optimization problems in (6.21) and (6.16).

Theorem 6.1. *The optimal threshold λ^* for the optimization problems $\mathcal{OP}1^{(N)}_{CCCS}$ and $\mathcal{OP}1^{(c)}_{CCCS}$ satisfies the constraint $P_d^{CCCS} \geq \overline{P}_d$ with equality, and is given by*

$$\lambda^* = \sigma_w^2(1+\gamma)\left\{\sqrt{2\mathsf{c}NP}Q^{-1}(\overline{P}_d) + \mathsf{c}NP\right\}. \tag{6.25}$$

Proof. See Appendix C.1.

As a consequence of the above theorem, it is shown that the other constraint in (6.21) and (6.23), namely $P_f^{CCCS} \leq \overline{P}_f$, reduces to an upper bound on the product $\mathsf{c}N$. By substituting $\lambda = \lambda^*$ in

the constraint $P_f^{CCCS} \leq \overline{P}_f$, $\overline{P}_f$ is given by

$$\overline{P}_f \geq Q\left(\frac{\frac{\sigma_w^2(1+\gamma)\left\{\sqrt{2\mathsf{c}NP}Q^{-1}(\overline{P}_d)+\mathsf{c}NP\right\}}{\sigma_w^2} - \mathsf{c}NP}{\sqrt{2\mathsf{c}NP}}\right). \tag{6.26}$$

Rearranging the above equation, this condition reduces to

$$\mathsf{c}N \leq \frac{2}{\gamma^2 P}\left\{Q^{-1}(\overline{P}_f) - (1+\gamma)Q^{-1}(\overline{P}_d)\right\}^2. \tag{6.27}$$

Now, the optimization problems $\mathcal{OP}1_{CCCS}^{(N)}$ and $\mathcal{OP}1_{CCCS}^{(\mathsf{c})}$ given in (6.21) and (6.23) can be respectively reformulated as

$$\mathcal{OP}2_{CCCS}^{(N)} : \max_{N} \quad \tilde{EE}_{cccs}(\lambda^*, \mathsf{c}, N) \tag{6.28}$$

$$s.t.\ N \leq N_{\max} \triangleq \frac{2\left\{Q^{-1}(\overline{P}_f) - (1+\gamma)Q^{-1}(\overline{P}_d)\right\}^2}{\gamma^2 \mathsf{c}P}, \tag{6.29}$$

and

$$\mathcal{OP}2_{CCCS}^{(\mathsf{c})} : \max_{\mathsf{c}} \quad \tilde{EE}_{cccs}(\lambda^*, \mathsf{c}, N) \tag{6.30}$$

$$s.t.\ \mathsf{c} \leq \mathsf{c}_{\max} \triangleq \frac{2\left\{Q^{-1}(\overline{P}_f) - (1+\gamma)Q^{-1}(\overline{P}_d)\right\}^2}{\gamma^2 NP}. \tag{6.31}$$

In the next theorem, the problem (6.31) is considered in particular, and shown that the corresponding objective function is monotonically increasing (and concave) for $\mathsf{c} \in (0, \mathsf{c}_{\max})$, for a given N. Therefore, the optimal c^* which maximizes $\tilde{EE}_{cccs}(\lambda^*, \mathsf{c}, N)$ for a given N is given as $\mathsf{c}^* = \mathsf{c}_{\max}$.

Theorem 6.2. *For a given N, the objective function in the optimization problem $\mathcal{OP}2_{CCCS}^{(\mathsf{c})}$ is monotonically increasing in $\mathsf{c} \in (0, \mathsf{c}_{\max})$. Therefore, optimal c, $\mathsf{c}^* = \mathsf{c}_{\max}$.*

Proof. See Appendix C.2.

A similar argument can be made for the problem in (6.29), vide the following theorem.

Theorem 6.3. *For a given* c*, the objective function in the optimization problem* $\mathcal{OP}2^{(N)}_{CCCS}$ *is monotonically increasing in* $N \in (0, N_{\max})$*. Therefore, optimal N,* $N^* = N_{\max}$.

Proof. The proof is in similar lines to that of Theorem 6.2, and is omitted for brevity.

This completes the analysis on finding the optimal c, (c^*) for a given N, or to find the optimal N, (N^*) for a given c, such that the energy efficiency of the CRN is maximized. In the next section, the performance analysis of the CRN with a deterministic PU signal is considered.

6.5 Performance with Deterministic PU Signal

In this section, the EE performance of the CR network is considered for the case when PU signal is deterministic. Although unrealistic in practice, performance study of a CRN with a deterministic PU signal has been studied earlier in the context of capacity analysis [167], spectrum sensing [168], etc., which serves as an upper bound on the performance of a system employed in practice. In the case of a deterministic PU signal, asymptotic distribution of the test statistic at the FC under either hypotheses can be written as [53]

$$T(\mathbf{X}) \triangleq\sim \begin{cases} \mathcal{N}(0, \sigma_w^2 N \|\widehat{\mathbf{P}}\mathbf{x}\|_2^2), & \text{under } \mathcal{H}_0 \\ \mathcal{N}(N\|\widehat{\mathbf{P}}\mathbf{x}\|_2^2, \sigma_w^2 N \|\widehat{\mathbf{P}}\mathbf{x}\|_2^2) & \text{under } \mathcal{H}_1 \end{cases}, \tag{6.32}$$

where $\|\widehat{\mathbf{P}}\mathbf{x}\|_2^2 \triangleq \mathbf{x}^T\boldsymbol{\phi}^T(\boldsymbol{\phi}\boldsymbol{\phi}^T)^{-1}\boldsymbol{\phi}\mathbf{x}$. From (6.32), the probabilities of false-alarm and signal detection at the FC following the CCCS scheme with deterministic PU signal are given by

$$P_f^{CCCS,det} \triangleq P(T(\mathbf{X}) > \lambda|\mathcal{H}_0) = Q\left(\frac{\lambda - N\mathsf{c}\gamma\sigma_w^2}{\sqrt{\sigma_w^2 N\|\widehat{\mathbf{P}}\mathbf{x}\|_2^2)}}\right) \tag{6.33}$$

$$P_d^{CCCS,det} = P(T(\mathbf{X}) > \lambda|\mathcal{H}_1) = Q\left(\frac{\lambda - N\mathsf{c}\gamma\sigma_w^2}{\sqrt{\sigma_w^2 N\|\widehat{\mathbf{P}}\mathbf{x}\|_2^2)}}\right) \tag{6.34}$$

As discussed in the random signal case, using the concept of ϵ-stable embedding, for larger value of NM the approximation $\|\widehat{\mathbf{P}}\mathbf{x}\|_2^2 \approx \frac{M}{P}\|\mathbf{x}\|_2^2 = \mathsf{c}\|\mathbf{x}\|_2^2$ [53]. Therefore,

$$P_f^{CCCS,det}=Q\left(\frac{\lambda}{\sigma_w^2\sqrt{N\mathsf{c}\gamma}}\right), P_d^{CCCS,det}=Q\left(\frac{\lambda - N\mathsf{c}\gamma\sigma_w^2}{\sigma_w^2\sqrt{N\mathsf{c}\gamma}}\right) \tag{6.35}$$

It is easy to show that the detection threshold $\lambda = \frac{N}{2}\mathbf{x}^T\boldsymbol{\phi}^T(\boldsymbol{\phi}\boldsymbol{\phi}^T)^{-1}\boldsymbol{\phi}\mathbf{x} = \frac{N}{2}\|\widehat{\mathbf{P}}\mathbf{x}\|_2^2 = \frac{N}{2}\mathsf{c}\gamma\sigma_n^2$. Therefore, the final expressions for $P_f^{CCCS,det}$ and $P_d^{CCCS,det}$ are given by

$$P_f^{CCCS,det} = Q\left(\frac{\sqrt{\mathsf{c}N\gamma}}{2}\right), \;\; P_d^{CCCS,det} = Q\left(-\frac{\sqrt{\mathsf{c}N\gamma}}{2}\right) \tag{6.36}$$

Note that the expressions for average achievable throughput, average energy consumption and the energy efficiency expressions across all four scenarios **S1** $-$ **S4** for the deterministic case remains similar to the random case, except that P_f^{CCCS} and P_d^{CCCS} are replaced by $P_f^{CCCS,det}$ and $P_d^{CCCS,det}$, respectively. The approximations discussed in the previous case also hold for the deterministic case. For a given c, the corresponding optimization problem for the deterministic case can be written as

$$\mathcal{OP}1_{CCCS,det}^{(N)} : \max_{N} \qquad \tilde{EE}_{cccs,det}(\mathsf{c},N) = \frac{\tilde{R}_{cccs,det}(\mathsf{c},N)}{\tilde{E}_{cccs,det}(\mathsf{c},N)} \tag{6.37}$$

$$\text{s.t.} \quad \begin{cases} P_f^{CCCS,det} \leq \overline{P_f}, \\ P_d^{CCCS,det} \geq \overline{P_d}, \end{cases} \tag{6.38}$$

and the optimization problem for given N is given by

$$\mathcal{OP}1_{CCCS,det}^{(\mathsf{c})} : \max_{\mathsf{c}} \qquad \tilde{EE}_{cccs,det}(\mathsf{c},N) = \frac{\tilde{R}_{cccs,det}(\mathsf{c},N)}{\tilde{E}_{cccs,det}(\mathsf{c},N)} \tag{6.39}$$

$$\text{s.t.} \quad \begin{cases} P_f^{CCCS,det} \leq \overline{P_f}, \\ P_d^{CCCS,det} \geq \overline{P_d}, \end{cases} \tag{6.40}$$

for some $0 < P_f^{CCCS,det} < P_d^{CCCS,det} < 1$. Later, it is shown that the errors due to these approximations are negligible. Again, note that both $P_f^{CCCS,det}$ and $P_d^{CCCS,det}$ depend on c and N through the product $\mathsf{c}N$.

Theorem 6.4. *The optimal threshold λ^* for the optimization problems $\mathcal{OP}1^{(N)}_{CCCS,det}$ and $\mathcal{OP}1^{(\mathsf{c})}_{CCCS,det}$ satisfies the constraint $P_d^{CCCS} \geq \overline{P}_d$ with equality, and is given by*

$$\lambda^* = \sigma_w^2 \sqrt{N\mathsf{c}\gamma} \left\{ Q^{-1}(\overline{P}_d) + \sqrt{N\mathsf{c}\gamma} \right\}. \tag{6.41}$$

Proof. See Appendix C.3.

Similar to the previous case, as a consequence of the above theorem, it is shown that the other constraint in (6.37) and (6.39), namely $P_f^{CCCS} \leq \overline{P}_f$, reduces to an upper bound on the product $\mathsf{c}N$. By substituting $\lambda = \lambda^*$ in the constraint $P_f^{CCCS} \leq \overline{P}_f$, $\overline{P}_f$ is given by

$$\overline{P}_f \geq Q\left(\frac{\sqrt{\mathsf{c}N\gamma}\sigma_w^2 (Q^{-1}(\overline{P}_d) + \sqrt{N\mathsf{c}\gamma})}{\sigma_w^2 \sqrt{\mathsf{c}N\gamma}} \right) \tag{6.42}$$

Rearranging the above equation, this condition reduces to

$$\mathsf{c}N \leq \frac{1}{\gamma} \left\{ Q^{-1}(\overline{P}_f) - Q^{-1}(\overline{P}_d) \right\}^2. \tag{6.43}$$

Now, the optimization problems $\mathcal{OP}1^{(N)}_{CCCS,det}$ and $\mathcal{OP}1^{(\mathsf{c})}_{CCCS,det}$ given in (6.37) and (6.39) can be respectively reformulated as

$$\mathcal{OP}2^{(N)}_{CCCS,det} : \max_{N} \quad \tilde{EE}_{cccs}(\lambda^*, \mathsf{c}, N) \tag{6.44}$$

$$s.t.\ N \leq N_{\max} \triangleq \frac{\left\{ Q^{-1}(\overline{P}_f) - Q^{-1}(\overline{P}_d) \right\}^2}{\gamma \mathsf{c}}, \tag{6.45}$$

and

$$\mathcal{OP}2^{(\mathsf{c})}_{CCCS,det} : \max_{\mathsf{c}} \quad \tilde{EE}_{cccs}(\lambda^*, \mathsf{c}, N) \tag{6.46}$$

$$s.t.\ \mathsf{c} \leq \mathsf{c}_{\max} \triangleq \frac{\left\{ Q^{-1}(\overline{P}_f) - Q^{-1}(\overline{P}_d) \right\}^2}{\gamma N}, \tag{6.47}$$

In the next theorem, the problem (6.47) is considered in particular, and shown that the corresponding objective function is monotonically increasing (and concave) for $\mathsf{c} \in (0, \mathsf{c}_{\max})$, for a given N.

Theorem 6.5. *For a given N, the objective function in the optimization problem $\mathcal{OP}1^{(\mathsf{c})}_{CCCS,det}$ is monotonically increasing in $\mathsf{c} \in (0, \mathsf{c}_{\max})$, and hence optimal c, $\mathsf{c}^* = \mathsf{c}_{\max}$.*

Proof. See Appendix C.4.

A similar argument can be made for the problem in (6.45).

Theorem 6.6. *For a given c, the objective function in the optimization problem $\mathcal{OP}1^{(N)}_{CCCS,det}$ is monotonically increasing in $N \in (0, N_{\max})$, and hence optimal N, $N^* = N_{\max}$.*

Proof. The proof is in similar lines to that of Theorem 6.2, and is omitted for brevity.

6.6 Numerical Results and Discussion

In this section, the performance of the CCCS technique is studied in comparison with the CCS technique, in terms of energy efficiency and validate the analysis, through numerical techniques. MATLAB is used as a simulation tool. The parameter values are fixed as follows. The target probability of detection, $\overline{P}_d$, and false-alarm probability, $\overline{P}_f$, are fixed to be 0.9 and 0.1, respectively. The prior probabilities π_0 and π_1 are set to be 0.5 each. The total frame duration is assumed to be $T_{Total} = 200$ ms. The sampling frequency at the local SUs is assumed to be $f_s = 1$ MHz, and the sensing power $P_s = 0.1$ W. The length of the uncompressed received signal vector, $P = 100$. The sensing time, τ_s, and reporting time, τ_r, for the CCCS scheme are set to 30 ms and 100 μs, respectively. The achievable rate of secondary transmission is chosen to be $\mathcal{C} = \log_2(1 + \text{SNR}_s) = 6.6582$ bits/sec/Hz, where the SNR_s for the secondary transmission is assumed to be $\text{SNR}_s = 20$ dB. The transmission power of individual sensors, P_t, is assumed to be 3 W. Also, the partial throughput factor, κ_c, and the penalty factor, ϕ, are set to be 0.5 each.

Figure 6.3 shows the variation of energy efficiencies for the random and deterministic signal cases, as a function of parameters c and N. Observe that the energy efficiency is concave in both c and N. Furthermore, it can be seen that as N increases, c decreases, which means indicates a better compression. Also, the maximum energy efficiency can also be improved with N.

Figures 6.4 (a) and 6.4 (b) show the variation of the optimal compression ratio $\mathtt{c}^*$ for the CCCS scheme, as a function of N for different values of SNR γ. First, note that the optimal values of $\mathtt{c}$ are nearly equal for the actual and approximate energy efficiency values, thereby establishing the earlier claim on approximating the energy efficiency. The decrease in $\mathtt{c}^*$ with an increase in N is intuitive, since the loss due to compression is recovered in CCCS by increasing N, which results in a better throughput, and consequently, a better energy efficiency. Similarly, in Figure 6.5 (a) and 6.5 (b), the variation of optimal N for different values of $\mathtt{c}$ is considered.

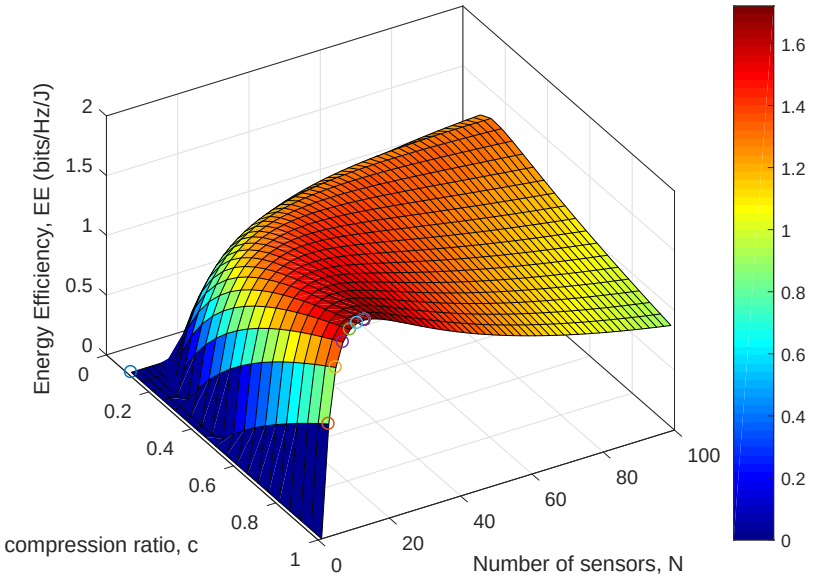

(a) deterministic signal case

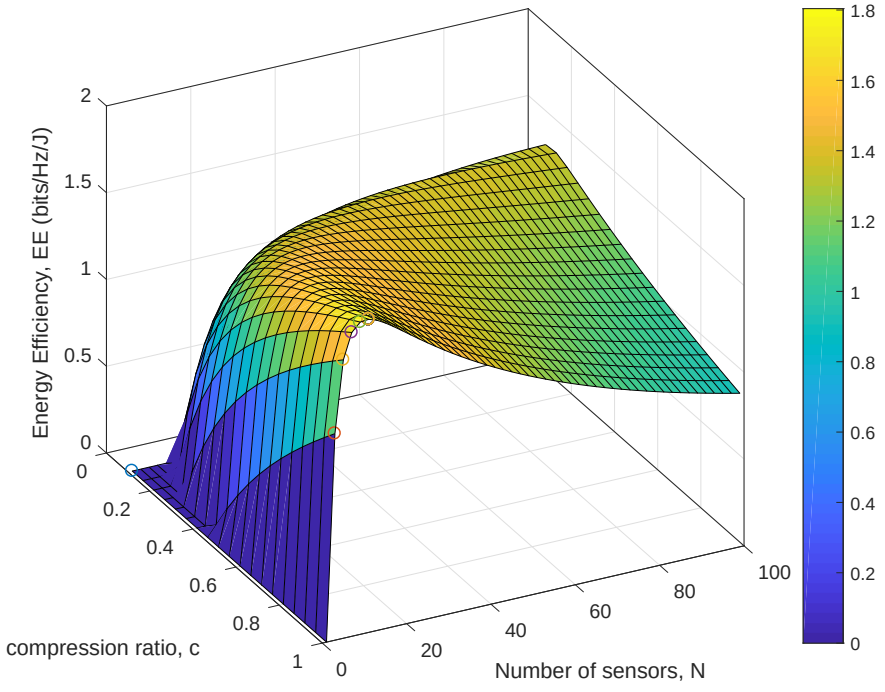

(b) random signal case

Figure 6.3. Energy efficiency as a function of number of sensors N and compression ratio c for (a) deterministic signal case, (b) random signal case.

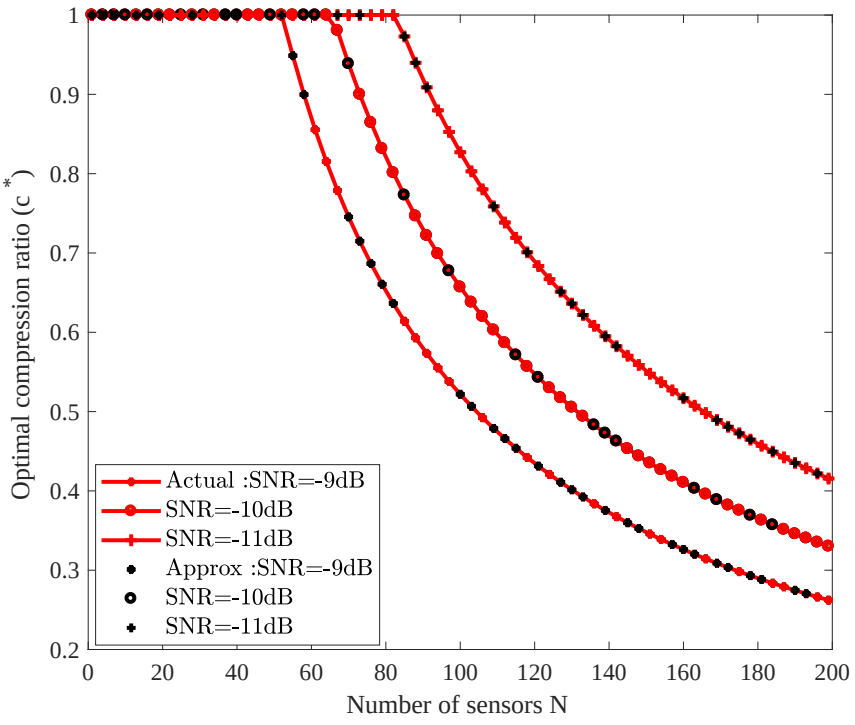

(a) deterministic signal case

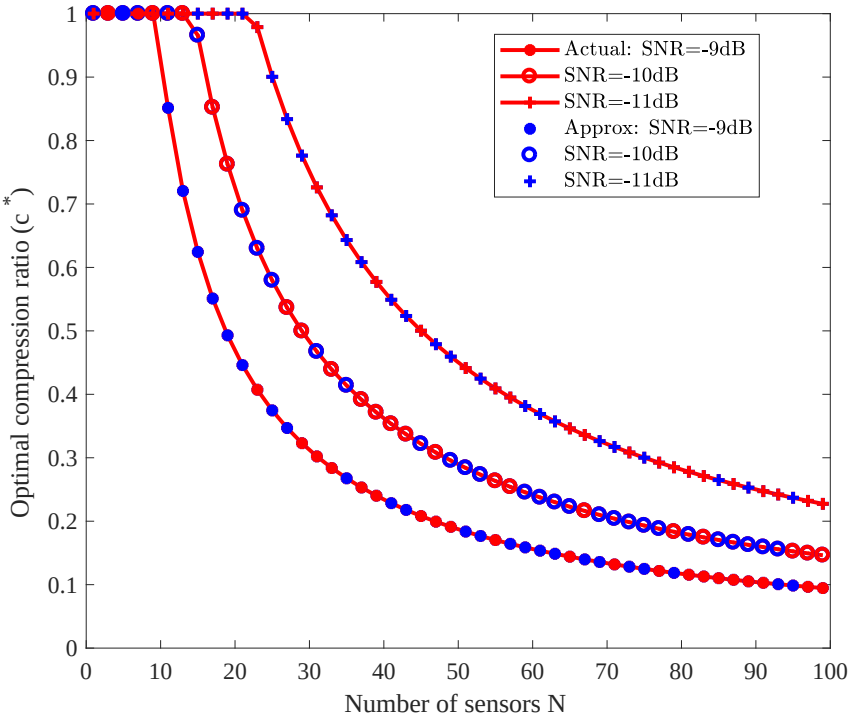

(b) random signal case

Figure 6.4. Variation of the optimal number of sensors (N^*) with compression ratio c^* for (a) deterministic signal case (b) random signal case.

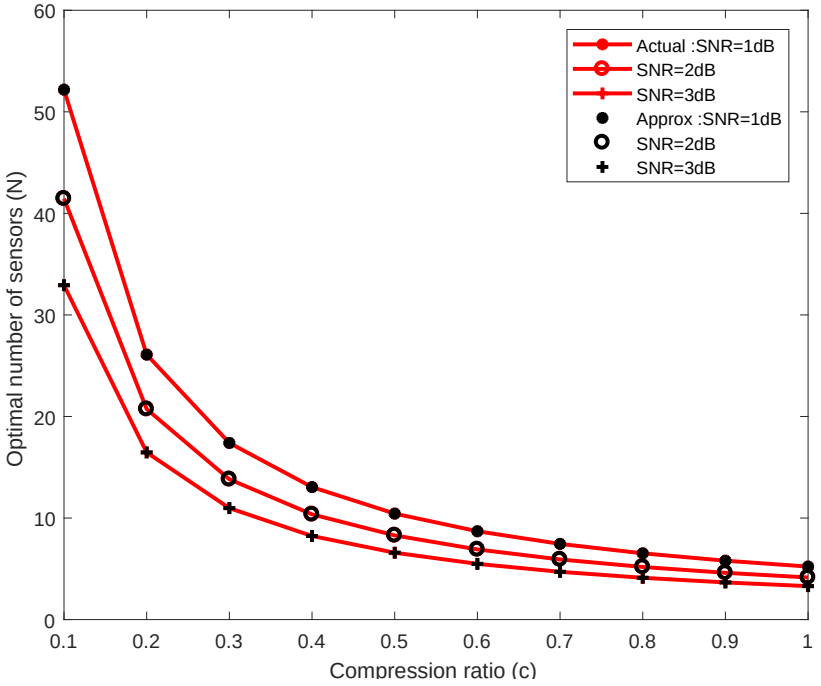

(a) deterministic signal case

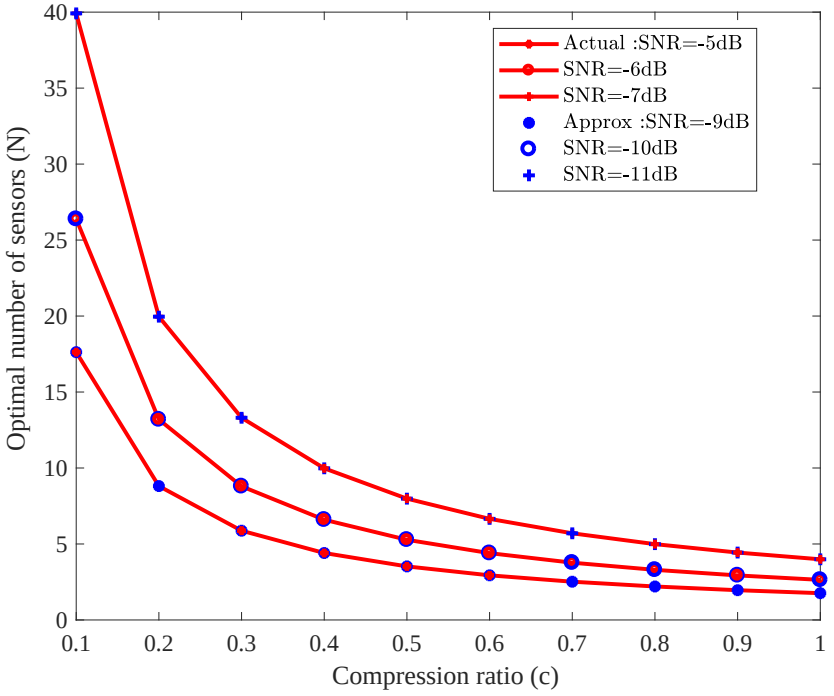

(b) random signal case

Figure 6.5. Variation of the optimal compression ratio (c^*) with number of sensors N for (a) deterministic signal case (b) random signal case.

Figures 6.6 (a) and 6.6 (b) show the variation of optimal energy efficiency values with the actual and approximate expressions, for different values of N. Note that for low values of N, performances of both CCS and CCCS schemes are similar, due to the fact that $\mathtt{c}^* = 1$ for sufficiently low N. As N increases, the system achieves a better compression, and therefore, the performance of CCCS scheme becomes better than that of the CCS scheme. Also, the energy efficiency for both CCS and CCCS schemes increase with an increase in SNR. Moreover, the loss due to the energy efficiency approximation is negligible. Therefore, in the subsequent results, only the approximated energy efficiency values are considered.

The reason for a better energy efficiency of the CCCS scheme in comparison to the CCS scheme can be either because CCCS achieves a better throughput, or it achieves a lower energy consumption. For a given N (or $\mathtt{c}$), since the detection performance of the CCS scheme is better than that of CCCS scheme, the achievable throughput of the CCS scheme will be higher as compared to the CCCS scheme. Therefore, the improvement in the energy efficiency of the CCCS scheme must be due to a significant reduction in energy consumption in comparison to the CCS scheme. Figures 6.7 and 6.8 corroborate this argument. In Figure 6.7, the achievable throughput of CCS and CCCS schemes are compared, where the former is found to be better. For larger values of N, the detection probability and hence the throughput of the CCS scheme improves faster. However, as shown in Figure 6.8, the energy consumption of the CCS scheme also increases rapidly with N, as opposed to the CCCS scheme, where the increase is much slower since $\mathtt{c}^*$ decreases with N. This is true for both random signal and deterministic signal cases. Hence, in scenarios where the energy consumption has a larger priority in a signal detection scenario CCCS scheme could be preferred. However, in the scenario where the sensing accuracy is a main concern, CCS scheme yields a better performance, in terms of energy efficiency.

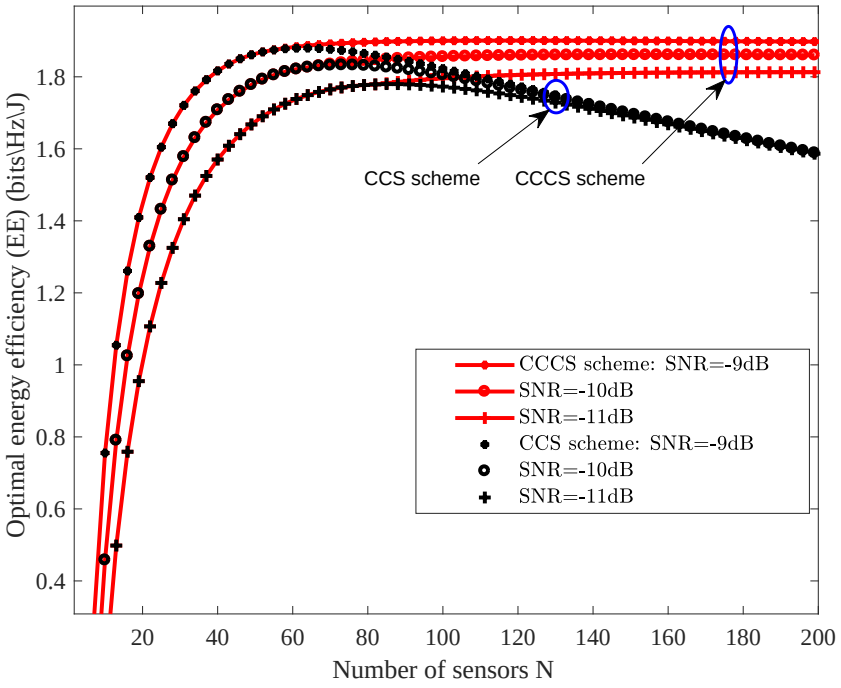

(a) deterministic signal case

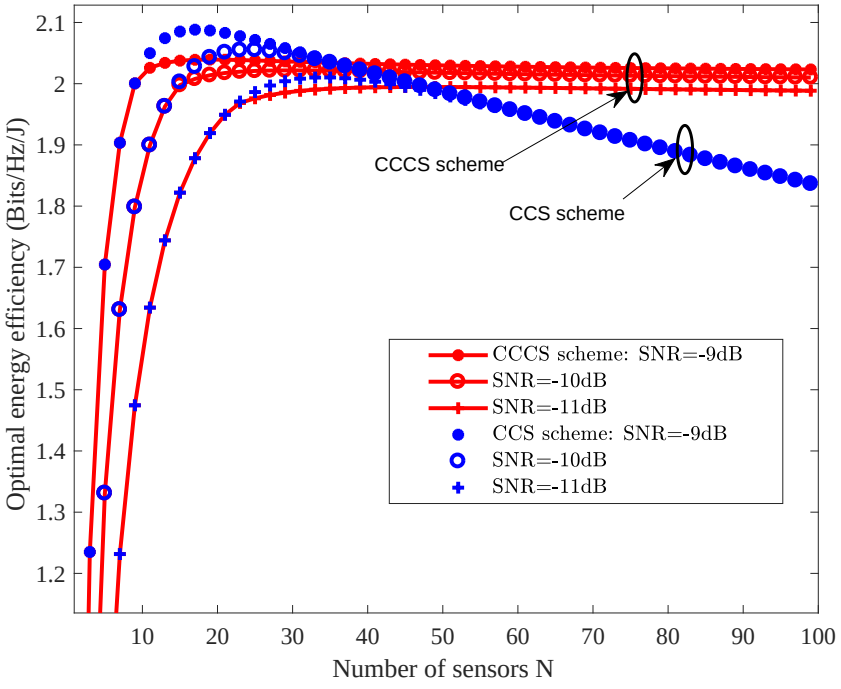

(b) random signal case

Figure 6.6. Variation of optimal energy efficiency with number of sensors N for (a) deterministic signal case (b) random signal case.

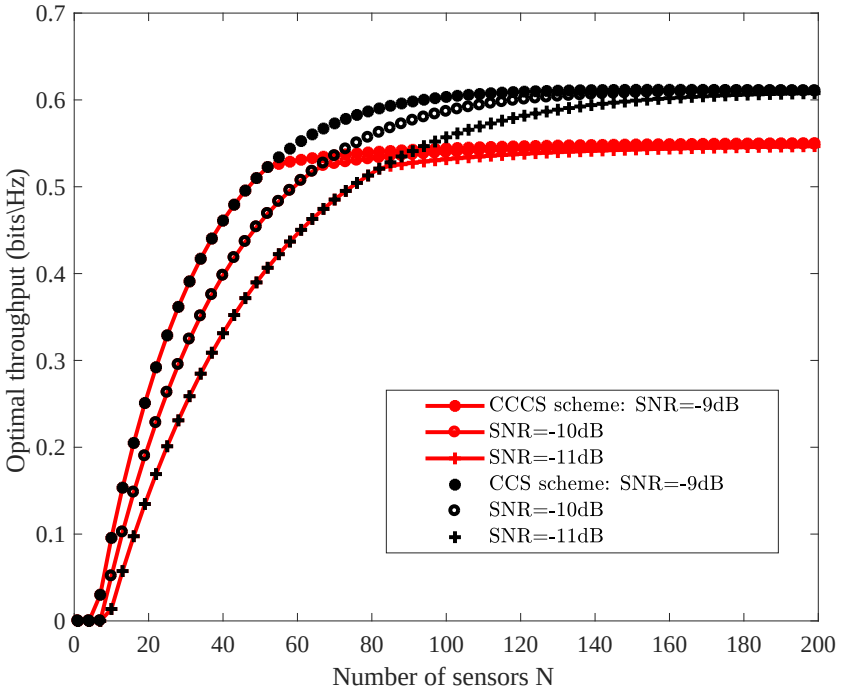

(a) deterministic signal case

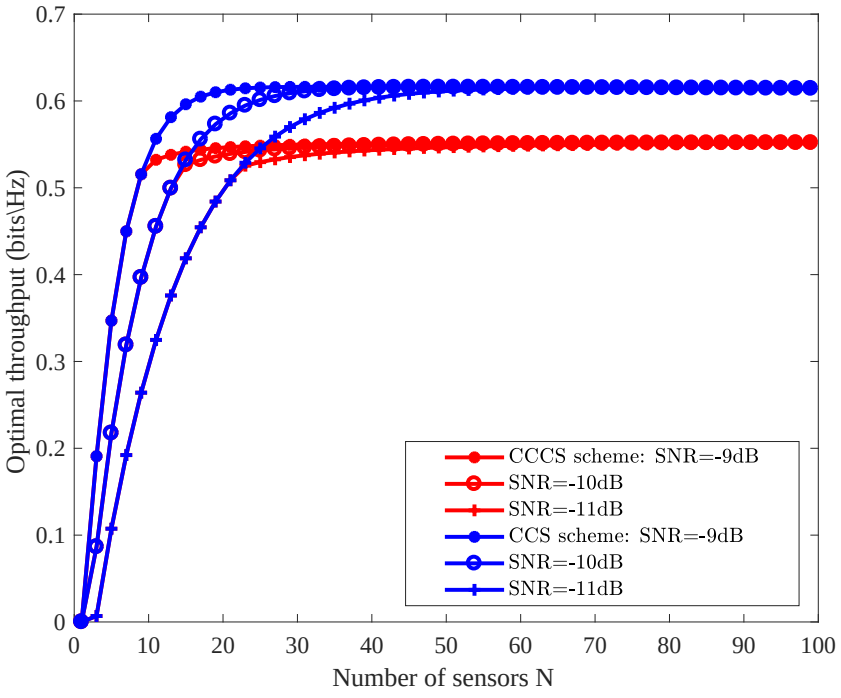

(b) random signal case

Figure 6.7. Variation of optimal achievable throughput with number of sensors N for (a) deterministic signal case (b) random signal case.

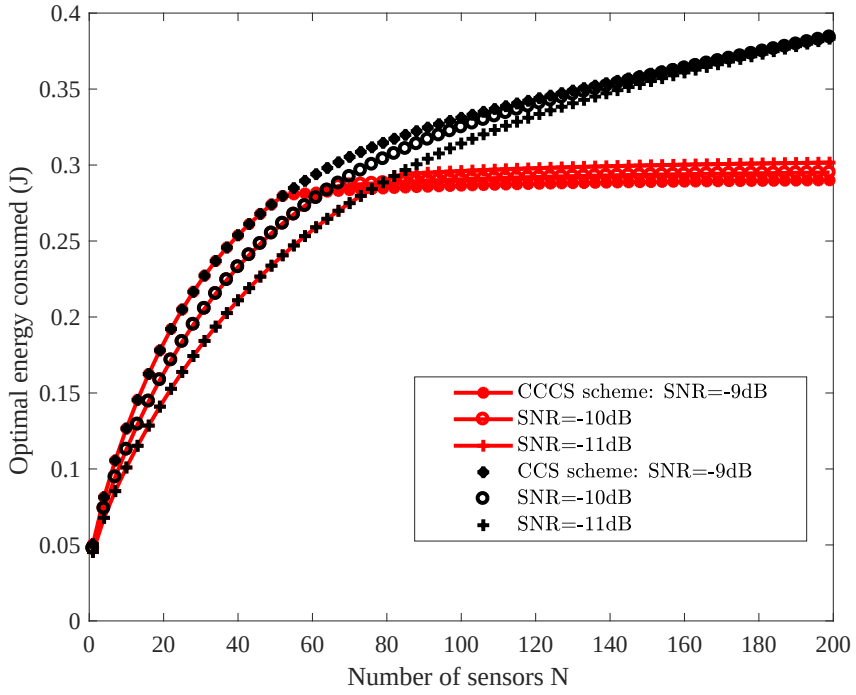

(a) deterministic signal case

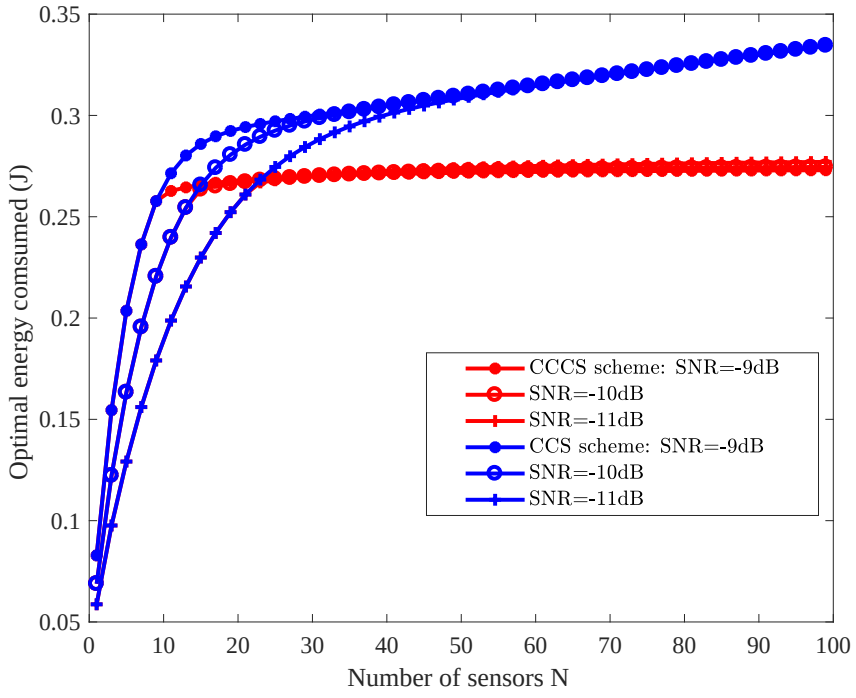

(b) random signal case

Figure 6.8. Variation of optimal energy consumption with number of sensors N for (a) deterministic signal case (b) random signal case.

6.7 Summary

The energy efficiency of compressed conventional collaborative sensing (CCCS) scheme is considered focusing on balancing the tradeoff between energy efficiency and detection accuracy in cognitive radio environment. First the existing CCCS scheme in the literature is considered , and the achievable throughput, energy consumption and energy efficiency is derived. Next, the energy efficiency maximization for the CCCS scheme is posed as a non-convex, optimization problem. The optimization problem is approximated to reduce it to a convex optimization problem, and showed that this approximation holds with sufficient accuracy in the regime of interest. The tradeoff between dimensionality reduction and collaborative sensing of CCCS scheme is analytically characterized as the implicit tradeoff between energy saving and detection accuracy, and shown that by combining compression and collaboration the loss due to one can be compensated by the other which improves the overall energy efficiency of the cognitive radio network.

Chapter 7

Conclusions and Future Work

In this chapter, the conclusions drawn from research work carried out are summarized and scope for future work is presented. Spectrum sensing plays a crucial role in the successful deployment of cognitive radio networks. To further improve the spectrum sensing performance, spectral and energy efficient cooperative spectrum sensing schemes, that reduces the sensing overhead, need to be employed. In most of the previous work, sequential sensing is employed for cooperative spectrum sensing wherein the same set of cooperating users sense a single channel in each sensing period to increase the sensing accuracy. However, this approach greatly limits the sensing efficiency and can result in a large cooperation overhead. In this thesis, more efficient cooperative spectrum sensing techniques are considered and the tradeoff between detection accuracy and energy efficiency at global detection level is analyzed to best leverage the achievable cooperative gain.

7.1 Conclusions

In this thesis, energy and throughput efficient cooperative spectrum sensing techniques are considered and efficient solutions at local sensing level and fusion level to best leverage the achievable cooperative gain are proposed. The main focus of this thesis was to theoretically analyze efficient cooperative spectrum sensing techniques for cognitive radio networks to maximize the achievable throughput, energy efficiency and reduce the energy consumption

while limiting the incurred cooperation overhead and sensing errors. Towards this end, initially the energy efficiency performance was studied for two selective reporting based cooperative sensing scheme namely SSR and its novel variation, OSSR scheme, to reduce the reporting overhead and extended the analysis to multichannel heterogeneous CR scenario. Later energy efficiency in collaborative compressed sensing scheme was considered. The main focus of this study is on three important design issues for energy efficient cooperative spectrum sensing which are selective reporting based cooperative user selection techniques, user scheduled based multichannel cooperative sensing technique and collaborative compressed sensing technique in the detection performance constraints.

In Chapter 2, the most common spectrum sensing techniques for cognitive radio networks is reviewed in energy efficiency perspective and detailed their advantages and disadvantages. To address the limitations of the spectrum sensing techniques by a single secondary user, cooperative spectrum sensing and its main elements and limiting factors have been discussed.

In Chapter 3, the energy efficiency of superior selective reporting (SSR)-based scheme for spectrum sensing is considered, and derived its achievable throughput, energy consumption and energy efficiency is derived. The energy efficiency maximization problem for the SSR scheme was formulated as a non-convex, multiple variable optimization problem and approximating it to a quasi-concave optimization problem is discussed, and showed that this approximation holds with sufficient accuracy. Through numerical results, it is shown that the energy efficiency achieved by the SSR scheme is larger as compared to the conventional cooperative sensing schemes based on OR and AND rules.

In Chapter 4, a variant of the SSR scheme called the opportunistic superior selective reporting (OSSR) scheme is proposed and its energy efficiency analysis is presented. Through numerical results, it is shown that the SSR and OSSR techniques outperform the conventional AND and OR fusion rule-based energy efficient schemes, and discussed the regimes where OSSR is preferred over SSR and vice-versa, in terms of the energy efficiency. It is shown that the trade off between the performances of SSR and OSSR schemes is the implicit trade off between the energy consumption and average throughput, and the results shows that the SSR scheme outperforms OSSR scheme in many scenarios. This indicates that the energy consumption gets a larger priority in a CRN, as

opposed to the achievable throughput and therefore, in the scenarios such as green cognitive radio systems, SSR scheme is a better choice. However, in the scenarios where the saving of sensing and transmission energy is not a main concern, OSSR scheme could be employed.

Sensing accuracy, in terms of probability of detection is essential to improve the average throughput, which can be achieved by using the optimal L-out-of-M rule [159]. However, as the number of sensors increases, the average throughput decreases due to an increase in reporting overhead, even though the sensing accuracy increases. Towards this end, methods to increase the channel available time by reducing the sensing overhead has also received considerable research attention. From Chapter 4, it follows that the SSR scheme reduces the decision reporting overhead, since only one selected node reports its decision to a center node/sink. Therefore, the SSR scheme results in a better data transmission time which enhances the achievable network throughput. Hence, a CR system incorporating the SSR scheme with energy harvesting nodes achieves a major improvement in the channel available time and network throughput in an HCRWSN, for a given primary interference constraint. Towards this end, in Chapter 5, the maximum achievable throughput of SSR-based spectrum sensing in a multichannel HCRN is considered. The impact of EH rate on maximum achievable throughput of SSR scheme is investigated and the average achievable throughput for multichannel HCRN is derived. The problem of maximizing the average throughput for multichannel HCRN is formulated. To solve this formulated optimization problem, the cross entropy (CE) algorithm is employed and is shown that the algorithm converges to an optimal value obtained through exhaustive search with fewer number of iterations. It is also shown that the achievable throughput increases with EH rate by optimally scheduling the spectrum sensors to sense a particular channel. Through numerical results, it is shown that SSR-based multichannel scheduled sensing scheme outperforms the CCS scheme employing the optimal L-out-of-M rule, and discussed the tradeoff between the average achievable throughput of both schemes. It is shown that this tradeoff is the inherent tradeoff between the channel available time and the detection accuracy, and discussed the regime where SSR is preferred over CCS scheme. The results show that the SSR scheme outperforms CCS scheme when the number of spectrum sensors is large, and therefore, the channel available time gets a larger priority in a HCRWSN than the detection accuracy. Hence, in a scenario where spectral efficiency needs to be improved, SSR is a better choice; CCS should be employed in the scenario where the PU protection and detection accuracy are important.

In Chapter 6, the energy efficiency of compressed conventional collaborative sensing (CCCS) scheme is considered focusing on balancing the tradeoff between energy efficiency and detection accuracy in cognitive radio environment. First, the existing CCCS scheme is considered, and derive the achievable throughput, energy consumption and energy efficiency. The energy efficiency maximization for the CCCS scheme is posed as a non-convex, optimization problem. The optimization problem is approximated to reduce it to a convex optimization problem, and showed that this approximation holds with sufficient accuracy in the regime of interest. The tradeoff between dimensionality reduction and collaborative sensing of CCCS scheme is analysed as an implicit tradeoff between energy saving and detection accuracy, and show that by combining compression and collaboration the loss due to one can be compensated by the other which improves the overall energy efficiency of the cognitive radio network.

7.2 Future work

Following are some of the topics which can be explored further in the context of work carried out in this thesis :

Throughout this thesis, several techniques that contributed to the spectral and energy efficient design of cooperative spectrum sensing schemes for cognitive radio networks is proposed and analyzed. Various existing tradeoff in CSS such as tradeoff between achievable throughput and energy consumption, tradeoff between channel available time and detection accuracy is identified and shown that there is high degree of freedom in the optimization of the energy efficiency in CSS network. These issues are addressed by focusing on some selected key aspects of CSS such as overhead reduction (Chapter 3, 4), improving the channel available time (Chapter 5) and employing compressed sensing in CSS (Chapter 6). However, there are some relevant issues that warrant further consideration in the future work.

- **Dispersiveness in the reporting channel:** The reporting channels are assumed to be error-free throughout this thesis, for analytical simplicity and do not consider the impairments such as dispersiveness in the reporting channels, which is unrealistic in practice [138, 169]. However the performance of SSR would degrade further in the case of dispersive

reporting channel errors [138], and hence the presented performance in this work can be considered as an upper bound for practical purposes.

- **Impact of PU mobility:** Another interesting idea for future work is to incorporate the impact of mobility of PU on the spectrum sensing performance with the objective to determine the parameters that affect the sensing performance. In this work, mobility aspects of the PU [145] is ignored, since each SU would then require an exact knowledge of the change in network topology due to the movement of PU, which makes the analysis more complex.

  A detailed analysis on the EE performance of SSR and OSSR schemes in the presence of dispersive reporting channel errors, and the impact of PU mobility on the performance are some directions in which this study can be extended in future.

- **Impact of fading channel:** In this work, the performance of cooperative spectrum sensing over the additive white Gaussian noise channel is examined. It will be beneficial to study the performance of the energy efficiency of CSS techniques over fading channels such as Rayleigh, Rician or Nakagami-m channels which results in more practical performance analysis. Depending on the fading model, the average probability of detection, achievable throughput, energy consumed and energy efficiency can be evaluated. Although this analysis exhibits performance degradation for cooperative spectrum sensing when fading is considered, this needs to be confirmed through analysis and simulations.

  The effect of topological aspects of nodes such as location of nodes, positioning of nodes in energy efficiency analysis is yet another interesting direction in which this work can be extended in future.

- **Incorporation of Ambient Backscatter Communication (ABC):** In overlay CR network, the performance of secondary systems is still much dependent on the activity of a primary channel. i.e., when the primary transmitter occupies the channel for most of the time, the secondary transmitter has less opportunity for data transmission during the limited channel idle period. As a result, the network performance of the secondary system is severely deteriorated. This scenario of existence of PU for a long period has not been considered in any of the analysis in this work. This problem can be further investigated and extended by incorporating Ambient Backscatter Communication (ABC) which is a novel and more

energy efficient communication technique. Since this will further increase the achievable throughput of CR network, efficient methods to integrate ABC technique in the system model considered in this work should be developed.

- **Efficient optimization Algorithm:** Cross entropy (CE) algorithm was used to maximize the channel available time under PU protection constraint in Chapter 5. Although the performance bound of the CE algorithm remains an open theoretical issue, it has been shown effective in solving a similar combinatorial optimization problem. This optimization problem can be further investigated and extended by in cooperating efficient heuristic optimization algorithm which can be considered as a future research direction.

Appendix A

Appendix for Chapter 3

A.1 Proof of Theorem 3.4 : To show that $[V_0(\beta) - V_1(\beta)] \geq 0$, for $\beta \to 0$

To show that $[V_0(\beta) - V_1(\beta)] \geq 0$, when $\beta \to 0$, $[V_0(\beta) - V_1(\beta)]$ can be expressed as

$$[V_0(\beta) - V_1(\beta)] = V_0^0(\beta)\tilde{E}_{SSR}(\beta) - V_1^0(\beta)\tilde{R}_{SSR}(\beta), \quad \text{where} \tag{A.1}$$

$$V_0^0(\beta) = P(\mathcal{H}_0)C(T_{Total} - \beta T)\left\{(\phi+1)(N+1)(1-P_f)^N\right\}, \tag{A.2}$$

$$V_1^0(\beta) = P(\mathcal{H}_0)\left\{(NP_s\eta\beta T + (1-2\eta)\beta T) + P_t(T_{Total} - \beta T)(1-P_f)^N(N+1)\right\}. \tag{A.3}$$

Observe that both $V_0^0(\beta) \geq 0$ and $V_1^0(\beta) \geq 0$, as $\beta \to 0$. Following the condition (D̲1) in lemma 3.1, when $\frac{\Phi+1}{\Phi} < \frac{1}{[1-P_f(\varepsilon)]^{N+1}}$, $\tilde{R}_{SSR}(\beta) < 0$, and $\tilde{E}_{SSR}(\beta) \geq 0$. Therefore, $[V_0(\beta) - V_1(\beta)] \geq 0$, which implies that $\lim_{\beta\to 0} \frac{\partial E_{SSR)}}{\partial \beta} > 0$.

A.2 Proof of Theorem 3.4: To show that $[V_0(\beta) - V_1(\beta)] \leq 0$, for $\beta \to 1$

When $\beta \to 1$, it can be seen that since $\frac{\partial P_f}{\partial \beta} \leq 0$, it is sufficient to prove that $[V_0(\beta) - V_1(\beta)]$ is a decreasing function of β. Towards this end, it suffices to show that $V_0(\beta)$ is decreasing, and $V_1(\beta)$ is an increasing function of β. Now, $\frac{\partial V_0(\beta)}{\partial \beta}$ can be expressed as:

$$\frac{\partial V_0(\beta)}{\partial \beta} = V_0^0(\beta)\frac{\partial \tilde{E}_{SSR}(\beta)}{\partial \beta} + \tilde{E}_{SSR}(\beta)\frac{\partial V_0^0(\beta)}{\partial \beta}, \quad \text{where} \tag{A.4}$$

$$\frac{\partial E_{SSR}(\beta)}{\partial \beta} = -([NP_s\eta T + P_t(1-2\eta)T][P(\mathcal{H}_1)P_d + P(\mathcal{H}_0)P_f - 1] + [NP_sT_1 + P_tT_2] + [P(\mathcal{H}_0)P_t(1 - P_f^{N+1}T] - P_s\eta T), \tag{A.5}$$

$$\frac{\partial V_0^0(\beta)}{\partial \beta} = -P(\mathcal{H}_0)\mathtt{C}(\phi+1)(N+1)\left\{(T_{Total} - \beta T)N(1-P_f)^{N-1}(\frac{\partial P_f}{\partial \beta}) + (1-P_f)^N T\right\}. \tag{A.6}$$

Since $V_0^0(\beta) \geq 0$ and $\tilde{E}_{SSR}(\beta) \geq 0$, it is easy to show that $V_0(\beta) \leq 0$. Thus $\frac{\partial V_0(\beta)}{\partial \beta}$ is a decreasing function of β. Similarly,

$$\frac{\partial V_1(\beta)}{\partial \beta} = V_1^0(\beta)\frac{\partial R_{SSR}(\beta)}{\partial \beta} + R_{SSR}(\beta)\frac{\partial V_1^0(\beta)}{\partial \beta}, \quad \text{where} \tag{A.7}$$

$$\frac{\partial R_{SSR}(\beta)}{\partial \beta} = -V^0(\beta)\frac{\partial P_f}{\partial \beta} + \left[\phi - (\phi+1)(1-P_f)^{N+1}\right]P(\mathcal{H}_0)\mathtt{C}T, \tag{A.8}$$

$$\frac{\partial V_1^0(\beta)}{\partial \beta} = -P(\mathcal{H}_0)\left\{P_t(N+1)\left\{(T_{Total} - \beta T)N(1-P_f)^{N-1}\frac{\partial P_f}{\partial \beta} + (1-P_f)^N T\right\} - (NP_s\eta T + (1-2\eta)T)\right\}. \tag{A.9}$$

Since $\frac{\partial P_f}{\partial \beta}$ is a decreasing function of β, $\frac{\partial \tilde{R}_{SSR}(\beta)}{\partial \beta} \geq 0$. Also, when $\tilde{R}_{SSR} \leq 0$ and $\frac{\partial V_1^0(\beta)}{\partial \beta} \leq 0$, then $V_1(\beta)$ is an increasing function of β. Therefore, if ϕ meets the requirement (D̲1) in lemma 3.1, $V_0(\beta)$ and $V_1(\beta)$ are monotonically decreasing and increasing in β, respectively. According to the constraints on β and P_f^{SSR}, β_{min} can calculated by considering the optimal detection threshold, and can be shown as

$$\beta_{min} = \left[\frac{1}{\left(\frac{\varepsilon^*}{\sigma^2} - 1\right)(\sqrt{\eta T f_s})}Q^{-1}\left(1 - (1-\overline{P}_f)^{\frac{1}{N+1}}\right)\right]^2. \tag{A.10}$$

Hence, $[V_0(\beta) - V_1(\beta)]$ is monotonic decreasing in $\beta_{min} \leq \beta \leq 1$.

Since the energy efficiency is quasi- concave in β, it is shown that the first derivative is positive as $\beta \to 0$ and negative as $\beta \to 1$. This indicates that there could be multiple points between 0 and 1, for which the first derivative is zero. The global optimum will be picked by the algorithm used to solve this problem. However, in case of a concave function, the point at which the first derivative is zero will be unique, and this existence of a unique maximum can be established by considering the second derivative.

A.3 Proof of Lemma 3.3 : To Show that $\frac{\partial \tilde{EE}_{SSR}}{\partial \eta} \geq 0$

The first order derivative of the cost function with respect to η can be expressed as

$$\frac{\partial \tilde{EE}_{SSR}}{\partial \eta} = -\left[V_0(\eta) - V_1(\eta)\right] \frac{\partial P_f}{\partial \eta} - V_2(\eta), \tag{A.11}$$

where $\frac{\partial P_f}{\partial \eta}$ is given by

$$\frac{\partial P_f}{\partial \eta} = -\frac{1}{2}\sqrt{\frac{\beta T f_s}{2\pi\eta}}\left(\frac{\varepsilon}{\sigma^2} - 1\right) \exp\left(\frac{-(\frac{\varepsilon}{\sigma^2} - 1)^2 \eta \beta T f_s}{2}\right). \tag{A.12}$$

It is straightforward to see that $\frac{\partial P_f}{\partial \eta} \leq 0$, i.e., P_f is a monotonic decreasing function with η. Now,

$$V_0(\eta) = V^0(\eta)\tilde{E}_{SSR}(\eta), \quad \text{where} \tag{A.13}$$

$$V^0(\eta) = \left\{P(\mathcal{H}_0)C(T_{Total} - \beta T)\left[(\Phi + 1)(N + 1)(1 - P_f)^N\right]\right\}. \tag{A.14}$$

Also,

$$V_1(\eta) = R_{SSR}(\eta)V^1(\eta), \quad \text{where} \tag{A.15}$$

$$V^1(\eta) = P(\mathcal{H}_0)\left\{(NP_s\eta\beta T + P_t(1 - 2\eta)\beta T) - P_t(T_{Total} - \beta T)(1 - P_f)^N(N + 1)\right\}. \tag{A.16}$$

Similarly, $V_2(\eta)$ can be expressed as

$$V_2(\eta) = R_{SSR}(\eta)(P_s\beta T - P(\mathcal{H}_1)\left[NP_s\beta T - 2P_t\beta T\right] \\ - \left[NP_s\eta\beta T + P_t + P_t(1-2\eta)\beta T\right] P_f P(\mathcal{H}_0) - \left[NP_s\beta T + 2P_t\beta T\right]). \tag{A.17}$$

It can be seen from the above expressions that when $0 \leq \eta \leq 1/3$, $\frac{\partial P_f}{\partial \eta} \rightarrow -\infty$ and $[V_0(\eta) - V_1(\eta)] \geq 0$, provided that $V_2(\eta) \leq 0$. Hence, $\frac{\partial \tilde{E}_{SSR}}{\partial \eta} \geq 0$ for all η.

Appendix B

Appendix for Chapter 4

B.1 Proof of Theorem 4.1

The proof technique is similar to the SSR scheme. $\frac{\partial \tilde{EE}_{OSSR}}{\partial \varepsilon}$ can be expressed as

$$\frac{\partial \tilde{EE}_{OSSR}}{\partial \varepsilon} = \frac{\left[-(V_1(\varepsilon)\tilde{E}_{OSSR}(\varepsilon) + V_2(\varepsilon))\right]}{\tilde{E}^2_{OSSR}(\varepsilon)} \frac{\partial P_f}{\partial \varepsilon} - R_{OSSR}(\varepsilon) V_3(\varepsilon) \frac{\partial P_d}{\partial \varepsilon} + V_4(\varepsilon), \quad \text{with} \tag{B.1}$$

$$V_1(\varepsilon) = \mathtt{C}(T_{Total} - T_0)P(\mathcal{H}_0) + \mathtt{C}(T_{Total} - \beta T)P(\mathcal{H}_0)\left\{\phi + (\phi+1)P^{OSSR}_{f,F} N (1 - P^{OSSR}_{f,F})^{N-1}\right\} - (1 - P^{OSSR}_{f,F})^N, \tag{B.2}$$

$$V_2(\varepsilon) = NP_sT_1P(\mathcal{H}_0) + P_tT_2 + P_t(T_{Total} - \beta T)(1-P_f)^N + P_t(T_{Total} - \beta T)(1-P_f)^N + P_t(T_{Total} - T_0)P(H_0), \tag{B.3}$$

$$V_3(\varepsilon) = NP_sT_1P(\mathcal{H}_1) - P_t(T_{Total} - T_0)P(\mathcal{H}_1), \text{ and} \tag{B.4}$$

$$V_4(\varepsilon) = (P_tT_2 + P_t(T_{Total} - \beta T))(P(\mathcal{H}_0)P_f N(1-P_f)^{N-1} + P_f, \tag{B.5}$$

each of which are greater than or equal to zero. Also, it can be shown that

$$\frac{\partial P_f}{\partial \varepsilon} = -\frac{1}{\sigma^2}\sqrt{\frac{\eta\beta T f_s}{2\pi}} \exp\left(\frac{-(\frac{\varepsilon}{\sigma^2} - 1)^2 \eta\beta T f_s}{2}\right) \leq 0. \tag{B.6}$$

$$\frac{\partial P_d}{\partial \varepsilon} = -\frac{1}{\sigma^2}\sqrt{\frac{\eta\beta T f_s}{2\pi(2\gamma+1)}} \exp\left(-\frac{\eta\beta T f_s}{4\gamma+2}\left(\frac{\varepsilon}{\sigma^2} - \gamma - 1\right)^2\right) \leq 0. \tag{B.7}$$

Appendix C

Appendix for Chapter 6

C.1 Proof of Theorem 6.1

To establish that $P_d^{CCCS} \geq \overline{P}_d$ is satisfied with equality, it is shown that $\frac{\partial \tilde{EE}_{cccs}(\lambda,\mathsf{c},N)}{\partial \lambda} \geq 0$, for all λ. Observe that

$$\frac{\partial \tilde{EE}_{cccs}(\lambda,\mathsf{c},N)}{\partial \lambda} = \frac{\frac{\partial \tilde{R}_{cccs}(\lambda)}{\partial \lambda}\tilde{E}_{cccs}(\lambda) - \tilde{R}_{cccs}(\lambda)\frac{\partial \tilde{E}_{cccs}(\lambda)}{\partial \lambda}}{\tilde{E}^2_{cccs}(\lambda)}, \tag{C.1}$$

where

$$\frac{\partial \tilde{R}_{cccs}(\lambda,\mathsf{c},N)}{\partial \lambda} = -\frac{\partial P_f}{\partial \lambda}(1+\phi)\pi_0 \mathcal{C}(T_{Total} - \mathsf{c}T_s), \tag{C.2}$$

and

$$\frac{\partial \tilde{E}_{cccs}(\lambda,\mathsf{c},N)}{\partial \lambda} = -\frac{\partial P_f}{\partial \lambda}\pi_0 P_t(T_{Total} - \mathsf{c}T_s). \tag{C.3}$$

Upon further simplification, $\frac{\partial \tilde{E}_{cccs}(\lambda,\mathsf{c},N)}{\partial \lambda}$ is given by

$$\frac{\partial \tilde{E}_{cccs}(\lambda,\mathsf{c},N)}{\partial \lambda} = -\frac{\partial P_f}{\partial \lambda}V_1(\lambda,\mathsf{c},N), \tag{C.4}$$

where

$$V_1(\lambda, \mathsf{c}, N) = \left[\frac{(1+\phi)\pi_0 \mathcal{C}(T_{Total} - \mathsf{c}T_s)\tilde{E}_{cccs}(\lambda, \mathsf{c}, N)}{\tilde{E}^2_{cccs}(\lambda, \mathsf{c}, N)} - \frac{\pi_0 P_t (T_{Total} - \mathsf{c}T_s) * \tilde{R}_{cccs}(\lambda, c, N)}{\tilde{E}^2_{cccs}(\lambda, \mathsf{c}, N)}\right] \tag{C.5}$$

Now, to show that $\frac{\partial E E_{CCCS}(\lambda, \mathsf{c}, N)}{\partial \lambda} \geq 0$, it is enough to show that $V_1(\lambda, \mathsf{c}, N) \geq 0$, since

$$\frac{\partial P_f}{\partial \lambda} = -\frac{1}{2\sigma_w^2 \sqrt{\mathsf{c}NP\pi}} \exp\left[-\frac{\left(\frac{\lambda}{\sigma_w^2} - \mathsf{c}NP\right)^2}{(4\mathsf{c}NP)}\right] \leq 0.$$

In general, it is hard to analytically show that $V_1(\lambda, \mathsf{c}, N) \geq 0$. However, since $\tilde{R}_{cccs}(\lambda, \mathsf{c}, N) \geq 0$ and $\tilde{E}_{cccs}(\lambda, \mathsf{c}, N) \geq 0$, the parameters $\phi, \mathcal{C}, T_{Total}$ and T_s can be chosen such that $(1+\phi)\pi_0 \mathcal{C}(T_{Total} - \mathsf{c}T_s)\tilde{E}_{cccs}(\lambda, \mathsf{c}, N) \geq \pi_0 P_t (T_{Total} - \mathsf{c}T_s)\tilde{R}_{cccs}(\lambda, \mathsf{c}, N)$. Later, in Sec. 6.6, it can be seen that the above condition is satisfied for those parameter values which are of practical interest. Therefore,

$$\overline{P}_d = Q\left(\frac{\frac{\lambda^*}{\sigma_x^2 + \sigma_w^2} - \mathsf{c}NP}{\sqrt{2\mathsf{c}NP}}\right) = Q\left(\frac{\frac{\lambda^*}{\sigma_w^2}\left(\frac{1}{1+\gamma}\right) - \mathsf{c}NP}{\sqrt{2\mathsf{c}NP}}\right). \tag{C.6}$$

Rearranging the equation gives the expression for λ^*.

C.2 Proof of Theorem 6.2

Note that

$$\frac{\partial \tilde{EE}_{cccs}(\lambda, \mathsf{c}, N)}{\partial \mathsf{c}} = \frac{\frac{\partial \tilde{R}_{cccs}(\mathsf{c})}{\partial \mathsf{c}} \tilde{E}_{cccs}(\mathsf{c}) - \tilde{R}_{cccs}(\mathsf{c}) \frac{\partial \tilde{E}_{cccs}(\mathsf{c})}{\partial \mathsf{c}}}{\tilde{E}^2_{cccs}(\mathsf{c})}. \tag{C.7}$$

As $\mathsf{c} \to 0$, it can be shown that

$$\lim_{\mathsf{c}\to 0} \frac{\partial \tilde{EE}_{cccs}(\lambda, \mathsf{c}, N)}{\partial \mathsf{c}} \geq \lim_{\mathsf{c}\to 0} \left\{-\frac{\partial P_f}{\partial \mathsf{c}}\left(\frac{\mathcal{C}}{P_t}\right) + V_2(\mathsf{c}, N)\right\}, \tag{C.8}$$

where

$$V_2(\mathsf{c}, N) = \frac{\left[NP_s\tau_s + NP_t\tau_r\right]\pi_0\mathcal{C}}{P_t^2} \geq 0 \tag{C.9}$$

Also, note that

$$\frac{\partial P_f}{\partial \mathsf{c}} = -\frac{1}{\sqrt{\pi}}\exp(\frac{(\frac{\lambda^*}{\sigma_w^2} - \mathsf{c}NP)^2}{4\mathsf{c}NP}) \left[-\frac{NP}{2\sqrt{\mathsf{c}NP}} - \frac{NP((\frac{\lambda^*}{\sigma_w^2} - \mathsf{c}NP))}{4(\mathsf{c}NP^{3/2})}\right] \tag{C.10}$$

Therefore, P_f is a monotonically decreasing function of c. When $\mathsf{c} \to 0$, it can be shown that $\frac{\partial P_f(\lambda,\mathsf{c},N)}{\partial \mathsf{c}} \to -\infty$. Since $V_2(\mathsf{c}, N)$ is a positive constant, $\lim_{\mathsf{c}\to 0}\frac{\partial \tilde{EE}_{cccs}(\lambda,\mathsf{c},N)}{\partial \mathsf{c}} = +\infty$. Furthermore, using a well-known bound on the Q function, the following lower bound P_f is obtained and is given by

$$P_f \geq \left[1 - \frac{2\mathsf{c}NP}{(\frac{\lambda}{\sigma_w^2} - cNP)^2}\right]\exp\left[-\frac{(\frac{\lambda}{\sigma_w^2} - \mathsf{c}NP)^2}{4\mathsf{c}NP}\right], \tag{C.11}$$

which can be used to get a lower bound on the first derivative of $\tilde{EE}_{cccs}(\lambda, \mathsf{c}, N)$ as

$$\begin{aligned}\frac{\partial \tilde{EE}_{cccs}(\lambda, \mathsf{c}, N)}{\partial \mathsf{c}} \geq\ & \underbrace{(BA - BD - BC - \mathsf{c}AC)}_{\triangleq X_1} \\ & + \underbrace{(BC + \mathsf{c}AC - 2BA + 2BD)\left[1 - \frac{2\mathsf{c}NP}{(\frac{\lambda}{\sigma_w^2} - \mathsf{c}NP)^2}\right]\exp\left[-\frac{(\frac{\lambda}{\sigma_w^2} - \mathsf{c}NP)^2}{4\mathsf{c}NP}\right]}_{\triangleq X_2} \\ & + \underbrace{(BA - BD)\left[1 - \frac{2\mathsf{c}NP}{(\frac{\lambda}{\sigma_w^2} - \mathsf{c}NP)^2}\right]^2\exp\left[-\frac{(\frac{\lambda}{\sigma_w^2} - \mathsf{c}NP)^2}{4\mathsf{c}NP}\right]}_{\triangleq X_3} - \underbrace{(AC)\frac{\partial P_f(\lambda, \mathsf{c}, N)}{\partial \mathsf{c}}}_{\triangleq X_4},\end{aligned} \tag{C.12}$$

where $A = \pi_0\mathcal{C}\left[T_{Total} - \mathsf{c}T_s\right]$, $B = \pi_0 P_t T_s$, $C = NP_s\mathsf{c}\tau_s + NP_t\mathsf{c}\tau_r$, $D = P_t\left[T_{Total} - \mathsf{c}T_s\right]\pi_0$

As seen earlier, $\frac{\partial P_f}{\partial \mathsf{c}}$ is negative, and it is easy to show that $BC + AE - 2BA + 2BD > 0, BA - BD > 0$, and consequently, $X_2 \geq 0$, $X_3 \geq 0$ and $X_4 \geq 0$. Now,

$$\begin{aligned}
\frac{\partial \tilde{EE}_{cccs}(\lambda, \mathsf{c}, N)}{\partial \mathsf{c}} &\geq X_1 + X_2 + X_3 + X_4 \\
&\geq X_1 \\
&= BA - BD - BC - AE \\
&= (\pi_0^2 P_t T_s)\pi_0 \mathcal{C}(T_{Total} - \mathsf{c}T_s) - (\pi_0^2 P_t^2 T_s)(T_{Total} - \mathsf{c}T_s) \\
&\quad - (\pi_0 P_t T_s)(NP_s c\tau_s + NP_t c\tau_r) \\
&\quad -\pi_0 \mathcal{C}(T_{Total} - \mathsf{c}T_s)(NP_s\tau_s + NP_t\tau_r)) \\
&= \underbrace{\pi_0 \left\{ P_t T_s \mathcal{C} - P_t^2 T_s - \mathcal{C}(NP_s\tau_s + NP_t\tau_r) \right\}}_{\triangleq W} (T_{Total} - \mathsf{c}T_s) \\
&\quad - \mathsf{c}\underbrace{\pi_0 P_t T_s (NP_s\tau_s + NP_t\tau_r)}_{\triangleq Y}
\end{aligned} \tag{C.13}$$

To ensure that $\frac{\partial \tilde{EE}_{cccs}(\lambda,\mathsf{c},N)}{\partial \mathsf{c}} \geq 0$, the right hand side of (C.13) has to be ≥ 0. Rearranging (C.13), observe that this is true when $\mathsf{c} \leq \mathsf{c}_{UB} \triangleq \frac{T_{Total}W}{T_s W + Y}$. In other words, it is shown that $\frac{\partial \tilde{EE}_{cccs}(\lambda,\mathsf{c},N)}{\partial \mathsf{c}} \geq 0$ whenever $\mathsf{c} \in (0, \mathsf{c}_{UB})$. Finally, to establish that $\mathsf{c}^* = \mathsf{c}_{\max}$, it is required to show that $\mathsf{c}_{\max} \leq \mathsf{c}_{UB}$. Although hard to show analytically, it is verified to be indeed true numerically, for moderate values of N and for low SNR, which is of practical relevance.

C.3 Proof of Theorem 6.4

Note that the first derivative of P_f is negative as given below.

$$\frac{\partial P_f}{\partial \lambda} = -\frac{1}{\sigma_w^2 \sqrt{2\pi \mathsf{c} N\gamma}} \exp\left[\frac{-\lambda^2}{(2\mathsf{c}N\gamma\sigma_w^4)}\right] \leq 0 \tag{C.14}$$

As mentioned earlier, since the expressions for average achievable throughput, average energy consumption and the energy efficiency expressions across all four scenarios **S1** $-$ **S4** for the deterministic case remains similar to the previous case, and similar set of arguments hold true for the deterministic case too. These can be used to prove that the first derivative of $\tilde{EE}_{cccs}$ is

greater than or equal to 0. Therefore,

$$\overline{P}_d = Q\left(\frac{\lambda^* - \mathsf{c}N\sigma_w^2}{\sigma_w^2\sqrt{\mathsf{c}N\gamma}}\right). \tag{C.15}$$

Rearranging the above equation gives the expression for λ^*.

C.4 Proof of Theorem 6.5

Note that the first derivative of $P_f^{CCCS,det}$ with respect to c from (6.36) is given by,

$$\frac{\partial P_f(\lambda, N, \mathsf{c})}{\partial \mathsf{c}} = -\frac{\exp(-(\frac{\lambda^2}{2N\gamma\sigma_w^4})N\gamma\lambda}{2\sqrt{2\pi}(cN\gamma)^{3/2}\sigma_w^2} \leq 0. \tag{C.16}$$

Therefore, $\lim_{\mathsf{c}\to 0}\frac{\partial P_f(\lambda,\mathsf{c},N)}{\partial \mathsf{c}} \to -\infty$. Similar arguments given in Sec. C.2 can be used to show that $\mathsf{c}^* = \mathsf{c}_{\max}$, even in this case.

Appendix D

Detection Performance of SSR Scheme

D.1 Bayesian Detector

Performance of Bayesian detector are better when compared to energy detector in terms of spectrum utilization and secondary user throughput. According to binary hypothesis testing, test statistics of Bayesian rule is to compute the likelihood ratio and compare with the threshold δ [170]. The probability ratio test (PRT) of the hypothesis H_1 and H_0 for the received signal r(t) can be defined as

$$T_{PRT}(r) = \frac{P(r/H_1)}{P(r/H_0)} \tag{D.1}$$

Finally, the probability ratio test $T_{PRT}(r)$ is compared with a threshold δ that depends on the cost function, which is properly chosen to reduce the estimated posterior cost defined as

$$C = \sum_{i=0}^{1} \sum_{j=0}^{1} C_{ij} p(\mathcal{H}_j) p(\mathcal{H}_i|\mathcal{H}_j) \tag{D.2}$$

Thus based on [13], it is known that at low SNR the detection probability and false alarm probability of Bayesian detector are respectively given as

$$P_D = Q\left(\frac{\ln\delta - 2N\gamma^2}{\gamma\sqrt{2N(1+4\gamma)}}\right) \tag{D.3}$$

$$P_F = Q\left(\frac{\ln\delta}{\gamma\sqrt{2N}}\right) \tag{D.4}$$

Usually the threshold is calculated by fixing individual false alarm probability and is given by

$$\delta = \exp(\gamma\sqrt{2N}Q^{-1}(P_F)) \tag{D.5}$$

Where Q^{-1} is the inverse function of marcum-Q function. Thus by using (5) on (3), individual detection probability using Bayesian detector is obtained.

D.2 Detection Performance Analysis of Proposed BD-SSRCS Scheme

Performance analysis of BD-SSRCS in terms of detection probability, false alarm probability and average sensing time is considered in this section.

D.2.1 Overall detection Probability of BD-SSRCS strategy

Overall, SSR probability of false alarm and probability of detection are evaluated as

$$P_f^{\mathrm{SSR}} = P_{f,F}^{\mathrm{SSR}} + \left(1 - P_{f,F}^{\mathrm{SSR}}\right) P_{f,F,1}^{\mathrm{SSR}} \tag{D.6}$$

$$P_d^{\mathrm{SSR}} = P_{d,F}^{\mathrm{SSR}} + \left(1 - P_{d,F}^{\mathrm{SSR}}\right) P_{d,F,1}^{\mathrm{SSR}} \tag{D.7}$$

Figure.D.1 plots probability of detection versus false alarm probability (P_f) for both Bayesian and energy based detectors. It is apparent that SSR scheme with Bayesian detector outperforms other strategies by providing improved detection performance.The reason is of two fold; one is due to

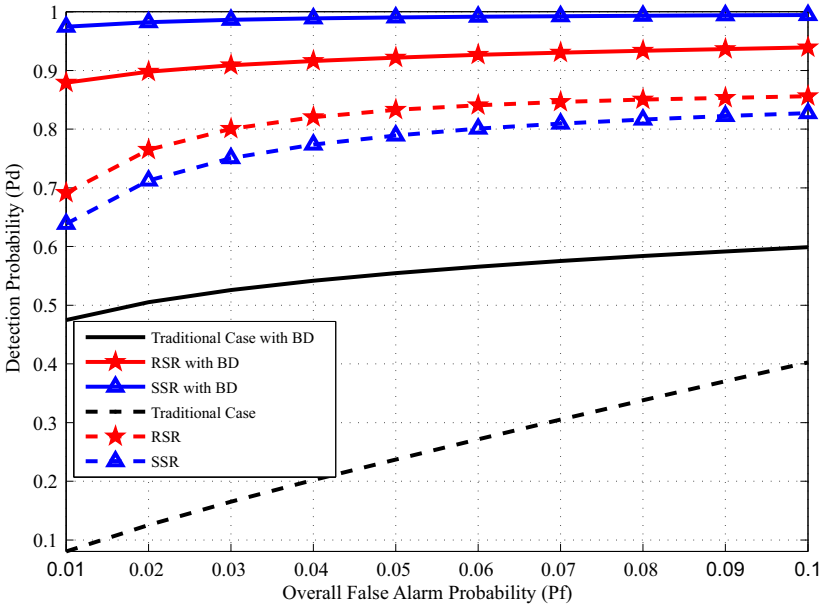

Figure D.1. Detection Probability versus false alarm probability for the traditional, RSR and SSR Scheme.

the fact that sensing by individual SUs are carried out by Bayesian detector which performs well under low SNR. Secondly due to the selection of superior reporting SU. SSR combined with BD results in 16.71% increase in detection probability. While the increase in RSR is 8.32%, traditional case exhibits 19.65% increase in detection probability. Improvement of probability of detection using Bayesian detector in suggested cooperative sensing scheme is listed in Table. D.1.

Table D.1. Probability of detection (P_d) for different sensing scheme for both Bayesian and energy detector for SNR=-6dB, $(P_f = 0.1)$

Cooperative sensing Scheme	**Local Sensing**	P_d	**% of improvement in** P_d
Traditional	BD	0.599	19.65%
	ED	0.4025	
RSR	BD	0.9392	8.32%
	ED	0.856	
SSR	BD	0.9946	16.71%
	ED	0.8275	

Figure.D.2 show influence of η on miss detection probability. Modification of η to an optimal value lessens miss detection probability for a given β. Incrementing η ensures an increment in local detection time, thus decreasing miss detection probability. However, more time allotment to sensing phase decreases reporting time which leads to reporting performance degradation. Hence there exists a trade-off between local decision performance and decision reporting for the

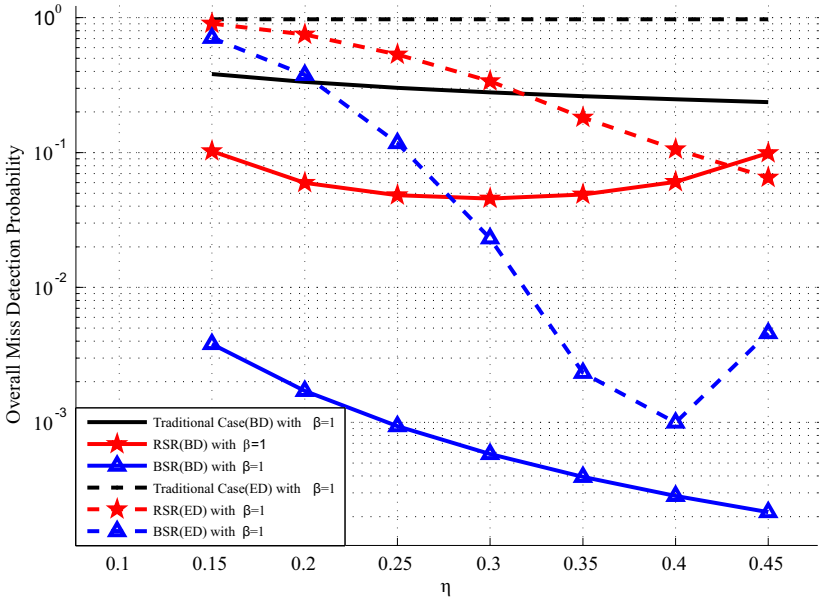

Figure D.2. Miss detection Probability versus η for the traditional,RSR and SSR Scheme for β=1

Table D.2. Percentage reduction in miss detection probability using Bayesian in different sensing scheme with different values of β

Cooperative sensing Scheme	**Local Sensing**	**Pm**		**% reduction of Pm**	
		$\beta = 1$	$\beta = 0.5$	$\beta = 1$	$\beta = 0.5$
Traditional	BD	0.302	0.416	68.98%	56.68%
	ED	0.975	0.961		
RSR	BD	0.048	0.369	48.63%	56.79%
	ED	0.534	0.855		
SSR	BD	0.0009	0.006	99.20%	99.25%
	ED	0.117	0.855		

proposed strategy. Improvement of local detection probability by using Bayesian detector ensures improvement in overall reporting performance at reduced β value. This in turn reduces overall miss detection probability. Percentage reduction in miss detection probability using Bayesian in suggested cooperative sensing scheme with different values of β is listed in Table D.2.

Table D.3. AST for BD-SSRCS and ED-SSRCS for different values of γ_P and σ^2_{PF}

γ_P	σ^2_{PF}	**Average Sensing Time**		**% reduction of Average Sensing Time**
		SSR-BD	**SSR-ED**	
-10	0.6	1.738	1.894	8.23%
-6	0.6	1.189	1.699	30.01%
-6	1	1.045	1.559	32.96%

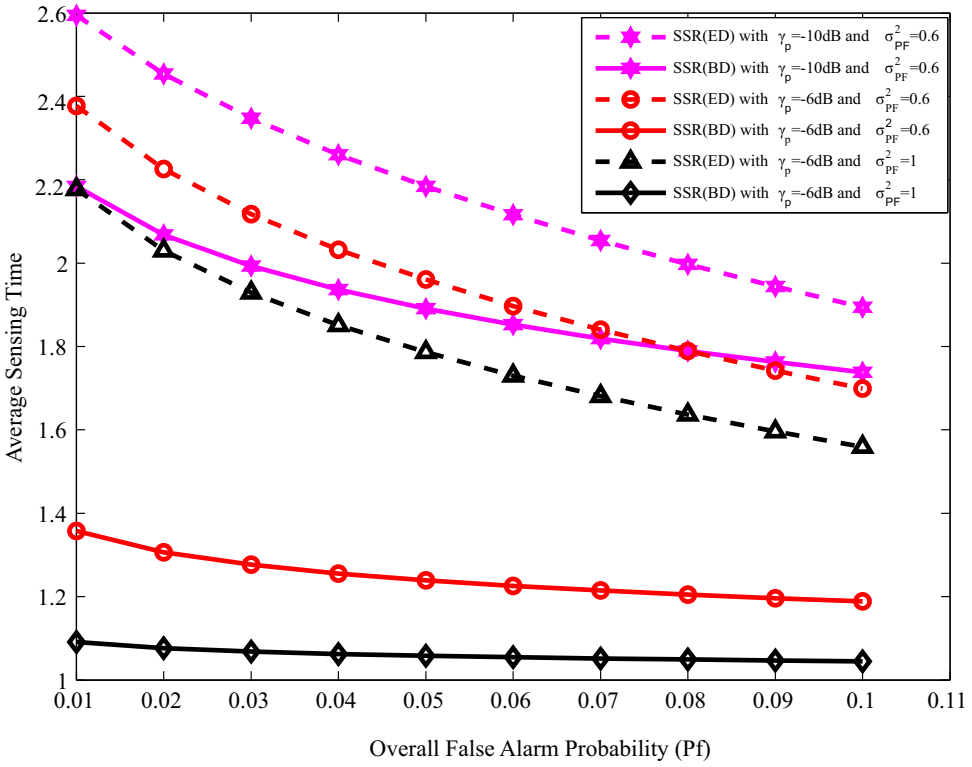

Figure D.3. AST versus false alarm probability for SSR scheme for different γ_p and σ^2_{PF} values

Table D.4. AST for different sensing scheme using energy detector and Bayesian detector with η=0.25 , σ^2_{PF}=1 , γ_P = -6dB , P_f = 0.01

β	**Sensing Scheme**	**AST**	**% reduction in AST**
0.5	SSR/RSR-BD	1.533	48.27%
	SSR/RSR-ED	2.964	
1	SSR/RSR-BD	2.328	52.18%
	SSR/RSR-ED	4.869	

D.2.2 Average Sensing Time (AST)

Average Sensing Time (AST) is the time needed to arrive at a final conclusion about the existence of PU in a sensing phase. In the conventional case, cooperative SUs use up all the subslots to report their local decisions. The total sensing time for the traditional scheme is

$$\bar{t}_{Tra} = N + 1 \tag{D.8}$$

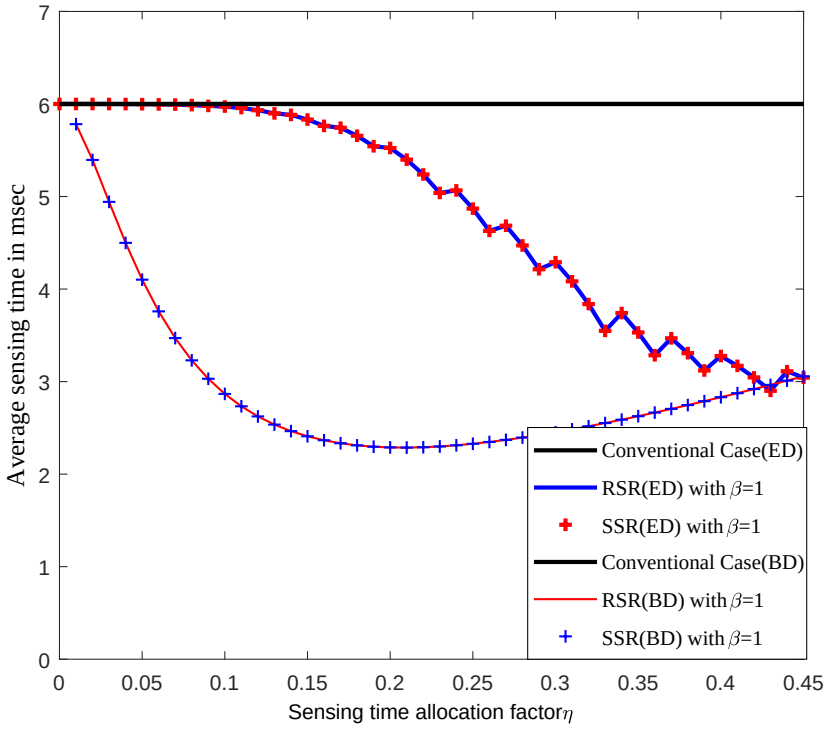

Figure D.4. Average Sensing Time versus false alarm probability for the traditional, RSR and SSR scheme for β=1

In SSR strategies, detection of presence of PU by center SU merely requires time slot T_0, else T_1 and T_2 add to the time. Hence the AST of SSR is expressed as

$$\bar{t}_{SSR} = \beta(N+1)\left(1 - P_{d,F}^{\mathrm{SSR}} + \eta P_{d,F}^{\mathrm{SSR}}\right) \tag{D.9}$$

Above equations distinctly claim that when local detection by center SU(F) is high, i.e. when $P_{d,F}^{SSR}$ tends to 1, it does not need assistance from other cooperative SUs for sensing, which reduces the AST of BD-SSRCS scheme. Furthermore, when F cannot detect presence of PU by itself, i.e when $P_{d,F}^{SSR}$ tends to 0, the suggested schemes use up to (N + 1) subslots. Even in this worst case scenario, the suggested schemes have lower ASTs as compared to the conventional scheme since η is considered to be a small value.

From the simulation results, it is evident that ASTs for the suggested methods can be minimized by choosing appropriate η for any given β value.Figure D.3 Probability of false alarm plot for SSR schemes under different values of SNR and noise variance for both energy detector and Bayesian detector. From the time slot structure it is clear that AST depends on sensing time allocation

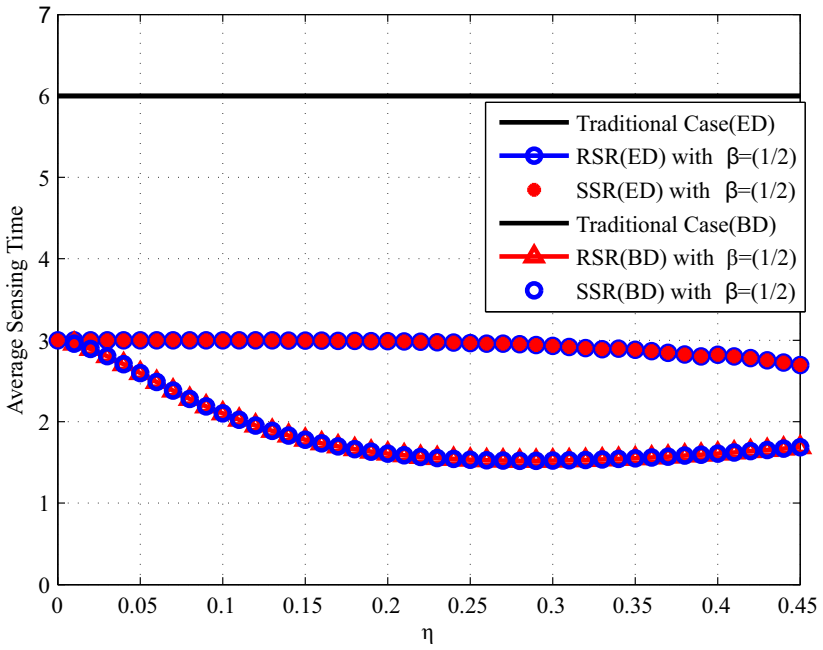

Figure D.5. Average Sensing Time versus false alarm probability for the traditional, RSR and SSR scheme for β=0.5

factor β, η and the local detection probability of center SU. Since the local detection is carried by Bayesian detector which works well under low SNR regime this improves the local sensing probability of center SU which further reduces the AST of BD-SSRCS scheme. Table. D.3. shows quantitative comparison of BD-SSRCS and ED-SSRCS based on γ_P and σ^2_{PF}. It is observed that AST is reduced in BD-SSRCS when compared to ED-SSRCS. Also it can be noticed that average sensing time is deceased as γ_P grows or when channel quality from Primary user, P to center SU, F is improved. This situation avoids cooperation of other SUs since center SU (F) itself will detect the presence of PU. Figures.D.4 and D.5 shows the influence of β and η on AST. Increase in β and η results in longer sensing time. Fig.6 illustrates that choosing an optimum value of η leads to minimization of average sensing time. Moreover, since AST in SSR and RSR depends on β,η and the local detection probability of F, ASTs of both the scheme are nearly identical to each other. It is understood from (D.9) that AST of the proposed BD-SSRCS scheme reduces as $P^{SSR}_{d,F}$ tends to 1. Therefore, in this scenario F seldom needs assistance from cooperative SUs for spectrum sensing. Although β increases, higher local detection probability leads to decrease in AST of the proposed scheme. Table D.4 illustrates the reduction in AST when Bayesian detector is used for local sensing when compared to energy detector. It can be concluded that by adjusting β and η AST can be minimized.

Bibliography

[1] S. Eryigit, G. Gur, S. Bayhan, and T. Tugcu, "Energy efficiency is a subtle concept: fundamental trade-offs for cognitive radio networks," *IEEE Commun. Mag.*, vol. 52, no. 7, pp. 30–36, Jul. 2014.

[2] J. Mitola and G. Q. Maguire, "Cognitive radio: making software radios more personal," *IEEE Personal Commun. Mag.*, vol. 6, no. 4, pp. 13–18, Aug. 1999.

[3] J. Mitola, "Cognitive Radio — An Integrated Agent Architecture for Software Defined Radio," DTech thesis, Royal Institute of Technology (KTH), Kista, Sweden, May 2000.

[4] S. K. Sharma, T. E. Bogale, L. B. Le, S. Chatzinotas, X. Wang, and B. Ottersten, "Dynamic spectrum sharing in 5G wireless networks with full-duplex technology: Recent advances and research challenges," *IEEE Commun. Surveys Tuts.*, vol. PP, no. 99, pp. 1–1, 2017.

[5] FCC, "Unlicensed operation in the TV broadcast bands," *in Notice of Proposed Rule Making (NPRM) Docket No. 04-113*, May 2004.

[6] H. R. Imam, K. Inage, M. Ohta, and T. Fujii, "Measurement based radio environment database using spectrum sensing in cognitive radio," in *Proc. iCOST (2011 International Conference on Selected Topics in Mobile and Wireless Networking)*, Oct. 2011, pp. 110–115.

[7] T. Yucek and H. Arslan, "A survey of spectrum sensing algorithms for cognitive radio applications," *IEEE Commun. Surveys Tuts.*, vol. 11, no. 1, pp. 116–130, Mar. 2009.

[8] I. F. Akyildiz, B. F. Lo, and R. Balakrishnan, "Cooperative spectrum sensing in cognitive radio networks : A survey," *Physical Communication*, vol. 4, no. 1, pp. 40–62, 2011.

[9] E. Axell, G. Leus, E. G. Larsson, and H. V. Poor, "Spectrum sensing for cognitive radio : State-of-the-art and recent advances," *IEEE Signal Process. Mag.*, vol. 29, no. 3, pp. 101–116, May 2012.

[10] F. F. Digham, M. S. Alouini, and M. K. Simon, "On the energy detection of unknown signals over fading channels," *IEEE Trans. Commun.*, vol. 55, no. 1, pp. 21–24, Jan. 2007.

[11] M. S. Murty and R. Shrestha, "Reconfigurable memory-efficient cyclostationary spectrum sensor for cognitive-radio wireless networks," *IEEE Trans. Circuits Syst. II*, vol. PP, no. 99, pp. 1–1, 2018.

[12] X. Zhang, R. Chai, and F. Gao, "Matched filter based spectrum sensing and power level detection for cognitive radio network," in *Proc. GlobalSIP*, Dec. 2014, pp. 1267–1270.

[13] S. Zheng, P. Y. Kam, Y. C. Liang, and Y. Zeng, "Bayesian spectrum sensing for digitally modulated primary signals in cognitive radio," in *Proc. VTC (Spring)*, May 2011, pp. 1–5.

[14] G. Sanjeev, K. V. K. Chaythanya, and C. R. Murthy, "Bayesian decentralized spectrum sensing in cognitive radio networks," in *Proc. SPCOM*, Jul. 2010, pp. 1–5.

[15] J. Song, Z. Feng, P. Zhang, and Z. Liu, "Spectrum sensing in cognitive radios based on enhanced energy detector," *IET Commun.*, vol. 6, no. 8, pp. 805–809, May 2012.

[16] A. Ghasemi and E. S. Sousa, "Collaborative spectrum sensing for opportunistic access in fading environments," in *Proc. DySPAN*, Nov. 2005, pp. 131–136.

[17] D. J. Lee, "Adaptive random access for cooperative spectrum sensing in cognitive radio networks," *IEEE Trans. Wireless Commun.*, vol. 14, no. 2, pp. 831–840, Feb. 2015.

[18] S. Hussain and X. N. Fernando, "Performance analysis of relay-based cooperative spectrum sensing in cognitive radio networks over non-identical nakagami- m channels," *IEEE Trans. Commun.*, vol. 62, no. 8, pp. 2733–2746, Aug. 2014.

[19] X. Chen, H. H. Chen, and W. Meng, "Cooperative communications for cognitive radio networks from theory to applications," *IEEE Commun. Surveys Tuts.*, vol. 16, no. 3, pp. 1180–1192, Mar. 2014.

[20] K. Cichon, A. Kliks, and H. Bogucka, "Energy-efficient cooperative spectrum sensing: A survey," *IEEE Commun. Surveys Tuts.*, vol. 18, no. 3, pp. 1861–1886, Apr. 2016.

[21] D. Cohen and Y. C. Eldar, "Sub-nyquist sampling for power spectrum sensing in cognitive radios: A unified approach," *IEEE Trans. Signal Process.*, vol. 62, no. 15, pp. 3897–3910, Aug. 2014.

[22] S. Chaudhari, J. Lunden, V. Koivunen, and H. V. Poor, "Cooperative sensing with imperfect reporting channels: Hard decisions or soft decisions?" *IEEE Trans. Signal Process.*, vol. 60, no. 1, pp. 18–28, Jan. 2012.

[23] D. Hamza, S. Aïssa, and G. Aniba, "Equal gain combining for cooperative spectrum sensing in cognitive radio networks," *IEEE Trans. Wireless Commun.*, vol. 13, no. 8, pp. 4334–4345, Aug. 2014.

[24] R. Bouraoui and H. Besbes, "Cooperative spectrum sensing for cognitive radio networks: Fusion rules performance analysis," in *Proc. IWCMC*, Sept. 2016, pp. 493–498.

[25] Q. WANG, D. wu YUE, and Q. na YAN, "Optimal fusion rule for cooperative spectrum sensing in cognitive radio networks," *The Journal of China Universities of Posts and Telecommunications*, vol. 19, no. 5, pp. 58 – 65, 2012.

[26] S. Maleki, S. P. Chepuri, and G. Leus, "Energy and throughput efficient strategies for cooperative spectrum sensing in cognitive radios," in *Proc. SPAWC*, Jun. 2011, pp. 71–75.

[27] E. C. Y. Peh, Y. C. Liang, Y. L. Guan, and Y. Zeng, "Cooperative spectrum sensing in cognitive radio networks with weighted decision fusion schemes," *IEEE Trans. Wireless Commun.*, vol. 9, no. 12, pp. 3838–3847, Dec. 2010.

[28] S. Althunibat, "Towards Energy Efficient Cooperative Spectrum Sensing in Cognitive Radio Networks," Ph.D thesis, University of Trento, Trento, Italy, 2014.

[29] X. Huang, T. Han, and N. Ansari, "On green-energy-powered cognitive radio networks," *IEEE Commun. Surveys Tuts.*, vol. 17, no. 2, pp. 827–842, Jan. 2015.

[30] M. Emara, H. S. Ali, S. E. Khamis, and F. E. Abd El-Samie, "Spectrum sensing optimization and performance enhancement of cognitive radio networks," *Wirel. Pers. Commun.*, vol. 86, no. 2, pp. 925–941, Jan. 2016.

[31] E. C. Y. Peh, Y. C. Liang, Y. L. Guan, and Y. Pei, "Energy-efficient cooperative spectrum sensing in cognitive radio networks," in *Proc. GLOBECOM*, Dec. 2011, pp. 1–5.

[32] Z. Li, B. Liu, J. Si, and F. Zhou, "Optimal spectrum sensing interval in energy-harvesting cognitive radio networks," *IEEE Trans. Cognitive Commun. Netw.*, vol. 3, no. 2, pp. 190–200, Jun. 2017.

[33] M. Monemian and M. Mahdavi, "Analysis of a new energy-based sensor selection method for cooperative spectrum sensing in cognitive radio networks," *IEEE Sensors J.*, vol. 14, no. 9, pp. 3021–3032, Sept. 2014.

[34] Z. Dai, J. Liu, and K. Long, "Selective-reporting-based cooperative spectrum sensing strategies for cognitive radio networks," *IEEE Trans. Veh. Technol.*, vol. 64, no. 7, pp. 3043–3055, Jul. 2015.

[35] B. Wang, K. J. R. Liu, and T. C. Clancy, "Evolutionary cooperative spectrum sensing game: how to collaborate?" *IEEE Trans. Commun.*, vol. 58, no. 3, pp. 890–900, Mar. 2010.

[36] R. Kishore, C. Ramesha, and K. Anupama, "Bayesian detector based superior selective reporting mechanism for cooperative spectrum sensing in cognitive radio networks," *Procedia Computer Science*, vol. 93, pp. 207 – 216, 2016.

[37] N. Zhao, F. Pu, X. Xu, and N. Chen, "Optimisation of multi-channel cooperative sensing in cognitive radio networks," *IET Commun.*, vol. 7, no. 12, pp. 1177–1190, Aug. 2013.

[38] F. Zeng, C. Li, and Z. Tian, "Distributed compressive spectrum sensing in cooperative multihop cognitive networks," *IEEE J. Sel. Topics Signal Process.*, vol. 5, no. 1, pp. 37–48, Feb. 2011.

[39] Y. L. Polo, Y. Wang, A. Pandharipande, and G. Leus, "Compressive wide-band spectrum sensing," in *Proc. ICASSP*, Apr. 2009, pp. 2337–2340.

[40] W. S., F. Granelli, L. Y., and C. S., "Energy-efficient cognitive radio networks," *IEEE Commun. Mag.*, vol. 52, no. 7, pp. 12–13, Jul. 2014.

[41] X. Gan, M. Xu, and H. Li, "Energy efficient sequential sensing in multi-user cognitive ad hoc networks: A consideration of an adc device," *J. Commun. Networks*, vol. 14, no. 2, pp. 188–194, Apr. 2012.

[42] F. Kong, J. Cho, and B. Lee, "Optimizing spectrum sensing time with adaptive sensing interval for energy-efficient crsns," *IEEE Sensors J.*, vol. 17, no. 22, pp. 7578–7588, Nov. 2017.

[43] A. Kaur, S. Sharma, and A. Mishra, "Sensing period adaptation for multiobjective optimisation in cognitive radio using jaya algorithm," *Electron. Lett.*, vol. 53, no. 19, pp. 1335–1336, Sept. 2017.

[44] H. Wu, F. Yao, Y. Chen, Y. Liu, and T. Liang, "Cluster-based energy efficient collaborative spectrum sensing for cognitive sensor network," *IEEE Commun. Lett.*, vol. 21, no. 12, pp. 2722–2725, Dec. 2017.

[45] A. Ebrahimzadeh, M. Najimi, S. M. H. Andargoli, and A. Fallahi, "Sensor selection and optimal energy detection threshold for efficient cooperative spectrum sensing," *IEEE Trans. Veh. Technol.*, vol. 64, no. 4, pp. 1565–1577, Apr. 2015.

[46] J. Lai, E. Dutkiewicz, R. P. Liu, and R. Vesilo, "Cooperative sensing with detection threshold optimization in cognitive radio networks," in *2012 International Symposium on Communications and Information Technologies (ISCIT)*, Oct. 2012, pp. 781–786.

[47] Y. Wang, C. Feng, C. Guo, and F. Liu, "Optimization of parameters for spectrum sensing in cognitive radios," in *2009 5th International Conference on Wireless Communications, Networking and Mobile Computing*, Sept. 2009, pp. 1–4.

[48] L. Luo, C. Ghosh, and S. Roy, "Joint optimization of spectrum sensing for cognitive radio networks," in *Proc. GLOBECOM*, Dec. 2010, pp. 1–5.

[49] L. Luo and S. Roy, "Efficient spectrum sensing for cognitive radio networks via joint optimization of sensing threshold and duration," *IEEE Trans. Commun.*, vol. 60, no. 10, pp. 2851–2860, Oct. 2012.

[50] S. K. Sharma, E. Lagunas, S. Chatzinotas, and B. Ottersten, "Application of compressive sensing in cognitive radio communications: A survey," *IEEE Commun. Surveys Tuts.*, vol. 18, no. 3, pp. 1838–1860, Feb. 2016.

[51] T. Xiong, H. Li, P. Qi, Z. Li, and S. Zheng, "Predecision for wideband spectrum sensing with sub-nyquist sampling," *IEEE Trans. Veh. Technol.*, vol. 66, no. 8, pp. 6908–6920, Aug. 2017.

[52] J. Zhao, Q. Liu, X. Wang, and S. Mao, "Scheduled sequential compressed spectrum sensing for wideband cognitive radios," *IEEE Trans. Mobile Comput.*, vol. PP, no. 99, pp. 1–1, Aug. 2017.

[53] B. Kailkhura, T. Wimalajeewa, and P. K. Varshney, "Collaborative compressive detection with physical layer secrecy constraints," *IEEE Trans. Signal Process.*, vol. 65, no. 4, pp. 1013–1025, Feb. 2017.

[54] Y. Ma, Y. Gao, A. Cavallaro, C. G. Parini, W. Zhang, and Y. C. Liang, "Sparsity independent sub-nyquist rate wideband spectrum sensing on real-time tv white space," *IEEE Trans. Veh. Technol.*, vol. 66, no. 10, pp. 8784–8794, Oct. 2017.

[55] L. Arienzo and D. Tarchi, "Stochastic optimization of cognitive networks," *IEEE Trans. Green Commun. Netw.*, vol. 1, no. 1, pp. 40–58, Mar. 2017.

[56] M. Costa and A. Ephremides, "Energy efficiency versus performance in cognitive wireless networks," *IEEE J. Sel. Areas Commun.*, vol. 34, no. 5, pp. 1336–1347, May 2016.

[57] T. D. P. Perera, D. N. K. Jayakody, S. K. Sharma, S. Chatzinotas, and J. Li, "Simultaneous wireless information and power transfer (swipt): Recent advances and future challenges," *IEEE Commun. Surveys Tuts.*, vol. 20, no. 1, pp. 264–302, Dec. 2018.

[58] R. Paul, W. Pak, and Y. J. Choi, "Selectively triggered cooperative sensing in cognitive radio networks," *IET Commun.*, vol. 8, no. 15, pp. 2720–2728, Oct. 2014.

[59] W. Lee, J. Kang, and J. Kang, "Joint resource allocation for throughput enhancement in cognitive radio femtocell networks," *IEEE Wireless Communications Letters*, vol. 4, no. 2, pp. 181–184, Apr. 2015.

[60] P. Cheng, R. Deng, and J. Chen, "Energy-efficient cooperative spectrum sensing in sensor-aided cognitive radio networks," *IEEE Wireless Commun.*, vol. 19, no. 6, pp. 100–105, Dec. 2012.

[61] S. Xie, Y. Liu, Y. Zhang, and R. Yu, "A parallel cooperative spectrum sensing in cognitive radio networks," *IEEE Trans. Veh. Technol.*, vol. 59, no. 8, pp. 4079–4092, Oct. 2010.

[62] Y. Wang, C. Feng, Z. Zeng, and C. Guo, "A robust and energy efficient cooperative spectrum sensing scheme in cognitive radio networks," in *2009 11th International Conference on Advanced Communication Technology*, vol. 01, Feb. 2009, pp. 640–645.

[63] A. Baharlouei and B. Jabbari, "A stackelberg game spectrum sensing scheme in cooperative cognitive radio networks," in *Proc. WCNC*, Apr. 2012, pp. 2215–2219.

[64] Y. Pei, Y. C. Liang, K. C. Teh, and K. H. Li, "Energy-efficient design of sequential channel sensing in cognitive radio networks: Optimal sensing strategy, power allocation, and sensing order," *IEEE J. Sel. Areas Commun.*, vol. 29, no. 8, pp. 1648–1659, Sept. 2011.

[65] S. H. Hojjati, A. Ebrahimzadeh, M. Najimi, and A. Reihanian, "Sensor selection for cooperative spectrum sensing in multiantenna sensor networks based on convex optimization and genetic algorithm," *IEEE Sensors J.*, vol. 16, no. 10, pp. 3486–3487, May 2016.

[66] S. Maleki, A. Pandharipande, and G. Leus, "Energy-efficient distributed spectrum sensing with convex optimization," in *2009 3rd IEEE International Workshop on Computational Advances in Multi-Sensor Adaptive Processing (CAMSAP)*, Dec. 2009, pp. 396–399.

[67] S. Maleki, A.Pandharipande, and G.Leus, "Energy-efficient distributed spectrum sensing for cognitive sensor networks," *IEEE Sensors J.*, vol. 11, no. 3, pp. 565–573, Mar. 2011.

[68] C. H. Lee and W. Wolf, "Energy efficient techniques for cooperative spectrum sensing in cognitive radios," in *2008 5th IEEE Consumer Communications and Networking Conference*, Jan. 2008, pp. 968–972.

[69] Z. Khan, J. Lehtomaki, K. Umebayashi, and J. Vartiainen, "On the selection of the best detection performance sensors for cognitive radio networks," *IEEE Signal Process. Lett.*, vol. 17, no. 4, pp. 359–362, Apr. 2010.

[70] L. Li, Y. Lu, and H. Zhu, "Half-voting based twice-cooperative spectrum sensing in cognitive radio networks," in *2009 5th International Conference on Wireless Communications, Networking and Mobile Computing*, Sept. 2009, pp. 1–3.

[71] W. Yuan, H. Leung, W. Cheng, and S. Chen, "Optimizing voting rule for cooperative spectrum sensing through learning automata," *IEEE Trans. Veh. Technol.*, vol. 60, no. 7, pp. 3253–3264, Sept. 2011.

[72] S. Chaudhari, J. Lunden, V. Koivunen, and H. V. Poor, "Cooperative sensing with imperfect reporting channels: Hard decisions or soft decisions?" *IEEE Trans. Signal Process.*, vol. 60, no. 1, pp. 18–28, Jan. 2012.

[73] E. C. Y. Peh, Y. C. Liang, Y. L. Guan, and Y. Pei, "Energy-efficient cooperative spectrum sensing in cognitive radio networks," in *Proc. GLOBECOM*, Dec. 2011, pp. 1–5.

[74] S. Saha, A. Kumar, Priyanka, and R. Bhattacharya, "An llr based cooperative spectrum sensing with hard-soft combining for cognitive radio networks," in *2017 XXXIInd General Assembly and Scientific Symposium of the International Union of Radio Science (URSI GASS)*, Aug. 2017, pp. 1–4.

[75] W. Ejaz, G. Hattab, N. Cherif, M. Ibnkahla, F. Abdelkefi, and M. Siala, "Cooperative spectrum sensing with heterogeneous devices: Hard combining versus soft combining," *IEEE Systems J.*, vol. PP, no. 99, pp. 1–12, 2017.

[76] S. Nallagonda, Y. R. Kumar, and P. Shilpa, "Analysis of hard-decision and soft-data fusion schemes for cooperative spectrum sensing in rayleigh fading channel," in *2017 IEEE 7th International Advance Computing Conference (IACC)*, Jan. 2017, pp. 220–225.

[77] Y. H. Bae and J. W. Baek, "Achievable throughput analysis of opportunistic spectrum access in cognitive radio networks with energy harvesting," *IEEE Trans. Commun.*, vol. 64, no. 4, pp. 1399–1410, Apr. 2016.

[78] S. Park, H. Kim, and D. Hong, "Cognitive radio networks with energy harvesting," *IEEE Trans. Wireless Commun.*, vol. 12, no. 3, pp. 1386–1397, Mar. 2013.

[79] G. Anastasi, M. Conti, M. D. Francesco, and A. Passarella, "Energy conservation in wireless sensor networks: A survey," *Ad Hoc Networks*, vol. 7, no. 3, pp. 537 – 568, 2009.

[80] A. O. Ercan, O. Sunay, and I. F. Akyildiz, "Rf energy harvesting and transfer for spectrum sharing cellular IoT communications in 5G systems," *IEEE Trans. Mobile Comput.*, vol. PP, no. 99, pp. 1–1, Aug. 2017.

[81] S. Hussain and X. N. Fernando, "Performance analysis of relay-based cooperative spectrum sensing in cognitive radio networks over non-identical nakagami- m channels," *IEEE Trans. Commun.*, vol. 62, no. 8, pp. 2733–2746, Aug. 2014.

[82] Y. Feng, Y. Luo, W. Xu, S. Li, Z. He, and J. Lin, "Energy-efficient power allocation algorithms for OFDM-based cognitive relay networks with imperfect spectrum sensing," in *Proc. ICC*, Jun. 2014, pp. 337–342.

[83] J. Wei and X. Zhang, "Energy-efficient distributed spectrum sensing for wireless cognitive radio networks," in *2010 INFOCOM IEEE Conference on Computer Communications Workshops*, Mar. 2010, pp. 1–6.

[84] Z. Javed, K. L. A. Yau, H. Mohamad, N. Ramli, J. Qadir, and Q. Ni, "Rl-budget: A learning-based cluster size adjustment scheme for cognitive radio networks," *IEEE Access*, vol. 6, pp. 1055–1072, Nov. 2018.

[85] C. H. Lee and W. Wolf, "Energy efficient techniques for cooperative spectrum sensing in cognitive radios," in *2008 5th IEEE Consumer Communications and Networking Conference*, Jan 2008, pp. 968–972.

[86] W. Xia, S. Wang, W. Liu, and W. Chen, "Cluster-based energy efficient cooperative spectrum sensing in cognitive radios," in *2009 5th International Conference on Wireless Communications, Networking and Mobile Computing*, Sept. 2009, pp. 1–4.

[87] Y. Xu, C. Wu, C. He, and L. Jiang, "A cluster-based energy efficient mac protocol for multi-hop cognitive radio sensor networks," in *Proc. GLOBECOM*, Dec. 2012, pp. 537–542.

[88] H. Wu, F. Yao, Y. Chen, Y. Liu, and T. Liang, "Cluster-based energy efficient collaborative spectrum sensing for cognitive sensor network," *IEEE Commun. Lett.*, vol. 21, no. 12, pp. 2722–2725, Dec. 2017.

[89] F. Salahdine, N. Kaabouch, and H. El Ghazi, "A survey on compressive sensing techniques for cognitive radio networks," *Phys. Commun.*, vol. 20, no. C, pp. 61–73, Sept. 2016.

[90] L. Zhang, M. Xiao, G. Wu, S. Li, and Y. C. Liang, "Energy-efficient cognitive transmission with imperfect spectrum sensing," *IEEE J. Sel. Areas Commun.*, vol. 34, no. 5, pp. 1320–1335, May 2016.

[91] M. R. Mili, L. Musavian, K. A. Hamdi, and F. Marvasti, "How to increase energy efficiency in cognitive radio networks," *IEEE Trans. Commun.*, vol. 64, no. 5, pp. 1829–1843, May 2016.

[92] R. Kishore, C. K. Ramesha, S. Gurugopinath, and K. R. Anupama, "Performance analysis of superior selective reporting-based energy efficient cooperative spectrum sensing in cognitive radio networks," *Ad Hoc Networks*, vol. 65, pp. 99 – 116, 2017.

[93] H. Hu, H. Zhang, and Y. C. Liang, "On the spectrum- and energy-efficiency tradeoff in cognitive radio networks," *IEEE Trans. Commun.*, vol. 64, no. 2, pp. 490–501, Feb. 2016.

[94] N. I. Miridakis, T. A. Tsiftsis, G. C. Alexandropoulos, and M. Debbah, "Green cognitive relaying: Opportunistically switching between data transmission and energy harvesting," *IEEE J. Sel. Areas Commun.*, vol. 34, no. 12, pp. 3725–3738, Dec. 2016.

[95] A. E. Shafie, N. Al-Dhahir, and R. Hamila, "A sparsity-aware cooperative protocol for cognitive radio networks with energy-harvesting primary user," *IEEE Trans. Commun.*, vol. 63, no. 9, pp. 3118–3131, Sept. 2015.

[96] J. Ren, J. Hu, D. Zhang, H. Guo, Y. Zhang, and X. Shen, "RF energy harvesting and transfer in cognitive radio sensor networks: Opportunities and challenges," *IEEE Commun. Mag.*, vol. 56, no. 1, pp. 104–110, Jan. 2018.

[97] S. Lee, R. Zhang, and K. Huang, "Opportunistic wireless energy harvesting in cognitive radio networks," *IEEE Trans. Wireless Commun.*, vol. 12, no. 9, pp. 4788–4799, Sept. 2013.

[98] S. Bi, Y. Zeng, and R. Zhang, "Wireless powered communication networks: an overview," *IEEE Wireless Commun. Mag.*, vol. 23, no. 2, pp. 10–18, Apr. 2016.

[99] S. H. Kim and D. I. Kim, "Hybrid backscatter communication for wireless-powered heterogeneous networks," *IEEE Trans. Wireless Commun.*, vol. 16, no. 10, pp. 6557–6570, Oct. 2017.

[100] D. T. Hoang, D. Niyato, P. Wang, D. I. Kim, and Z. Han, "Ambient backscatter: A new approach to improve network performance for RF-powered cognitive radio networks," *IEEE Trans. Commun.*, vol. 65, no. 9, pp. 3659–3674, Sept. 2017.

[101] L. R. Varshney, "Transporting information and energy simultaneously," in *Proc. IEEE Int. Symp. Inf. Theory*, Jul. 2008, pp. 1612–1616.

[102] X. Lu, P. Wang, D. Niyato, D. I. Kim, and Z. Han, "Wireless networks with RF energy harvesting: A contemporary survey," *IEEE Commun. Surveys Tuts.*, vol. 17, no. 2, pp. 757–789, Nov. 2015.

[103] A. S. Cacciapuoti, I. F. Akyildiz, and L. Paura, "Correlation-aware user selection for cooperative spectrum sensing in cognitive radio ad hoc networks," *IEEE J. Sel. Areas Commun.*, vol. 30, no. 2, pp. 297–306, Feb. 2012.

[104] W. Yuan, H. Leung, S. Chen, and W. Cheng, "A distributed sensor selection mechanism for cooperative spectrum sensing," *IEEE Trans. Signal Process.*, vol. 59, no. 12, pp. 6033–6044, Dec. 2011.

[105] M. Monemian, M. Mahdavi, and M. J. Omidi, "Optimum sensor selection based on energy constraints in cooperative spectrum sensing for cognitive radio sensor networks," *IEEE Sensors J.*, vol. 16, no. 6, pp. 1829–1841, Mar. 2016.

[106] A. Ebrahimzadeh, M. Najimi, S. M. H. Andargoli, and A. Fallahi, "Sensor selection and optimal energy detection threshold for efficient cooperative spectrum sensing," *IEEE Trans. Veh. Technol.*, vol. 64, no. 4, pp. 1565–1577, Apr. 2015.

[107] A. Bhowmick, A. Chandra, S. D. Roy, and S. Kundu, "Double threshold-based cooperative spectrum sensing for a cognitive radio network with improved energy detectors," *IET Commun.*, vol. 9, no. 18, pp. 2216–2226, Dec. 2015.

[108] S. Althunibat, S. Narayanan, M. D. Renzo, and F. Granelli, "On the energy consumption of the decision-fusion rules in cognitive radio networks," in *2012 IEEE 17th International Workshop on Computer Aided Modeling and Design of Communication Links and Networks (CAMAD)*, Sept. 2012, pp. 125–129.

[109] T. Wang, Y. Li, G. Wang, J. Cao, M. Z. A. Bhuiyan, and W. Jia, "Sustainable and efficient data collection from wsns to cloud," *IEEE Trans. on Sustainable Computing*, pp. 1–1, Mar. 2017.

[110] D. Djenouri and M. Bagaa, "Energy-aware constrained relay node deployment for sustainable wireless sensor networks," *IEEE Trans. on Sustainable Computing*, vol. 2, no. 1, pp. 30–42, Jan. 2017.

[111] W. Xu, Y. Zhang, Q. Shi, and X. Wang, "Energy management and cross layer optimization for wireless sensor network powered by heterogeneous energy sources," *IEEE Trans. Wireless Commun.*, vol. 14, no. 5, pp. 2814–2826, May 2015.

[112] J. Huang, H. Wang, Y. Qian, and C. Wang, "Priority-based traffic scheduling and utility optimization for cognitive radio communication infrastructure-based smart grid," *IEEE Trans. on Smart Grid*, vol. 4, no. 1, pp. 78–86, Mar. 2013.

[113] J. Zhao, Q. Liu, X. Wang, and S. Mao, "Scheduling of collaborative sequential compressed sensing over wide spectrum band," *IEEE/ACM Transactions on Networking*, vol. 26, no. 1, pp. 492–505, Feb. 2018.

[114] X. Liu, B. G. Evans, and K. Moessner, "Energy-efficient sensor scheduling algorithm in cognitive radio networks employing heterogeneous sensors," *IEEE Trans. Veh. Technol.*, vol. 64, no. 3, pp. 1243–1249, Mar. 2015.

[115] J. B. Rao and A. O. Fapojuwo, "An analytical framework for evaluating spectrum/energy efficiency of heterogeneous cellular networks," *IEEE Trans. Veh. Technol.*, vol. 65, no. 5, pp. 3568–3584, May 2016.

[116] M. E. Ozçevik, B. Canberk, and T. Q. Duong, "End to end delay modeling of heterogeneous traffic flows in software defined 5G networks," *Ad Hoc Networks*, vol. 60, no. C, pp. 26 – 39, 2017.

[117] D. Zhang, Z. Chen, J. Ren, N. Zhang, M. K. Awad, H. Zhou, and X. S. Shen, "Energy-harvesting-aided spectrum sensing and data transmission in heterogeneous cognitive radio sensor network," *IEEE Trans. Veh. Technol.*, vol. 66, no. 1, pp. 831–843, Jan. 2017.

[118] M. I. B. Shahid and J. Kamruzzaman, "Interference protection in cognitive radio networks," in *Proc. VTC*, May 2010, pp. 1–5.

[119] Q. Tan, W. An, Y. Han, Y. Liu, S. Ci, F.-M. Shao, and H. Tang, "Energy harvesting aware topology control with power adaptation in wireless sensor networks," *Ad Hoc Networks*, vol. 27, no. Supplement C, pp. 44 – 56, 2015.

[120] Z. Zhang, X. Wen, H. Xu, and L. Yuan, "Sensing nodes selective fusion scheme of spectrum sensing in spectrum-heterogeneous cognitive wireless sensor networks," *IEEE Sensors J.*, vol. 18, no. 1, pp. 436–445, Jan. 2018.

[121] W. Ejaz and M. Ibnkahla, "Multiband spectrum sensing and resource allocation for IoT in cognitive 5G networks," *IEEE Internet of Things Journal*, vol. 5, no. 1, pp. 150–163, Feb. 2018.

[122] O. Simpson, Y. Abdulkadir, Y. Sun, and B. Chi, "Relay-based cooperative spectrum sensing with improved energy detection in cognitive radio," in *2015 10th International Conference on Broadband and Wireless Computing, Communication and Applications (BWCCA)*, Nov. 2015, pp. 227–231.

[123] Y. A. Chau, "Energy-efficient cooperative spectrum sensing with relay switching based on decision variables for cognitive radio," in *2013 16th International Symposium on Wireless Personal Multimedia Communications (WPMC)*, Jun. 2013, pp. 1–6.

[124] J. Habibi, A. Ghrayeb, and A. G. Aghdam, "Energy-efficient cooperative routing in wireless sensor networks: A mixed-integer optimization framework and explicit solution," *IEEE Trans. Commun.*, vol. 61, no. 8, pp. 3424–3437, Aug. 2013.

[125] S. Wang, M. Ge, and W. Zhao, "Energy-efficient resource allocation for OFDM-based cognitive radio networks," *IEEE Trans. Commun.*, vol. 61, no. 8, pp. 3181–3191, Aug. 2013.

[126] H. Su and X. Zhang, "Energy-efficient spectrum sensing for cognitive radio networks," in *2010 IEEE International Conference on Communications*, May 2010, pp. 1–5.

[127] Y. Pei, A. T. Hoang, and Y. C. Liang, "Sensing-throughput tradeoff in cognitive radio networks: How frequently should spectrum sensing be carried out?" in *Proc. PIMRC*, Sept. 2007, pp. 1–5.

[128] F. Kong, J. Cho, and B. Lee, "Optimizing spectrum sensing time with adaptive sensing interval for energy-efficient crsns," *IEEE Sensors J.*, vol. 17, no. 22, pp. 7578–7588, Nov. 2017.

[129] S. Zhang, A. S. Hafid, H. Zhao, and S. Wang, "Cross-layer rethink on sensing-throughput tradeoff for multi-channel cognitive radio networks," *IEEE Trans. Wireless Commun.*, vol. 15, no. 10, pp. 6883–6897, Oct. 2016.

[130] Y. J. Choi, W. Pak, Y. Xin, and S. Rangarajan, "Throughput analysis of cooperative spectrum sensing in Rayleigh-faded cognitive radio systems," *IET Commun.*, vol. 6, no. 9, pp. 1104–1110, Jun. 2012.

[131] B. Wang, K. Huang, X. Xu, and Y. Wang, "Secure spectral-energy efficiency tradeoff in random cognitive relay networks," *China Communications*, vol. 14, no. 12, pp. 45–58, Dec. 2017.

[132] G. Ozcan, M. C. Gursoy, and J. Tang, "Spectral and energy efficiency in cognitive radio systems with unslotted primary users and sensing uncertainty," *IEEE Trans. Commun.*, vol. 65, no. 10, pp. 4138–4151, Oct. 2017.

[133] X. Xu, W. Yang, Y. Cai, and S. Jin, "On the secure spectral-energy efficiency tradeoff in random cognitive radio networks," *IEEE J. Sel. Areas Commun.*, vol. 34, no. 10, pp. 2706–2722, Oct. 2016.

[134] W. Zhang, C. X. Wang, D. Chen, and H. Xiong, "Energy spectral efficiency tradeoff in cognitive radio networks," *IEEE Trans. Veh. Technol.*, vol. 65, no. 4, pp. 2208–2218, Apr. 2016.

[135] S. Althunibat, V. Sucasas, H. Marques, J. Rodriguez, R. Tafazolli, and F. Granelli, "On the trade-off between security and energy efficiency in cooperative spectrum sensing for cognitive radio," *IEEE Commun. Lett.*, vol. 17, no. 8, pp. 1564–1567, Aug. 2013.

[136] J. Dai, J. Liu, C. Pan, J. Wang, C. Cheng, and Z. Huang, "MAC based energy efficiency in cooperative cognitive radio network in the presence of malicious users," *IEEE Access*, vol. 6, pp. 5666–5677, Jan. 2018.

[137] Y. C. Liang, Y. Zeng, E. C. Y. Peh, and A. T. Hoang, "Sensing-throughput tradeoff for cognitive radio networks," *IEEE Trans. Wireless Commun.*, vol. 7, no. 4, pp. 1326–1337, Apr. 2008.

[138] A. S. Cacciapuoti, M. Caleffi, D. Izzo, and L. Paura, "Cooperative spectrum sensing techniques with temporal dispersive reporting channels," *IEEE Trans. Wireless Commun.*, vol. 10, no. 10, pp. 3392–3402, Oct. 2011.

[139] S. Althunibat, M. Di Renzo, and F. Granelli, "Cooperative spectrum sensing for cognitive radio networks under limited time constraints," *Journal on Computer Communications*, vol. 43, pp. 55–63, May 2014.

[140] W. Ejaz, G. A. Shah, N. ul Hasan, and H. S. Kim, "Energy and throughput efficient cooperative spectrum sensing in cognitive radio sensor networks," *Trans. Emerg. Telecom. Tech.*, vol. 26, no. 7, pp. 1019–1030, 2015.

[141] X. Li, J. Cao, Q. Ji, and Y. Hei, "Energy efficient techniques with sensing time optimization in cognitive radio networks," in *Proc. WCNC*, Apr. 2013, pp. 25–28.

[142] S. Nallagonda, S. D. Roy, and S. Kundu, "Performance evaluation of cooperative spectrum sensing scheme with censoring of cognitive radios in rayleigh fading channel," *Wireless Personal Communications*, vol. 70, no. 4, pp. 1409–1424, 2013.

[143] D. Huang, G. Kang, B. Wang, and H. Tian, "Energy-efficient spectrum sensing strategy in cognitive radio networks," *IEEE Commun. Lett.*, vol. 17, no. 5, pp. 928–931, May 2013.

[144] S. Atapattu, C. Tellambura, and H. Jiang, "Energy detection based cooperative spectrum sensing in cognitive radio networks," *IEEE Trans. Wireless Commun.*, vol. 10, no. 4, pp. 1232–1241, Apr. 2011.

[145] A. S. Cacciapuoti, I. F. Akyildiz, and L. Paura, "Primary-user impact on spectrum sensing in cognitive radio networks," in *2011 IEEE 22nd International Symposium on Personal, Indoor and Mobile Radio Communications*, Sept. 2011, pp. 451–456.

[146] A. Bletsas, A. Khisti, D. P. Reed, and A. Lippman, "A simple cooperative diversity method based on network path selection," *IEEE J. Sel. Areas Commun.*, vol. 24, no. 3, pp. 659–672, Mar. 2006.

[147] H. Hu, H. Zhang, and Y. C. Liang, "On the spectrum- and energy-efficiency tradeoff in cognitive radio networks," *IEEE Trans. Commun.*, vol. 64, no. 2, pp. 490–501, Feb. 2016.

[148] S. Althunibat, M. D. Renzo, and F. Granelli, "Optimizing the k-out-of-n rule for cooperative spectrum sensing in cognitive radio networks," in *Proc. GLOBECOM*, Dec. 2013, pp. 1607–1611.

[149] Y. Zheng and L. Zheng, "Sensing transmission tradeoff over penalty for miss detection in cognitive radio network," *Wireless Personal Communications*, vol. 92, no. 3, pp. 1089–1105, 2017.

[150] X. Liu, W.-z. Zhong, and K.-q. Chen, "Optimization of sensing time and cooperative user allocation for or-rule cooperative spectrum sensing in cognitive radio network," *Journal of Central South University*, vol. 22, no. 7, pp. 2646–2654, Jul 2015.

[151] C. R. Stevenson, G. Chouinard, Z. Lei, W. Hu, S. J. Shellhammer, and W. Caldwell, "IEEE 802.22: the first cognitive radio wireless regional area network standard," *IEEE Commun. Mag.*, vol. 47, no. 1, pp. 130–138, Jan. 2009.

[152] H. V. Dang and W. Kinsner, "An analytical multiobjective optimization of joint spectrum sensing and power control in cognitive radio networks," in *2015 IEEE 14th International Conference on Cognitive Informatics Cognitive Computing (ICCI*CC)*, Jul. 2015, pp. 39–48.

[153] W. Y. Lee and I. F. Akyildiz, "Optimal spectrum sensing framework for cognitive radio networks," *IEEE Trans. Wireless Commun.*, vol. 7, no. 10, pp. 3845–3857, Oct. 2008.

[154] W. Zhang and C. K. Yeo, "Joint iterative algorithm for optimal cooperative spectrum sensing in cognitive radio networks," *Comput. Commun.*, vol. 36, no. 1, pp. 80–89, Dec. 2012.

[155] R. Xie, F. R. Yu, H. Ji, and Y. Li, "Energy-efficient resource allocation for heterogeneous cognitive radio networks with femtocells," *IEEE Trans. Wireless Commun.*, vol. 11, no. 11, pp. 3910–3920, Nov. 2012.

[156] T. Qiu, N. Chen, K. Li, D. Qiao, and Z. Fu, "Heterogeneous ad hoc networks: Architectures, advances and challenges," *Ad Hoc Networks*, vol. 55, no. Supplement C, pp. 143 – 152, 2017.

[157] X. Liu, F. Li, and Z. Na, "Optimal resource allocation in simultaneous cooperative spectrum sensing and energy harvesting for multichannel cognitive radio," *IEEE Access*, vol. 5, pp. 3801–3812, Mar. 2017.

[158] A. Gokceoglu, S. Dikmese, M. Valkama, and M. Renfors, "Enhanced energy detection for multi-band spectrum sensing under RF imperfections," in *Proc. CROWNCOM*, Jul. 2013, pp. 55–60.

[159] I. Y. Hoballah and P. K. Varshney, "Distributed bayesian signal detection," *IEEE Trans. Inf. Theory*, vol. 35, no. 5, pp. 995–1000, Sept. 1989.

[160] Y. C. Liang, Y. Zeng, E. C. Y. Peh, and A. T. Hoang, "Sensing-throughput tradeoff for cognitive radio networks," *IEEE Trans. Wireless Commun.*, vol. 7, no. 4, pp. 1326–1337, Apr. 2008.

[161] H. Yu, W. Tang, and S. Li, "Optimization of cooperative spectrum sensing in multiple-channel cognitive radio networks," in *Proc. GLOBECOM*, Dec. 2011, pp. 1–5.

[162] Q. Zhao, Z. Wu, and X. Li, "Energy efficiency of compressed spectrum sensing in wideband cognitive radio networks," *EURASIP Journal on Wireless Communications and Networking*, vol. 2016, no. 1, p. 83, Mar 2016.

[163] S. J. Zahabi, A. A. Tadaion, and S. Aissa, "Neyman-pearson cooperative spectrum sensing for cognitive radio networks with fine quantization at local sensors," *IEEE Trans. Commun.*, vol. 60, no. 6, pp. 1511–1522, Jun. 2012.

[164] S. Gurugopinath, "Near-optimal detection thresholds for bayesian spectrum sensing under fading," in *Proc. SPCOM*, Jul. 2014, pp. 1–6.

[165] S. Gurugopinath, C. R. Murthy, and V. Sharma, "Error exponent analysis of energy-based bayesian decentralized spectrum sensing under fading," *Phys. Commun.*, vol. 17, no. C, pp. 94–106, Dec. 2015.

[166] Y. Gao, W. Xu, K. Yang, K. Niu, and J. Lin, "Energy-efficient transmission with cooperative spectrum sensing in cognitive radio networks," in *Proc. WCNC*, Apr. 2013, pp. 7–12.

[167] H. Urkowitz, "Energy detection of unknown deterministic signals," *Proceedings of the IEEE*, vol. 55, no. 4, pp. 523–531, Apr. 1967.

[168] N. Reisi, V. Jamali, and M. Ahmadian, "Linear decision fusion based cooperative spectrum sensing in cognitive radio networks," in *Proc. AISP*, May 2012, pp. 211–215.

[169] S. Atapattu, C. Tellambura, and H. Jiang, "Energy detection based cooperative spectrum sensing in cognitive radio networks," *IEEE Trans. Wireless Commun.*, vol. 10, no. 4, pp. 1232–1241, Apr. 2011.

[170] H. V. Poor, *An introduction to signal detection and estimation*. Springer Science & Business Media, 2013.

List of Publications From This Thesis

Journal Papers

1. Rajalekshmi Kishore, Ramesha C.K., Sanjeev Gurugopinath, Anupama K.R., "Performance analysis of superior selective reporting-based energy efficient cooperative spectrum sensing in cognitive radio networks", in Ad Hoc Networks, Volume 65, 2017, Pages 99-116, ISSN 1570-8705.

2. Rajalekshmi Kishore, Sanjeev Gurugopinath, Ramesha C.K., Anupama K.R., Eshan Sangodkar "Optimal Sensor Scheduling for Cognitive Radio Networks with Energy Harvesting Nodes", submitted to Transactions on Emerging Telecommunication Technologies, Wiley.

Conference Papers

1. Rajalekshmi Kishore, Sanjeev Gurugopinath, Ramesha C.K., Anupama K.R., Eshan Sangodkar, "Sensor Scheduling for Selective Reporting-based Spectrum Sensing in Energy Harvesting-Aided Heterogeneous Cognitive Radio Sensor Networks" accepted in IEEE SENSORS 2018.

2. Rajalekshmi Kishore, Ramesha C. K., Sanjeev Gurugopinath, and Eshaan Sangodkar, "Energy Efficiency Optimization for Superior Selective Reporting-based Spectrum Sensing," 2017 IEEE 28th Annual International Symposium on Personal, Indoor, and Mobile Radio Communications (PIMRC), Montreal,Canada, 2017, pp. 1-6.

3. Rajalekshmi Kishore, Ramesha C K, George Joseph and Eshaan Sangodkar, "Waveform and Energy Based Dual Stage Sensing Technique for Cognitive Radio using RTL-SDR," 2016 Annual IEEE India Conference (INDICON), IISc Bangalore, Dec. $16^{th} - 18^{th}$, 2016, pp. 1-6.

4. Rajalekshmi Kishore, C.K. Ramesha, K.R. Anupama, "Bayesian Detector Based Superior Selective Reporting Mechanism for Cooperative Spectrum Sensing in Cognitive Radio

Networks," Procedia Computer Science, 6th International Conference on Advances in computing and Communication (ICACC), Kochi, Sep. $6^{th} - 8^{th}$, Vol 93, 2016, pp. 207-216, ISSN 1877-0509, http://dx.doi.org/10.1016/j.procs.2016.07.202.

5. R. Kishore, Ramesha C K and T. Sawant, "Superior Selective Reporting mechanism for cooperative spectrum sensing in cognitive radio networks," 2016 International Conference on Wireless Communications, Signal Processing and Networking (WiSPNET), Chennai, March 23^{rd} -25^{th} ,2016, pp. 426-431.doi: 10.1109/WiSPNET.2016.7566169.

6. R. Kishore, C. K. Ramesha, V. Sharma and R. Joshi, "Performance evaluation of energy based spectrum sensing in multipath fading channel for cognitive radio system," 2014 IEEE National Conference on Communication, Signal Processing and Networking (NCCSN), Palakkad, Oct.$10^{th} - 12^{th}$, 2014, pp. 1-6. doi: 10.1109/NCCSN.2014.7001153.

Brief Biography of the Candidate

Rajalekshmi Kishore is a Ph.D. student at BITS PIlani, K.K.Birla Goa Campus, Goa, India. Rajalekshmi completed her ME in Communication Systems from National Engineering College affiliated to Anna University in 2005. Rajalekshmi obtained her B.E degree from N.I. College of Engineering, Tamil Nadu in 2003. Her current work is focused on Cooperative Communication, Energy Efficiency and harvesting in Cognitive radio network.

Brief Biography of the Supervisor

Ramesha C K received the M.Sc degree from Mangalore University, Konaje, Mangalore in 1990 and Ph.D degree in Electronics from University of Mysore, Mysore, India in 2007. He is currently working as Associate Professor in the Department of Electrical and Electronics Engineering, BITS Pilani, K.K Birla Goa Campus. He has published more than 14 articles in referred journals, and has been author or co-author of over 26 conference papers. He is also actively involved in Major Research Projects sponsored by UGC and DST, New Delhi, India. His current research interests are (i) Ohmic and Schottky Contacts to wide-band gap semiconductors, (ii) Surface analysis of III-V and II-VI semiconductors, Low power VLSI design, RF Antenna design and cognitive radio.

Brief Biography of the Co-Supervisor

K.R.Anupama received her Ph.D in Mobile Networking from BITS Pilani, Pilani Campus. She is currently a Professor, in the Department of Electrical & Electronics Engineering, BITS Pilani, K.K.Birla Goa Campus. Her area of specialization is network embedded systems and teaches courses related to embedded systems and architecture. Her research interest are in the area of mobile adhoc network, wireless sensor network, network embedded application and deeply embedded systems.